Nicolaas Westerhof
Nikos Stergiopulos
Mark I.M. Noble

Snapshots
of Hemodynamics

An Aid for
Clinical Research and
Graduate Education

Second Edition

Springer

Snapshots of Hemodynamics

Nicolaas Westerhof · Nikolaos Stergiopulos
Mark I.M. Noble

Snapshots of Hemodynamics

An Aid for Clinical Research
and Graduate Education

Second edition

Springer

Nicolaas Westerhof
Departments of Physiology and
Pulmonology
ICaR-VU
VU University Medical Center
Amsterdam, the Netherlands
n.westerhof@vumc.nl

Mark I.M. Noble
Cardiovascular Medicine
Aberdeen University
Aberdeen, Scotland
mimnoble@abdn.ac.uk

Nikolaos Stergiopulos
Laboratory of Hemodynamics and
Cardiovascular Technology
Swiss Federal Institute of Technology
Lausanne, Switzerland
Nikolaos.stergiopulos@epfl.ch

Preface

This book is written in a quick reference style to help clinical and basic researchers, as well as graduate students, in the understanding of hemodynamics. Recent developments in genetics and molecular biology on the one hand, and new noninvasive measurement techniques on the other hand, make it possible to measure and understand the hemodynamics of heart and vessels better than ever before. Hemodynamics makes it possible to characterize, in a quantitative way, and even with noninvasive techniques the function of the heart and the arterial system, separately and in combination, thereby producing information about what genetic and molecular processes are of importance for cardiovascular function.

We have made the layout of the book such that it gives a succinct overview of individual topics in short chapters Therefore every chapter starts with a "box" containing a figure and caption, describing the main aspects of the subject. It is often sufficient to study the contents of this box alone to obtain this basic information, and therefore it is not necessary to read the book from cover to cover.

Each chapter is further written in such a way that one is able to grasp the basic and applied principles of the hemodynamic topic. The part, called "Description", can be used to get more detailed information and find some references to more detailed work. If more details or broader perspectives are desired one can go to the other, related, chapters to which the text refers, or to the textbooks listed in the "Reference books" section (Appendix 6). More literature can easily be found on the internet.

Chapters end with a section "Physiological and Clinical relevance" to place the information into perspective.

<div align="right">

Nicolaas Westerhof
Nikolaos Stergiopulos
Mark I.M. Noble

</div>

Acknowledgement

Contents

How to use
Snapshots of Hemodynamics

Parabolic velocity profile

v_{max}

$Q = (\Delta P/l)\cdot(\pi/8\eta)\cdot r_i^4$

$v(r) = (\Delta P/l)\cdot(r_i^2 - r^2)/4\eta$

$\tau = 4\eta\cdot Q/(\pi\, r_i^3)$

The law of Poiseuille describes the relation between pressure drop, $\Delta P/l$, and blood flow, Q, in a stiff tube under steady flow conditions. This figure shows a tube with circular cross-section where the blood flows in a laminar fashion, i.e., each fluid layer stays at the same constant distance from the center. The flow depends strongly on the radius of the tube (fourth power), the pressure drop over the tube length ($\Delta P/l$) and viscosity of blood (η). The velocity profile, $v(r)$, is parabolic (second formula). The wall shear stress, τ, (third formula) acting on the intimal layer (endothelium) equals $4\eta\, Q/(\pi r^3) = (\Delta P/l)\cdot(r_i/2)$. Resistance can be calculated as $R = \Delta P/Q = 8\,\eta l/\pi r_i^4$.

The box contains a figure and a short text that illustrates the main message of the chapter.

Description
With laminar flow through a uniform tube the velocity profile over the cross-section is a parabola.

The "Description" section gives the essential background and discusses the different aspects of the subject.

Physiological and Clinical Relevance
The more general form of Poiseuille's law given above, i.e., $Q = DP/R$ allows us to derive resistance, R, from measurements of mean pressure and mean flow.

The "Physiological and clinical relevance" section places the subject in a broader patho-physiological context and shows clinical applications.

References
1. Murgo JP, Westerhof N, Giolma JP, Altobelli SA. Aortic input impedance in normal man: relationship to pressure wave forms. *Circulation* 1980; 62: 101–116.
2. Murgo JP, Westerhof N, Giolma JP, Altobelli, SA. Manipulation...

A limited number of references are given. Major reference books are given in Appendix 6.

Part A
Basics of Hemodynamics

Chapter 1
Viscosity

The definition of viscosity. A fluid is located between two parallel plates. The shear force, F, divided by the contact area, A, between the liquid and the plate gives the shear _stress_, $F/A = \tau$. The shear _rate_ is the difference in velocity between the different fluid layers, and can here be calculated as the velocity of the top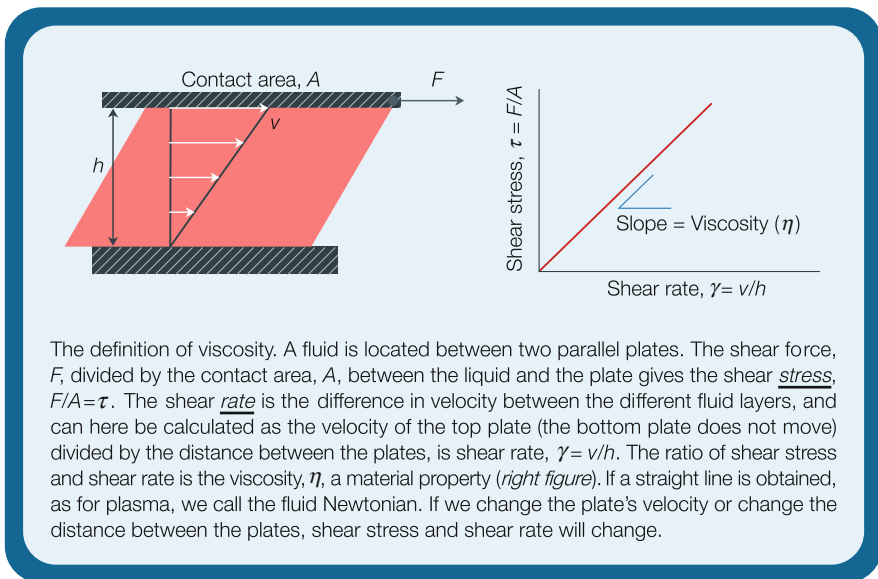 plate (the bottom plate does not move) divided by the distance between the plates, is shear rate, $\gamma = v/h$. The ratio of shear stress and shear rate is the viscosity, η, a material property (_right figure_). If a straight line is obtained, as for plasma, we call the fluid Newtonian. If we change the plate's velocity or change the distance between the plates, shear stress and shear rate will change.

Description

Consider the experiment shown in the Figure in the box. The top plate is moved with constant velocity, v, by the action of a shear force F, while the bottom plate is kept in place (velocity is zero). The result is that the different layers of blood move with different velocities. The difference in velocity in the different blood layers causes a shearing action between them.

The rate of shear, γ, is the relative displacement of one fluid layer with respect to the next. In general, the shear rate is the slope of the velocity profile, as shown in Fig. 1.1. In our particular example the velocity profile is linear, going from zero at
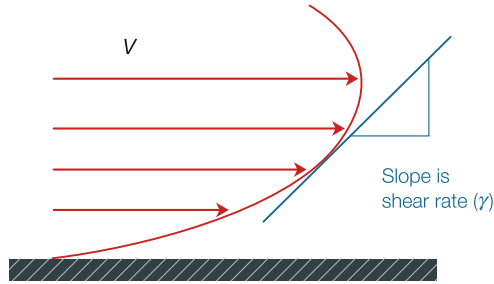
Fig. 1.1 Velocity and shear rate for a general flow profile

the bottom to v at the top plate. Therefore, the slope of the velocity profile, and thus the rate of shear, is equal to v/h, h being the distance between the plates. The units of shear rate are 1/s. The force needed to obtain a certain velocity, is proportional to the contact area, A, between fluid and plates. It is therefore convenient to use the term shear stress, defined as the force per area $\tau = F/A$, with units Pa or N/m^2.

We may think of the following experiment: we pull the top plate at different velocities v and we measure the shear force F. Then we plot the shear stress, τ, against the shear rate, γ. The resulting relation is given in the Figure in the box and the slope is the viscosity, η:

$$\eta = shearstress/shear\,rate = \tau/\gamma$$

The units of viscosity are Pa·s=Ns/m^2, or Poise (dynes·s/cm^2), with 1 Pa·s=10 Poise.

Fluids with a straight relationship between shear stress and shear rate are called Newtonian fluids, i.e., viscosity does not depend on shear stress or shear rate. This is not the case for blood (Fig. 1.2). Viscosity is sometimes called dynamic viscosity in contrast to the kinematic viscosity, which is defined as viscosity divided by fluid density ρ, thus η/ρ.

Viscosity of Blood

Blood consists of plasma and particles, with 99% of the particle volume taken by the red blood cells, RBC's or erythrocytes. Thus the red blood cells mainly determine the difference between plasma and blood viscosity (Fig. 1.2). The viscosity of blood therefore depends on the viscosity of the plasma, in combination with the hematocrit (volume % of red blood cells, Ht) and red cell deformability. Higher hematocrit and less deformable cells imply higher viscosity. The relation between hematocrit and viscosity is complex and many formulas exist. One of the simplest is the one by Einstein (Fig. 1.3):

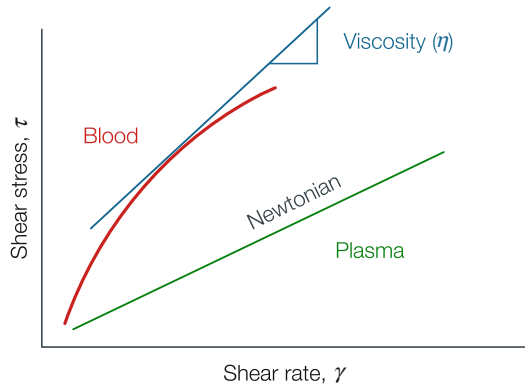$$\eta = \eta_{plasma} \cdot (1 + 2.5Ht)$$

Fig. 1.2 Viscosity of plasma and blood
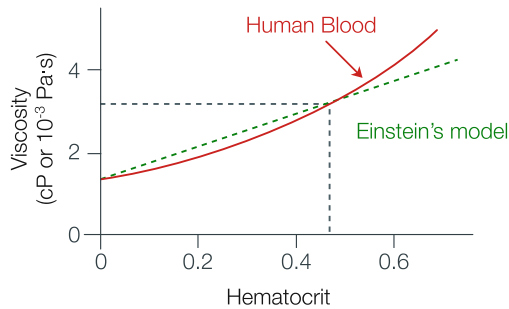
Fig. 1.3 Viscosity as a function of hematocrit

   Einstein's relation for the viscosity of fluids containing particles applies only to very low particle concentrations. Nevertheless, it gives some indication. The viscosity of plasma is about 0.015 Poise (1.5 centipoise, cP) and the viscosity of whole blood at a physiological hematocrit of 40–45% is about 3.2 cP, or $3.2 \cdot 10^{-3}$ Pa·s.
   Blood viscosity depends not only on plasma viscosity and hematocrit, but also on the size, shape and flexibility of the red blood cells. For instance, the hematocrit of camel blood is about half of that of human blood, but the camel's red blood cells are more rigid, and the overall effect is a similar blood viscosity.

Anomalous Viscosity or Non-Newtonian Behavior of Blood

The viscosity of blood depends on its velocity. More exactly formulated, when shear rate increases, viscosity decreases (Fig. 1.4). At high shear rates the doughnut-shaped RBC's orient themselves in the direction of flow and viscosity is lower. For extremely low shear rates formation of RBC aggregates may occur, thereby increasing viscosity to very high values. It has even been suggested that a certain minimum shear stress is required before the blood will start to flow, the so-called yield stress. In large and medium size arteries shear rates are higher than
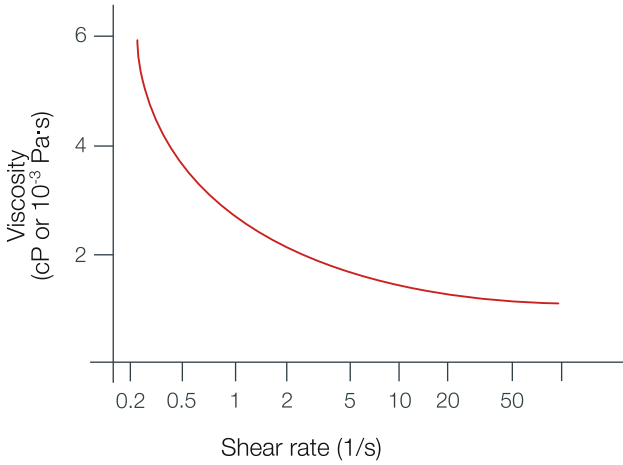
Fig. 1.4 Viscosity of blood as function of shear rate for a hematocrit of 48
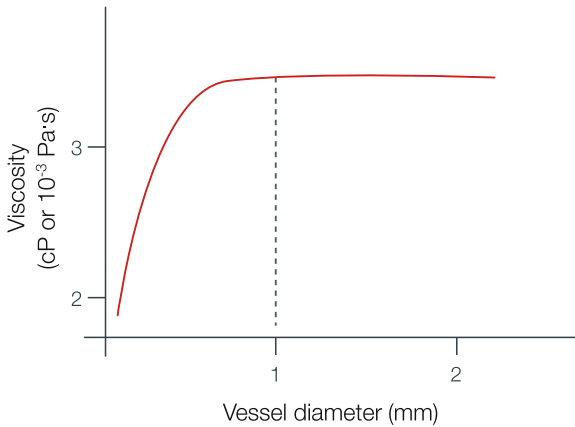
Fig. 1.5 Blood viscosity as function of vessel size

100 s^{-1}, and the viscosity is practically independent of velocity, and thus constant. The physiological range of wall shear stress is 10–20 dynes/cm², or 1–2 Pa, with 1 Pa = 0.0075 mmHg. Several equations exist that relate shear stress and shear rate of blood, e.g., Casson fluid, and Herschel-Bulkley fluid [1, 2].

Viscosity also depends on the size of blood vessel (Fig. 1.5). In small blood vessels and at low velocities, blood viscosity apparently decreases with decreasing vessel size. This is known as the Fahraeus-Lindqvist effect, and it begins to play a role in vessels smaller than 1 mm in diameter. Therefore the non-Newtonian character of blood only plays a role in the microcirculation.

Red blood cells show axial accumulation (plasma skimming), while the concentration of platelets appears highest at the wall.

Viscosity depends on temperature. A decrease of 1°C in temperature yields a 2% increase in viscosity. Thus in a cold foot blood viscosity is much higher than in the brain.

How to Measure Viscosity

Blood viscosity is measured using viscometers. Viscometers consist essentially of two rotating surfaces, as a model of the two plates shown in the box Figure. Blood is usually prevented from air contact and temperature is controlled. When comparing data on viscosity one should always keep in mind that results are often device dependent.

Physiological and Clinical Relevance

The anomalous character of blood viscosity results from the red blood cells, and the effects are mainly found in the microcirculation at low shear and small diameters. The effects are of little importance for the hemodynamics of large arteries. Thus, in large vessel hemodynamics, it may be assumed that viscosity is independent of vessel size and shear rate.

Determination of blood viscosity *in vivo* is almost impossible. In principle, the pressure drop over a blood vessel and the flow through it, together with vessel size, can be used to derive viscosity on the basis of Poiseuille's law. However, the vessel diameter in Poiseuille's law (Chap. 2) appears as the fourth power, so that a small error in the vessel diameter leads to a considerable error in the calculated viscosity. Also, the mean pressure drop over a uniform segment of artery is typically a fraction of 1 mmHg. Moreover, hematocrit is not the same in all vessels due to plasma skimming effects. Finally, Poiseuille's law may only be applied when there are no effects of inlet length (see Chap. 2) and pressure and flow are not pulsatile (Chap. 8).

The main purpose of the circulation is to supply tissues with oxygen. Oxygen supply is the product of flow and oxygen content of the blood. The hematocrit determines the (maximum) oxygen carrying capacity of blood and its viscosity, and therefore the resistance to blood flow. These counteracting effects on oxygen transport result in an optimal hematocrit of about 45 in the human at sea level, with a small difference between males and females. It appears that in mammals, blood viscosity is similar, but the hematocrit is not because of the different size, shape and flexibility of the red blood cells as mentioned above.

Low hematocrit, as in anemia, decreases oxygen content and viscosity of blood. The former lowers oxygen supply and the latter increases blood flow thus increasing supply. Inversely, polycythemia increases oxygen content but lowers blood flow. At high altitude, where oxygen tension is lower and thus oxygen saturation in the blood is lower, a larger hematocrit is advantageous. In endurance sports higher hematocrit is more efficacious during increased oxygen demand. This is the reason EPO is sometimes used by the athletes.

References

1. Merrill EW. Rheology of blood. *Physiol Rev* 1969;49:863–888.
2. Scott Blair GW, Spanner DC. *An introduction to biorheology*. 1974, Amsterdam, Elsevier.

Chapter 2
Law of Poiseuille

Parabolic velocity profile

$Q = (\Delta P/l) \cdot (\pi/8\eta) \cdot r_i^4$

$v(r) = (\Delta P/l) \cdot (r_i^2 - r^2)/4\eta$

$\tau = 4\eta \cdot Q/(\pi\, r_i^3)$

The law of Poiseuille describes the relation between pressure drop, $\Delta P/l$, and blood flow, Q, in a stiff tube under steady flow conditions. This figure shows a tube with circular cross-section where the blood flows in a laminar fashion, i.e., each fluid layer stays at the same constant distance from the center. The flow depends strongly on the radius of the tube (fourth power), the pressure drop over the tube length ($\Delta P/l$) and viscosity of blood (η). The velocity profile, $v(r)$, is parabolic (second formula). The wall shear stress, τ, (third formula) acting on the intimal layer (endothelium) equals $4\eta\, Q/(\pi r^3) = (\Delta P/l) \cdot (r_i/2)$. Resistance can be calculated as $R = \Delta P/Q = 8\,\eta l/\pi r_i^4$.

Description

With laminar and steady flow through a uniform tube of radius r_i, the velocity profile over the cross-section is a parabola. The formula that describes the velocity (v) as a function of the radius, r is:

$$v_r = \frac{\Delta P \cdot (r_i^2 - r^2)}{4 \cdot \eta \cdot l} = v_{max}(1 - r^2/r_i^2)$$

ΔP is the pressure drop over the tube of length (l), and η is blood viscosity. At the axis ($r=0$), velocity is maximal, v_{max}, with $v_{max}=\Delta P r_i^2/4\eta l$, while at the wall ($r=r_i$) the velocity is assumed to be zero. Mean velocity is:

$$v_{mean} = \Delta P \cdot r_i^2/8 \cdot \eta \cdot l = v_{max}/2 = Q/\pi r_i^2$$

and is found at $r \approx 0.7\ r_i$.

Blood flow (Q) is mean velocity, v_{mean}, times the cross-sectional area of the tube, πr_i^2, giving:

$$Q = \Delta P \cdot \pi \cdot r_i^4/8 \cdot \eta \cdot l$$

This is Poiseuille's law relating the pressure difference, ΔP, and the steady flow, Q, through a uniform (constant radius) and stiff blood vessel. Hagen, in 1860, theoretically derived the law and therefore it is sometimes called the law of Hagen-Poiseuille. The law can be derived from very basic physics (Newton's law) or the general Navier-Stokes equations.

The major assumptions for Poiseuille's law to hold are:

- The tube is stiff, straight, and uniform
- Blood is Newtonian, i.e., viscosity is constant
- The flow is laminar and steady, not pulsatile, and the velocity at the wall is zero (no slip at the wall)

In curved vessels and distal to branching points the velocity profile is not parabolic and the parabolic flow profile needs some length of straight tube to develop, this length is called inlet length (Fig. 2.1). The inlet length, l_{inlet}, depends on the Reynolds number (Re, see Chap. 4) as:

$$l_{inlet}/D \approx 0.06\,Re$$

with D vessel diameter. For the aorta mean blood flow is about 6 l/min, and the diameter 3 cm, so that the mean velocity is ~15 cm/s. The Reynolds number is
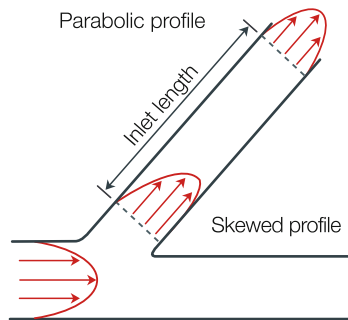

Fig. 2.1 Inlet length. Flow entering a side branch results in skewed profile. It takes a certain inlet length before the velocity develops into a parabolic profile again

therefore ~1,350 (Chap. 4). This means that l_{inlet}/D is ~80, and the inlet length ~240 cm, which is much longer than the length of the entire aorta. In the common iliac artery the Reynolds number is about 500 and diameter ~0.6 cm, giving an inlet length of ~18 cm. In other, more peripheral arteries the inlet length is much shorter but their length is shorter as well. Clearly, a parabolic flow profile is not even approximated in the arterial system. Nevertheless, the law of Poiseuille can be used as a concept relating pressure drop to flow.

A less detailed and thus more general form of Poiseuille's law is $Q = \Delta P/R$ with resistance R being:

$$R = 8 \cdot \eta \cdot l / \pi r_i^4$$

This law is used in analogy to Ohm's law of electricity, where resistance equals voltage drop/current. The analogy is that voltage difference is compared to pressure drop and current to volume flow. In hemodynamics we also call it Ohm's law. Thus:

$$\Delta P/Q = R$$

This means that resistance can be calculated from pressure and flow measurements.

Calculation of Wall Shear Stress

The wall shear rate can be calculated from the slope of the velocity profile near the wall (angle θ in Fig. 2.2), which relates to the velocity gradient, $\tan \theta = dv/dr$, near the wall (see Chap. 1). The derivative of the velocity profile gives the shear rate $\gamma = (\Delta P/l) \cdot r/2\eta$. Shear stress is shear rate times viscosity $\tau = (\Delta P/l) \cdot r/2$. The shear rate at the vessel axis, $r=0$, is zero, and at the wall, $r=r_i$, it is $\tau = (\Delta P/l) \cdot r_i/2$, so the blood cells encounter a range of shear stresses and shear rates over the vessel's cross-section.

The shear stress at the wall can also be calculated from basic principles (Fig. 2.3). For an arterial segment of length l, the force resulting from the pressure difference
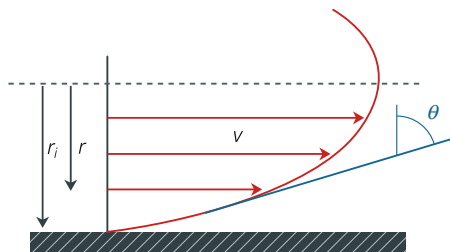

Fig. 2.2 The shear rate at the wall of a blood vessel can be calculated from the 'rate of change of velocity' at the wall, as indicated by angle θ. Relations between shear rate and flow or pressure gradient are given in the text
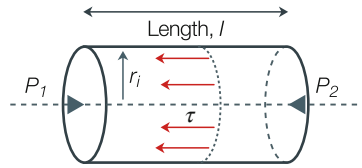
Fig. 2.3 Shear stress at the wall can also be calculated directly by the balance of pressure, $\Delta P = P_1 - P_2$, and frictional forces: $\tau = (\Delta P/l) \cdot (r_i/2)$

$(P_1 - P_2) = \Delta P$, times the cross-sectional area, πr_i^2, should equal the opposing force generated by friction. This frictional force on the wall equals the shear stress, τ, times the lateral surface, $2\pi r_i \cdot l$. Equating these forces gives, $\Delta P \cdot \pi r_i^2 = \tau \cdot 2\pi r_i \cdot l$, and

$$\tau = (\Delta P/l) \cdot (r_i/2)$$

This formulation shows that with constant perfusion pressure an increase in viscosity does not affect wall shear stress.

The wall shear stress may also be expressed as a function of volume flow using Poiseuille's law

$$\tau = 4 \cdot \eta \cdot Q / \pi r_i^3$$

this is a more useful formula for estimating shear stress because flow and radius can be measured noninvasively using ultrasound or MRI, whereas pressure gradient cannot.

Example of the Use of Poiseuille's Law to Obtain Viscosity

A relatively simple way to obtain viscosity is to use a reservoir that empties through a capillary (Fig. 2.4). Knowing the dimensions of the capillary and using Poiseuille's law viscosity can be calculated. Even simpler is the determination of viscosity relative to that of water. In that case only a beaker and stopwatch are required. The amounts of blood and water obtained for a chosen time are inversely proportional to their viscosities. The practical design based on this principle is the Ostwald viscometer.

Murray's Law

Murray's law (1926) was originally proposed by Hess in 1913 and assumes that the energy required for blood flow and the energy needed to maintain the vasculature is assumed minimal [1]. The first term equals pressure times flow and, using Poiseuille's law, this is $P \cdot Q = Q^2 \cdot 8 \cdot \eta \cdot l / \pi r_i^4$. The second term is proportional
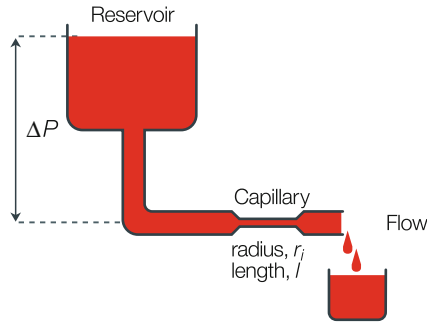
Fig. 2.4 A wide bore reservoir, maintaining constant pressure, provides the blood flow through a capillary. The application of Poiseuille's law, or comparison with water, gives absolute or relative viscosity, respectively

to vessel volume and thus equals $b \cdot \pi\, r_i^2 l$, with b proportionality constant. The total energy, E_m, is:

$$E_m = Q^2 \cdot 8\eta \cdot l / \pi r_i^4 + b \cdot \pi r_i^2 l$$

The minimal value is found for $dE_m/dr = 0$ and this leads to:

$$Q = (\pi/4l) \cdot (b/\eta)^{0.5} \cdot r_i^3 = k \cdot r_i^3$$

For a bifurcation it holds that

$$Q_{mother} = Q_{daughter1} + Q_{daughter2}$$

and thus

$$k_m r_{mother}^3 = k_{d,1} r_{daughter1}^3 + k_{d,2} r_{daughter2}^3$$

with two equal daughters, same radii and lengths, thus equal k's, it holds that:

$$r_{mother}^3 = 2 \cdot r_{daughter}^3$$

and we find that

$$r_{daughter} = (\tfrac{1}{2})^{\tfrac{1}{3}} r_{mother} \approx 0.79 r_{mother}$$

The area of both daughters together is $2 \cdot 0.79^2 \approx 1.25$ the area of the mother vessel. This area ratio is close to the area ratio predicted by Womersley on the basis of the oscillatory flow theory (Chap. 8), to obtain minimal reflection of waves at a bifurcation, namely between 1.15 and 1.33 [2]. Thus Murray's law suggests a minimal size of blood vessels and an optimum bifurcation [1].

Physiological and Clinical Relevance

The more general form of Poiseuille's law given above, i.e., $Q = \Delta P/R$ allows us to derive resistance, R, from mean pressure and mean flow measurement.

The wall shear stress, i.e., the shear force on the endothelial cells plays an important role in the short term, seconds to minutes, and the long term, weeks, months or years (Chap. 27). Short-term effects are vasomotor tone and flow mediated dilatation (FMD). Long-term effects are vascular remodeling, endothelial damage, changes in barrier function, and atherosclerosis (Chap. 27).

Shear stress plays a role in the embryonic development of the cardiovascular system. On the one hand shear stress, through gene expression, affects (ab)normal cardiovascular growth [3], and on the other hand it activates blood-forming stem cells [4]. It is of interest to mention that shear stress depends on vessel size and is different between similar vessels (e.g., aorta) of mammals [5].

It is still not possible to directly measure wall shear stress or shear rate *in vivo*. Shear rate is therefore derived from the velocity profile and blood viscosity at the wall. Velocity profiles can be measured with MRI and Ultrasound Doppler. However, the calculations to obtain shear rate require extrapolation of a flow velocity profile, because very near the wall velocity measurements are not possible. From the velocity profile, based on either Poiseuille or Womersley's oscillatory flow theory (Chap. 8), the velocity gradient, $dv/dr = \gamma$, at the wall is then calculated. To calculate wall shear stress, $\tau = \eta\,\gamma$, the blood viscosity near the wall has to be known as well, but viscosity close to the wall is not known because of plasma skimming. Plasma skimming refers to the relative absence of erythrocytes in the region near the wall. Also the diameter variation over the heartbeat is almost impossible to account for. All in all wall shear stress cannot be estimated accurately.

Wall shear stresses are ~10–20 dynes/cm^2, which is about 10,000 times less than the hoop stress (Chap. 9). Despite this enormous difference in magnitude, both stresses are equally important in the functional wall behavior in physiological and pathological conditions (see Chaps. 27 and 28).

References

1. Weibel E. *Symmorphosis*. 2000, Cambridge, MA, Harvard University Press.
2. Womersley JR. *The mathematical analysis of the arterial circulation in a state of oscillatory motion*. 1957, Wright Air Dev. Center, Tech Report WADC-TR-56-614.
3. Poelmann RE, Gittenberger-de Groot AC, Hierck BP. The development of the heart and microcirculation: role of shear stress. *Med Biol Eng Comput* 2008;46:479–84.
4. Adamo L, Naveiras O, Wenzel PL, McKinney-Freeman S, Mack PJ, Gracia-Sancho J, Suchy-Dicey A, Yoshimoto M, Lensch MW, Yoder MC, García-Cardeña G, Daley GQ. Biomechanical forces promote embryonic haematopoiesis. *Nature* 2009;459(7250):1131–5.
5. Cheng C, Helderman F, Tempel D, Segers D, Hierck B, Poelmann R, van Tol A, Duncker DJ, Robbers-Visser D, Ursem NT, van Haperen R, Wentzel JJ, Gijsen F, van der Steen AF, de Crom R, Krams R. Large variations in absolute wall shear stress levels within one species and between species. *Atherosclerosis* 2007;195:225–35.

Chapter 3
Bernoulli's Equation

Bernoulli's equation relates blood pressure, P, and blood flow velocity, v. It expresses the conservation of energy in the flowing blood. If pressure losses due to friction or turbulence are neglected, Bernoulli's equation states that the sum of mechanical, P, kinetic, $1/2\rho v^2$, and potential energy, $\rho g z$, stays constant. In any organ filled with blood the sum of pressures or total energy is constant. For a blood vessel in the supine human the term $\rho g z$ is usually neglected. Thus, when velocity is high, $v_2 > v_1$, pressure is low (*right hand figure*). In reality pressure distal to the narrowing section does not recover completely as suggested by Bernoulli's equation. The law helps to understand the effect of valvular stenosis and coarctation. The pressure drop over a stenosed valve can be estimated by $\Delta P = 4 v_s^2$ with ΔP in mmHg and with v_s, the maximal velocity in the stenosis, given in m/s.

Description

The Bernoulli equation can be viewed as an energy law. It relates blood pressure (P) to flow velocity (v). Bernoulli's law says that if we follow a blood particle along its path (dashed line in left Figure in the box) the following sum remains constant:

$$P + \tfrac{1}{2}\cdot \rho \cdot v^2 + \rho \cdot g \cdot z = \text{constant}$$

where ρ is blood density, g acceleration of gravity, and z elevation with respect to a horizontal reference surface (i.e., ground level or heart level). The equation of Bernoulli says that as a fluid particle flows, the sum of the hydrostatic pressure, P, potential energy, $\rho \cdot g \cdot z$, and the dynamic pressure or kinetic energy, $\frac{1}{2} \cdot \rho \cdot v^2$, remains constant. One can easily derive Bernoulli's equation from Newton's law: Pressure forces + gravitational forces = mass × acceleration.

Strictly speaking, the Bernoulli equation is applicable only if there are no viscous losses and blood flow is steady.

Physiological and Clinical Relevance

Bernoulli's law tells us that when a fluid particle decelerates pressure increases. Conversely, when a fluid particle accelerates, such as when going through a severe stenosis, pressure drops.

Because of the direct relationship between pressure and velocity, the Bernoulli equation has found several interesting clinical applications, such as the Gorlin [1] equation for estimating the severity of an aortic or mitral valve stenosis. Let us consider flow through a stenosed valve, s, as shown in Fig. 3.1.

Applying Bernoulli's Law

$$P_v + \tfrac{1}{2} \cdot \rho \cdot v_v^2 = P_s + \tfrac{1}{2} \cdot \rho \cdot v_s^2$$

and

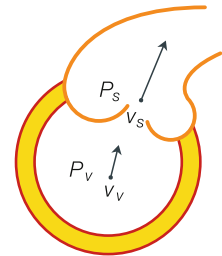$$P_v - P_s = \tfrac{1}{2} \cdot \rho \cdot (v_s^2 - v_v^2)$$

Fig. 3.1 Pressures, P_v and P_s, and velocities, v_v, and v_s, in ventricular lumen and valvular stenosis

The flow Q is the same at both locations, thus $A_v \cdot v_v = A_s \cdot v_s = Q$, where A_v and A_s are the cross-sectional areas of ventricle and valve, respectively. Substituting this into the Bernoulli's equation we obtain:

$$\Delta P = P_v - P_s = \tfrac{1}{2} \cdot \rho \cdot Q^2 \cdot (1/A_s^2 - 1/A_v^2)$$

Since the cross-sectional area of the stenosed valve A_s is much smaller than the cross-sectional area of the ventricle ($A_s \ll A_v$), the equation can be simplified to:

$$\Delta P = \tfrac{1}{2} \cdot \rho \cdot Q^2 / A_s^2 = \tfrac{1}{2} \cdot \rho \cdot v_s^2$$

When velocity in the stenosis, v_s, is expressed in m/s the pressure drop (P, in mmHg) is approximately $4 \cdot v_s^2$.

Earlier this approach was used to estimate effective area [1], A_s, of the valvular stenosis by measuring flow and pressure gradient (e.g., using a pressure wire).

$$A_s = Q\sqrt{\frac{\rho}{2\Delta P}}$$

When the pressure is in mmHg and flow in ml/s, this gives an effective area: A_s (in cm²)$=0.02 \cdot Q/\sqrt{\Delta P}$. If pressure recovery downstream of the vena contracta (see below) is included then: $A_s = 0.0225 \cdot Q/\sqrt{\Delta P} = Q/(44\sqrt{\Delta P})$, [2].

Calculation of Aortic Valvular Area

Doppler velocimetry applied to both the valvular annulus and the aorta allows for the direct calculation of valve area (Fig. 3.2). Since volume flow is the same, the product of velocity and area is also the same at both locations. Thus

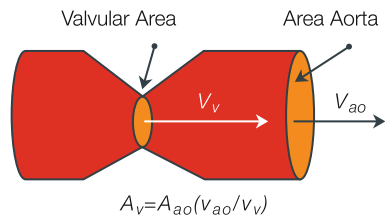$$A_{valve} = A_{aorta} \cdot v_{aorta} / v_{valve}$$

Fig. 3.2 Aortic valve area, A_v, can be derived from Doppler velocity measurements, in aorta and valve, v_{ao} and v_v, and aortic area, A_{ao}
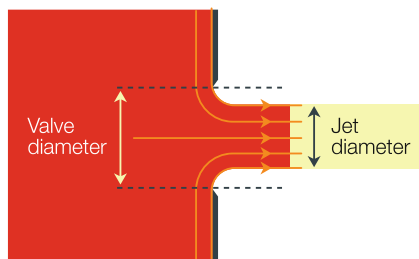
Fig. 3.3 Vena contracta effect is the result of the inability of the fluid to turn a sharp corner. The contraction coefficient A_{jet}/A_{valve} depends on the anatomical shape

Jets and Vena Contracta

Jets and vena contracta (Fig. 3.3) are formed when blood flow emerges from an opening such as a valve, and play a role in valvular stenosis and regurgitation. The contraction coefficient, i.e., the area ratio of the jet (color) and the valve (dashed lines) depends on the shape of the valve. The coanda effect is the phenomenon that a jet along the atrial or ventricular wall appears smaller than a free jet. Estimation of valvular area from the jet area is therefore not straightforward. Computational flow dynamics, i.e., the numerical solution of the Navier-Stokes equations (Appendix 5), allows the calculation flow velocity in complex geometries and makes it possible to learn more about jets.

Kinetic Energy

Bernoulli's equation pertains to conservation of energy. The term $\frac{1}{2} \cdot \rho \cdot v^2$ is the kinetic energy. At peak systole ($P = 130$ mmHg), the blood flowing in the lower abdominal aorta with a velocity $v = 1$ m/s hits the wall of the apex of the iliac bifurcation. When it would come to a rest there, velocity is negligible ($v = 0$). On the basis of the Bernoulli equation this implies a pressure rise of $\frac{1}{2} \cdot \rho \cdot v^2 = 1/2 \cdot 1{,}060 \cdot 1^2 = 530$ N/m$^2 \approx 0.5$ kPa. With 1 kPa$= 7.5$ mmHg, this pressure due to flow deceleration is thus about 3.5 mmHg.

The Hydrostatic Pressure

Most measurements are performed in the supine position. However, most activity takes place in the standing position. Figure 3.4 shows the pressures in the arterial and venous systems when a person is in the supine and the (motionless) standing position. It may be seen that the arterio-venous pressure gradients are not much affected.
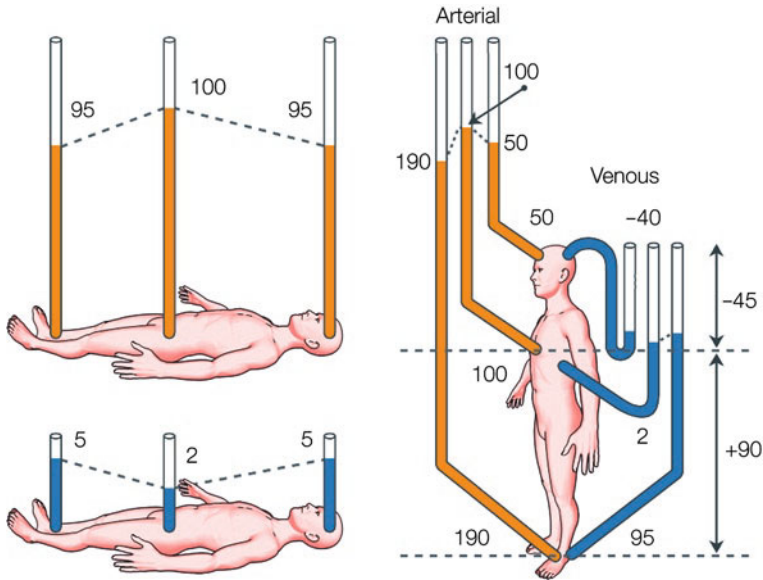
Fig. 3.4 Effect of posture on arterial and venous pressures (estimates, in mmHg). Effect of level is given by the hydrostatic pressure $\rho\, g\, h$, with ρ blood density, g, acceleration of gravity, and h height difference $z_1 - z_2$. *Dashed line* indicates the heart level. Adapted from ref. [3], used by permission
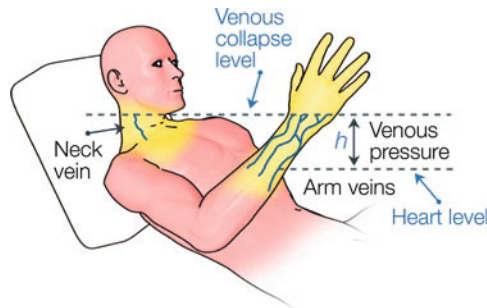

Fig. 3.5 Estimation of venous pressure by collapse. The level above the heart where collapse takes place, h, is measured in cm. The central venous pressure is then $h/1.33$ mmHg. Adapted from ref. [3], used by permission

Thus the driving forces for the flow are not much different in the two positions. The transmural pressures are strongly different and this mainly has an effect on the venous and capillary systems since the arterial system is rather stiff. The venous pooling of blood reduces cardiac filling and therefore has a, temporary, effect on the pump function of the heart. The capillary transmural pressure increase gives rise to edema formation.
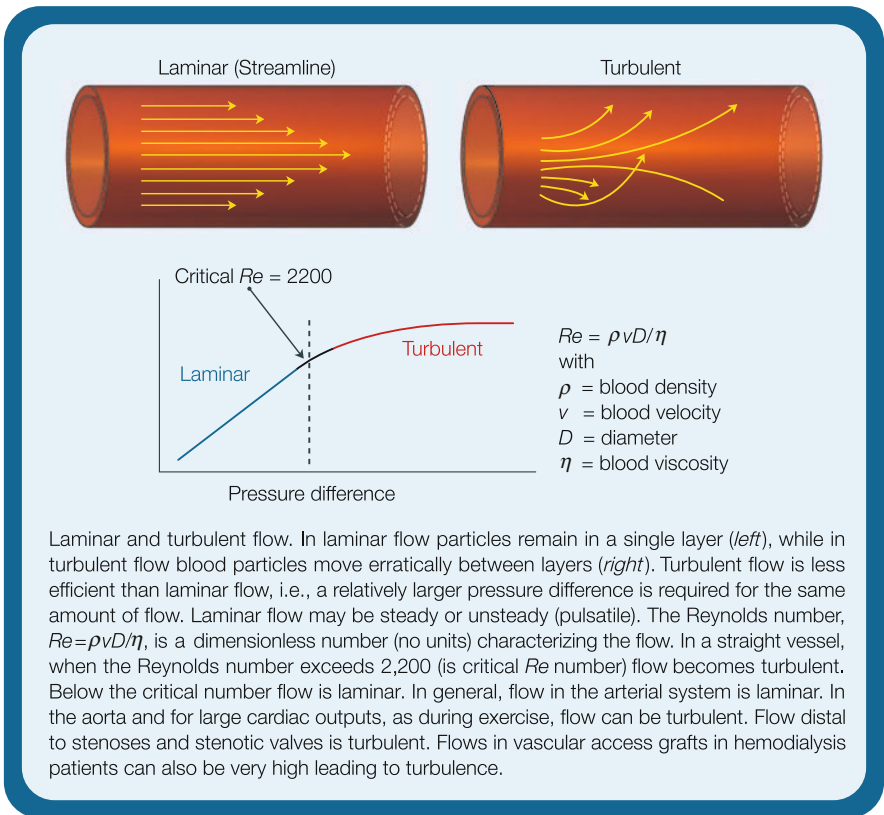
When a person is lying in a reclined position the venous pressure can be estimated in the veins of the neck and hand (Fig. 3.5). The height difference between

the point of collapse of superficial veins and the heart is the venous pressure. If the height difference is z in cm, the venous pressure can be calculated as $\rho \cdot g \cdot z = 1.05 \cdot 980 \cdot z$ dynes/cm^2 or $1.05 \cdot 980 \cdot z/1{,}360 = z/1.33$ mmHg, and thus for $z = 10$ cm the pressure equals ~7 mmHg.

References

1. Gorlin R, Gorlin SG. Hydraulic formula for calculations of the area of the stenotic mitral valve value, orthocardiac values and central circulating shunts. *Am Heart J* 1951;41:1–29.
2. Wilkinson JL. Haemodynamic calculations in the catheter laboratory. *Heart* 2001;85:113–120.
3. Burton AC. *Physiology and Biophysics of the Circulation*. 1972, Chicago, Year Book Medical Publ., 2nd edn.

Chapter 4
Turbulence

Laminar (Streamline)　　　　　Turbulent

Critical Re = 2200

Laminar

Turbulent

$Re = \rho vD/\eta$
with
ρ = blood density
v = blood velocity
D = diameter
η = blood viscosity

Pressure difference

Laminar and turbulent flow. In laminar flow particles remain in a single layer (*left*), while in turbulent flow blood particles move erratically between layers (*right*). Turbulent flow is less efficient than laminar flow, i.e., a relatively larger pressure difference is required for the same amount of flow. Laminar flow may be steady or unsteady (pulsatile). The Reynolds number, $Re = \rho vD/\eta$, is a dimensionless number (no units) characterizing the flow. In a straight vessel, when the Reynolds number exceeds 2,200 (is critical Re number) flow becomes turbulent. Below the critical number flow is laminar. In general, flow in the arterial system is laminar. In the aorta and for large cardiac outputs, as during exercise, flow can be turbulent. Flow distal to stenoses and stenotic valves is turbulent. Flows in vascular access grafts in hemodialysis patients can also be very high leading to turbulence.

Description

When flow in a straight cylindrical tube is relatively low, fluid particles move smoothly in concentric layers (box Figure, left). This type of flow is called laminar flow. The relation between the pressure gradient and flow is linear and described

by Poiseuille's law. As flow increases, the smooth parallel fluid motion becomes wavy, leading to vortices propagated downstream, subsequently the number of vortices increases and finally fluid motion becomes irregular [1]. This irregular and seemingly random fluid particle motion is called turbulence. Turbulent flow is energetically more costly than laminar flow, because part of the mechanical energy used to maintain flow (i.e., pressure gradient) is lost in the erratic motion between the fluid particles. The resistance to flow is thus higher, which is reflected by the change in slope in the relation between pressure drop and flow (box Figure, right).

To judge whether a fluid flow is laminar or turbulent, the Reynolds number, Re, is often used. Re is defined as $Re = \rho \cdot v \cdot D/\eta$, with ρ the fluid density, v the mean fluid velocity, D the tube inner diameter and η fluid viscosity. The Reynolds number reflects the ratio of inertia and viscous effects. For low Reynolds numbers (<2,200, critical Reynolds number) the viscous effects are dominant and laminar flow prevails, while for Re >2,200, flow is turbulent. Thus, it is not only the fluid velocity that determines whether or not the flow is laminar, but tube size, viscosity and blood density also play a role.

There exists a transitional zone around the critical Reynolds number of 2,200 where flow is neither strictly laminar nor strictly turbulent. Also when flow is slowly increased turbulence may start at Reynolds numbers somewhat higher than 2,200 and, inversely, when flow is decreased from a turbulent case it may remain turbulent for Reynolds numbers smaller than 2,200. In some hemodynamic texts the radius is used instead of the diameter; the critical Reynolds number is then 1,100.

Physiological and Clinical Relevance

At normal resting conditions arterial flows are laminar. For instance, in the human aorta at rest with a Cardiac Output, CO, of 6 l/min the Reynolds number can be calculated as follows. Mean velocity $v = CO/\pi r_i^2$, and with $r_i = 1.5$ cm, $v = 6,000/(60 \cdot \pi \cdot 1.5^2) \approx 15$ cm/s. Assuming blood density to be 1.06 g/cm^3 and blood viscosity to be 3.5 cP the Reynolds number equals $Re = v \cdot D \cdot \rho/\eta = 1.06 \cdot 15 \cdot 2 \cdot 1.5/0.035 \approx 1,350$. This Reynolds number is far below the critical number of 2,200 and thus flow is laminar. With heavy exercise, where flow can increase by a factor of 5 or so, the Reynolds number increases to values above 2,200 and turbulence occurs (Fig. 4.1).

The criterion for transition to turbulence, i.e., Re >2,200 applies to steady flow in straight tubes. Because arterial flow is highly pulsatile, this criterion does not strictly apply. For pulsatile flow laminar flow persists longer and transition to turbulence takes place at higher Reynolds numbers.

Turbulence is delayed when the fluid is accelerating whereas transition to turbulence occurs faster in decelerating flows. Loss of pressure due to turbulence is an effective means to decelerate flow fast. A classical example is turbulence distal to a stenosis. Fluid particles, which have been accelerated through the converging part
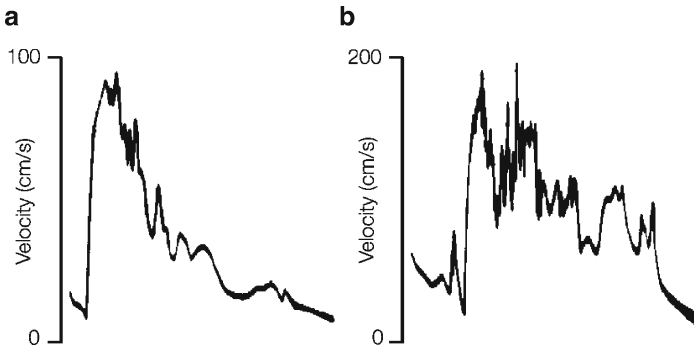
Fig. 4.1 Turbulence evidenced as rapid fluctuation in the aortic velocity signal measured in (**a**) a patient with normal aortic valve and a normal cardiac output of 5.3 l/min, and (**b**) a patient with normal aortic valve but with an elevated cardiac output of 12.9 l/min. Turbulence is much more present and intense in the case of high aortic flow. Adapted from ref. [2], used by permission

of the stenosis, decelerate fast in the distal expanding part, flow separates and turbulence develops. Turbulence in severe stenoses can be initiated for Reynolds numbers as low as 50.
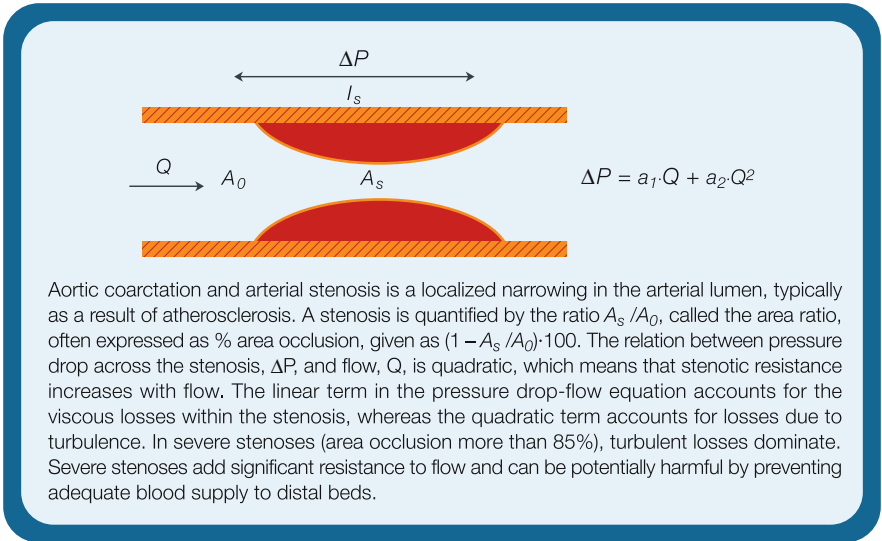
Turbulence may affect endothelial function and plays an important role in certain pathologies. For example, it has been suggested that turbulence distal to stenoses contributes to the phenomenon of post-stenotic dilatation. Aortic dilatation in valvular stenosis is also known to exist. Also, turbulence occurring at the venous anastomoses of vascular access grafts used in hemodialysis patients is correlated with the local development of intima hyperplasia, which ultimately leads to a stenosis and graft failure.

References

1. Munson BR, Young DF, Okiishi TH. *Fundamentals of fluid mechanics*. 1994, New York, NY: Wiley.
2. Nichols WW, O'Rourke MF. *McDonald's blood flow in arteries*. 2005, New York, NY: Oxford University Press, 5th edn.

Chapter 5
Arterial Stenosis

Aortic coarctation and arterial stenosis is a localized narrowing in the arterial lumen, typically as a result of atherosclerosis. A stenosis is quantified by the ratio A_s/A_0, called the area ratio, often expressed as % area occlusion, given as $(1 - A_s/A_0) \cdot 100$. The relation between pressure drop across the stenosis, ΔP, and flow, Q, is quadratic, which means that stenotic resistance increases with flow. The linear term in the pressure drop-flow equation accounts for the viscous losses within the stenosis, whereas the quadratic term accounts for losses due to turbulence. In severe stenoses (area occlusion more than 85%), turbulent losses dominate. Severe stenoses add significant resistance to flow and can be potentially harmful by preventing adequate blood supply to distal beds.

Description

Stenosis, from the Greek word for 'narrowing', is a medical term used to describe a localized constriction in an artery. Stenoses are usually caused by the development of atheromatous plaques in the subintimal layer of the arterial wall, which subsequently protrude into the lumen of the artery, thus causing a narrowing to the free passage of blood.

A coarctation or arterial stenosis consists of a converging section, a narrow section, with the minimal luminal section defining the degree of stenosis, and a diverging section (Fig. 5.1). In the converging section, Bernoulli's equation holds (see Chap. 3). Within the narrow section Poiseuille's law is assumed to apply, provided that this narrow section is long enough with approximately constant diameter. In the diverging
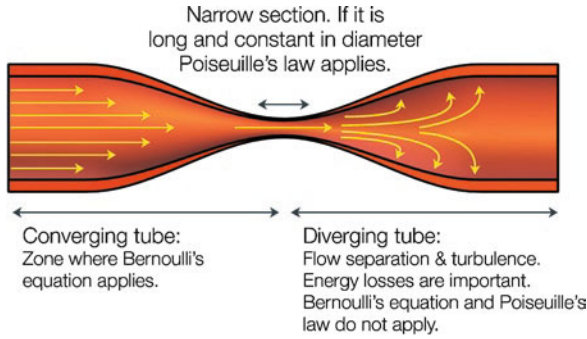
Narrow section. If it is
long and constant in diameter
Poiseuille's law applies.

Converging tube:
Zone where Bernoulli's
equation applies.

Diverging tube:
Flow separation & turbulence.
Energy losses are important.
Bernoulli's equation and Poiseuille's
law do not apply.

Fig. 5.1 A coarctation consists of a converging section, a narrow section and a diverging section, each with their particular pressure-flow relations

section flow separates and is often turbulent with significant viscous losses, which means that in this region neither Bernoulli's nor Poiseuille's law applies.

The severity of a stenosis can be expressed as % area or % diameter occlusion as $(1 - A_s/A_o)\cdot 100$ or $(1 - D_s/D_o)\cdot 100$, with subscripts s and o denoting stenotic and unstenosed vessel segments, respectively (Figure in the box). Pressure losses over a coarctation can be treated through semi-empirical relations. Such a relationship was developed by Young and Tsai [1] who performed a series of experiments of steady and pulsatile flows in models of concentric and eccentric stenosis. Young and Tsai found that the pressure drop, ΔP, across an arterial stenosis can be related to flow, Q, through the following relation:

$$\Delta P = \frac{8\pi\cdot\eta\cdot l_s}{A_s^{2}}\cdot Q + \frac{K_t\cdot\rho}{2A_0^{2}}\cdot[A_0 / A_s - 1]^2\cdot Q^2 = a_1 Q + a_2 Q^2$$

where A_0 is the unobstructed cross-sectional lumen area and A_s the minimal free cross-sectional lumen area within the coarctation (see Box Figure). The first term of the stenosis equation accounts for the viscous losses (Poiseuille's law) as blood flows through the narrow coarctation lumen. The second term accounts for the pressure losses distal to the stenosis and is derived from the mechanics of flow in a tube with an abrupt expansion. The K_t is an empirical coefficient approximately equal to 1.5, but strongly depending on the shape of the stenosis. The equation is derived for steady flow, but for oscillatory pressure-flow relations a similar equation holds [2].

Post-Stenotic Dilatation

The arterial diameter distal of a stenoses is often increased, a phenomenon called post-stenotic dilatation. The mechanism causing the dilatation is still not clear.

It may be due to abnormal shear stress and turbulent flow downstream of the stenosis, leading to extracellular matrix remodeling in the vessel wall. It has also been suggested that vessel wall vibrations distal to the stenosis cause the dilatation [3]

Physiological and Clinical Relevance

The best way to characterize a stenosis by measurement is by constructing the relation between flow and pressure across the stenosis (see Fig. 5.2).

The empirical formula for the pressure drop across a stenosis shows that both flow and area appear as quadratic terms. This is an important aspect of the hemodynamics of a coarctation. To illustrate the significance of the quadratic terms, let us assume that the stenosis length, l_s, is very small so that the first term in the equation above, $a_1 \cdot Q$, is negligible. The pressure drop is then proportional to the flow squared. Suppose that a patient with a mild coarctation in the femoral artery has, at rest, a pressure drop over the narrowed section of 10 mmHg. When the patient starts walking, and the peripheral bed dilates to allow for more perfusion flow, the drop in pressure increases. When flow needs to increase by a factor three the pressure gradient should increase to $10 \cdot 3^2 = 90$ mmHg. This is clearly impossible and the decrease in peripheral resistance of the leg does not help to increase flow sufficiently.

The pressure drop is inversely related to the square of the cross-sectional area in the stenosis. For a 80% area stenosis, the term $[A_0/A_s - 1]^2$ equals $[1/0.2 - 1]^2 = 16$, whereas for a 90% stenosis this term increases to 81. Thus a 90% stenosis is 81/16 or about five times more severe than an 80% stenosis in terms of pressure drop for
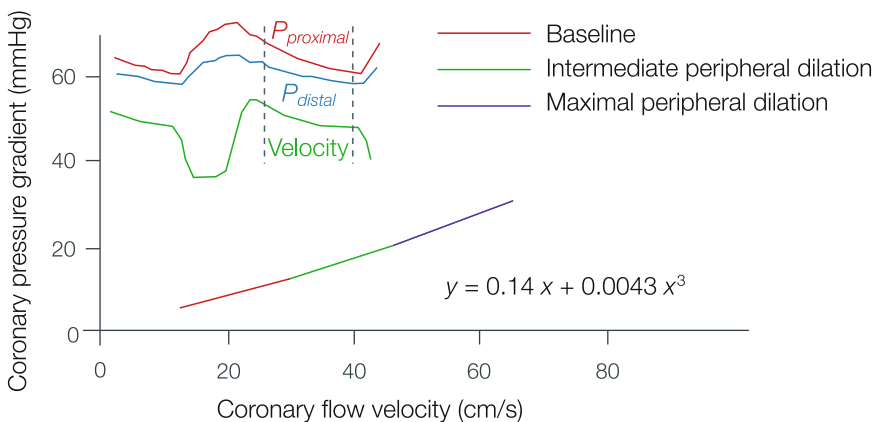

Fig. 5.2 Pressure drop over a coronary stenosis, as a function of blood flow velocity. The relations pertain to diastole and the range of velocities is obtained by vasodilation of the microcirculation. The quadratic expression can be applied. Adapted from ref. [4], used by permission

a similar flow, i.e., from 10 to 50 mmHg. This strongly nonlinear effect implies that complaints from ischemia will arise 'suddenly' when the narrowing becomes more severe, typically for a stenosis of >70%.

From Bernoulli's equation it follows that at high velocity pressure is low (Chap. 3). This implies that when flow and thus velocity is high, as is the case during vasodilation, the pressure in the narrow section may decrease to low values. For stenoses with compliant walls the decrease in transmural pressure may lead to extra narrowing, thereby worsening the situation.

Flow Reserve

Angiographic data often do not give accurate information about the functional aspects of a stenosis or coarctation. This has led several investigators to propose methods to obtain a quantitative description in functional terms. One approach is the determination of flow reserve. The, absolute, flow reserve is defined as the ratio of flow during maximal dilatation and flow during control (Q_{max}/Q_c). In Fig. 5.3, pressure distal to a stenosis, P_d, is plotted as a function of flow, while proximal (aortic) pressure is assumed to be constant. It is apparent that when the periphery dilates, i.e., the peripheral resistance decreases, from R_c to R_d, the flow increases. However, in the presence of a severe stenosis (lower curve in Fig. 5.3), the flow increase is limited and distal pressure greatly decreases, and this pressure decrease is accentuated when flow is high. In control conditions, at rest, flow may be hardly affected by the presence of the stenosis, since peripheral dilation may compensate for the stenosis 'resistance', i.e., Q_c depends on stenosis severity and on microvascular resistance. At maximal vasodilation a severe stenosis limits maximal flow Q_{max} considerably, but the peripheral resistance remains playing a role. Thus, in presence of a stenosis, flows are not determined by the stenosis alone, but by both the stenosis and the microvasculature resistance. In other words, the flow reserve (Q_{max}/Q_c) is not determined by the severity of a stenosis alone.

Fractional Flow Reserve

Another estimate of stenosis severity is the Fractional Flow Reserve, FFR, which is the ratio of the maximal flow, $Q_{max,s}$ in the bed perfused by the stenosed artery and the maximal flow in a normal, unstenosed area, $Q_{max,n}$. The FFR is thus

$$FFR = [(P_d - P_v)/R_{st}]/[(P_{prox} - P_v)/R_n] \cong P_d/P_{prox} \cong P_d/P_{aorta}$$

with P_d being the distal pressure during maximal dilation, and P_{prox} the proximal pressure. For coronary stenoses the proximal pressure equals aortic pressure. Under
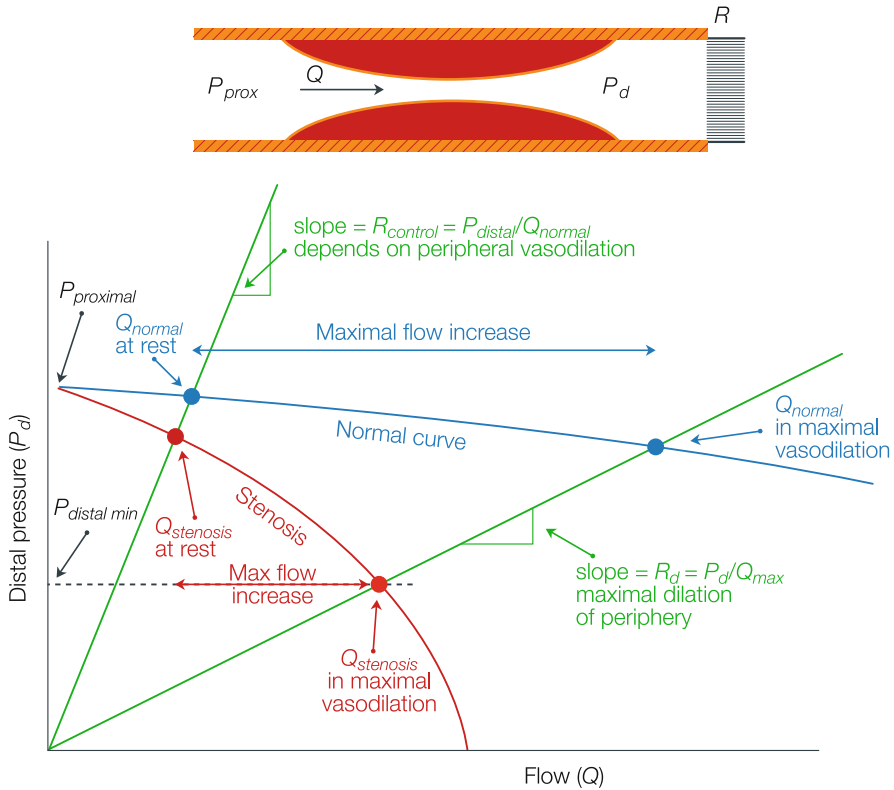
Fig. 5.3 Flow reserve is defined as the ratio of flow during maximal vasodilation and flow during control. In the unstenosed artery the ratio $Q_{max,n}/Q_n$ is much larger than when a stenosis is present, $Q_{max,s}/Q_s$. In this figure distal pressure is plotted as a function of flow. When the peripheral bed is maximally vasodilated, peripheral resistance decreases from R_c to R_d and flow increases, but distal pressure decreases. The decrease in distal pressure limits the maximal flow under vasodilation, thereby reducing the flow reserve. Thus, the flow reserve depends on the stenosis severity and microvascular resistance. The Fractional Flow Reserve, FFR, is the ratio of the maximal flow with the stenosis present and maximal flow in the unaffected bed, $Q_{max,s}/Q_{smax,n}$. The FFR also depends on the stenosis severity and how much the distal bed can dilate. The FFR is close to the ratio of the distal pressure during dilation and the proximal pressure, P_{dmin}/P_{prox}. The, nonlinear, relation between pressure drop over the stenosis and flow through it, $(P_{prox} - P_{dmin})/Q$, depends on the stenosis severity only

the assumption that the microvascular bed of the stenosed area has the same resistance as the bed of the normal area, $R_{st} = R_n$, and assuming that venous or intercept pressure, P_v, (Chap. 18) is small with respect to P_d it holds that the FFR is close to the ratio P_d/P_{aortax}. [5].

Although a normal periphery and the periphery distal to the stenosis may not have similar resistance, the FFR appears a workable parameter. The cut-off value of the FFR is 0.74, i.e., for values higher than 0.74 the stenosis is not considered functionally important.

For segmented stenoses, i.e., stenoses severity changes over its length, and for multiple stenoses the approach is more complicated.
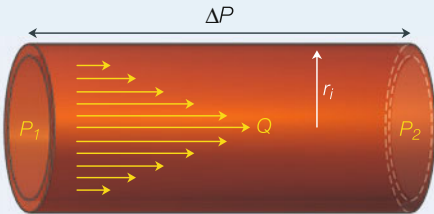
Spaan et al. [6] have reviewed the principles and limitations of flow reserve.

References

1. Young DF, Tsai FY. Flow characteristics in models of arterial stenoses: I Steady flow. *J Biomech* 1973;6:395–410.
2. Newman DL, Westerhof N, Sipkema P. Modelling of aortic stenosis. *J Biomech* 1979;12:229–235.
3. Roach MR, Stockley D. The effects of the geometry of a stenosis on poststenotic flow in models and poststenotic vibration of canine carotid arteries in vivo. *J Biomech* 1980;13:623–634.
4. Marques KM, Spruijt HJ, Boer C, Westerhof N, Visser CA, Visser FC. The diastolic flow-pressure gradient relation in coronary stenoses in humans. *J Am Coll Cardiol* 2002;39:1630–1636.
5. Pijls NHJ, De Bruyne B. *Coronary pressure*. 1997, Dordrecht & Boston, Kluwer.
6. Spaan JAE, Piek JJ, Hoffman JIE, Siebes M. Physiological basis of clinically used coronary hemodynamic indices. *Circulation* 2006;113;446–455.

Chapter 6
Resistance

$$\Delta P$$

P_1 Q r_i P_2

$$R = \Delta P/Q$$
$$= 8\eta l/\pi\, r_i^4$$

Resistance is a practical quantitative description of the relation between pressure difference and flow through a blood vessel. For a single uniform vessel Poiseuille's law gives its resistance, but in practice resistance can be obtained using Ohm's law. In other words, resistance although depending on the vascular geometry and blood viscosity, can be calculated directly from measurements of mean pressure difference and mean blood flow. Detailed knowledge of the vascular geometry is not required. Ohm's law not only pertains to single blood vessels but may also be applied to combinations of vessels, whole organ beds, and the whole systemic or pulmonary circulation. Rules for addition of resistances are discussed below. Resistance should always be calculated from a pressure *difference*, $P_1 - P_2$, indicated by ΔP. However, in the systemic circulation venous pressure is usually much lower than aortic pressure and can be disregarded. This is not the case in the pulmonary circulation. The systemic, and pulmonary vascular resistances are mainly determined by the resistance of small arteries and arterioles. This means that the mean pressure in all conduit arteries is almost the same. The arterioles act as resistances to regulate flow to the local tissue.

Description

Poiseuille's law (Chap. 2) shows that resistance depends on the length and diameter of the vessel and the viscosity of blood. However, even for a single blood vessel, it is difficult to derive the relation between pressure and flow on the basis of Poiseuille's law. The diameter of the vessel needs to be accurately known because of the fourth power law. Furthermore, the vessel should be uniform, and, especially for small vessels, the anomalous viscous properties of blood make it impossible to use a single number for viscosity. Accurate calculation of resistance on the basis of

Poiseuille's law is therefore virtually impossible. However, resistance can be calculated from the ratio of the pressure gradient and flow constituting a practical experimental approach. Thus although Poiseuille's law makes it possible to arrive at several important conclusions regarding vascular function, in practice we use resistance, calculated using Ohm's law.

To understand where resistance is located in the arterial tree we need to know some rules about resistances.

Addition of Resistances

Two resistances in series result in a total resistance equal to the sum of the resistances. This rule can be derived as follows. The total pressure drop over two resistances in series is the sum of the individual pressure drops, i.e., $\Delta P_{total} = \Delta P_1 + \Delta P_2$ and flow is the same through both. Thus $\Delta P_{total} = Q \cdot R_1 + Q \cdot R_2 = Q \cdot (R_1 + R_2) = Q \cdot R_{total}$. Thus, $R_{total} = R_1 + R_2$, and the total resistance is the sum and thus larger than each individual resistance.

Two resistances in parallel add up in a so-called 'inverse' fashion (Fig. 6.1). When in parallel, the pressure drop, ΔP, over both vessels is the same, and the two flows add up to total flow, Q_{total}, thus

$$Q_{total} = Q_1 + Q_2 = \Delta P / R_1 + \Delta P / R_2 = \Delta P / (1/R_1 + 1/R_2) = \Delta P / R_{total}$$

and we find

$$1/R_{total} = 1/R_1 + 1/R_2$$
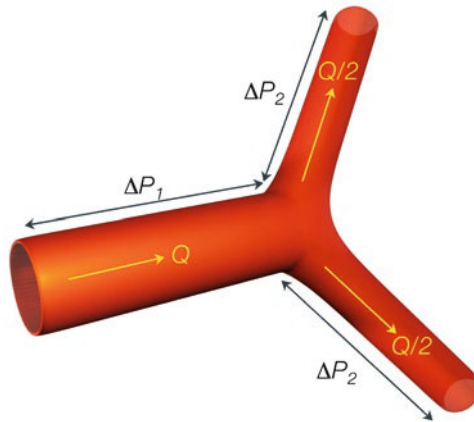
Fig. 6.1 A blood vessel, mother, divides into two smaller, daughter vessels. We determine the resistance of this network by proper addition of the two distal vessels in parallel and then add the resistance of the mother vessel. Note that we work from the distal end

An easier calculation is through conductance (G), which is the inverse of resistance, $G = 1/R$. Ohm's law written in terms of conductance is $Q = \Delta P \cdot G$. Parallel conductances can be added directly: $G_{total} = G_1 + G_2$.

Thus two equal resistances in parallel add to a total resistance of half the resistance of each. Ten equal arterioles in parallel result in an overall resistance equal to 1/10 of a single arteriole.

Physical Reason Why the Resistance Is Located in the Arterioles

We first compare the resistance of the aorta with the resistance of an arteriole using Poiseuille's law. Assuming an aortic radius of 15 mm and an (arbitrary) length of 50 cm and an arteriole with a radius of 7.5 μm and a length of 1 mm we can estimate the resistance ratio of these two. The radius ratio is 2,000 and the length ratio is ~500, thus the resistance ratio is $(2,000)^4/500$, i.e., ~$3 \cdot 10^{10}$. Thus the resistance of a single arteriole is $3 \cdot 10^{10}$ as large as that of a 50 cm long aorta.

However, there is only one aorta and about $3 \cdot 10^8$ arterioles, and since these arterioles all sprout (indirectly) from the single aorta we can consider them as in parallel. Thus the total arteriolar resistance is about $3 \cdot 10^{10}/3 \cdot 10^8 \approx 100$ times as large as the resistance of the aorta.

Therefore, the pressure drop over the aorta is about 1% of the total pressure drop over the systemic arterial system, which is about 100 mmHg. Indeed, the mean pressure in the dorsalis pedis artery is, in the supine human, only a few mmHg lower than mean pressure the ascending aorta.

Resistance of Capillaries and Veins

Capillaries have diameters that are of the same order as arterioles but their number is larger (four to five capillaries per arteriole) and therefore their resistance is about four to five times smaller. Recently is became clear that the glycocalyx, the carbohydrate structures on the luminal surface of the microvascular endothelial cells, not only protects against edema, but also reduces the effective capillary diameter and thus increases capillary resistance [1]. Still capillaries contribute little to total resistance.

Venules and veins have larger diameters than their accompanying arteries and often appear as two veins to one artery. Therefore, total venous resistance in the systemic circulation is about 1/20 of total resistance.

Thus, the total vascular resistance is mainly located in the small arteries and arterioles and is often called peripheral resistance, R_p.

Calculation of Vascular Resistance

The total resistance of the systemic circulation can be calculated as follows. When mean aortic pressure is taken to be about 105 mmHg and central venous pressure is about 5 mmHg the pressure difference is 100 mmHg. With a Cardiac Output of 6 l/min, thus 100 ml/s, the total resistance is $100/100 = 1$ mmHg/ml/s. The units mmHg/ml/s or mmHg·s/ml are called peripheral resistance units, PRU. Often physical units are used in the clinic and resistance is then expressed in dyn·s·cm^{-5} or Pa·s/m^3. As can be seen from Appendix 7 the following holds: $7.5·10^{-9}$ mmHg s/ml $= 10^{-5}$ dyn·s/cm$^5 = 1$ Pa·s/m^3 or a resistance of 1 mmHg/ml/s $= 1.3·10^3$ dyn·s/cm$^5 = 1.3·10^8$ Pa·s/m^3.

For the systemic circulation subtraction of venous pressure is often omitted without introducing large errors. However, in the pulmonary circulation with mean pulmonary artery pressure of about 20 mmHg and a pulmonary venous pressure of 5 mmHg, calculation of the pressure difference is mandatory. Pulmonary resistance thus is $(20 - 5)/100 = 0.15$ PRU, which is about 15% of the resistance of the systemic circulation.

Physiological and Clinical Relevance

The small arteries and arterioles mainly determine peripheral resistance. Resistance can be regulated by the arterioles, because they are muscular arteries and it follows from Poiseuille's law that rather small changes in diameter result in large resistance changes. A 10% change in diameter corresponds to a change in resistance by 1.1^4, or about 50%.

The resistance of the aorta and conduit arteries is so low that the mean pressure hardly decreases from heart to the small peripheral arteries, the pressure drop being only a few mmHg. This means that in the supine human, mean blood pressure is practically the same in all conduit arteries, and therefore mean blood pressure may be determined in any conduit artery. This also implies that conduit arteries can be seen as a supply reservoir with peripheral resistances adjusting themselves such that demand of flow to the tissue is met (Fig. 6.2).

When perfusion flow is high, e.g., during exercise, the large arteries could cause a sizable pressure drop. However, with increased flow conduit arteries dilate through 'Flow Mediated Dilation', FMD, to decrease their resistance. An FMD of 7% gives a resistance decrease of more than 30%.

Vascular smooth muscle tone is regulated by the nervous and hormonal systems and through autoregulation. Autoregulation is based on metabolic, myogenic, and endothelial mechanisms. During increased pressure arteriolar resistance increases thereby keeping capillary pressure constant to maintain tissue fluid equilibrium, the Starling equilibrium.

The total cross-sectional area is the largest in capillaries. It is not correct to apply Poiseuille's law using total cross-sectional area. The area (radius) of individual vessels should be used to calculate resistance and then resistances must be added in series
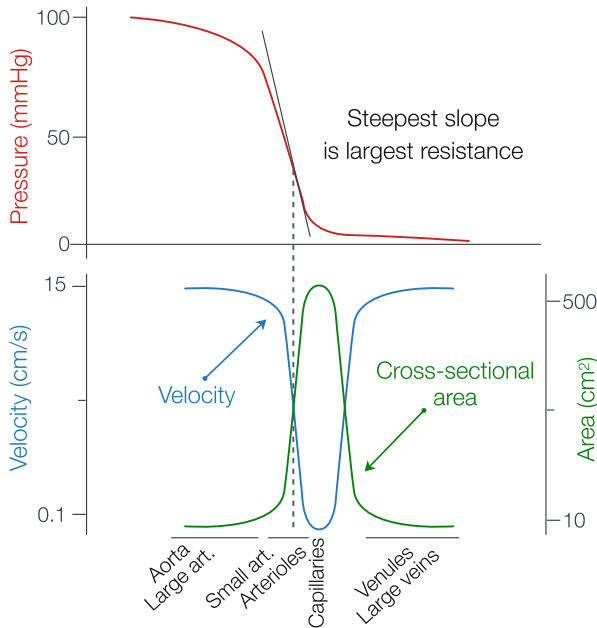
Fig. 6.2 Pressure, velocity and area distribution in the systemic circulation. Resistance must be calculated from individual vessels and cannot be obtained from total cross-sectional area directly. Adapted from ref. [2], used by permission

and in parallel according to the anatomy. The velocity of blood is lowest in the capillaries allowing ample time for exchange with the tissues.

Low Resistance of an Arterio-Venous Fistula

Several arterio-venous fistulas may exist, such as an open ductus arteriosus, and the fistula between the radial artery and vein made for dialysis. As an example, the latter shunt causes a low resistance in parallel with the resistance of the lower arm. However, the shunt does not always cause ischemia in the hand for the following reason (steal syndrome). The mean blood pressure in the aorta is 100 mmHg, and is in the radial artery normally about 3 mmHg lower, and thus 97 mmHg. The venous pressure is about 5 mmHg and in the vena cava pressure is 2 mmHg. The low resistance of the conduit arteries and veins will, with the much larger shunt flow, decrease arterial pressure by, say only 10 mmHg and increase the venous pressure by the same amount. The driving pressure for the hand is then $87 - 15 = 72$ mmHg, which is high enough to avoid ischemia. The fistula will, however, lower the total systemic peripheral resistance and increase Cardiac Output thereby affecting cardiac function.

Qualitatively stated: the conduit arterial system and venous system can be viewed as pressure reservoirs.

References

1. Van den Berg BM, Vink H, Spaan JAE. The endothelial glycocalyx protects against myocardial edema. *Circ Res* 2003;92:592–594.
2. Berne RM, Levy MN, Koeppen BM, Stanton BA. *Physiology.* 2003, St Louis & Baltimore, Mosby-Elsevier, 5th edn.

Chapter 7
Inertance
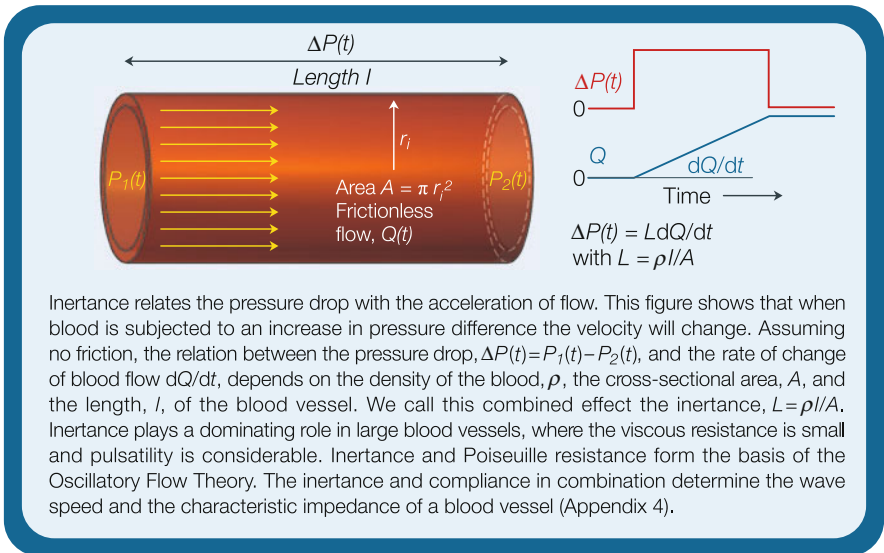
Inertance relates the pressure drop with the acceleration of flow. This figure shows that when blood is subjected to an increase in pressure difference the velocity will change. Assuming no friction, the relation between the pressure drop, $\Delta P(t) = P_1(t) - P_2(t)$, and the rate of change of blood flow dQ/dt, depends on the density of the blood, ρ, the cross-sectional area, A, and the length, l, of the blood vessel. We call this combined effect the inertance, $L = \rho l/A$. Inertance plays a dominating role in large blood vessels, where the viscous resistance is small and pulsatility is considerable. Inertance and Poiseuille resistance form the basis of the Oscillatory Flow Theory. The inertance and compliance in combination determine the wave speed and the characteristic impedance of a blood vessel (Appendix 4).

Description

Blood is accelerated and decelerated with every heartbeat, and the mass of the blood plays a role. The mass is density times volume, and the volume depends on the geometry of the blood vessel or heart. Blood density is a material property and is about 1.06 g/cm³. In hemodynamics, we calculate the effective mass and call it inertance. Inertance connects the oscillatory pressure drop with the rate of change of blood flow.

We can derive inertance by using Newton's law relating force, F, mass, m, and the rate of change of velocity, dv/dt, which is the acceleration, a:

$$F = m \cdot a = m \cdot dv/dt$$

For a vessel, the net force $F(t) = (P_1(t) - P_2(t)) A = \Delta P A$, A being the luminal cross-sectional area. The mass in the segment equals blood density, ρ, times the volume (length times area): $\rho\,(l\,A)$. The acceleration is the rate of change of velocity with time, i.e., dv/dt. In terms of volume flow this is $(1/A)\,dQ/dt$. With Newton's equation this gives:

$$\Delta P(t) \cdot A = \rho \cdot l \cdot A \cdot (1/A) \cdot dQ/dt = \rho \cdot l \cdot$$

and

$$\Delta P(t) = \rho \cdot l\,/\,A\,(dQ/dt) = L \cdot dQ/dt$$

where $L = \rho \cdot l/A$ is called inertance. We recall that resistance is inversely proportional to r_i^4 (Chap. 2) while inertance is inversely related to r_i^2. Thus, in large vessels the inertance plays a larger role than resistance while in very small arteries and arterioles it is the resistance that plays the larger role.

The inertance in combination with the compliance of a vessel segment determines the characteristic impedance and the wave speed (see Chap. 20 and Appendix 3).

Addition of Series and Parallel Inertances

The principal rules for addition of inertance of vessels in parallel and in series are as for resistances (see Chap. 6).

Physiological and Clinical Relevance

The inertance is determined by the cross-sectional area and length of the blood vessel, and by blood density. Blood density varies little, even in pathologic conditions. Inertance is therefore primarily a geometrically determined parameter.

An example where the effect of the inertance can be seen is when left ventricular and aortic pressures are measured simultaneously (Fig. 7.1). During the ejection period aortic flow is first accelerating (early ejection) and then decelerating. When the blood is accelerated the left ventricular pressure is higher than aortic pressure. When the blood is decelerated the pressure difference reverses, as in the later phase of ejection. It may be seen that the pressure difference and the time derivative of flow are almost proportional in systole, suggesting inertance effects.

Inertance in combination with reflections (see Chap. 21) can result in flow reversal, i.e., negative flow during part of the cardiac cycle (Fig. 7.2). This negative flow is therefore physiologic. The mean flow is, of course, always in the direction of the periphery.

Another example (see Fig. 7.3) is the diastolic filling of the ventricle through the mitral valve. As a result of the inertance, flow persists when left ventricular pressure is higher than left atrial pressure.
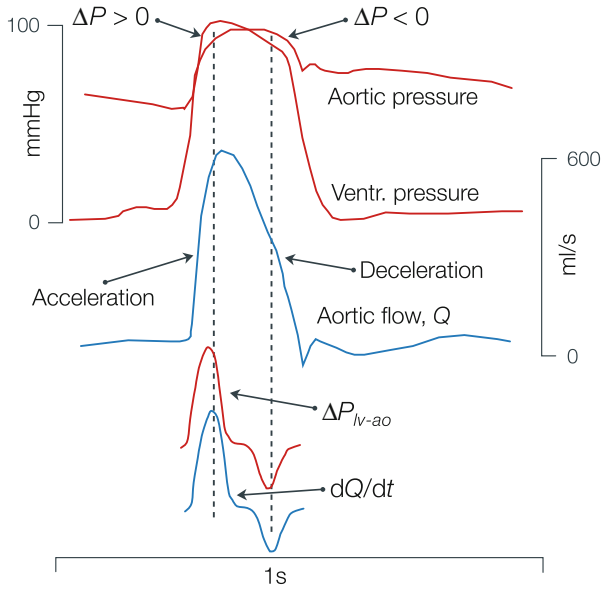
Fig. 7.1 Inertance plays a role in accelerating and decelerating the blood. In early systole, when left ventricular pressure is higher than aortic pressure the blood accelerates, i.e., flow increases. In late systole, aortic pressure is higher than ventricular pressure the blood still flows forward but the velocity decreases (deceleration). Adapted from ref. [1], used by permission
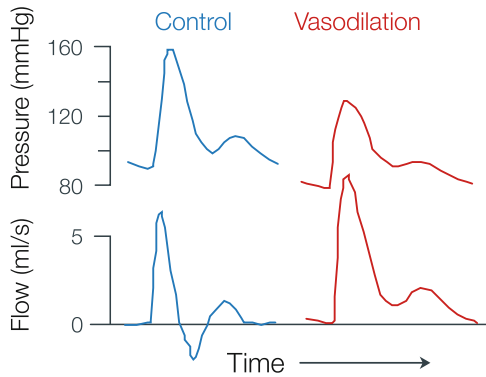

Fig. 7.2 Blood flow may be reversed, or negative, during part of the cardiac cycle. This results from inertia and reflections. With vasodilation the reflections decrease and flow reversal disappears (example from femoral artery). Adapted from ref. [2], used by permission
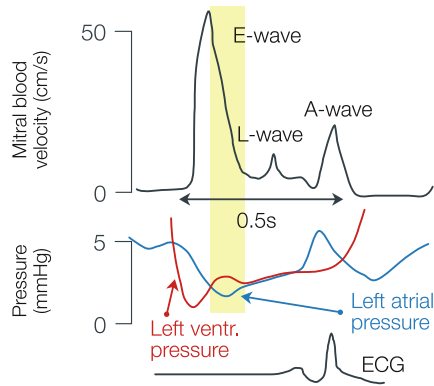
Fig. 7.3 In diastolic filling of the ventricle inertia plays a role. Flow is still forward, but decelerates, while the pressure difference between atrium and ventricle reverses. Adapted from ref. [3], used by permission

References

1. Noble MIM. The contribution of blood momentum to left ventricular ejection in the dog. *Circ Res* 1968;23:663–670.
2. O'Rourke MF, Taylor MG. Vascular impedance of the femoral bed. *Circ Res* 1966;18:126–139.
3. Solomon SB, Nikolic SD, Glantz SA, Yellin EL. Left ventricular diastolic function of remodeled myocardium in dogs with pacing induced heart failure. *Am J Physiol* 1998;274:H945–H954.

Chapter 8
Oscillatory Flow Theory

$\alpha = 2$, viscosity dominates $\alpha = 7$ $\alpha = 14$, inertia dominates

r_i

Axial velocity

Oscillatory flow velocity profiles in a stiff tube during laminar sinusoidal flow. Flow is driven by a sinusoidal, oscillatory, pressure gradient. The velocity profile varies over the sinusoidal cycle and only the profile at the moment of maximal forward flow is depicted here. The velocity profile depends on the Womersley parameter, $\alpha^2 = r_i^2\, \omega\rho/\eta$, where r_i is the internal radius, ω the circular frequency ($2\pi f$, f frequency), ρ the blood density, and η the blood viscosity. Womersley's parameter α expresses the relative importance of inertial effects over viscous (frictional) effects. For low values of the Womersley parameter ($\alpha < 3$, low frequency, small radius), viscous effects dominate and the profile becomes parabolic, as in Poiseuille flow (left figure). For a medium range of α values the velocity profile becomes flatter and the maximum velocity does not occur at the tube's center (middle figure). For large values of α, $\alpha > 10$, i.e., high frequency and/or large vessels the profile becomes flat, because inertial effects dominate. The theory is based on sinusoidal oscillations of pressure and flow. This implies that application of the theory to hemodynamics requires Fourier analysis (Appendix 1). From work on comprehensive models we conclude that the contribution of oscillatory flow theory only gives a small correction over and above the use of a resistance with inertance in series (Appendix 3). However, in the calculation of wall shear and in the calculations and measurements of local flow profiles, the theory is of great importance.

Description

The pressure-flow relation for steady flow, where only frictional losses are considered (resistance, law of Poiseuille), and the relation between oscillatory or pulsatile pressure and flow when only blood mass (inertance) is taken into consideration, are simplifications of reality.

The relation between oscillatory, sinusoidal, pressure drop and flow through a blood vessel can be derived from the Navier-Stokes equations. The assumptions are to a large extent similar to the derivation of Poiseuille's law: uniform and straight blood vessel, rigid wall, Newtonian viscosity, etc. The result is that flow is still laminar but pulsatile, i.e., not constant in time, and the flow profile is no longer parabolic. The theory is based on sinusoidal pressure-flow relations, and therefore called oscillatory flow theory.

The flow profile depends on the, circular, frequency of oscillation, ω, with $\omega = 2\pi f$, with f the frequency; the tube radius, r_i, the viscosity, η, and density, ρ, of the blood. These variables were taken together in a single dimensionless (no units) parameter called Womersley's alpha parameter [1]:

$$\alpha^2 = r_i^2 \omega \cdot \rho / \eta$$

If the local pressure gradient, $\Delta P/l$, is a sinusoidal wave with amplitude A^* and circular frequency, ω, then the corresponding velocity profile is given by the formula [1]:

$$v(r,t) = \mathrm{Real}\left[(A^*/i\omega\rho) \cdot \{1 - J_0(\alpha \cdot y \cdot i^{3/2})/J_0(\alpha \cdot i^{3/2})\} \cdot e^{i\omega t} \right]$$

where y is the relative radial position, $y = r/r_i$, and $i = \sqrt{-1}$. Flow is given as:

$$Q(t) = \mathrm{Real}\left[(\pi r_i^2 A^*/i\omega\rho) \cdot \{1 - 2J_1(\alpha \cdot i^{3/2})/\alpha \cdot i^{3/2} J_0(\alpha \cdot i^{3/2})\} \cdot e^{i\omega t} \right]$$

with $i = \sqrt{-1}$, and J_0 and J_1 are Bessel functions of order 0 and 1, respectively. The Real means that only the real part of the mathematically complex formula is taken.

Since the heart does not generate a single sine wave but a sum of sine waves (see Appendix 1) the flow profile *in vivo* is found by addition of the velocity profiles of the various harmonics, and is very complex. The relation between pressure drop and flow as given above is the so-called longitudinal impedance of a vessel segment (see Appendix 3). Experiments have shown that the theory is accurate.

On the basis of the oscillatory flow theory Womersley predicted that for $\alpha > 0.5$, the area ratio of two equal daughters and a mother vessel should be between 1.33 and 1.15 to minimize local wave reflection (Chap. 21). For large α, i.e., $\alpha > 10$, where inertia dominates the viscous effects, this area ratio is 1.15, while Murray's law predicts 1.25 for the area ratio (Chap. 2).

Physiological and Clinical Relevance

Womersley's oscillatory flow theory [1] reduces to Poiseuille's law for very low α. This means that in the periphery with small blood vessels (small r) and little oscillation, there is no need for the oscillatory flow theory and we can describe the pressure-flow relation with Poiseuille's law. For the very large conduit arteries,

where $\alpha > 10$, friction does not play a significant role and the pressure-flow relation can be described with inertance alone. For α values in between, the combination of the resistance plus the inductance approximates the oscillatory pressure-flow relations (see Appendix 3).

Models of the entire arterial system have indicated that, even in intermediate size arteries, the oscillatory effects on the velocity profiles are not large. The main factors contributing to pressure and flow wave shapes in the arterial tree are due to branching, non-uniformity and bending of the blood vessels etc. Thus for global hemodynamics, i.e., wave travel, input impedance, Windkessel models etc., the longitudinal impedance of a segment of artery (Appendix 3) can be described, in a sufficiently accurate way, by an inertance only in the aorta and major arteries, an inertance in series with a resistance in medium sized conduit vessels, and a resistance only in peripheral arteries.

The oscillatory flow theory is, however, of importance when local phenomena are studied. For instance, detailed flow profiles and calculation of shear stress at the vascular wall require the use of the oscillatory flow theory.

There is another dimensionless parameter of importance in unsteady, oscillatory flow problems: the Strouhal number. The Strouhal number can be written as $St = \omega D/v$, where D is diameter, ω circular frequency, $2\pi f$, with f frequency in cycles per second, and v velocity. It represents a measure of the ratio of inertial forces due to oscillatory flow and the inertial forces due to convective acceleration. It can be shown that the Strouhal number relates in combination with the Reynolds number (Re, Chap. 4) to the square of Womersley's parameter α:

$$St \cdot Re = (\omega D / v) \cdot (\rho v D / \eta) = D^2 \omega \rho / \eta = 4\alpha^2$$

The Strouhal number has been used in experimental studies of arterial flows in the past, such as vortex shedding phenomena distal of a cardiac (mitral) valve. It is widely accepted, however, that the most relevant parameter expressing the relative significance of inertial effects due to oscillatory flow is the Womersley parameter α.

Before Ultrasound Doppler velocity and other flow measurement techniques became available, attempts were made to derive blood flow wave shapes and Cardiac Output from the measurement of two pressures in the aorta a few centimeters apart. The pressure drop and aortic size allowed for the calculation of flow using the oscillatory flow theory.

Reference

1. Womersley JR. The mathematical analysis of the arterial circulation in a state of oscillatory motion. 1957, Wright Air Dev. Center, Tech Report WADC-TR-56-614.

Chapter 9
Law of Laplace

Wall stress $\sigma = P_t r_i / h$ Wall stress $\sigma = P_t r_i / (2h)$

The law of Laplace relates transmural pressure, P_t, with wall stress, σ. In a (*cylindrical*) blood vessel and in a (*spherical*) heart model there is a simple relation between pressure and circumferential wall stress. The law gives the average stress over the wall, thus how the stress varies over the wall cannot be derived. The law holds only for simple geometries. Often P_t can be approximated by pressure in the organ.

Description

The original law of Laplace pertains to soap bubbles, with radius r, and gives the relation between transmural pressure, P_t, and wall tension, T_s, in a thin-walled sphere as $T_s = P_t \cdot r$. The law can be used, for example, to calculate tension in alveoli. This tension is directly related to surface tension and has the dimension N/m. The form of the law of Laplace most often used in hemodynamics gives the relation between transmural pressure and the stress in the wall in organs with a wall thickness h. We here use the Cauchy stress formulation, which is defined as the ratio of the normal (perpendicular) force acting on a surface divided by the area of the surface at its deformed configuration. Stress has the dimension N/m^2 (see Figure in the box).

For a circular cylinder, as model of a blood vessel, the transmural pressure acts to push the two halves apart with a force equal to pressure times the area (left Figure in the box). Thus force is $2P_t \cdot l \cdot r_i$. The two halves are kept together by wall stress, σ, acting in the wall only. This force is thus $2 \cdot \sigma \cdot h \cdot l$. These forces are in equilibrium and thus: $2\,P_t \cdot l \cdot r_i = 2\sigma \cdot h \cdot l$, which gives $\sigma = P_t \cdot r_i / h$. This form of the law of Laplace is more correctly called Lamé's equation. For a sphere, a similar derivation holds and the result is $\sigma = P_t \cdot r/2h$.

We see that transmural pressure and wall stress are related by the ratio of radius over wall thickness, r_i/h.

Applicability of the Law of Laplace

The law of Laplace applies to cylindrical or spherical geometries, irrespective of whether the material is linear or nonlinear or if the wall is thin or thick. The only limitation of Laplace's law is that it yields the average wall stress and thus it cannot give any information on the stress distribution across the wall. For cylindrical geometries, and assuming linearly elastic (Hookean) material the distribution of circumferential stress or hoop stress across the wall thickness can be approximated by:

$$\sigma(r) = P_t r_i^2 \cdot (1 + r_o^2 / r^2) / [r_o^2 - r_i^2]$$

where r_i and r_o is the internal and external radius, respectively, and r is the position within the wall for which local stress is calculated.

There is a large body of literature, especially for the thick-walled heart, where (local) wall stress or muscle fiber stress is related with pressure for different complex geometries (for information see ref. [1]).

Hefner [2] extended the Law of Laplace for the left ventricle by showing that the equatorial wall force (F) is $P \cdot A_e$, where A_e = equatorial cavity cross-sectional area and P luminal pressure. The wall stress, σ, is given by F/A_w with A_w the equatorial cross-sectional area of the muscle ring. Thus $\sigma = P \cdot A_e/A_w$.

Mirsky and Rankin [3] suggested an often used estimation of mid-wall stress. For an ellipsoidal heart shape the mid-wall stress is:

$$\sigma / P_t = \sigma / P_{lv} \cdot (D / 2h) \cdot (1 - h / D - D^2 / 2l^2)$$

with D and l the mid-wall diameter and mid-wall long axis of the ventricle (see Figure in box). Transmural pressure, P_t, is often replaced by luminal pressure, P_{lv}, assuming external pressure (e.g. thorax pressure) to be negligible.

Arts et al. [4] derived a simple and practical relation between fiber stress, σ_f, and ventricular pressure, P_{lv}, which reads:

$$P_{lv} / \sigma_f = 1 / 3 \ln(1 + V_\omega / V_{lv})$$

where V_{lv} and V_w are ventricular lumen and ventricular wall volume, respectively and the ln signifies the natural logarithm. This equation can be used in all moments of the cardiac cycle and thus allows the calculation of fiber stress in both diastole and systole, including the ejection period.

Many other relations between wall force or stress and ventricular pressure have been reported, but since measurement of wall force is still not possible [1], it is difficult to decide which relation is best.

The law of Laplace pertains to geometrically simple bodies but may be applied to nonlinear material. Assuming a simple shape such as a sphere, or circular cylinder, the law may be applied to the ventricular wall in diastole and systole, as well as to the vessel wall. The Law of Laplace can also be used in the contracting heart, where the force is generated in the wall and the rise in pressure is the result of the contracting muscle.

Relation to the Young Modulus

Assuming that the arterial wall is relatively thin ($h \ll r_i$) and incompressible, one can use Laplace's Law to derive the following expression for the incremental elastic modulus (Chaps. 10 and 11):

$$E_{inc} = (r_i^2 / h)\ \Delta P_t / \Delta r_i$$

where the Δr_i and the ΔP_t, are the change in internal radius and transmural pressure.

If the wall cannot be considered thin, as is often the case in muscular arteries, the Young modulus is best derived from the measurement of pressure and radius using the following expression [5].

$$E_{inc} = 3r_i^2 \cdot r_o \cdot (\Delta P_t / 2\Delta r_o) / [r_o^2 - r_i^2]$$

Physiological and Clinical Relevance

The Law of Laplace, although basic and pertaining to simple geometries only, helps in understanding cardiac and vascular function. The law is therefore of great conceptual importance. For instance, the ratio r_i/h is a main determinant of the wall stress. The radius of curvature of the left ventricle is smaller at the apex than at the base, and so is the wall thickness h. In other words, the ratio r_i/h at the apex and base is the same resulting in similar wall stress at these locations in the wall. In hypertension the cardiac muscle cells increase in thickness by building more contractile proteins in parallel, leading to concentric hypertrophy. The thicker wall, but
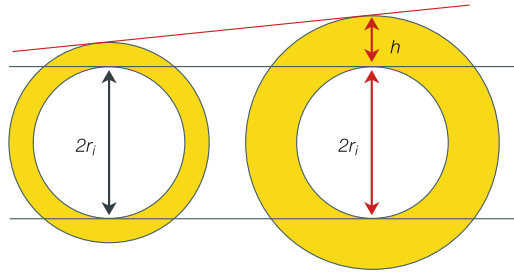
Fig. 9.1 In concentric hypertrophy, when compensated, ventricular pressure, P, and wall thickness, h, both are increased in approximately the same proportion, thus Pr_i/h is the same, and wall stress remains similar (see Chap. 9)

similar lumen, i.e., decreased r_i/h, causes the systolic wall stress to return to presumably normal levels despite the higher pressure in systole (Fig. 9.1). In hypertension the large arteries hypertrophy and the thicker wall decreases wall stress.

When the heart dilates in disease, often without much change in wall thickness, the increase in radii leads to an increase in wall stress, and therefore less shortening of the muscle and increased energy needs of the muscle. The higher muscle stress leads to higher oxygen demand (Chap.16), often too large for oxygen supply, and adding to the deleterious effect of the dilatation.

How stresses in the cells are sensed is still largely unknown.

References

1. Huisman RM, Sipkema P, Westerhof N, Elzinga G, Comparison of models used to calculate left ventricular wall force. *Med Biol Eng Comput* 1980;18:133–144.
2. Hefner LL, Sheffield LT, Cobbs GC, Klip W. Relation between mural force and pressure in the left ventricle of the dog. *Circ Res* 1962;11:654–663.
3. Mirsky I, Rankin JS. The effects of geometry, elasticity, and external pressures on the diastolic pressure-volume and stiffness-stress relations. How important is the pericardium? *Circ Res* 1979;44:601–611. Review.
4. Arts T, Bovendeerd HHM, Prinzen FW, Reneman RS. Relation between left ventricular cavity pressure and volume and systolic fiber stress and strain in the wall. *Biophys J* 1991;59:93–102.
5. Love AEH. *A treatise on mathematical elasticity*. 1952, London & New York, Cambridge University Press, third edn.

Chapter 10
Elasticity

The Young's modulus of elasticity is a material constant. A strip of material subjected to a force will lengthen. Force per cross-sectional area, $A = \frac{1}{4}\pi d_o^2$, is stress, $\sigma = F/A$, and the relative length change, $\varepsilon = \Delta l/l_o$, is the strain. Stress-strain relations of elastic materials are given at the right. If the stress-strain relationship is linear, the material obeys Hooke's law and the slope of the relation is called the Young's modulus of elasticity. The stress-strain relation of biological tissues is curved, and the local slope gives the incremental elastic modulus, E_{inc}, which is strain (or stress) dependent. The Young's modulus of elasticity is a stiffness modulus.

Description

When a force, F, is applied to a specimen with cross-sectional area $A = \frac{1}{4}\pi d^2$, and length l_0, the length will be increased by Δl (left Figure in box). With a specimen of larger cross-sectional area the same force will result in a smaller length change. Also, when the starting length of the specimen, l_0, is longer the same force will result in a larger length change. To be able to give a unique characterization of the material, independent of the sample size, we normalize force by the area and the LaGrangian stress is obtained, $\sigma = F/A$. Similarly we normalize the length change to the starting length, l_o, and obtain strain, $\varepsilon = \Delta l/l_o$.

The relation between stress and strain is given in the right part of the Figure in the box. When the relation is straight we say that the law of Hooke applies, and the

material is called Hookean or linearly elastic. The slope of the graph is called the Young modulus of elasticity $E = \sigma/\varepsilon$. The Young modulus is a material property and is a measure of the stiffness, not elasticity, of the material. The units of the Young modulus are force per area, thus the same units as for stress and pressure, i.e., $N/m^2 = Pa$, or mmHg.

When lengthened the specimen also gets thinner. The strain in the transverse direction, ε_t, is $\varepsilon_t = \Delta d/d_o = (d - d_0)/d_0$. The ratio of the transverse strain and the longitudinal strain, $\varepsilon_t/\varepsilon$, is called the Poisson ratio. When with stretch the specimen's volume remains constant, as appears to be the case for most biological tissues, the Poisson ratio is 0.5.

Biological materials almost always exhibit a curved stress-strain relationship with convexity towards the strain axis (Fig. 10.1). The curved relation implies that the material cannot be characterized by a single Young modulus. The solution is to introduce an incremental modulus, E_{inc}, defined as the local slope of the stress-strain relation. For biological tissue the incremental elastic modulus increases with strain, i.e., the biological material becomes stiffer with increasing stress and strain.

There are no clear conventions about the choice of the horizontal and vertical axes for stress and strain. This often leads to confusion when the slope of the relation
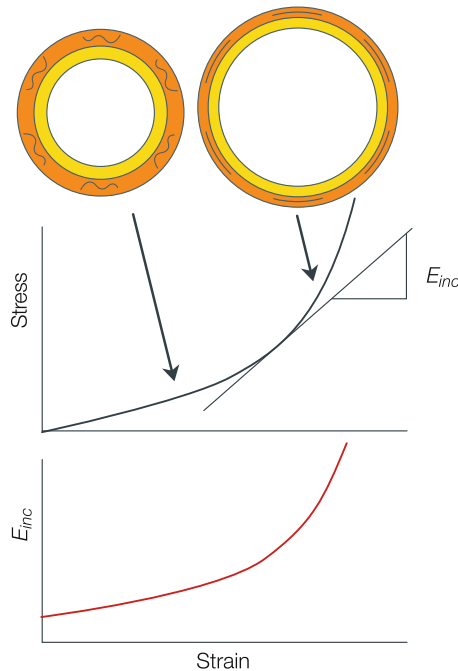
Fig. 10.1 Biological tissues show a stress-strain relation that is convex to the strain axis. The local slope gives the incremental Young modulus, E_{inc}, which increases with strain (or stress) mainly as a result of unfolding of collagen molecules

is determined. It should be remembered that biological relations are convex towards the strain axis, i.e., the strain is limited. This limitation protects against overstretch and damage.

Viscoelasticity

Viscoelasticity (see Figs. 10.2 and 10.3) means that a material is not only elastic but also has viscous ('fluid-like') properties [1]. Viscoelasticity can be made visible and quantified in different ways. If one wants to stretch (strain) a viscoelastic material rapidly to a new length, initially a larger force is needed for the same amount of stretch as for a purely elastic material. With time the viscous contribution to the stress decreases. This is called stress relaxation. Inversely, with a sudden increase in stress the strain (stretch) is delayed. The delayed stretch is called creep.
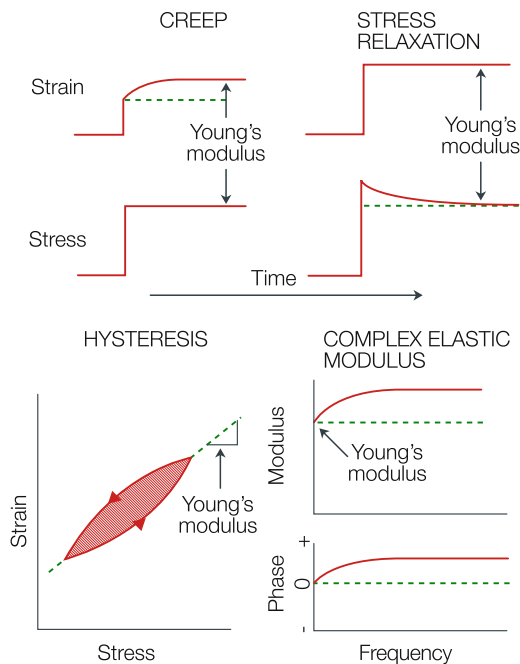
Fig. 10.2 The viscoelastic properties of biological material appear in four forms depending on the intervention and measurements. Step increases in stress and strain lead to creep and stress-relaxation, respectively. Repeated increases and decreases in stress and strain result in a hysteresis loop, the area within the loop equals energy loss (*red area*). Application of sinusoidal forces and measuring strains permits the determination of the complex Young modulus in the frequency domain. The *dashed*, *green*, *lines* pertain to purely elastic material. Viscoelasticity also appears in a similar fashion in pressure-diameter and pressure-volume relations
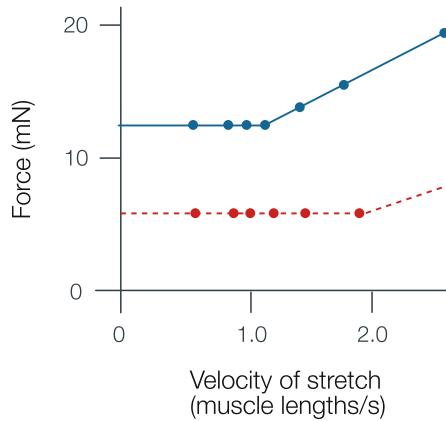
Fig. 10.3 Viscoelasticity of heart muscle requires extra pressure during filling. At velocities of stretch above one muscle length per second an additional force appears in excess of the force due to the elastic force/length curve; this effect is more obvious at high length. Adapted from ref. [2]

When, stress and strain are pulsatile, as *in vivo*, strain always lags stress. Plotting strain versus stress yields a hysteresis loop. The area of the loop is the energy lost due to the viscosity of the material. When sinusoidal force or pressure is applied, the amplitude ratio and phase difference between stress and strain describe the complex elastic modulus. The complex elastic modulus depends on the frequency of oscillation. When the stress or strain is applied very slowly the viscous aspects do not become apparent and the material behaves as purely elastic.

Viscoelastic Models

Several models have been proposed to describe the viscoelastic properties of biological tissue (Fig. 10.4). Some of these models fall short in the sense that they do not describe all aspects of viscoelasticity. One of the examples is the Maxwell model where a spring and dash-pot or damper, are placed in series. With a constant stress this model predicts a continuous, never ending, increase in length, which is clearly not true in biological tissue. Adding another spring in parallel to the Maxwell model yields Kelvin's viscoelastic model, which is the simplest, yet realistic viscoelastic model of the vascular wall.

Residual Stresses and Stress Distribution at Physiological Loads

The vascular tissue is not at a zero stress state when all loads, i.e., pressure and longitudinal tension, are removed. The same holds true for cardiac tissue. Stresses that still exist in the tissue when no external loads are applied are called residual stresses.
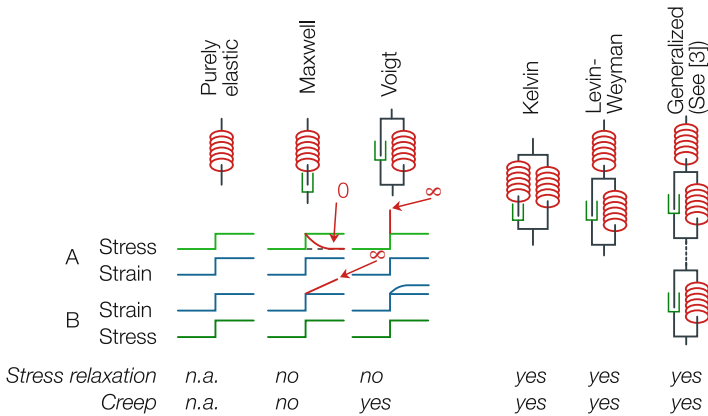
Fig. 10.4 Models of viscoelastic material in the form of springs and dashpots (dampers). A step-change in strain (blue, experiment A) results in a stress response (*green*). A step change in stress (*green*, experiment B) gives a response in strain (*blue*). A purely elastic material can be described by a spring, stress and strain follow each other. The simplest two-element models (*left part*) represent biological material poorly, they either show (*red lines*) stress relaxation to zero and strain that is unlimited for a step in stress (Maxwell) or show an infinite stress response to a step change in strain (Voigt). The three-element models (Kelvin and Levin-Weyman) are equivalent and qualitatively sufficient. To quantitatively describe viscoelasticity in greater detail more elements are usually required (Appendix 3)

The classical experiment to illustrate the existence of residual stress in arteries after removal of all loads is to excise a ring of artery and cut it longitudinally (Fig. 10.5). The ring springs open and takes the shape of a circular arc, as shown in Fig. 10.5 on the right. The change in configuration means that stresses existed within the wall before the cut. Further cuts do not seem to release more stresses, therefore we assume that the opened-up configuration after the first cut is a stress free configuration. This stress free state or zero stress state, ZSS, can be characterized by the 'opening angle' φ, which is the angle formed by the two ends and the midpoint of the inner arc length.

Knowledge of the ZSS is of primary importance when one wants to calculate the detailed stress field within the arterial wall. This is because strains can be calculated only in reference to the ZSS. Knowledge of the ZSS is not required when one calculates the average circumferential stress in the wall using Laplace's law. Residual stresses play an important role in maintaining a fairly uniform stress distribution across the arterial wall at physiological loads. This can be visualized with the help of the schematic drawings shown in Fig. 10.5. The left column shows an arterial cross-section where the ZSS is a circular ring (top). This means that at $P=0$ mmHg there are no residual stresses (middle). At a physiological transmural pressure level ($P=100$ mmHg) however, significant stresses develop with a pronounced stress peak at the inner most layer of the wall (bottom). The higher stress concentration in the inner wall is a direct consequence of the fact that these layers are stretched much more during the pressure-induced inflation.
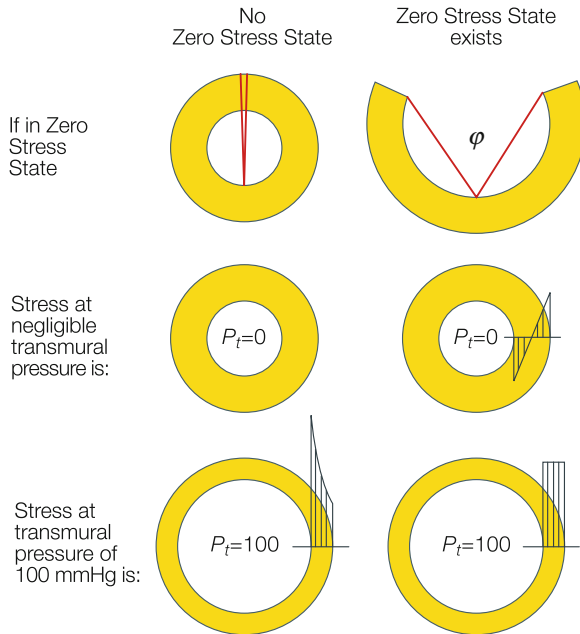
Fig. 10.5 Influence of zero stress state on wall stress distribution at operating pressures. *Left column:* stress distribution if no pre-stresses exist. *Right column:* arterial ring after being cut open (*top*). The ring is now in its stress-free or zero stress state (ZSS). This is characterized by the opening angle φ. Pre-stresses in the wall at zero load ($P_t=0$) are shown in the middle figure. Stress distribution at operating pressure are shown in the *bottom panel*

The right column shows an artery where the ZSS is characterized by an opened-up configuration (top). The ZSS means that at zero load, and in a closed ring configuration (middle row of Fig. 10.5) residual stresses exist. Residual stresses are compressive in the inner wall and tensile in the outer wall. During inflation, the inner layers will be stretched more than the outer layers of the wall. However, because at the beginning of the inflation, $P=0$ mmHg, the inner wall was under compression whereas the outer wall already was under some extension, at the physiological pressure level the degree of extension is the same in both inner and outer wall layers. The stress distribution is therefore uniform across the wall (bottom).

Physiological and Clinical Relevance

Elasticity plays an important role in the circulation. All blood vessels are elastic and their elastic moduli do not differ greatly. A typical value of the incremental elastic modulus of arteries in the normal human at a pressure of 100 mmHg,

is about $5 \cdot 10^6$ dyn/cm^2 or 500 kPa. With 1 kPa $= 7.5$ mmHg the elastic modulus is 3,750 mmHg. For diastolic heart tissue the incremental elastic modulus at a filling pressure of 5 mmHg is about $4 \cdot 10^5$ dyn/cm^2 or 40 kPa. In systole these values are about 20 or more times larger. Thus cardiac muscle is much stiffer in systole than in diastole.

The Elasticity of Cardiovascular Tissue

Vascular tissue is mainly composed of elastin, vascular smooth muscle and collagen. Elastin fibers are highly extensible and even at large deformations they can be characterized by an almost constant Young modulus. Collagen fibers, on the other hand, are very stiff: $E_{collagen} \approx 1,000\, E_{elastin}$. At lower strains, collagen fibers are wavy are bearing no load, and the elastin and smooth muscle mainly determine the wall elasticity. At larger strains collagen waviness decreases and collagen begins to bear more load leading to an increasingly stiff wall, i.e., a larger E_{inc} (see Fig. 10.1). The same holds for cardiac tissue.

The curved relation between stress and strain can be described in several ways. One simple relation, with only two parameters, is the equation originally suggested by Fung [3].

$$\sigma = a \cdot [e^{b \cdot (\varepsilon - 1)} - 1]$$

This model gives fairly accurate fits of the stress-strain relations.

The nonlinear relation between stress and strain has led to much confusion. An example is in hypertension. When elastic properties are derived at the working point, i.e., the operating mean pressure of the individual patient, the vessels of hypertensive patients are found to have a higher incremental elastic modulus as compared with normal human subjects. However, this apparently increased stiffness in hypertensive patients is mainly the result of their higher blood pressure (see Chap. 27). Thus either a stress-strain graph should be made or the incremental elastic modulus should be compared at similar strains or stresses to be able to conclude if mechanical properties have changed or not.

Elasticity of the conduit arteries stands at the basis of their Windkessel function (see Chap. 24).

Determination of the Young Modulus

In practice the Young modulus is often not measured directly, because isolated tissue samples without perfusion are not viable. Therefore, for hollow organs like heart and vessels, pressure-volume or, for vessels, pressure-diameter relations are

determined. However, through the law of Laplace, and accounting for geometry, the calculation of the Young modulus is feasible (Chaps. 9 and 11).

References

1. Westerhof N, Noordergraaf A. Arterial elasticity: A generalized model. Effect on input impedance and wave travel in the systemic arterial tree. *J Biomech* 1970;3:357–379.
2. Noble MIM. The diastolic viscous properties of cat papillary muscle. *Circ Res* 1977;40:287–292.
3. Fung YC. Elasticity of soft tissues in simple elongation. *Am J Physiol* 1967;28,1532–1544.

Chapter 11
Compliance

Compliance $C = \Delta V/\Delta P$

Elastance $E = \Delta P/\Delta V$
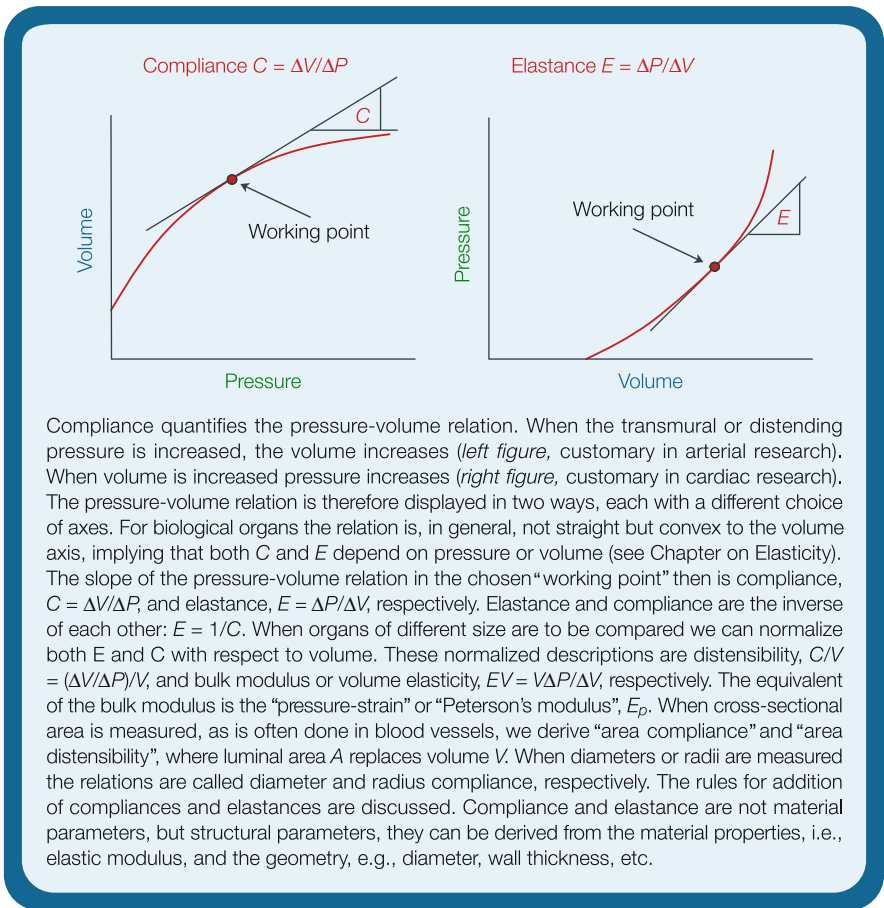
Compliance quantifies the pressure-volume relation. When the transmural or distending pressure is increased, the volume increases (*left figure,* customary in arterial research). When volume is increased pressure increases (*right figure,* customary in cardiac research). The pressure-volume relation is therefore displayed in two ways, each with a different choice of axes. For biological organs the relation is, in general, not straight but convex to the volume axis, implying that both C and E depend on pressure or volume (see Chapter on Elasticity). The slope of the pressure-volume relation in the chosen "working point" then is compliance, $C = \Delta V/\Delta P$, and elastance, $E = \Delta P/\Delta V$, respectively. Elastance and compliance are the inverse of each other: $E = 1/C$. When organs of different size are to be compared we can normalize both E and C with respect to volume. These normalized descriptions are distensibility, $C/V = (\Delta V/\Delta P)/V$, and bulk modulus or volume elasticity, $EV = V\Delta P/\Delta V$, respectively. The equivalent of the bulk modulus is the "pressure-strain" or "Peterson's modulus", E_p. When cross-sectional area is measured, as is often done in blood vessels, we derive "area compliance" and "area distensibility", where luminal area A replaces volume V. When diameters or radii are measured the relations are called diameter and radius compliance, respectively. The rules for addition of compliances and elastances are discussed. Compliance and elastance are not material parameters, but structural parameters, they can be derived from the material properties, i.e., elastic modulus, and the geometry, e.g., diameter, wall thickness, etc.

Description

The advantage of the pressure-volume (or -diameter and -radius) relation (Figures in the box) is that it can be measured *in vivo*. It is important to note that pressure-volume relations do not characterize the material but includes the structure of the organ as a whole.

If the pressure-volume relations were straight and going through the origin, the slope, compliance or elastance would give the full characterization of the organ by a single quantity. However, the pressure-volume relations are never straight. For a small change around a chosen working point, the curve is approximately straight, and the tangent of the pressure-volume curve is used. We can determine compliance in the 'working point' as $C = \Delta V / \Delta P$. The elastance, the inverse of compliance is $E = \Delta P / \Delta V$. Of course, these local slopes depend on the (ventricular) pressure or volume chosen. Thus, when comparing compliance or elastance data one should report the chosen working point, i.e., the pressure at which compliance or elastance was determined. For instance, when the elastance of a heart in diastole is studied and appears increased, the increase can result from either a higher filling pressure but otherwise normal heart, or a normal filling pressure but a hypertrophied heart with thicker wall (Fig. 11.1).

The curvature of the pressure-volume relation is mainly the result of the fact that the Young modulus increases with stretch, therefore C decreases and E increases, with volume.

Measurement of Elastance and Compliance

Elastance is customarily used for the heart while compliance is mostly used to describe blood vessels.
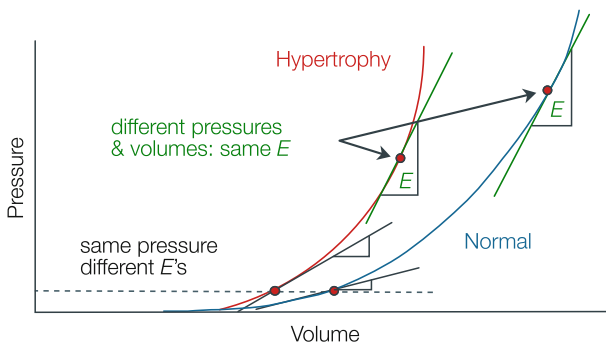
Fig. 11.1 Diastolic pressure-volume relations of a normal and hypertrophied heart are shown. If only the similar elastance values are reported without further information on pressure or volume, it cannot be decided if the heart is normal and overfilled, or hypertrophied, since both have the same E. At similar pressure the hypertrophied heart is stiffer (larger E). The full graph is required to give the complete information

Fig. 11.2 For geometrically simple shapes, like blood vessels, measurement of changes in internal radius or diameter is sufficient to obtain compliance. In complex geometries as that of the heart this cannot be done
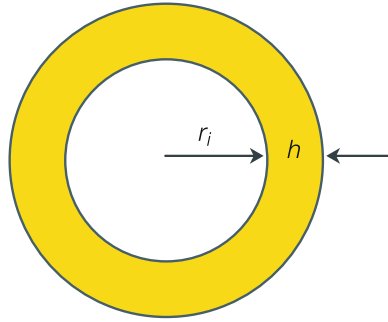
Ventricular elastance is best determined by the measurement of pressure and volume. A number of noninvasive techniques are now available to determine volumes, such as Computed Tomography, Magnetic Resonance Imaging, Ultrasound Echo, while the Pressure-Volume catheter allows for determination of elastance in experimental situations. Cardiac elastance determination requires volume and pressure measurements in systole and diastole, because of the varying properties of the cardiac muscle. Diameter as estimate of volume is inaccurate.

Arterial (*volume*) compliance, $C = \Delta V/\Delta P$, is usually determined from pressure and diameter measurements (Fig. 11.2). Diameter changes can be measured noninvasively by wall-tracking and for large vessels like the aorta by MRI. From the local diameter the cross-sectional area is calculated assuming a circular cross-section. When area and pressure are related the term *area* compliance, $C_A = \Delta A/\Delta P$, is used to distinguish it from (volume) compliance. Volume compliance is then lC_A, with l vessel length. For instance, the systolic-diastolic differences in area, ΔA, and pressure, ΔP, i.e., Pulse Pressure, when measured *in vivo*, can be used to obtain the area compliance. When the diameter change is related to the pressure change one obtains *diameter* compliance, $\Delta D/\Delta P$. The area compliance, C_A, and diameter compliance, C_D, are related by: $C_A = \pi \cdot D \cdot C_D/2$.

Distensibility and Bulk Modulus

Compliance depends on the size of the organ under study. To compare properties of blood vessels, or hearts from different animal species we can normalize compliance and elastance with respect to the volume of the organ. We use $C/V = (\Delta V/V)/\Delta P$, called distensibility, and the inverse, $E \cdot V = \Delta P/(\Delta V/V)$, called bulk modulus or volume elasticity. Area and diameter distensibilities are also used, area distensibility is $(\Delta A/A)/\Delta P$ and diameter distensibility is $2 \cdot (\Delta D/D)/\Delta P$.

The Pressure-Strain Elastic Modulus

Peterson et al. [1] introduced the pressure-strain elastic modulus in blood vessel research. This measure of blood vessel elasticity requires the measurement of diameter and pressure only, and can be used to compare vessels of different size. The pressure-strain elastic modulus, or Peterson modulus [1], is defined as $E_p = \Delta P/(\Delta r_o/r_o)$, where usually external radius, r_o, instead of the internal radius r_i is used. The E_p compares to the bulk modulus.

Summary of structural[a] parameters of elasticity for blood vessels

	Volume	Area[b]	Diameter	Radius
Compliance, C	$\Delta V/\Delta P$	$\Delta A/\Delta P$	$\frac{1}{2}\cdot(\Delta D/\Delta P)\pi D$	$2\cdot(\Delta r/\Delta P)\pi r$
Elastance, E	$\Delta P/\Delta V$	$\Delta P/\Delta A$	$2\cdot(\Delta P/\Delta D)/\pi D$	$(\Delta P/\Delta r)/2\pi r$
Distensibility, K	$1/V\cdot(\Delta V/\Delta P)$	$(1/A)\cdot\Delta A/\Delta P$	$2\cdot(\Delta D/\Delta P)/D$	$2\cdot(\Delta r/\Delta P)/r$
Bulk Modulus, BM[c]	$V\cdot\Delta P/\Delta V$	$A\cdot\Delta P/\Delta A$	$\frac{1}{2}\cdot(\Delta P/\Delta D)D$	$\frac{1}{2}\cdot(\Delta P/\Delta r)$[rd]

P, V, A, D, r are pressure, volume, area, diameter and radius, respectively.
[a]Structural: parameters depend on organ geometry and material properties.
[b]It is generally assumed that vessel length does not change with pressure.
[c]Bulk modulus or Volume elasticity.
[d]The Pressure-Strain modulus or Peterson's modulus, $E_p = r_0\cdot\Delta P/\Delta r_0 \approx 2/K \approx 2\cdot BM$; where outer radius is used. In all other relations internal diameter or radius is used.

The Stiffness Index

Compliance, distensibility and Peterson's modulus depend strongly on pressure, because diameter-pressure relationships are nonlinear. To overcome this pressure-dependence, Hayashi et al. [2] introduced a logarithmic stiffness index (or parameter) β, defined by the following relation (β-stiffness)

$$\ln\left(P/P_s\right) = \beta\cdot\left(D_o/D_s\right)$$

where P_s is a reference pressure (working point), typically mean pressure or 100 mmHg and D_s is the outer diameter at pressure P_s. Basic research and also several clinical studies have shown that the stiffness parameter does not depend on pressure within the physiological pressure range. However, outside the physiological pressure range and for pressures far from the reference pressure P_s the β-stiffness indexes are not constant anymore.

Describing the Pressure-Area or Pressure-Diameter Relation of Blood Vessels

The pressure-area and pressure-diameter relations of blood vessels have been described in a number of ways. At a working pressure the slope of the relation

From [4]
(in pressure and diameter)

$P = (P_0 + b)e^{a(D - D_0)} - b$

From [2]

$\ln (P/P_0) = \beta (D/D_0 - 1)$

$P = P_0\, e^{\,\beta(D/D_0 - 1)}$

From [3]

$A = A_m[1/2 + 1/\pi \tan^{-1}(P - P_0)/P_1]$
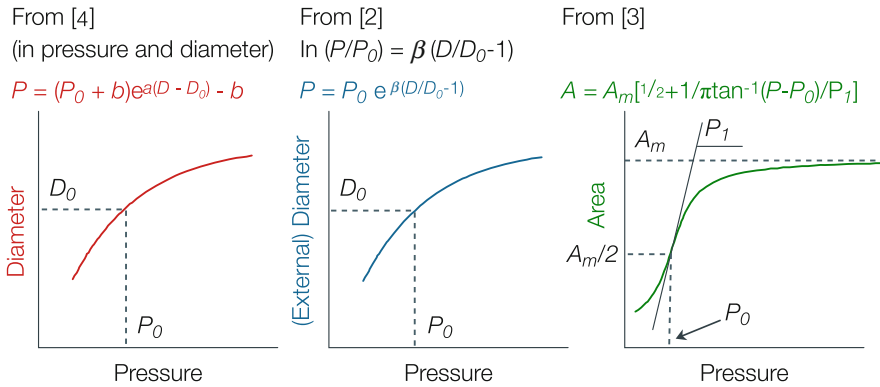
Fig. 11.3 Mathematical models of pressure-diameter and pressure-area relations

gives compliance. However, description of the relation over a range of pressures and volumes gives more insight. Although these descriptions are phenomeno-logical, we mention them here because of their general utility in arterial mechanics (Fig. 11.3).

The relation proposed by Langewouters et al. [3], describes the pressure-area relation over the widest range of pressures, i.e., from 0 to 200 mmHg. The relations of Fung [4] and Hayashi et al. [2] can be applied over the physiological range of pressures. The D_0 and P_0 are reference values for the relations of Fung [4] and Hayashi et al. [2]. In the relation by Langewouters $A_m/2$ and P_0 designate the inflection point and P_1 relates to the slope at the inflection point; A_m is the maximal, asymptotic, vessel area. The relations can also be presented in terms of volumes.

Addition of Compliances and Elastances

Let us consider the compliance of the entire aorta (Fig. 11.4), the individual compliances of three sections of the aorta are shown in this figure. In all sections the pressure is virtually equal (see also Chap. 6). This implies that

$$C_1 + C_2 + C_3 = \Delta V_1 / \Delta P + \Delta V_2 / \Delta P + \Delta V_3 / \Delta P$$
$$= (\Delta V_1 + \Delta V_2 + \Delta V_3) / \Delta P = \Delta V_{total} / \Delta P = C_{total}$$

Thus, simple addition of compliances is allowed and the total compliance is their sum and is therefore larger than the individual compliances.

If an organ with compliance C_1 is enveloped with an organ with compliance C_2, the total volume change equals the individual volume changes (Fig. 11.5). In that case the pressures need to be added. The distending pressure of the inner organ is the luminal pressure minus the pressure in between the organs. The distending pressure of the outer organ is the pressure between the organs minus the pressure of the
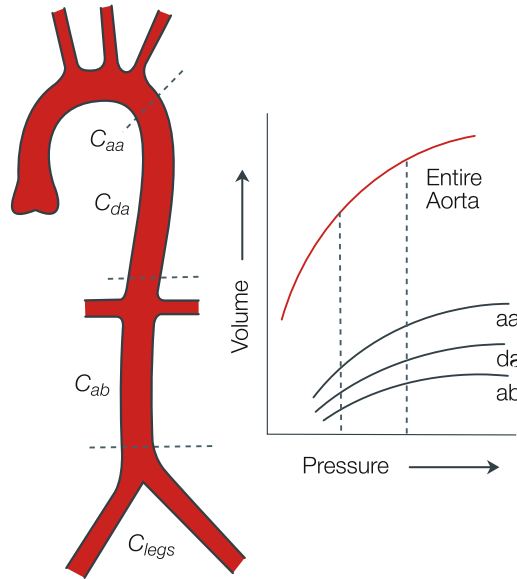
Fig. 11.4 Addition of compliances. Note the choice of axes. The compliances of different sections can be added to obtain total aortic compliance. The whole graphs may also be summed, by adding volumes at similar pressures (*dashed lines*). The aa, da, and ab are ascending, descending, and abdominal aorta

environment. Thus, the distending pressure acting on the two organs combined, i.e., the luminal pressure minus the external pressure is the sum of the distending pressures of each organ. In this situation addition of the elastances is easier. As an example we use the heart with pericardium. When the transmural pressure over the ventricular wall is ΔP_v and over the pericardium is ΔP_{pe}, for the heart inside the pericardium the transmural pressure equals $\Delta P_{total} = \Delta P_v + \Delta P_{pe}$. Therefore

$$E_{total} = \Delta P_{total} \, / \, \Delta V = (\Delta P_v + \Delta P_{pe}) \, / \, \Delta V = \Delta P_v \, / \, \Delta V + \Delta P_{pe} \, / \, \Delta V = E_v + E_{pe}$$

with E_v, and E_{pe} the ventricular elastance and pericardial elastance, respectively. When using compliances this would give: $1/C_{total} = 1/C_v + 1/C_{pe}$. The implicit assumption is that the intrapericardial pressure, ΔP_{pe}, is the same at all locations. There are indications that the situation is more complex.

Relating Compliance to Young Modulus

The measurement of pressure-volume or pressure-radius relationships in arteries allows for derivation of compliance but not of the Young modulus or incremental elastic modulus. As discussed in the chapter on Laplace's law, estimation of Young modulus or incremental elastic modulus requires, in addition to radius and pressure,
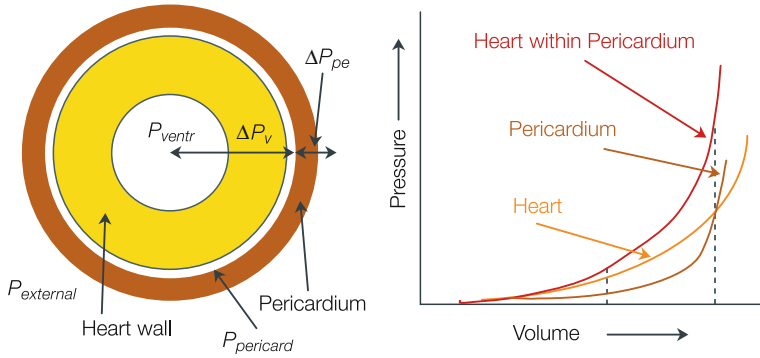
Fig. 11.5 Addition of elastances. Note the choice of axes. Heart and pericardium have their individual elastances and the total elastance of the heart in the pericardial sac can be obtained directly from addition of their individual elastances. Addition of the whole graphs is also allowed, at similar volumes (*dashed lines*). Thus, for structures within each other the elastances can be added directly to obtain overall elastance. Transmural pressure over the ventricular wall is $\Delta P_v = P_{ventr} - P_{pericard}$ and transmural pressure of the pericardium is $\Delta P_{pe} = P_{pericard} - P_{external}$

the measurement of wall thickness. An accurate relation between the Young modulus and compliance is given by Love [5], and used to model transverse impedance of an arterial segment (Appendix 3):

$$C_A = 3\pi \cdot r_i^2 \left(r_i + h\right)^2 / \text{E} \cdot \left(2r_i + h\right)h = 3\pi \cdot r_i^2 \left(a + 1\right)^2 / \text{E} \cdot \left(2a + 1\right), \quad \text{with } a = r_i / h$$

A simpler formula relating the area compliance with the incremental elastic modulus is:

$$C_A \approx (k\pi \cdot r_i^3) / (E_{inc} \cdot h), \text{ both k} = 1.5 \text{ and 2 have been reported}$$

(Area) compliance, being a structural property, should be plotted against distending pressure. The incremental elastic modulus, being a material property, should be plotted against stress or strain. Plotting E_{inc} against pressure, as is often done, leads to misinterpretation of vessel properties.

An example where the structural aspect of compliance can be seen is the comparison of the elastic properties of veins and arteries. The main reason why pressure-volume relations of veins differ from those of arteries is not the difference in wall material but their difference in wall thickness. More accurately stated, the ratio of wall thickness to radius is much smaller in veins than in arteries.

Physiological and Clinical Relevance

Compliance or elastance gives a quantitative measure of the mechanical and structural properties of an organ. Changes with disease and aging can be quantitatively investigated.

In general arterial compliance decreases with age and this is the main reason why arterial Pulse Pressure, systolic minus diastolic pressure, increases with age. The concomitant increase in systolic pressure is an extra load on the heart possibly leading to (concentric) hypertrophy. Concentric hypertrophy increases the elastance of the left ventricle in both diastole and systole. The increase in diastolic elastance (Fig. 11.6) results in decreased filling for the same filling pressure and filling can only return to near normal values with an increase in diastolic filling pressure, which in turn may lead to pulmonary edema (see Chap. 13).

With the now available wall-track technique arterial diameters can be measured noninvasively in superficial arteries and if pressure is simultaneously determined as well (see Chap. 26), diameter compliance can be derived in large groups of patients. However, we should realize that this is the local area compliance of a single, often peripheral, artery, such as the carotid or radial artery, and may not be a good measure of aortic compliance or total arterial compliance (see below and Chap. 24).

Compliance and elastance depend on volume and pressure. Comparison should thus be carried out at similar pressure. However, compliance and elastance, in contrast to the Young modulus, also depend on the size of the organ. Distensibility and volume elasticity account for vessel size and are often used for comparisons of groups (Fig. 11.6).

Buffering Function of Compliance

Arterial compliance is the buffering element for pressure so that the oscillations in pressure during the cardiac cycle are limited. The Pulse Pressure in the aorta, the
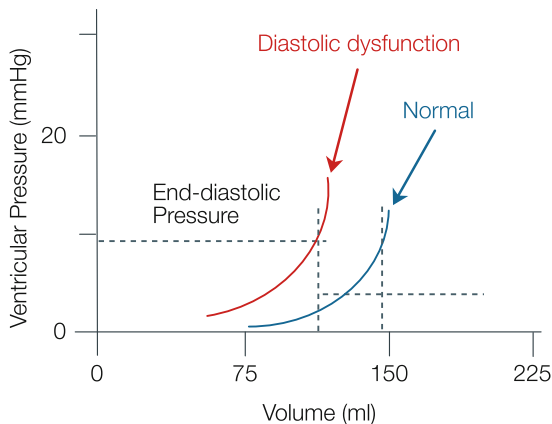
Fig. 11.6 Loss of diastolic ventricular compliance means that distension of the left ventricle in diastole becomes more difficult. Even a higher filling pressure is not capable to reach sufficient end-diastolic volume. An increase in diastolic filling pressure implies an increase in the pulmonary venous pressure, leading to pulmonary edema
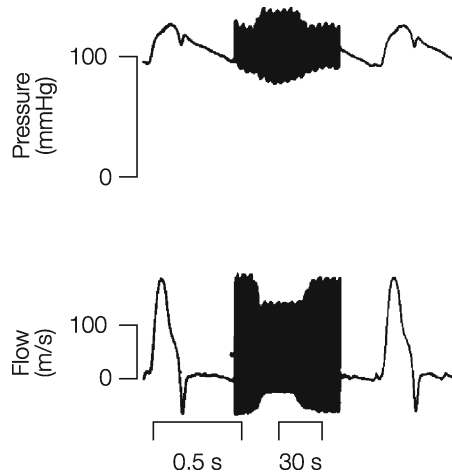
Fig. 11.7 Aortic pressure and flow in the intact dog during an acute decrease in aortic compliance, but constant peripheral resistance. Cardiac filling increases along with the decrease in compliance. The compliance decrease causes an increase in pulse pressure. Adapted from ref. [6], used by permission

difference between systolic and diastolic aortic pressure, is about 40 mmHg in the young healthy adult. It was shown by Randall et al. [6] that, *in vivo*, an acute reduction of total arterial compliance results in a considerable increase in Pulse Pressure (Fig. 11.7). The effect of long term, i.e., ~60 days reduction of aortic compliance to 60%, increased systolic pressure by 31 mmHg and diastolic pressure by 10 mmHg without affecting Cardiac Output and peripheral resistance [7].

It now accepted knowledge that increased Pulse Pressure is the strongest pressure-based indicator of cardiac mortality and morbidity [8, 9]. It has also been reported that diastolic cardiac function is affected when arterial compliance is decreased [10]. The scientific community is becoming more and more convinced that decreased compliance plays a major role in hypertension. In Chap. 29 it is shown that the change in compliance, with age, is considerable and contributes importantly to Pulse Pressure.

References

1. Peterson LH, Jensen RE, Parnell J. Mechanical properties of arteries in vivo. *Circ Res* 1960;8:622–639.
2. Hayashi, K, Handa H, Nagasawa S, Okumura A, Moritake K. Stiffness and elastic behavior of human intracranial and extracranial arteries. *J Biomech* 1980;13:175–184.
3. Langewouters GJ, Wesseling KH, Goedhard WJ. The static elastic properties of 45 human thoracic and 20 abdominal aortas in vitro and the parameters of a new model. *J Biomech* 1984;17:425–435.
4. Fung, Y. C. *Biomechanics. Mechanical Properties of Living Tissues.* 1981, New York & Heidelberg, Springer.

5. Love AEH. *A Treatise on the Mathematical Theory of Elasticity*. 1952, Cambridge, Cambridge University Press, 4th edn.

6. Randall OS, van den Bos GC, Westerhof N. Systemic compliance: does it play a role in the genesis of essential hypertension? *Cardiovasc Res* 1984;18:455–462.

7. Ioannou CV, Morel DR, Katsamouris AN, Katranitsa S, Startchik I, Kalangos A, Westerhof N, Stergiopulos N. Left ventricular hypertrophy induced by reduced aortic compliance. *J Vasc Res* 2009;46:417–425.

8. Benetos A, Safar M, Rudnichi A, Smulyan H, Richard JL, Ducimetieere P, Guize L. Pulse pressure: a predictor of long-term cardiovascular mortality in a French male population. *Hypertension* 1997;30:1410–1415.

9. Mitchell GF, Moye LA, Braunwald E, Rouleau JL, Bernstein V, Geltman EM, Flaker GC, Pfeffer MA. Sphygmomanometrically determined pulse pressure is a powerful independent predictor of recurrent events after myocardial infarction in patients with impaired left ventricular function. *Circulation* 1997;96:4254–4260.

10. Kawaguchi M, Hay I, Fetics B, Kass DA. Combined ventricular systolic and arterial stiffening in patients with heart failure and preserved ejection fraction: implications for systolic and diastolic reserve limitations. *Circulation* 2003;107:714–720.

Part B
Cardiac Hemodynamics

Chapter 12
Cardiac Muscle Mechanics
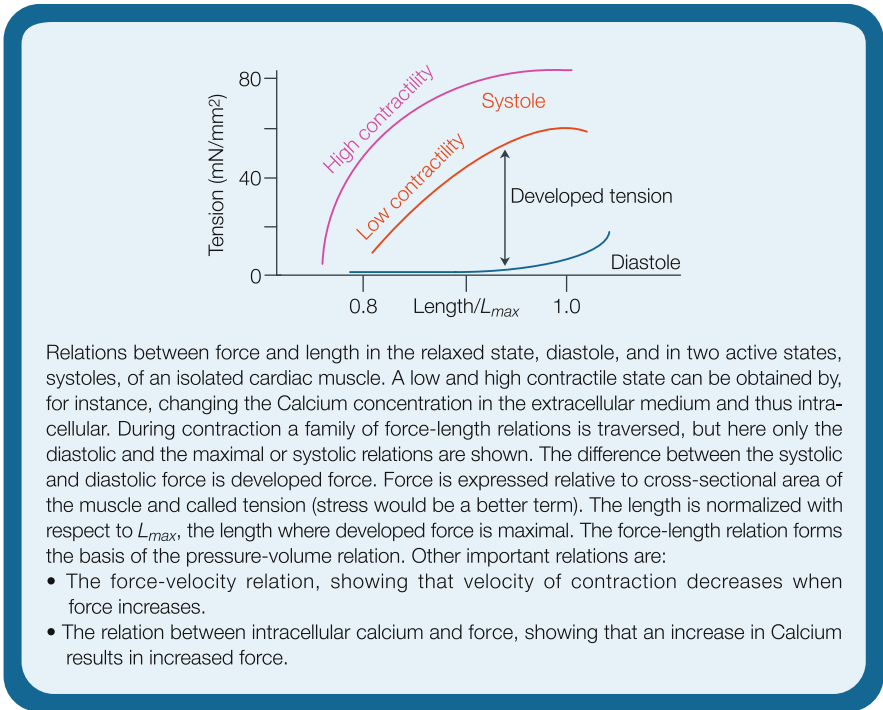
Relations between force and length in the relaxed state, diastole, and in two active states, systoles, of an isolated cardiac muscle. A low and high contractile state can be obtained by, for instance, changing the Calcium concentration in the extracellular medium and thus intracellular. During contraction a family of force-length relations is traversed, but here only the diastolic and the maximal or systolic relations are shown. The difference between the systolic and diastolic force is developed force. Force is expressed relative to cross-sectional area of the muscle and called tension (stress would be a better term). The length is normalized with respect to L_{max}, the length where developed force is maximal. The force-length relation forms the basis of the pressure-volume relation. Other important relations are:
- The force-velocity relation, showing that velocity of contraction decreases when force increases.
- The relation between intracellular calcium and force, showing that an increase in Calcium results in increased force.

Description

The cardiac muscle cells, also called fibers, branch and interdigitate. They are typically 40 μm long and about 10 μm in diameter; the fibers contain fibrils that are built up by the basic contractile units the sarcomeres (Fig. 12.1). Each sarcomere is bounded at the ends by Z-discs about 2 μm apart. The thin actin filaments about 1 μm long, are attached to the Z-discs, and extend towards the center of the sarcomere. They can
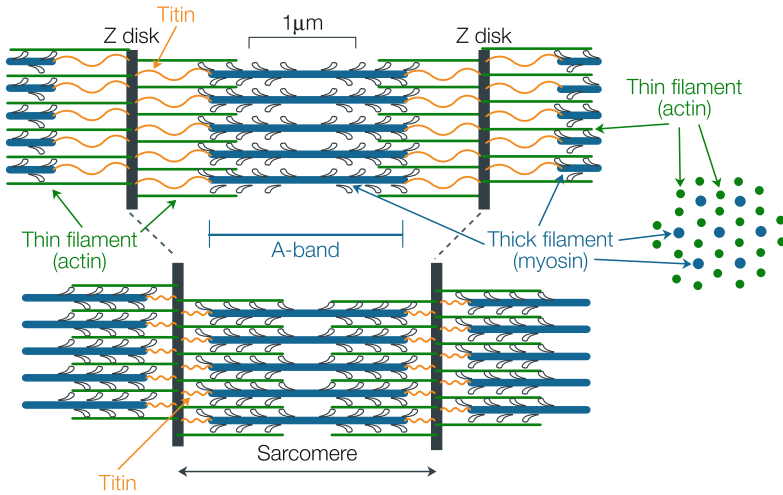
Fig. 12.1 The contractile unit of cardiac muscle is the sarcomere. The basic mechanical elements are presented here at two muscle lengths in the longitudinal direction. On the right hand side the cross section at overlap of thin and thick filaments is shown. Only one (instead of 6) titin molecule per half thick filament is shown for simplicity

either meet in the center, when sarcomere length is about 2.0 μm, overlap each other when sarcomere length is <2.0 μm, or not quite reach each other when sarcomere length >2.0 μm. Spanning the center of the sarcomere length are the thick myosin filaments, 1.6 μm long, which interdigitate with the thin filaments. They are connected to the Z-discs with a titin molecule, the third filament. The titin filament contains several spring sections, each with their own stiffness. The titin is the main determinant of muscle stiffness in diastole [1]. Changes in sarcomere length are achieved by sliding of thin between thick filaments; the sliding filament model. This sliding is caused by the action of the active, heavy meromyosin ATPase, i.e., ATP consuming unit, the 'cross-bridge'. The cross-bridges project sideways from the thick filaments, apart from a 'bare area' in the central zone of approximately 0.2 μm in length. The physiological range of sarcomere lengths (SL) is 1.6–2.3 μm, so that the number of cross-bridges in apposition to thin filaments is constant.

Calcium

Depolarization of the heart muscle cell membrane causes influx of calcium ions, Ca^{2+}, over the cell membrane. This increase in Ca causes a further and larger release of calcium ions from the Sarcoplasmatic Reticulum, SR, the so-called calcium-induced calcium release. Calcium reacts with myosin ATPase to produce a contraction.
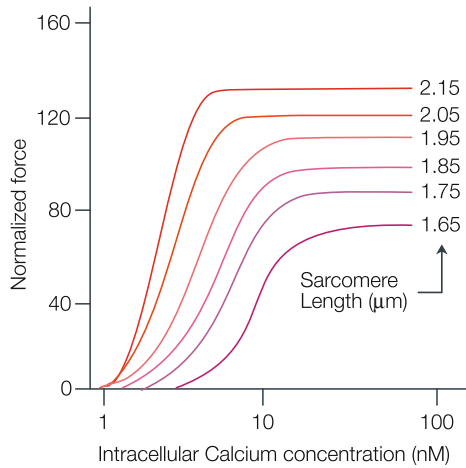
Fig. 12.2 Relation between intracellular calcium ion concentration and isometric force. Normalization is with respect to isometric force at a sarcomere length of 1.85 μm. Adapted from ref. [2], used by permission

The magnitude of the force of contraction produced when the sarcomere is prevented from shortening, i.e., isometric sarcomeres, is a function of sarcomere length and of intracellular calcium ion concentration, $[Ca]_i$.

The interrelationships between this isometric force, F_0, with sarcomere length, SL, and $[Ca]_i$ are sigmoidal (Fig. 12.2). On the up-sloping part of this curve, an increase in $[Ca]_i$ resulting from increased Ca^{2+} release, causes an increase in F_0, called an increase in contractility, or positive inotropic effect. This must be distinguished from an increase of F_0 due to increase in sarcomere length, which is due to increased sensitivity of the contractile filaments to Ca^{2+}. Increased sensitivity implies an upward and leftward shift of the $F_0 - [Ca]_i$ curve. This effect forms the basis of the Frank-Starling Law that states that 'the energy of contraction is a function of initial fiber length'. This effect is brought about by the presence of regulatory proteins on the thin filaments, namely the tropomyosin and the troponin complex. Other proteins and factors also play a role, e.g., Titin and lattice spacing.

The curvilinear shapes of the F_0 versus SL (or length) vary with the level of $[Ca]_i$, as shown in the Figure in the box.

The Force-Length Relation

The force-length relation of cardiac muscle (see Figure in box) forms the basis of the ventricular pressure-volume relation. The relation between pressure and (local) tension can in principle be obtained by Laplace's law, but more sophisticated

approaches are advised. Many models have been proposed with varying success. The main problems are:

- *(Local) wall stress* can not be measured in the intact heart, so that verification of models is not yet possible [3]. Subendocardial shortening is larger than subepi-cardial shortening, but forces may or may not be different.
- *Cardiac geometry is complex*. Cylindrical or ellipsoidal heart models are only rough approximations of reality.
- *Relations between ventricular volume and (local) fiber length*, as well as between volume changes and changes in fiber length also suffer from heterogeneity and geometric complexity. The simplest approach is to assume that the heart is a cylinder, with the volume proportional to fiber length squared, or a sphere, with volume proportional to fiber length to the third power.
- *The force-length relation* of the muscle therefore only qualitatively relates to the pressure-volume relation of the heart.

The Force-Velocity Relation

Another basic property of cardiac muscle is that for larger force the velocity of shortening is smaller (Fig. 12.3). This inverse relation between force and velocity is called the force-velocity relation (F-v relation). *In vivo*, heart muscle shortens against a force F that is less than the isometric force, F_0; these forces (stresses) are also called 'loads'. The F-v relation can be described by a hyperbola with the Hill equation:

$$(F_0 - F) \cdot b = (F + a) \cdot v$$

The maximal velocity, v_0, depends on the maximum velocity of ATP splitting by the myosin ATPase.

In Fig. 12.4, two sets of Force-velocity (F-v) relations are given. The F-v curves are hyperbolic except near F_0. The left hand side presents F-v relations for two
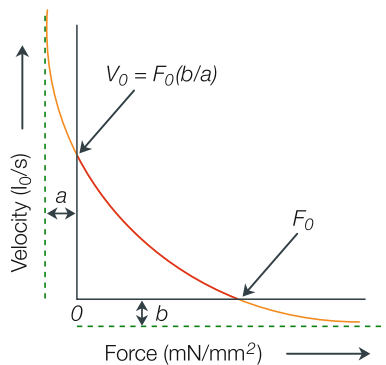
Fig. 12.3 Force-velocity relation of cardiac muscle. The hyperbola can be described by the Hill equation
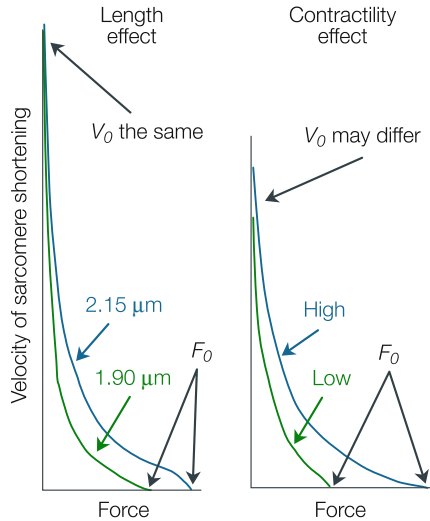
Fig. 12.4 Force-sarcomere shortening velocity relations are influenced by muscle length and contractility. Two lengths and two levels of contractility are depicted. Adapted from ref. [4], used by permission

sarcomere lengths, 1.90 and 2.15 μm. It shows that the increase in F_0 is not accompanied by an increase in the maximum velocity of sarcomere shortening, v_0, at zero force. This phenomenon depends on muscle length and disappears at short lengths. The right hand part of Fig. 12.4 shows the F-v relation for two contractility levels, or two levels of intracellular Calcium, $[Ca]_i$. With an increasing level of $[Ca]_i$ the v_0 increases until a saturation level is reached. In the rat this level is below the physiological $[Ca]_i$ so that v_0 will then not increase with increased contractility of increased intracellular Calcium. In the human there exists a range of Calcium concentrations where v_0 will increase.

The F-v Relation and Pump Function

F and v relate, through geometric transformations (Laplace) with pressure, e.g., pressure in the left ventricle, and (velocity to volume change) to flow. The F-v curves above refer to an instant in time within a contraction, whereas CO is a time-integrated quantity and not directly related. In other words, during the cardiac cycle the F-v relation is not constant but rises from one at the end of diastole, to one in systole and subsequently wanes down to the diastolic one again. This waxing and waning is not simply a 'parallel' shift because the time course of v_0 is more rapid

than that of F_0. A greater duration of contraction results in a higher Stroke Volume, *SV*, which is related to the average velocity. It is considered by some that the relevant *F-v* curve for the intact heart is the relationship between average *F* and average *v*, which is equivalent to the pump function graph relating mean ventricular pressure *LVP* to *CO* (see Chap. 14).

Experimental Problems

Studies on cardiac muscle are usually performed on isolated muscle strips, papillary muscle or trabeculae. These preparations are generally not perfused and therefore conditions have to be chosen such that a so-called anoxic core is avoided. These conditions are low temperature, low frequency, high P_{O2} of the superfusion fluid, etc. If *in vivo* conditions are desired, such as 37°C and physiological rate of contraction, a perfused preparation is required. Single skinned (permeable outer membrane) myocytes have been studied in terms of length and tension and calcium sensitivity, and very recently data on intact single myocytes have been reported [5].

Isolated cardiac muscle allows for studies of basic phenomena, such as tension development, calcium handling, effects of drugs, disease, etc. The advantage is that the muscle can be studied without the confounding effects of changes in cardiac loading. The disadvantage is that conditions are not physiological.

Determination of maximal isometric force requires that one stretches the preparation during contraction to prevent the sarcomeres from shortening because of compliant attachments of the preparation to the apparatus. This requires feedback control of the stretching apparatus keeping sarcomere length constant. The, average, sarcomere length can be derived from light diffraction provided the preparation is sufficiently thin. The method is used successfully in trabeculae, which are fine muscle bundles from the inside of the heart cavity, usually taken from the right ventricle.

In most cell cultures cell shortening is used as a measure of function. Unfortunately the shortening depends on the adherence of the cells to the substrate, and this adherence is not known. Also the amount of shortening cannot be related to the force.

Nomenclature Problems

Another term for v_0, used in the past was v_{max}, but this is now avoided because of erroneous attempts to calculate it in intact hearts. Traditionally, isolated muscle experiments were arranged so that the force was constant during systole and early relaxation, whereas in life, force decreases during systole and falls to about zero in early relaxation (before diastolic lengthening). This constant force during systole

and early relaxation was called 'afterload', a term which is clearly inappropriate to use in the intact heart. Before it was possible to measure sarcomere length throughout an experiment, the muscle was hung vertically and its initial length was set with variable weights; these weights were called 'preloads'. This term is no longer appropriate because the fundamental independent variable, sarcomere length, can now be measured. It is unwise to apply terms derived from cardiac muscle mechanical studies, which are one-dimensional, to the intact heart, which is three-dimensional.

Limitations of the Sliding Filament Model

Students of cardiac muscle have traditionally tried to relate their findings to thinking arising from skeletal muscle studies, and the latter has been dominated by the idea that the cross-bridges attach mechanically to the thin filaments. Herzog et al. review one of the phenomena that are not compatible with the theory that the cross-bridges attach mechanically to the thin filaments [6]. Liu and Pollack provide evidence that filaments slide in steps of integers of 2.7 nm [7], and Kishino and Yanagida [8] show myosin heads alone, attached to glass can exert full ATP-dependent force. Finally Holohan and Marston [9] show that immobilized myosin in a motility assay can induce full bead-tailed actin filament force-velocity characteristics, when an electromagnetic field is applied in the presence of ATP.

Currently there is no sign of such critiques in the cardiac muscle literature, although it was shown in cardiac muscle that myosin binding can switch on actin filaments in rigor conditions but it does not contribute significantly under physiological conditions. The physiological mechanism of co-operative Ca^{2+} regulation of cardiac contractility must therefore be intrinsic to the thin filaments [10].

Rigor is a pathological condition characterized by cross-bridge attachment to filaments caused by ATP depletion. Physiological contraction takes place in the presence of ATP, which ensures absence of cross-bridge attachment to thin filaments and catalyses contraction through an electromagnetic or electrostatic mechanism.

Physiological and Clinical Relevance

The maintenance of the circulation requires that the heart muscles have a sufficiently high *F-v* relation and duration of active state. Failure of these, as for example due to reduced contractility, will lead to clinical heart failure. Clinical heart failure can also occur due to damage of part of the heart, e.g. myocardial infarction. Stimulation of contractility may be necessary in the treatment of acute heart failure, using positively inotropic drugs. Unfortunately, this seemingly logical treatment is contra-indicated in chronic heart failure because it causes earlier death, presumably because increased oxygen is required by the cardiac muscle sometimes

in excess of possible supply rate; positively inotropic drugs mostly work by increasing [Ca]$_i$ which can also cause (possibly fatal) arrhythmia. However, an increase of Ca-sensitivity seems an option [11].

References

1. Fukuda N, Granzier HL. Titin/connectin-based modulation of the Frank-Starling mechanism of the heart. *J Muscle Res Cell Motil* 2005;26:319–323. Review

2. Kentish JC, ter Keurs HEDJ, Ricciardi L, Bucx JJJ, Noble MIM. Cardiac muscle mechanics: comparison between the sarcomere length-force relations of intact and skinned trabeculae from rat right ventricle. *Circ Res* 1986;58:755–768.

3. Huisman RM, Elzinga G, Westerhof N, Sipkema P. Comparison of models used to calculate left ventricular wall force. *Cardiovasc Res* 1980;14:142–153.

4. Daniels M, Noble MIM, ter Keurs HEDJ, Wohlfart B. Force and velocity of sarcomere short-ening in rat cardiac muscle: relationship of force, sarcomere length, Ca^{++} and time. *J Physiol* 1984;355:367–381.

5. van der Velden J, Klein LJ, van der Bijl M, Huybregts MA, Stooker W, Witkop J, Eijsman L, Visser CA, Visser FC, Stienen GJ. Isometric tension development and its calcium sensitivity in skinned myocyte-sized preparations from different regions of the human heart. *Cardiovasc Res* 1999;42:706–719.

6. Herzog W, Lee EJ, Rassier DE. Residual force enhancement in skeletal muscle. *J Physiol* 2007;578:613–615.

7. Liu X, Pollack GH. Stepwise sliding of single actin and Myosin filaments. *Biophys J* 2004;86:353–358.

8. Kishino A, Yanagida T. Force measurements by micromanipulation of a single actin filament by glass needles. *Nature* 1988;334(6177):74–76.

9. Holohan SJ, Marston SB. Force-velocity relationship of single actin filament interacting with immobilised myosin measured by electromagnetic technique. *IEEE Proc Nanobiotechnol* 2005;152:113–120.

10. Sun YB, Lou F, Irving M. Calcium- and myosin-dependent changes in troponin structure during activation of heart muscle. *J Physiol* 2009;587(Pt 1):155–163.

11. Drake-Holland AJ, Lee JA, Hynd J, Clarke SB, Noble MI. Beneficial effect of the calcium-sensitizing drug EMD 57033 in a canine model of dilated heart failure. *Clin Sci (Lond)* 1997;93:213–218.

Chapter 13
The Pressure-Volume Relation
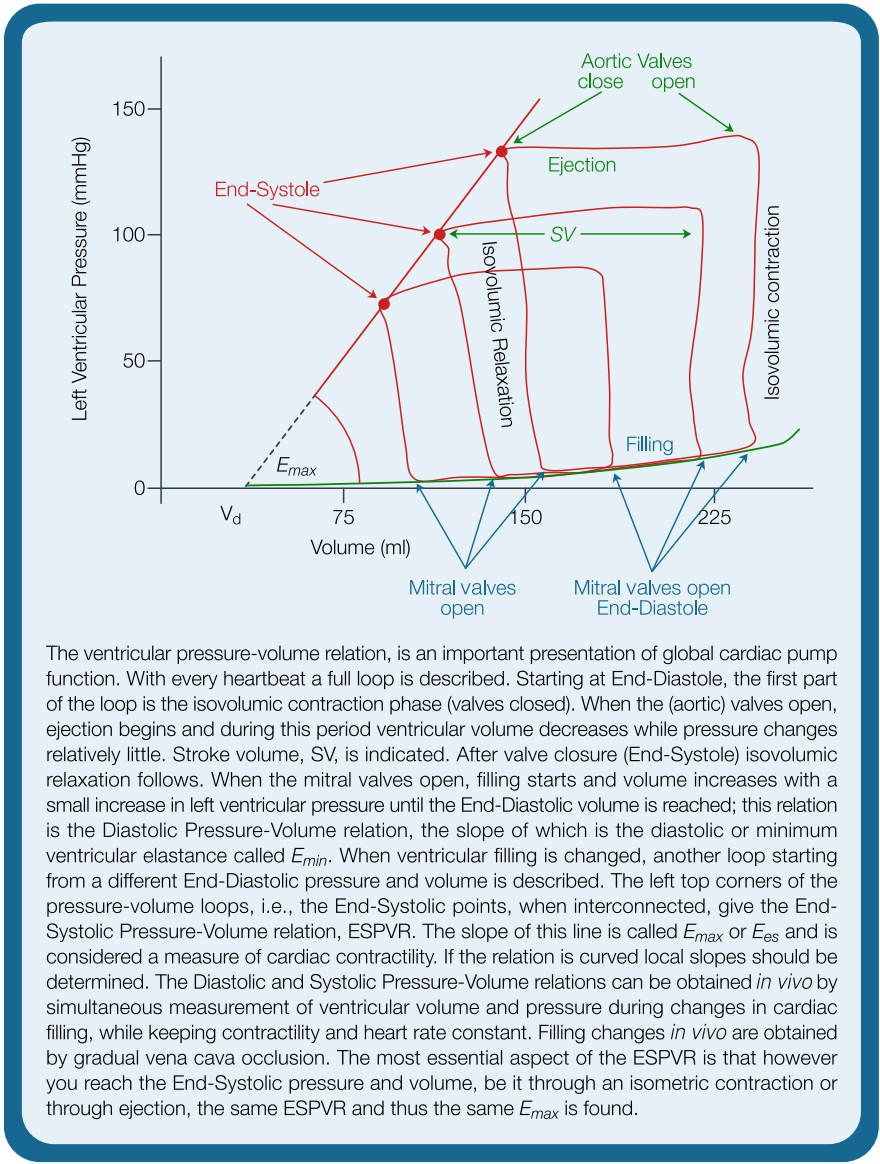
The ventricular pressure-volume relation, is an important presentation of global cardiac pump function. With every heartbeat a full loop is described. Starting at End-Diastole, the first part of the loop is the isovolumic contraction phase (valves closed). When the (aortic) valves open, ejection begins and during this period ventricular volume decreases while pressure changes relatively little. Stroke volume, SV, is indicated. After valve closure (End-Systole) isovolumic relaxation follows. When the mitral valves open, filling starts and volume increases with a small increase in left ventricular pressure until the End-Diastolic volume is reached; this relation is the Diastolic Pressure-Volume relation, the slope of which is the diastolic or minimum ventricular elastance called E_{min}. When ventricular filling is changed, another loop starting from a different End-Diastolic pressure and volume is described. The left top corners of the pressure-volume loops, i.e., the End-Systolic points, when interconnected, give the End-Systolic Pressure-Volume relation, ESPVR. The slope of this line is called E_{max} or E_{es} and is considered a measure of cardiac contractility. If the relation is curved local slopes should be determined. The Diastolic and Systolic Pressure-Volume relations can be obtained *in vivo* by simultaneous measurement of ventricular volume and pressure during changes in cardiac filling, while keeping contractility and heart rate constant. Filling changes *in vivo* are obtained by gradual vena cava occlusion. The most essential aspect of the ESPVR is that however you reach the End-Systolic pressure and volume, be it through an isometric contraction or through ejection, the same ESPVR and thus the same E_{max} is found.

Description

Otto Frank studied pressure-volume relations in the isolated frog heart. He found different End-Systolic Pressure-Volume Relations, ESPVR's, for the ejecting heart and the isovolumically contracting heart. In other words, a single unique End-Systolic Pressure-Volume Relation did not appear to exist.

The same measurements in the isolated blood perfused dog heart, where volume was accurately measured with a water-filled balloon, showed that the End-Systolic Pressure-Volume Relation is the same for ejecting beats and isovolumic beats. The original results suggested a linear ESPVR with an intercept with the volume axis, V_d. The linear relation implies that the slope of the ESPVR, the E_{max}, with the dimension of pressure over volume (mmHg/ml), can be determined. Increased contractility, (Fig. 13.1) as obtained with epinephrine, increases the slope of the ESPVR but leaves the intercept volume, V_d, unchanged [1]. Therefore with a linear ESPVR, the E_{max} can quantify contractility. Later it turned out that both the diastolic pressure-volume relation and the ESPVR are not linear. This implies that the slope depends on the pressure and volume chosen and when approximating this locally with a straight line a virtual intercept volume is obtained, which may be positive or negative. However, the load-independence of the ESPVR is generally shown to be true (some load-dependence of the ESPVR does exist but is small [1, 2]), which is of great significance in the understanding and characterization of cardiac pump function. An extensive treatment is given in [2].

The Varying Elastance Model

Pressure-volume loops can be analyzed by marking time points on the loop (Fig. 13.2). When different loops are obtained and the times indicated, we can connect points with the same times, and construct isochrones. The slopes of the isochrones can be determined, and the slope of an isochrone is the elastance at that moment in time. The fact that the elastance varies with time, leads to the concept of time-varying elastance, $E(t)$. This means that during each cardiac cycle the elastance increases from its diastolic value to its systolic value E_{max} and then returns to its diastolic value again (Fig. 13.2).

It has been shown that the $E(t)$ curve, when normalized with respect to its peak value and to the time of its peak (see Fig. 13.3), is similar for normal and diseased human hearts [3]. Similar $E(t)$ curves are found in the mouse, the dog and the human. It thus seems that there exists a universal $E(t)$ curve in mammals including man, which is unaltered in shape in health and disease. The only differences between hearts and state of health are in the magnitude and time of peak of the $E(t)$. This similarity of the varying $E(t)$-curve is very useful to construct lumped models of the heart [4, 5]. However, some doubt has been cast on the invariance of the normalized $E(t)$ curve [6].

The principle mechanism is that the cardiac muscle changes its stiffness (elastance) during the cardiac cycle (Fig. 13.4) independent of its load.
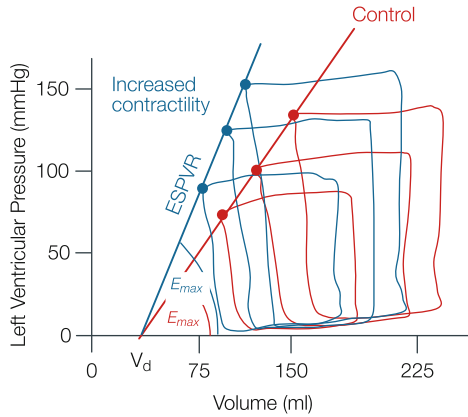
Fig. 13.1 The slope (E_{max}) of the End-Systolic Pressure-Volume Relation (ESPVR) is a measure of cardiac contractility. An increased slope implies increased contractility. Adapted from ref. [1] used by permission
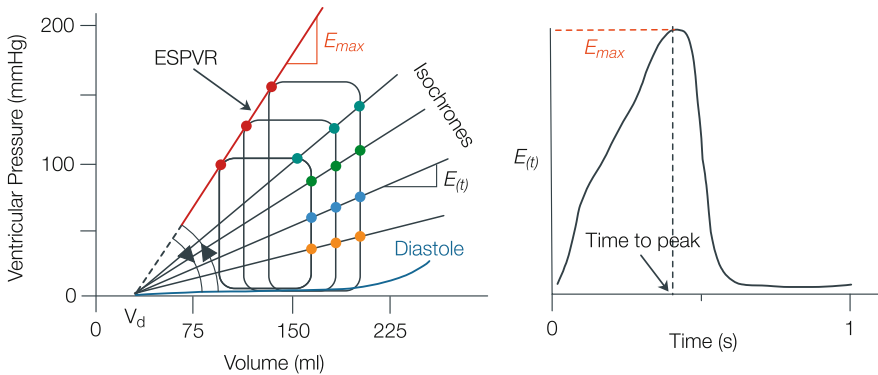
Fig. 13.2 Isochrones are lines connecting the pressures and volumes of different loops at the same moment in time. Isochrones are assumed to be straight and their slope is the instantaneous pressure-volume relation $E(t)$, with dimension mmHg/ml. The line connecting the End-Systolic corners of the loops is the End-Systolic Pressure-Volume Relation, ESPVR with slope E_{max}. The ESPVR is not an isochrone. The slopes of the isochrones plotted as a function of time, the $E(t)$-curve, exemplifies the varying elastance concept (*right part*)

Determination of E_{max}

The maximal slope of the pressure-volume relation is called maximal elastance, E_{max}. It is also called End-Systolic elastance, E_{es}. To determine E_{max} one needs to measure several pressure-volume loops to obtain a range of end-systolic pressure-volume points (see Figure in the box). The determination should be done sufficiently rapidly to avoid changes in contractility due to hormonal or nervous control systems. Both changes in arterial load and diastolic filling may, in principle, be used,
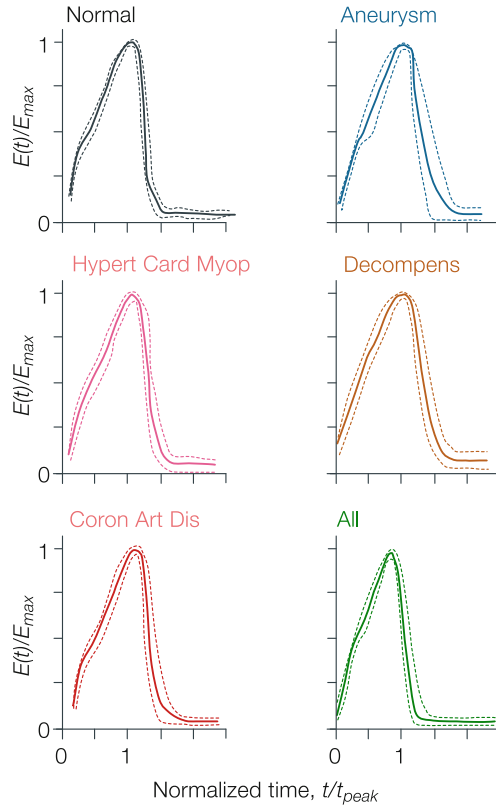
Fig. 13.3 The disease-independent $E(t)$ curve. The $E(t)$ curve, when normalized in amplitude and to time to peak, is similar in many disease states. Adapted from ref. [3], used by permission
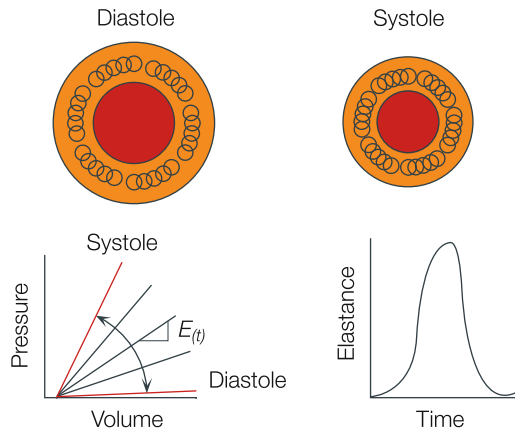
Fig. 13.4 The varying elastance concept assumes that the muscle stiffness increases from diastole to systole and back. This change in stiffness, expressed as the (varying) elastance curve, $E(t)$, is assumed to be unaffected by changes in load

but the former may illicit contractility changes. Changes in filling are therefore preferred and are also easier to accomplish in practice. For instance, blowing up a balloon in the vena cava may decrease filling over a sufficiently wide range and can be carried out sufficiently rapidly to obtain a series of loops and an accurate ESPVR. Measurement of both ventricular pressure and volume on a beat-to-beat basis can be carried out with the use of the so-called pressure-volume catheter [7].

Volume can be measured also using noninvasive techniques (US-Echo, X-ray, and MRI). Pressure can be measured invasively only. However, aortic pressure during the cardiac ejection period can be used as an acceptable approximation of left ventricular pressure to determine the systolic part of the pressure-volume loop [8]. Methods allowing for the calculation of ascending aortic pressure noninvasively from peripheral pressure (Chap. 26) could, if proven sufficiently accurate, allow for a completely noninvasive determination of E_{max}. Diastolic pressure can be estimated from pulmonary capillary wedge pressure and can thus be related to diastolic volume.

Physiological and Clinical Relevance

The ESPVR and E_{max} together with the diastolic pressure-volume relation, are important measures of cardiac pump function and they are often used in animal research; clinical use is still limited but increasing. The $E(t)$ curve depends on heart size and thus on body size: Pressures are similar in different animals but volumes are not. Volumes are proportional to body mass (Chap. 30). Thus E_{max} can be normalized with respect to ventricular lumen volume (see Chap. 11) or to heart mass or body mass to compare mammals. In diseased states the ratio of E_{max}/E_{min} may be a better measure of contractility than E_{max} alone (Chap. 30).

The Frank-Starling Law

The varying elastance concept contains both Frank's and Starling's original experimental results, as shown in Fig. 13.5. Frank studied the frog heart in isovolumic and ejecting beats, but we show here how isovolumic contractions behave in the pressure-volume plane when diastolic volume is increased. Starling also changed diastolic filling but studied an ejecting heart, which was loaded with a Starling resistor. This meant that in his experiments the aortic pressure was kept constant. This in turn implies that ventricular pressure during ejection was also constant. The increase in filling resulted in an increase in Stroke Volume and thus in Cardiac Output.

Systolic and Diastolic Dysfunction

It is important to realize that both diastole and systole play an important role in cardiac function (Fig. 13.6). This can be illustrated with the following example.
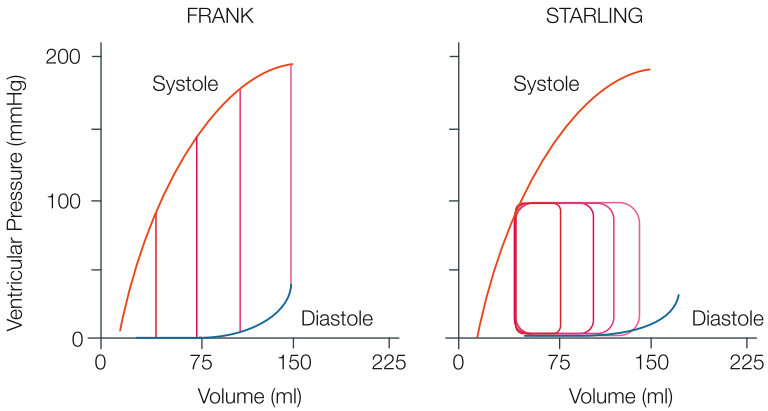
Fig. 13.5 The Frank (*left*, isovolumic contractions) and Starling (*right*, ejections against constant ejection pressure) experiments show the effect of ventricular filling in terms of pressure-volume relations
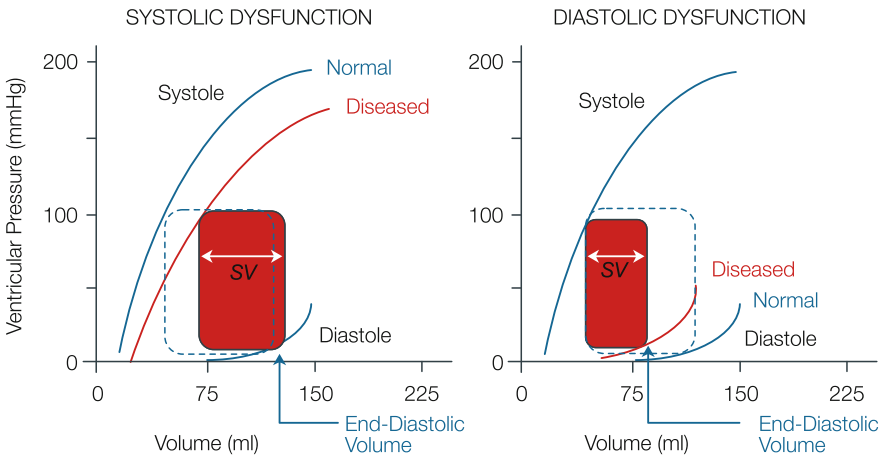
Fig. 13.6 Systolic and diastolic dysfunction are shown here by the *red lines*, and normal function by the *blue lines*. In systolic dysfunction the ESPVR is decreased and Stroke Volume, SV and Ejection Fraction, EF=SV/EDV, are decreased as well. In diastolic dysfunction, right, filling is decreased and, although filling pressure may be higher, End-Diastolic Volume and Stroke Volume are decreased, but EF may be similar

Systolic dysfunction results in a decreased Stroke Volume, and Cardiac Output, when not compensated by Heart Rate or diastolic filling. Diastolic dysfunction, with a stiffer ventricle in diastole causes decreased filling and higher filling pressure. This results in a decreased Cardiac Output, and an increased pulmonary venous pressure, the latter leading to shortness of breath.

Ejection Fraction, EF, defined as the ratio of Stroke Volume, SV, and End-Diastolic Volume, EDV, is decreased in systolic dysfunction but may be unaltered in diastolic dysfunction (Fig. 13.6). This is the case when SV and EDV decrease in similar proportion.

This situation is called diastolic dysfunction with maintained Ejection Fraction [9], and it shows that EF is not in all situations a measure of changed cardiac pump function. Also, since EF depends on the heart as a pump and the arterial load, EF can be affected by the mechanical coupling between the heart and arterial system and should therefore be considered as a ventriculo-arterial coupling factor (Chap. 17).

Concentric and Eccentric Hypertrophy

Interesting examples in the context of the varying elastance concept and the pressure-volume relation are concentric and eccentric hypertrophy (Fig. 13.7).

Concentric hypertrophy implies an increased wall thickness with similar lumen volume. This means a stiffer ventricle both in diastole and in systole, i.e., both E_{max} and E_{min} are increased. The increase in E_{max} does not necessarily imply increased contractility of the contractile apparatus of the muscle but is mainly a result of the fact that more sarcomeres are in parallel, i.e., thicker fibers and therefore increased wall thickness. Concentric hypertrophy, with its increased diastolic stiffness results in increased diastolic pressure but smaller end-diastolic volume, and higher systolic pressure with smaller volume in systole, but similar or slightly decreased Stroke Volume.

In eccentric hypertrophy the ventricular lumen volume is greatly increased, more sarcomeres in series, and longer cells, while the wall thickness may be unchanged or somewhat increased. The shift of the entire pressure-volume relation to larger volumes in eccentric hypertrophy implies, by virtue of the law of Laplace (Chap. 9), that wall forces are increased. The increased intercept volume, V_d, in eccentric hypertrophy emphasizes that the slope of the ESPVR cannot be determined from a single pressure and volume measurement because this is allowed only under the assumption that the intercept volume is negligible or known. Thus at least two
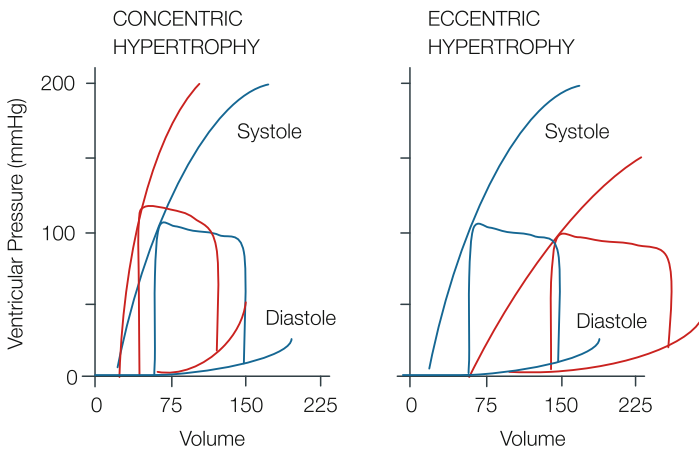
Fig. 13.7 Schematic drawings of pressure-volume relations in control (*blue lines*), severe concentric hypertrophy (*left*), and severe dilatation (*right*) (*red lines*)

points on the relation are required, necessitating a change in filling or systolic pressure. A second point may be obtained by estimating isovolumic pressure from the measured pressure (single beat method) as discussed in Chap. 17.

Modeling on the Basis of the Varying Elastance Concept

The finding that the normalized $E(t)$ curve appears to be quite independent of the cardiac condition (Fig. 13.3), and that it is similar in mammals (Chap. 30) allows quantitative modeling of the circulation [5, 10]. The nonlinearity of the isochrones (see below) appears of little consequence in this type of modeling [4].

Limitations

It should be emphasized that the time varying elastance concept pertains to the ventricle as a whole. It allows no distinction between underlying cardiac pathologies. For instance, asynchronous contraction, local ischemia or infarction etc., all decrease the slope of the End-Systolic Pressure-Volume Relation.

The pressure-volume relations, expressed by isochrones (Fig. 13.8), are not straight [11]. The diastolic relation is, as in most biological tissues, convex to the volume axis. The systolic pressure-volume relations may be reasonably straight when muscle contractility is low, but becomes (over the working range) more and more convex to the pressure axis with increasing contractility. A curved relation
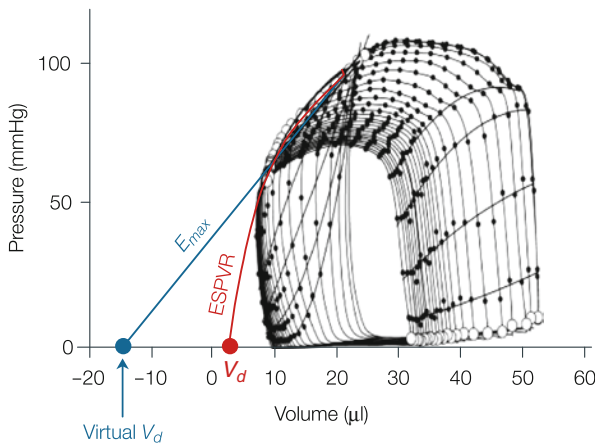
Fig. 13.8 Neither the isochrones nor the End-Systolic Pressure-Volume Relation is linear. Thus the linear approximation may not always be correct and may lead to, for instance, a negative volume intercept, Virtual V_d, which is physically impossible. Data of the mouse, adapted from ref. [11], used by permission

implies that the E_{max} depends on volume and pressure. It is customary to approximate the ESPVR's in the working range by a straight line. Although this sometimes gives an acceptable approximation of reality, often a negative, and thus a virtual, V_d is found by linear extrapolation of the ESPVR to the volume axis.

In the normal heart the intercept volume may be small, and when this is the case the E_{max} can be estimated from a single pressure-volume loop. However, when V_d is not small, large errors will result by using a single point estimation of the End-Systolic Pressure-Volume Relation to derive E_{max}, (see Fig. 13.8).

It has been shown by a number of investigators that load changes affect the End-Systolic Pressure-Volume Relation. However, the effect is rather small and may be due to the fact that, at high loads, the duration of ejection is curtailed and may not be long enough for E_{max} to be attained [2].

References

1. Suga H, Sagawa K, Shoukas AA. Load independence of the instantaneous pressure-volume ratio of the canine left ventricle and the effect of epinephrine and heart rate on the ratio. *Circ Res* 1973;32:314–322.
2. Sagawa K, Maughan, WL, Suga H, Sunagawa K. *Cardiac contraction and the pressure-volume relationship*. 1988, New York & Oxford, Oxford University Press.
3. Senzaki H, Chen C-H, Kass DA. Single beat estimation of end-systolic pressure-volume relation in humans: a new method with the potential for noninvasive application. *Circulation* 1996;94:2497–2506.
4. Lankhaar JW, Rövekamp FA, Steendijk P, Faes TJ, Westerhof BE, Kind T, Vonk-Noordegraaf A, Westerhof N. Modeling the instantaneous pressure-volume relation of the left ventricle: a comparison of six models. *Ann Biomed Eng* 2009;37:1710–1726.
5. Segers P, Stergiopulos N, Westerhof N. Quantification of the contribution of cardiac and arterial remodeling to hypertension. *Hypertension* 2000;36:760–765.
6. Palmer BM, Noguchi T, Wang Y, Heim JR, Alpert NR, Burgon PG, Seidman CE, Seidman JG, Maughan DW, LeWinter MM. Effect of cardiac myosin binding protein-C on mechanoenergetics in mouse myocardium. *Circ Res* 2004;94:1615–1622.
7. Baan J, van der Velde ET, de Bruin HG, Smeenk GJ, Koops J, van Dijk AD, Temmerman D, Senden J, Buis B. Continuous measurement of left ventricular volume in animals and humans by conductance catheter. *Circulation* 1984;70:812–823.
8. Lee WS, Nakayama M, Huang WP, Chiou KR, Wu CC, Nevo E, Fetics B, Kass DA, Ding PY, Chen CH. Assessment of left ventricular end-systolic elastance from aortic pressure-left ventricular volume relations. *Heart Vessels* 2002;16:99–104.
9. Paulus WJ, Tschöpe C, Sanderson JE, Rusconi C, Flachskampf FA, Rademakers FE, Marino P, Smiseth OA, De Keulenaer G, Leite-Moreira AF, Borbély A, Edes I, Handoko ML, Heymans S, Pezzali N, Pieske B, Dickstein K, Fraser AG, Brutsaert DL. How to diagnose diastolic heart failure: a consensus statement on the diagnosis of heart failure with normal left ventricular ejection fraction by the Heart Failure and Echocardiography Associations of the European Society of Cardiology. *Eur Heart J* 2007;20:2539–2550.
10. Westerhof N. Cardio-vascular interaction determines pressure and flow. In: *Biological Flows*. MY Jaffrin, CG Caro Eds., 1995, New York, Plenum.
11. Claessens TE, Georgakopoulos D, Afanasyeva M, Vermeersch SJ, Millar HD, Stergiopulos N, Westerhof N, Verdonck PR, Segers P. Nonlinear isochrones in murine left ventricular pressure-volume loops: how well does the time-varying elastance concept hold? *Am J Physiol* 2006;290:H1474–H1483.

Chapter 14
The Pump Function Graph
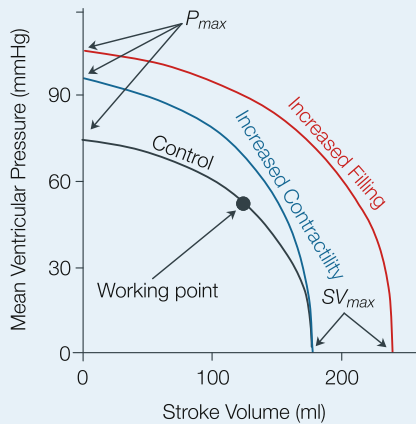
The heart as a pump can be described by the pump function graph, the relation between mean left ventricular pressure and Stroke Volume, *SV*. A pump function graph completely describes the heart as a pump [1] and is based on the characterization of industrial pumps. When the load on the heart is increased, it will generate a higher pressure but a smaller Stroke Volume, and vice versa, and a curved inverse relation is found. Contractility and diastolic filling modify the relation. Increased contractility "rotates" the pump function graph around the intercept with the *SV* axis SV_{max}, as shown by the *blue line*. When diastolic filling is increased, the pump function graph shifts in a "parallel" manner, and P_{max} and SV_{max} both increase, as shown by the *red line*. Thus, when a pump function graph is to be determined contractility and diastolic filling should be kept constant. The working point, i.e., the pressure and flow during normal function at rest, is indicated. The maximal mean pressure, P_{max}, i.e., the intercept with the pressure axis, is the pressure when the heart beats isovolumically. If the relation between Cardiac Output, CO, and mean left ventricular pressure is desired one can use $CO = HR \cdot SV$. The cardiac pump function graph is indirectly related to the force-velocity relation of muscle (see Chap. 12). There is also a simple relation between the pump function graph and the pressure-volume relationship.

Description

The heart is a pump that generates pressure and flow. It can be compared with other hydraulic pumps that are usually characterized by their head (pressure) – capacity (flow) curve. As an example consider a roller pump and make a pressure-flow relation by changing the load on the pump.

In Fig. 14.1 we show the pump function graph, PFG, of a roller pump used in the laboratory and in heart-lung machines. The pump function graph depends on the
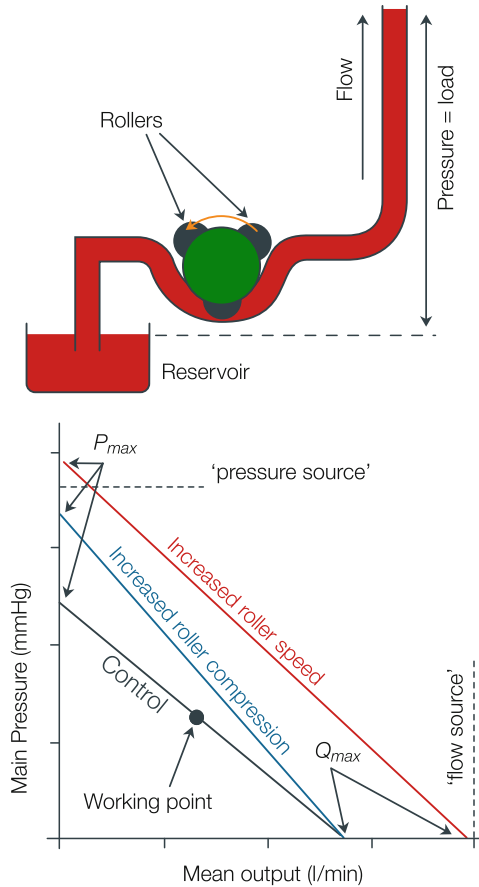
Fig. 14.1 The Pump Function Graph of a laboratory pump. When roller speed and compression of the tube by the rollers is kept constant, a Pump Function Graph can be determined by changing the load on the pump, here obtained by changes in height of the outflow tube. When the compression by the rollers is increased the *blue line* is obtained. When roller speed is increased, compare Heart Rate, the red Pump Function Graph is found. A pressure source is a pump that generates the same pressure for all flows obtained by the changes in the load. A flow source always generates the same flow. The pump shown here is neither a pressure source nor a flow source. Adapted from ref. [1], used by permission

roller speed and on how much the rollers compress the tube. A higher speed gives larger pressures and flows, pressure and flow intercept, P_{max} and Q_{max}, increase. Better compression of the rollers, increases the pressure generating capability because less leakage is present, the P_{max} increases. Since at low pressures the leakage is negligible, the maximal flow, Q_{max}, is hardly affected by changes in compression of the tube. Thus the result of the increased roller compression is a clockwise 'rotation' of the pump function graph around the intercept with the flow axis.

The pump function graph of a roller pump can be determined by changing the resistance in the outflow tube, while keeping the pump characteristics the same. Thus roller speed and roller compression, and the inflow pressure level are kept constant. For very high resistance values the pressure is maximal, P_{max}, but the flow is negligible. When the resistance is negligible and flow is maximal, Q_{max}, but the generated pressure is zero. Thus, an inverse relation between pressure and flow is obtained. The relation happens to be straight for this type of pump, and gives information about what pressures and flows the pump can generate. The pump function graph also shows that this particular pump is neither a pressure source, i.e., always generating the same pressure, nor a flow source, i.e., always keeping flow constant.

We can perform a similar experiment on the heart (Fig. 14.2). To avoid changes in pump function by humoral and nervous control mechanisms, these studies were originally carried out in the isolated perfused and ejecting cat heart. When ventricular filling pressure, cardiac contractility and Heart Rate are kept constant, variation in the load on the heart by either changing peripheral resistance or
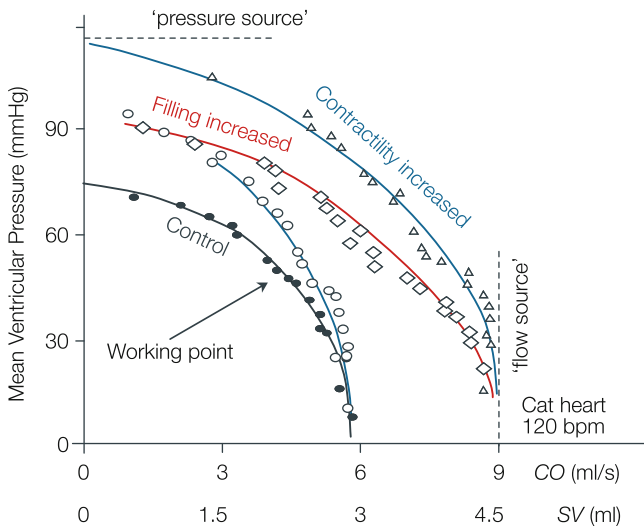
Fig. 14.2 Pump Function Graphs as originally measured in an isolated pumping cat heart. The *black line* gives the control situation. Increased diastolic filling (*black* to *red*) causes a 'parallel' shift. An increase in contractility 'rotates' the graph around the intercept with the flow axis (*black* to *blue* and *red* to *blue*). The *horizontal axis* is in terms of Stroke Volume. Adapted from ref. [4], used by permission

arterial compliance, or both, results in changes of mean left ventricular pressure and mean flow (or Stroke Volume) [1]. The relation between mean ventricular pressure and mean flow (Cardiac Output) is based on the reported inverse relation of mean force and mean velocity of isolated cardiac muscle [2, 3] and thus relates to basic muscle properties. The ventricular pressure is related with (aortic) flow because both quantities pertain to the cardiac side of heart and the very nonlinear aortic valves are avoided in the analysis. Mean ventricular pressure and mean flow are used as a first order approximation, comparable with the mean aortic pressure and mean flow to determine peripheral resistance. In principle Fourier analysis (Appendix 1) of ventricular pressure and flow can be used to derive the oscillatory aspects of the pump function graph, in analogy with the derivation of arterial input impedance (Chap. 23).

From the pump function graph we can see that the heart decreases its output when a higher pressure is generated. In other words the heart does neither generate the same flow, nor the same pressure under different loading conditions. This means that the heart is neither a pressure source, i.e., pressure is independent of the load, nor a flow source, i.e., the same flow and SV for all loads. At low flows the heart starts to resemble a pressure source and at high flows a flow source is approached. The intercept of the pump function graph with the pressure axis is the mean ventricular pressure for a non-ejecting or isovolumic beat, thus mean isovolumic ventricular pressure. The intercept with the flow axis is the Cardiac Output or Stroke Volume for the 'unloaded' or 'isobarically contracting' heart, i.e., contractions without build-up of pressure. The maximal Stroke Volume can be taken as End-Diastolic Ventricular Volume and together with measured Stroke Volume the End-Systolic Volume and Ejection Fraction can be estimated,

The changes in contractility [4] and filling are also shown in Fig. 14.2. An increase in cardiac contractility 'rotates' the pump function graph around the flow intercept, Q_{max}. Increased filling gives a 'parallel' shift of the graph. Increased Heart Rate in the physiological range results in a parallel shift, which is approximately proportional to the Heart Rate increase, thus P_{max} and Q_{max} are multiplied by the Heart Rate increase. If Stroke Volume instead of Cardiac Output is used on the horizontal axis and mean LV pressure per beat on the vertical axis the Heart Rate effect is eliminated, and only filling and contractility remain as determinants of the pump function graph.

At the intercept of the pump function graph with the pressure and flow axes, P_{max} and Q_{max}, respectively, the product of pressure and flow is zero and the external power is therefore negligible as well [5]. Thus external power generation exhibits a maximum for intermediate values (Chap. 15).

Relation Between the Pump Function Graph and the End-Systolic Pressure-Volume Relation

Figure 14.3 shows the qualitative comparison between the pressure-volume relation and the pump function graph [6]. We see a 'mirrored' relation between the two
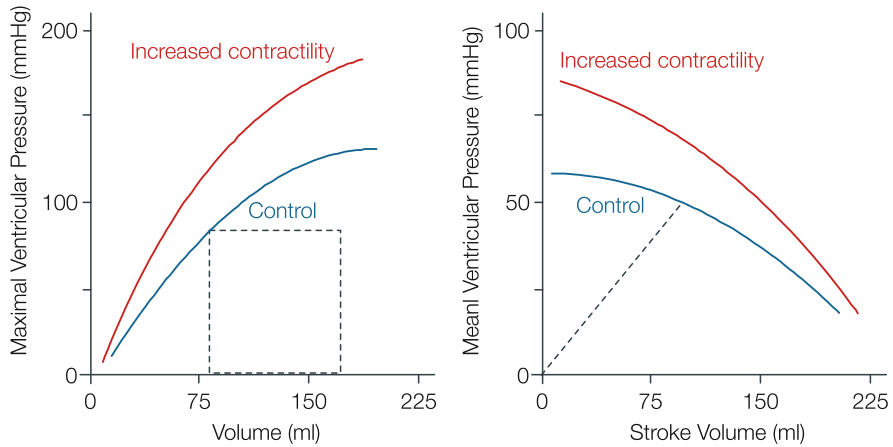
Fig. 14.3 The End-Systolic Pressure-Volume Relation (ESPVR, *left*) and the Pump Function Graph (PFG, *right*) show a 'mirrored' relationship. Increased contractility rotates the relations. Diastolic filling changes the pressure-volume loop but does not affect the ESPVR. Filling shifts the Pump Function Graph. The ESPVR is obtained by preload (filling) changes and the Pump Function Graph by afterload (resistance or comliance) changes. Note the scale difference in the pressure axes

characterizations of the heart. This follows from the fact that Stroke Volume is the decrease in ventricular volume during ejection. The main difference between the relations is that in the pressure-volume relation the end-systolic pressure, is used, while in the pump function graph the mean ventricular pressure is used.

Physiological and Clinical Relevance

The pump function graph describes the pump function of the heart for constant filling, Heart Rate and contractility. The graph is a relation between mean ventricular pressure, not mean aortic pressure, and Stroke Volume or Cardiac Output. The pump function graph teaches us that the heart is neither a flow source nor a pressure source. The flow source or in German the 'Harte Brunne' was the assumed heart model used until the 1960s. We see (Fig. 14.2) that contractility at constant loading pressure has only a small effect on Cardiac Output. Heart Rate and diastolic filling contribute importantly to CO.

The Frank-Starling Law

Figure 14.4 shows the effect of filling on the pump function graph and its meaning with respect to the Frank-Starling mechanism. Frank studied the effect of filling on isovolumic contractions. The effect of an increase in ventricular filling

EFFECT OF FILLING
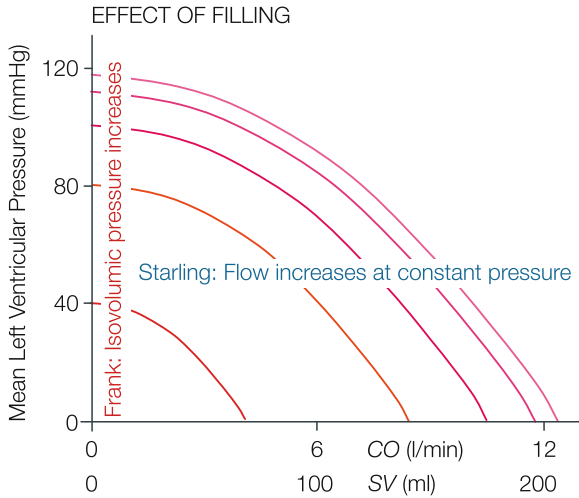
Fig. 14.4 The cardiac Pump Function Graph is a generalized description of the Frank-Starling mechanism. With increased filling the graph moves outward. One of Frank's experiments pertains to isovolumic conditions where pressure increases with filling (intercept with the pressure axis). Starling's experiment is one that keeps aortic pressure, and thus also ventricular pressure, constant so that cardiac output increases with filling

on non-ejecting, i.e., isovolumic, contractions is given by the intercepts of the pump function graphs with the pressure axis. Starling studied in the heart-lung preparation the effect of filling on Cardiac Output when aortic pressure and thus ventricular pressure was kept constant: Cardiac Output (and Stroke Volume) increases with cardiac filling.

Concentric Hypertrophy and Heart Failure

Figure 14.5 shows the pump function graph in hypertrophy and failure. In hypertrophy a flow source is approached while in failure the heart acts more like a pressure source [7].

These changes in pump function have an effect on reflected waves returning from the periphery (Chap. 21). In ventricular hypertrophy the backward pressure wave is reflected at the heart (flow source) and is added to the forward pressure wave resulting in augmentation of the wave. This extra augmentation of pressure in hypertrophy shows the contribution of the hypertrophied heart to hypertension. In failure, when the heart approaches a pressure source the reflected flow wave affects the forward flow wave negatively resulting in a decrease in Cardiac Output (Chaps. 21 and 22). Understanding of the contribution of the heart to reflected pressure and flow waves may assist in giving suggestions for possible therapy in heart failure [8].
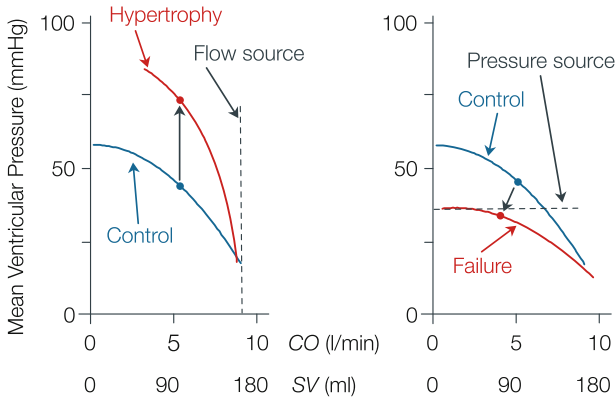
Fig. 14.5 The Pump Function Graph in hypertrophy and failure. The graph in hypertrophy has a greater slope in the working point, indicating that the heart approaches a flow source. In failure a pressure source is approached. The *dots* give the working points. Reflections against a flow source augment the pressure without affecting the flow. Reflection against a pressure source, as in failure, decreases flow but does not affect the pressure. Thus, in failure, cardiac output is diminished by reflections
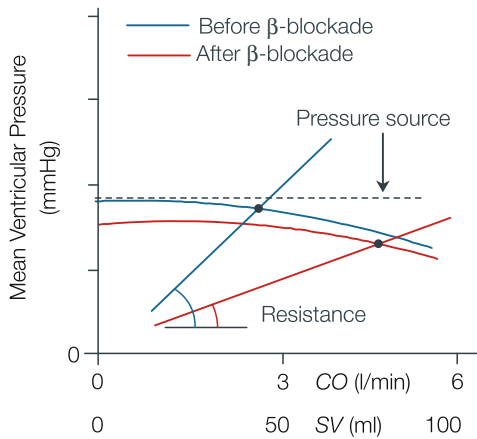
Fig. 14.6 The Pump Function Graph shows that in failure a pressure source is approached. A decrease in contractility in combination with vasodilation affects pressure little but increases cardiac output

From Fig. 14.6 it also becomes clear why in chronic heart failure beta-blockers may be beneficial even though blood pressure may be low. A decrease in contractility combined with peripheral vasodilation does, because of the 'pressure source' behavior of the heart, affect pressure little but increases Cardiac Output. Improved survival by beta-blockade was indeed shown in patients with severe chronic heart failure [9].
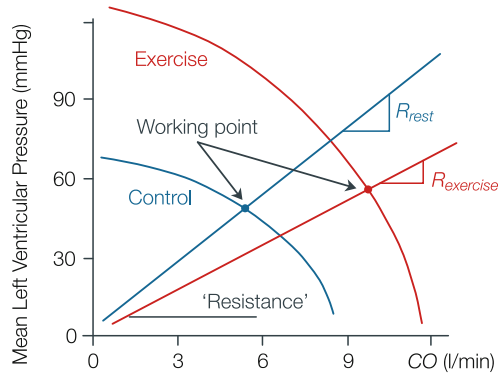
Fig. 14.7 During exercise vascular resistance decreases and the Pump Function Graph 'shifts' due to the increase in heart rate and filling, and 'rotates' since contractility increases. As a result cardiac output increases strongly with a limited increase in pressure

Exercise

Figure 14.7 shows what happens in moderate exercise. Due to the increase in Heart Rate, the (small) increase in filling, and the increase in contractility, the pump function graphs shifts outward, with a small rotation as well. The increase in Heart Rate forms the major contribution to the outward shift of the pump function graph. The systemic peripheral resistance is decreased. The overall result is an increase in Cardiac Output with only a small increase in pressure.

Limitations

The pump function graph is a global description of the heart as a pump. Changes in muscle contractility, in synchronicity or effects of local ischemia or infarction, all affect this global description.

The pump function graph, like the End Systolic Pressure Volume Relation requires at least two points for a full description. A second point can be obtained using the Single Beat Method (Chap. 17) and assuming the parabolic description of the pump function graph as proposed by van den Horn et al. [10].

Since the heart is under the influence of nervous and humoral control and the fact that diastolic filling shifts the pump function graph, the determination of the pump function graph in situ is difficult. During arterial load changes filling, Heart Rate and contractility may change due to control mechanisms so that the operating points move over a family of pump function graphs.

References

1. Elzinga G, Westerhof N. How to quantify pump function of the heart. *Circ Res* 1979;44:303–308.
2. Elzinga G, Westerhof N. Isolated cat trabeculae in a simulated feline heart and arterial system. *Circ Res* 1982;51:430–438.
3. Noble MIM. *The cardiac cycle.* 1979, Oxford & London, Blackwell.
4. Elzinga G, Westerhof N. The effect of an increase in inotropic state and end-diastolic volume on the pumping ability of the feline left heart. *Circ Res* 1978;42:620–628.
5. Elzinga G, Westerhof N. Pump function of the feline left heart: changes with heart rate and its bearing on the energy balance. *Cardiovasc Res* 1980;14:81–92.
6. Westerhof N. Cardio-vascular interaction determines pressure and flow. In: *Biological Flows.* MY Jaffrin, CG Caro Eds., 1995, New York, Plenum.
7. Elzinga G, Westerhof N. Workload as a determinant of ventricular hypertrophy. *Cardiovasc Res* 1985;19:524.
8. Westerhof N, O'Rourke MG. Haemodynamic basis for the development of left ventricular failure in systolic hypertension and for its logical therapy. *J Hypertens* 1995;13:943–952.
9. Rouleau JL, Roecker EB, Tendera M, Mohacsi P, Krum H, Katus HA, Fowler MB, Coats AJS, Castaigne A, Scherhag A, Holcslaw TL, Packer M. Influence of pretreatment systolic blood pressure on the effect of Carvedilol in patients with severe chronic heart failure (Copernicus study). *J Am Coll Cardiol* 2004;43:1423–1429.
10. van den Horn GJ, Westerhof N, Elzinga G. Optimal power generation by the left ventricle. A study in the anesthetized open thorax cat. *Circ Res* 1985;56:252–261.

Chapter 15
Cardiac Work, Energy and Power

Ventricular energy production or external work per beat can be determined from the area contained in the pressure-volume loop (*left*). External power (work per unit time) can be calculated from the product of ventricular (or aortic) pressure, *P(t)*, and flow, *Q(t)*, thus *P(t)* ·*Q(t)* in Watt (*right*). The area under the power curve equals energy per beat in Nm or Joules. Mean external power, in Watt equals energy times Heart Rate in beats per second. The calculation of energy and power does not require a linear system, as, for example, the calculation of resistance and impedance. This makes the use of energy and power very broadly applicable in hemodynamics. However, power is a characterization of heart and load together, while the End-Systolic Pressure-Volume Relation and Pump Function Graph characterize the heart and resistance and impedance characterize the arterial system.

Description

Work and the potential to do work, energy, are based on the product of force times displacement, the units being Newton times meter (Nm or Joule). When work is expressed per unit time it is called power (Nm/s or Watt). Linearity of the relations

between force and displacement (velocity) or, equivalently between pressure and volume is not required in the calculation of work and power, while it is required in the calculation of resistance and impedance.

In the heart, external work can be derived from pressure and volume through the pressure-volume loop (Chap. 13), it is the area contained within that loop. The so calculated work is, of course, the external work produced by the heart during that heartbeat and called stroke work.

Power delivered by the heart to the arterial load equals pressure times flow (Figure in box). Both pressure, P, and flow, Q, vary with time, and the instantaneous power, calculated as $P(t) \cdot Q(t)$ also varies with time. This means that instantaneous power varies over the heartbeat and is zero in diastole because aortic flow is zero. Thus, external work and power are only generated during ejection. Total energy is the integral of power, in mathematical form $\int P(t) \cdot Q(t) \, dt$, the integral sign, $\int$, together with dt implies that at all moments in time pressure and flow values are multiplied and the products added. The integration is carried out over the heart period T, but since flow is zero in diastole (assuming sufficient valves) integration over the ejection period is adequate. The average power over the heart beat is $(1/T) \cdot \int P(t) \cdot Q(t) \cdot dt$. Since aortic pressure and left ventricular pressure are practically equal during ejection, both ventricular pressure and aortic pressure may be used in the calculation.

Sometimes mean power is calculated as the product of mean pressure and mean flow (Cardiac Output). Here aortic pressure is to be used because it is the mean power delivered to the arterial system that we want to calculate. Since mean aortic pressure is about two to three times higher than mean left ventricular pressure, using ventricular pressure would lead to considerable errors [1]. The difference between total power and mean power is pulsatile power (also called oscillatory power). Pulsatile power is about 15% of total power (i.e., the oscillatory power fraction is 15%). In systemic hypertension the oscillatory power fraction is increased. In the pulmonary circulation the oscillatory power fraction is about 25%.

Physiological and Clinical Relevance

It has sometimes been reasoned that it is the mean power that is related to useful power while pulsatile power is related to moving blood forward and backward only. In other words it was thought that only mean power and work were useful quantities. The logical consequence was then to assume that pulsatile power would be minimal in physiological conditions. This in turn, was used to argue that if the Heart Rate is related to the frequency of the minimum in the input impedance modulus (Chap. 23), pulsatile power would be minimal. However, this is not correct since it is the real part of the impedance that is related to power, not the impedance modulus. Thus, the separation of mean and pulsatile power is not very useful as a measure of ventriculo-arterial coupling. Under physiological conditions the heart pumps at optimal external power [2]. See also Chap. 17.

Work and energy find their main importance in relation to cardiac oxygen consumption, metabolism, and optimal efficiency in ventriculo-arterial coupling.

Calculations

In hemodynamics the energy per beat equals pressure times volume, and power is calculated from pressure times flow. Energy per beat equals the area within the Pressure-Volume loop (the left part of the Figure in the box). This area equals about 90 ml times 100 mmHg. With 90 ml $= 0.09 \cdot 10^{-3}$ m^3 and 100 mmHg $=$ 13.3 kPa $= 13.3 \cdot 10^{+3}$ Pa $= 13.3 \cdot 10^{+3}$ N/m^2. The product of pressure and volume is then $0.09 \cdot 10^{-3}$ m$^3 \cdot 13.3 \cdot 10^{+3}$ N/m$^2 \approx 1.2$ Nm $= 1.2$ J. Multiplication by Heart Rate (beats per second) gives, with HR $= 60$ bpm, an average power output of 1.2 J/s $= 1.2$ W.

Power as a function of time is the instantaneous product of pressure and flow (right side of the Figure in the box). The area under the power curve is the work per beat, and assuming a triangular shape, the area is about ½ Peak Power times Ejection Time i.e., $\sim$½$\cdot 8 \cdot 0.3 = 1.2$ (Ws $=$ J). Multiplication by HR gives the average power output, also called mean external power.

References

1. Williams SG, Jackson M, Cooke GA, Barker D, Patwala A, Wright DJ, Albuoaini K, Tan L-N. How do different indicators of cardiac pump function impact upon the long-term prognosis of patients with chronic heart failure? *Am Heart J* 2005;150:983.
2. Toorop GP, Van den Horn GJ, Elzinga G, Westerhof N. Matching between feline left ventricle and arterial load: optimal external power or efficiency. *Am J Physiol* 1988;254:H279–H285.

Chapter 16
Cardiac Oxygen Consumption and Hemodynamics

Cardiac oxygen consumption can be determined from the product of coronary flow, Q_{coron}, and arterio-venous oxygen content difference, ΔAVO_2. Coronary artery oxygen content can be obtained from any arterial blood sample. Coronary venous or great cardiac vein oxygen content requires blood sampling at that location. Total coronary flow can be determined in the main stem coronary artery, in the periphery with microspheres, or at the venous side with thermodilution. These methods are difficult. To circumvent these preferentially simultaneous and difficult determinations, many indices for estimating oxygen consumption from mechanical variables have been proposed. It has been shown that heart rate is a primary determinant of oxygen consumption. The second major determinant is tension (stress) generation of the cardiac muscle, mostly measured as pressure generation. Pressure generation costs more oxygen than muscle shortening (flow). This means that systemic pressure generation rather than Cardiac Output determines oxygen consumption of the heart. Therefore almost all methods to derive oxygen consumption from hemodynamics are based on heart rate and pressure. The most used methods are the Rate Pressure Product (*RPP*), often used in biochemical studies, the Tension Time Index (*TTI*), and the Pressure Volume Area (*PVA*).

Description

It was shown by Sarnoff et al. [1] that the production of pressure costs much more oxygen than the production of flow or Cardiac Output (see Fig. 16.1). Also, it has been shown that oxygen consumption, VO_2, is almost proportional to Heart Rate. These findings imply that the main mechanical variables to estimate cardiac oxygen consumption are pressure and Heart Rate. If oxygen consumption is expressed per beat, pressure remains as major determinant.

Rate Pressure Product and Tension Time Index

In approximation, the product of the systolic ventricular pressure and Heart Rate can be used to estimate oxygen consumption. This so-called Rate Pressure Product, RPP, is simple to use, especially when limited to changes in oxygen consumption. The triple product, defined as $HR·P_{syst}·dP_{LV}/dt$, with dP_{LV}/dt the maximal rate of rise of ventricular pressure, has also been suggested as a measure of cardiac oxygen consumption.

Sarnoff introduced the Tension Time Index, TTI [1]. The oxygen consumption per beat is assumed to be proportional to the area under the ventricular pressure or (in absence of aorta stenosis) under the aortic pressure curve during the ejection period. Often the systolic period is used instead (Fig. 16.2). Implicitly the authors
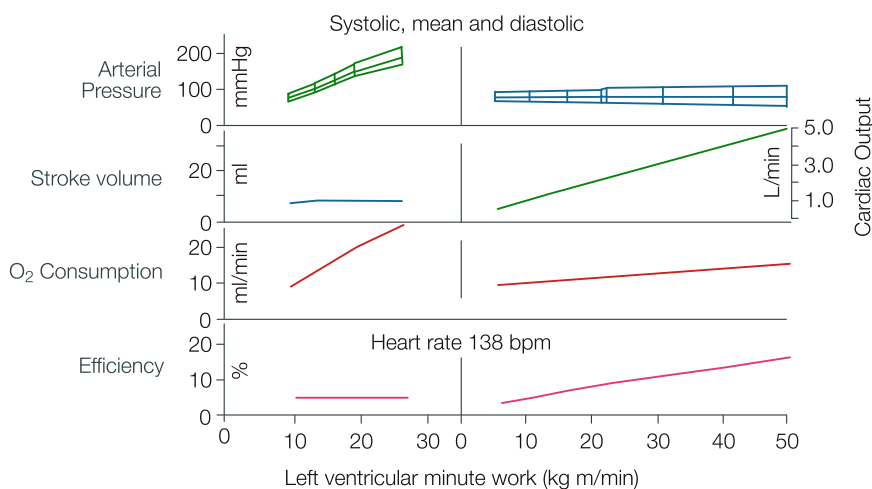
Fig. 16.1 Oxygen consumption is, at constant heart rate, primarily determined by pressure, not by flow or external work. In the *left panel* arterial pressure is increased while Stroke Volume and Cardiac Output are kept the same. The increase in pressure results in an increase in oxygen consumption. In the *right panel* Cardiac Output is increased while pressure is kept the same. Oxygen consumption changes only little. Adapted from ref. [1], used by permission

Fig. 16.2 Tension Time Index, TTI, equals the area under the pressure curve during the ejection period. Systolic and ejection periods are indicated

T_{ej}

T_{syst}
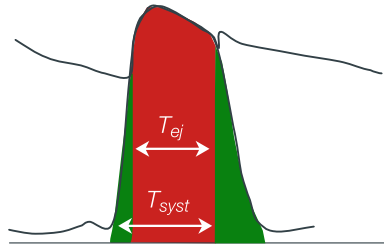
assumed this area to be proportional to the mean systolic left ventricular pressure times the duration of systole. However, it is better to use the total area under the *ventricular* pressure curve (red plus green in Fig. 16.2), and when we can neglect the contribution in diastole it follows that this area equals mean ventricular pressure, $P_{lv,mean}$, times heart period, T, i.e., TTI $\approx P_{lv,mean}$ T. In isolated heart studies where isovolumic contractions are studied, and the ejection period is negligible, the area under the *ventricular* pressure curve should be used as a measure of cardiac oxygen consumption. The TTI is a global measure of cardiac oxygen consumption, and the term tension is not meant to be local stress, but is pressure. The TTI is more difficult to measure than the RPP.

The Pressure Volume Area

Another way to estimate oxygen consumption per beat is the Pressure Volume Area (PVA, the red area in top part of Fig. 16.3). This method requires measurement of ventricular pressure and volume for at least two, and preferably more cardiac loading conditions (Chaps. 13 and 15). The relation between oxygen consumption and PVA is shown in the bottom part of Fig. 16.3, and can be written as:

$$VO_2 = a_1 \cdot PVA + a_2 \cdot E_{es} + a_3$$

where E_{es} or E_{max}, is the slope of the End-Systolic Pressure-Volume Relation (ESPVR), giving a measure of contractile state. The first term is the relation between mechanics and oxygen consumption. The two other terms together give the oxygen consumption for the unloaded or isobaric contraction, i.e., a contraction without build up of pressure. The second term is the energy cost of excitation-contraction coupling and depends on the contractile state of the cardiac muscle, expressed as E_{es}. The last term is the basal oxygen consumption, used for the maintenance of cell structure, etc. For details see Suga [2].

The following local measure of oxygen consumption has been suggested as well. The Stress Time Index, i.e., mean wall stress, derived from left ventricular pressure, times heart period, is the local formulation of the TTI. In analogy with the PVA the local Tension (or Stress) Area and Force Length Area have been suggested also (Fig. 16.3 with local area and stress or local length and stress on the axes).
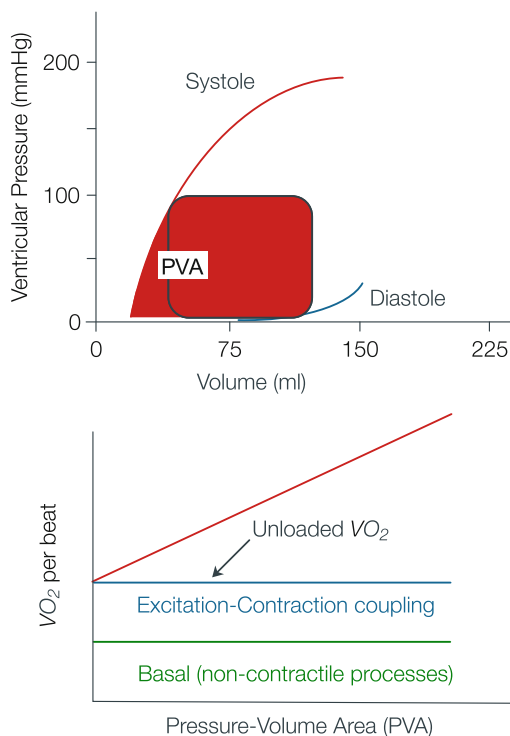
Fig. 16.3 The Pressure-Volume Area, PVA relates to cardiac oxygen consumption. Oxygen consumption is also determined by basal processes such as cell integrity and ion pumps, and by excitation-contraction coupling (activation energy). Increased contractility increases activation energy. The PVA is the third factor that determines the oxygen consumption. This is the oxygen consumption that is related to hemodynamics. The inverse slope of the relation is the so-called contractile efficiency. Adapted from ref. [2], used by permission

Since the TTI and the PVA predict oxygen consumption per beat, oxygen consumption per minute is found by multiplication with Heart Rate. If we assume the TTI to be equal to the mean ventricular pressure times heart period, multiplying with Heart Rate results in mean pressure as a measure of oxygen consumption.

An overview of other, more complex hemodynamic indicators of cardiac oxygen consumption can be found in Rooke and Feigl's report [3].

Heterogeneity of Metabolism

Not only local perfusion (Chap. 18), but also local myocardial oxygen consumption is heterogeneously distributed in the myocardium [4]. Thus perfusion and metabolism seem [5] related but the reason for this is still disputed.

Physiological and Clinical Relevance

Cardiac oxygen consumption, or oxygen demand, and cardiac oxygen supply, are in equilibrium in the normal healthy heart. The Tension Time Index (TTI) gives a measure of oxygen demand. Oxygen supply depends on coronary perfusion. Perfusion, especially to the subendocardial layers, mainly takes place in diastole when the cardiac muscle is relaxed. Thus, aortic pressure in diastole and the duration of diastole, together quantified by the area under the diastolic aortic pressure curve, and called the diastolic pressure-time index, gives a measure of oxygen supply. It has therefore been proposed that the ratio of areas under the diastolic aortic pressure and the area under the systolic pressure curve, gives an estimate of the supply-demand ratio of the subendocardial layers of the heart (see Fig. 16.4).

With increasing age wave reflections become more prominent in systole (Chaps. 21 and 22), resulting in an increase in mean systolic pressure and a decrease in mean diastolic pressure. This means that with age the supply-demand ratio decreases, which may result in ischemia in subendocardial layers. A similar reasoning can be applied to aortic valvular disease and tachycardia.

Limitations

The mechanical determinants of oxygen consumption, discussed above, can be used in individual hearts where pharmacological or other interventions are performed. The use of these determinants in different hearts should be done with care. When a dilated and hypertrophied heart is compared with a normal heart, pressures and Heart Rates may be similar, but with more muscle mass, oxygen consumption is not. In compensated concentric hypertrophy pressure is increased and wall thickness is increased in similar proportion while lumen radius is hardly changed, thereby keeping wall stresses the same (Chap. 9). This means that the Stress Volume
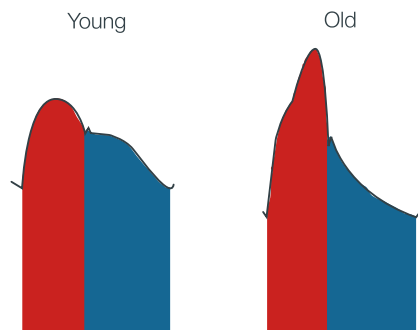
Fig. 16.4 The oxygen demand and supply. The areas under the systolic and diastolic part of the pressure curve, respectively. The ratio may be unfavorably influenced with increasing age

Area is similar in normal and hypertrophied hearts, while wall mass is increased and therefore oxygen consumption of the whole ventricle is increased. Therefore, correction for wall mass is required. Assuming wall stress to be the major determinant of oxygen consumption, total oxygen consumption would be proportional to wall mass.

Also by applying the Rate Pressure Product to mouse and man, where systolic ventricular pressure is similar but Heart Rate differs by a factor of ten, it can not be concluded that cardiac metabolism in the mouse heart is ten times that of the human heart. Even after normalizing for heart mass a difference remains because cardiac metabolism per gram of heart tissue is higher in the mouse than in the human (Chap. 30). The Pressure Volume Area, PVA, method also falls short when comparing different animals. Since the PVA predicts oxygen consumption per beat Heart Rate drops out of the equation. When normalized with respect to heart mass or body mass mouse and man would be more comparable but metabolism is not proportional to cardiac mass and body mass as will be discussed in Chap. 30.

References

1. Sarnoff SJ, Braunwald E, Welch GH, Case RB, Stainsby WN, Macruz R. Hemodynamic determinants of oxygen consumption of the heart with special relevance to the tension-time index. *Am J Physiol* 1958;192:148–156.
2. Suga H. Ventricular energetics. *Physiol Rev* 1990;70:247–277.
3. Rooke GA, Feigl EO. Work as a correlate of canine left ventricular oxygen consumption, and the problem of catecholamine oxygen wasting. *Circ Res* 1982;50:273–286.
4. van Beek JH, van Mil HG, King RB, de Kanter FJ, Alders DJ, & Bussemaker J. A (^{13})C NMR double-labeling method to quantitate local myocardial O(2) consumption using frozen tissue samples. *Am J Physiol* 1999;277:H1630–H1640.
5. Alders DJ, Groeneveld AB, de Kanter FJ, van Beek JH. Myocardial O2 consumption in porcine left ventricle is heterogeneously distributed in parallel to heterogeneous O2 delivery. *Am J Physiol* 2004;287:H1353–H1361.

Chapter 17
Cardiac Power and Ventriculo-Arterial Coupling

The heart pumps close to maximal external power and efficiency *(left)*. To test this, ventriculo-arterial coupling analysis is shown on the *right hand side*. On the left relations are shown as a function of *CO*. The *top panel* shows the Pump Function Graph, the *second panel* Oxygen Consumption, and the *third and fourth panels* show Mean Power Output and Cardiac Efficiency. The data were obtained by changing the arterial load while keeping the cardiac filling, contractility and heart rate constant. Both external power and efficiency exhibit a maximum. These maximums are not found at the same flow because O_2 consumption decreases with larger flow, i.e., with lower ventricular pressure (see Chap. 16). Both power and efficiency exhibit shallow relations without sharply defined maximum implying that under normal conditions the heart pumps close to maximal efficiency and maximal power, and efficiency is about 20−25%. The remaining energy is dissipated as heat and carried away by the coronary circulation and by diffusion to the thorax and cardiac lumen. It has been reasoned that the optimum of power results from size constraints of the heart. Whether the heart is pumping at optimal efficiency or optimal power (ventriculo-arterial coupling), or neither, depends on both the cardiac and the arterial state. The *right hand figure* shows how to analyze coupling. *The slope* of the ESPVR (E_{es}, see Chap. 13) characterizes the ventricle and the effective arterial elastance (E_a), which approximately equals total peripheral resistance over heart period, *R/T*, characterizes the arterial system. When $E_a /E_{es} \approx 1$, external work is maximized, and when $E_a /E_{es} \approx 0.5$ cardiac efficiency is maximal.

Description

Power and Efficiency

Cardiac efficiency is defined in analogy to that of a hydraulic pump. The external power is calculated from pressure times flow (Chap. 15) and the 'input power' is calculated from cardiac oxygen consumption (Chap. 16). The ratio of external, or produced power, and input power is defined as efficiency. Therefore, both external power and input power need to be expressed in the same units. When glucose or free fatty acids are consumed oxygen consumption can be expressed in Joules and oxygen consumption per time in Watts, through the so-called caloric equivalent. For carbohydrate and fat metabolism it holds that 1 ml $O_2 \approx 20$ J and 1 ml O_2/min ≈ 0.33 W. A review on cardiac energetics has been published by Suga [1].

Maximum Cardiac Efficiency and Maximum Power in the Intact Animal

The pressure and flow generated by the heart and the arterial load can be studied while keeping the Heart Rate, diastolic filling and contractility unaltered [2]. Power can be calculated from the pressure and flow. The Figure in the box, on the left, shows that, when power is plotted as a function of Cardiac Output it exhibits an optimal value. This can be understood with the cardiac pump function graph in mind, (top panel of box Figure, Chap. 14). For a high load (isovolumic contraction) pressure generated is high but flow is zero. Power, the product of pressure and flow, is therefore negligible. Inversely, for a very low load the heart generates a large flow but negligible pressure so that power is negligible as well. Thus, power, at some intermediate value of Cardiac Output, must be maximal. This power maximum was found, in the intact cat [3], to coincide with the working point, i.e., when a physiologic arterial load is present (see Fig. 17.1). It has also been reported that the left ventricle works at maximal efficiency [4].

Local Work and Power

It is of great interest if local power and efficiency could be derived. However, this is difficult since local work, and local oxygen consumption are hard to measure accurately. Local work can be derived by local shortening times local stress. The first, local shortening can be obtained from (surface) markers attached to the muscle or by MRI-tagging (magnetically induced markers in the myocardium). Local forces are only possible to derive indirectly from pressure and anatomy
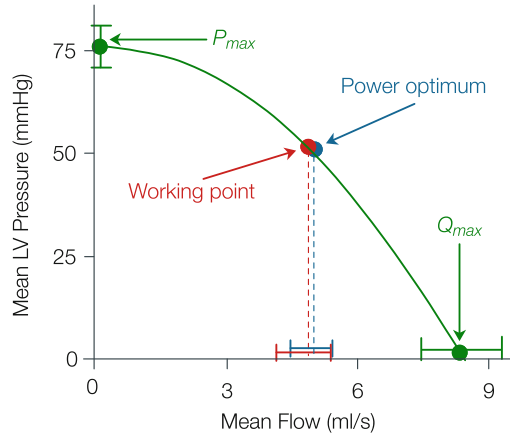
Fig. 17.1 The heart pumps at optimal power output. Power output of the heart studied in the intact animal for different arterial loads. Other determinants of pressure and flow, heart rate, diastolic filling and contractility, are kept constant. When the physiological arterial load is present, shown as the working point, power transfer is maximal. Adapted from ref. [3], used by permission

(sophisticated forms of Laplace's law, Chap. 9). This technique was used by Prinzen et al., to study effect of pacing site on local work [5]. When local oxygen consumption is also determined [6] local efficiency can be derived. However, local stresses derived from pressure are difficult to verify.

Heat Production and Transport

The heart is about 20–25% efficient. This implies that about 75% of the oxygen consumed is converted into heat. The heat is removed by diffusion to lumen and thorax, and convection by coronary flow, in about equal amounts (Fig. 17.2). In the mid-wall of the myocardium the temperature is a few tenths of a degree Celsius higher than in subepicardial and subendocardial layers allowing for diffusion of heat [7].

Assessment of Ventriculo-Arterial Coupling

Optimum power and efficiency are assumed measures of good ventriculo-arterial coupling. Whether the heart functions on optimum power or efficiency can be derived from hemodynamic principles. The two parameters assumed to be the determining ones are the slope of the left ventricular End-Systolic Pressure–Volume Relation, E_{es} or E_{max}, and effective arterial elastance, E_a. The effective arterial elastance is defined as $E_a = P_{es}/SV$, i.e., end-systolic (ventricular or aortic) pressure

Fig. 17.2 Oxygen consumption produces not only mechanical power but also heat. Convection by coronary flow and diffusion to thorax and cardiac lumen together, each account for about 50% of the heat loss, depending on the magnitude of the coronary flow
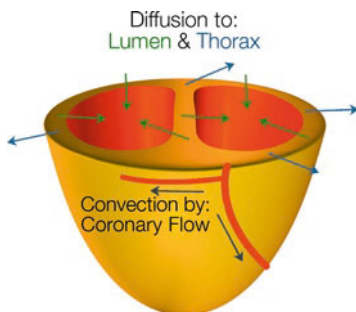
Fig. 17.3 End-systolic pressure is close to mean aortic pressure, allowing for noninvasive determination of P_{es}
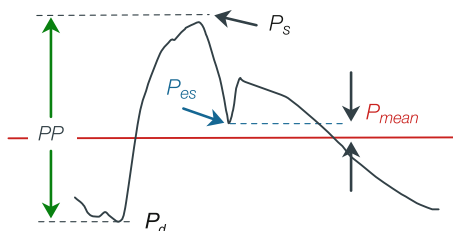
over Stroke Volume, (right side of the Figure in the box). The ratio E_a/E_{es} is considered a ventriculo-arterial coupling parameter and when $E_a/E_{es} \approx 1$ external work is maximized, while for $E_a/E_{es} \approx 0.5$ cardiac efficiency is maximal [8].

To determine these two parameters, several simplifications have been used. The E_a can be approximated as follows. End-systolic pressure is close to mean arterial pressure (Fig. 17.3). With Cardiac Output, CO, being $SV\ HR$, and Heart Period T, in seconds, the inverse of HR, $CO = SV/T$, we find that $P_{es}/SV \approx P_{mean}/CO \cdot T = R_p/T$. Thus the effective arterial elastance, E_a, is primarily a measure of vascular or peripheral resistance, R_p, and hardly reflects the compliant properties of the large conduit arteries. Therefore the term 'elastance' is misleading. Note that E_a depends on vascular resistance, which is a purely arterial variable, and on heart period, T, which is a purely cardiac variable. Therefore, E_a is a coupling parameter by itself. The E_a can be derived from noninvasive measurements: mean pressure (by sphygmomanometer) and Cardiac Output (US or MRI), and Heart Rate.

The maximum or End-Systolic elastance, E_{es} is calculated from $E_{es} = P_{es}/(V_{es} - V_d)$. End-Systolic volume can be measured noninvasively, but V_d is hard to estimate. To derive this intercept volume, at least one other point on the ESPVR should be obtained. This would require changes in diastolic filling that are often not feasible in very sick patients and in epidemiological studies. One method to determine the End-Systolic Pressure–Volume Relation is the one suggested by

Sunagawa et al. [8], where an isovolumic left ventricular pressure is predicted from the pressure of an ejecting beat (Single Beat Method). However, none of the so-called single beat methods to determine the ESPVR has been shown to give accurate estimates [9]. Nevertheless, the Single Beat Method is, at present the best approach in practice.

In a number of studies it has simply been assumed that $V_d = 0$ [10, 11]. This assumption leads to a very interesting simplification of the analysis. With the $V_d = 0$, $E_{es} = P_{es}/V_{es} = P_{es}/(V_{ed} - SV)$. The ratio E_a/E_{es} then becomes equal to:

$$E_a / E_{es} = (P_{es} / SV) / [P_{es} / (V_{ed} - SV)] = (V_{ed} - SV) / SV = 1 / EF - 1$$

with EF, the Ejection Fraction. We see that the P_{es} disappears altogether only leaving the determination of Ejection Fraction. This implies that work is maximal when $E_a / E_{es} = 1$, thus when EF = 0.5. Similarly, cardiac efficiency is maximal when $E_a/E_{es} = 0.5$ or when EF = 0.67.

Thus the assumption of a negligible V_d simplifies matters. However, negligible V_d values are difficult to verify, mostly not correct, and are certainly leading to large errors in case of a dilated heart (Chaps. 13 and 15).

The effective arterial elastance (E_a), has the units of elastance but is not an elastance; it is closely related to total peripheral resistance. It is approximately R_p/T and thus is not related to total arterial compliance. Several authors [12] have interpreted E_a as a measure of total arterial compliance, an interpretation that leads to confusion and is clearly wrong.

Theory of Optimal Heart Size

Why does the left ventricle pump at maximum power, while a feedback control for power is not known to exist? A simple answer to this question can be given based on the following reasoning [13]. Consider the pump function graph (Fig. 17.4). The working point, i.e., the point where maximum power is found, is for a flow which is about 58% maximal flow, Q_{max}. Mean ventricular pressure and Cardiac Output together determine the working point. Pressure is similar in mammals and Cardiac Output is determined by body size (Chap. 30). Several pump function graphs can be drawn through this working point. We begin by assuming that muscle stress is a given quantity, and that the ventricle is a sphere. On the one hand, a larger intercept of the pump function graph with the flow axis, i.e., a larger Q_{max}, implies a larger ventricular lumen requiring a thicker wall (Law of Laplace, Chap. 9), to maintain muscle, or wall stress. On the other hand, with a larger Q_{max} a smaller P_{max} results so that the wall may be less thick. In this way it is possible to calculate ventricular volume for the different pump function graphs through the working point, each with its own Q_{max}. Plotting ventricular volume as a function of Q_{max}, results in the graph given in Fig. 17.4. The minimum volume is found when the working point is at about 60% of Q_{max}, and this is the same value as where maximum power and efficiency
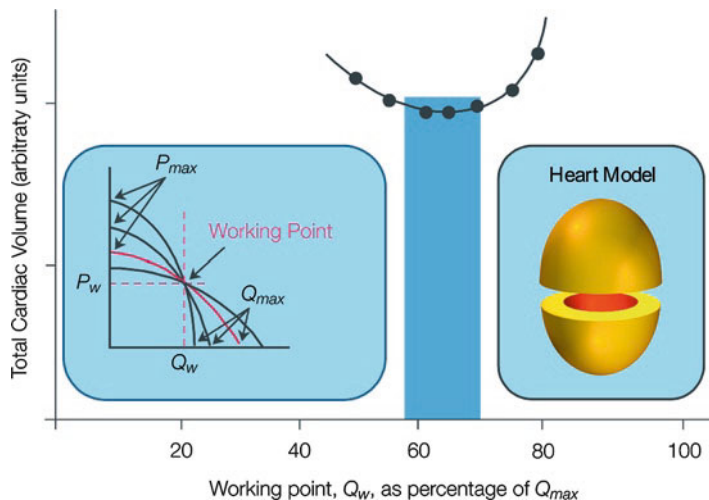
Fig. 17.4 Total ventricular volume, i.e., wall plus lumen volume, can be calculated assuming a spherical shape, right, and a fixed, maximal, wall stress, σ_m, for isovolumic contractions. Thus P_{max} relates to wall volume (Chap. 9), and larger P_{max} implies larger wall volume to keep wall stress the same. Increased Cardiac Output relates to ventricular lumen and wall volume. Many Pump Function Graphs through the working point are possible, left, but the Pump Function Graph where the working point is about 60% of Q_{max}, i.e., where maximal power and efficiency are found, corresponds with the smallest total (wall plus lumen) ventricular volume. Adapted from ref. [13], used by permission

are found. The minimum in heart volume thus corresponds to a working point where power and efficiency are about maximal. In other words, the size of the heart is minimized, and, for this minimal heart volume the heart pumps at maximal power.

Physiological and Clinical Relevance

Cardiac oxygen consumption and efficiency are still difficult to obtain in the patient. Modern techniques, such as Positron Emission Tomography (PET) and Magnetic Resonance Spectroscopy (MRS) may change this. Assessment of glucose metabolism with ^{18}F-fluorodeoxyglucose measures glucose uptake into myocardial cells, but not its conversion by glycolysis. Myocardial oxidative metabolism can be measured by ^{11}C-labeled acetate PET. For lipid metabolism, tracer examples are ^{123}I-beta-methyl-p-iodophenyl pentadecanoic acid and [15]-(O-^{123}I-phenyl)-pentadecanoic acid. These tracers can be detected by planar scintigraphy and single-photon emission computed tomography (SPECT), which are more economical and more widely available than PET. With current MRS techniques, ^{31}P-labeled magnetic resonance spectroscopy, Phosphate/Creatine and/or pH can be obtained in humans but this is not common yet. The hemodynamic determinants for oxygen consumption, as discussed in Chaps. 16 and 17,

are only valid in single hearts during acute interventions and cannot be used in comparing different patients.

'Output power' requires the measurement of aortic or ventricular pressure and flow. Thus for the calculation of efficiency, which is the ratio of 'Output power' and 'Input power', many measurements are required and therefore efficiency is not calculated routinely. In Chap. 30 it is shown that in healthy mammals cardiac metabolism is proportional to body mass to the power $-1/4$, implying that metabolism per gram of heart tissue decreases with body mass.

Related Issues

Contractile efficiency. On the basis of the Pressure Volume Area concept (Chap. 16) the contractile efficiency has been defined as the inverse of the slope of the Pressure Volume Area – VO_2 relation [1]. This definition of efficiency only accounts for the mechanical aspects of oxygen consumption and does not take into account the oxygen expenditure related to activation and basic metabolism. Therefore this contractile efficiency is about twice the actual cardiac efficiency.

Power in cardiogenic shock. Although power is a rather abstract measure, it has been shown that it is the strongest hemodynamic correlate of mortality in cardiogenic shock [14].

Economy. At the extremes of the pump function graph, the heart generates neither pressure nor flow. External power and thus efficiency is zero. In isolated heart studies (Langendorff preparations) where the heart contracts isovolumically or in isolated cardiac muscle studies, when the muscle contracts isometrically, contraction economy can be used instead. Economy of contraction is defined as oxygen consumption used for isovolumic or isometric contractions.

References

1. Suga H. Ventricular energetics. *Physiol Rev* 1990;70:247–277.
2. Elzinga G, Westerhof N. Pump function of the feline left heart: changes with heart rate and its bearing on the energy balance. *Cardiovascular Res* 1980;14:81–92.
3. Toorop GP, Van den Horn GJ, Elzinga G, Westerhof N. Matching between feline left ventricle and arterial load: optimal external power or efficiency. *Am J Physiol* 1988;254:H279–H285.
4. Burkhoff D, Sagawa K. Ventricular efficiency predicted by an analytical model. *Am J Physiol* 1986;250:R1021–R1027.
5. Prinzen FW, Hunter WC, Wyman BT, McVeigh ER. Mapping of regional myocardial strain and work during ventricular pacing: experimental study using magnetic resonance imaging tagging. *J Am Coll Cardiol* 1999;33:1735–1742.
6. van Beek JH, van Mil HG, King RB, de Kanter FJ, Alders DJ, Bussemaker J. A (^{13})C NMR double-labeling method to quantitate local myocardial O(2) consumption using frozen tissue samples. *Am J Physiol Heart Circ Physiol* 1999;277:H1630–H1640.

7. ten Velden GH, Elzinga G, Westerhof N. Left ventricular energetics. Heat loss and temperature distribution of canine myocardium. *Circ Res* 1982;50:63–73.
8. Sunagawa K, Maughan WL, Sagawa K. Optimal arterial resistance for the maximal stroke work studied in the isolated canine left ventricle. *Circ Res* 1985;56:586–595.
9. Kjorstad KE, Korvald C, Myrmel T. Pressure-volume-based single beat estimations cannot predict left ventricular contractility in vivo. *Am J Physiol* 2002;282:H1739–H1750.
10. Grosu A, BomGrosu A, Bombardini T, Senni M, Duino V, Gori M, Picano E. End-systolic pressure/volume relationship during dobutamine stress echo: a prognostically useful non-invasive index of left ventricular contractility. *Eur Heart J* 2005;26:2404–2412.
11. Saba PS, Roman MJ, Ganau A, Pini R, Jones EC, Pickering TG, Devereux RB. Relationship of effective arterial elastance to demographic and arterial characteristics in normotensive and hypertensive adults. *J Hypertens* 1995;13:971–977.
12. Senzaki H, Iwamoto Y, Ishido,H, Masutani S,Taketazu S, Kobayashi T, Katogi T, Kyo S. Ventricular–Vascular stiffening in patients with repaired coarctation of aorta. *Circulation* 2008;118:191–198.
13. Elzinga G, Westerhof N. Matching between ventricle and arterial load. An evolutionary process. *Circ Res* 1991;68:1495–1500.
14. Fincke R, Hochman JS, Lowe AM, Menon V, Slater JN, Webb JG, LeJemtel TH, Cotter G. Cardiac power is the strongest hemodynamic correlate of mortality in cardiogenic shock: a report from the SHOCK trial registry. *J Am Coll Cardiol* 2004;44:340–348.

Chapter 18
The Coronary Circulation
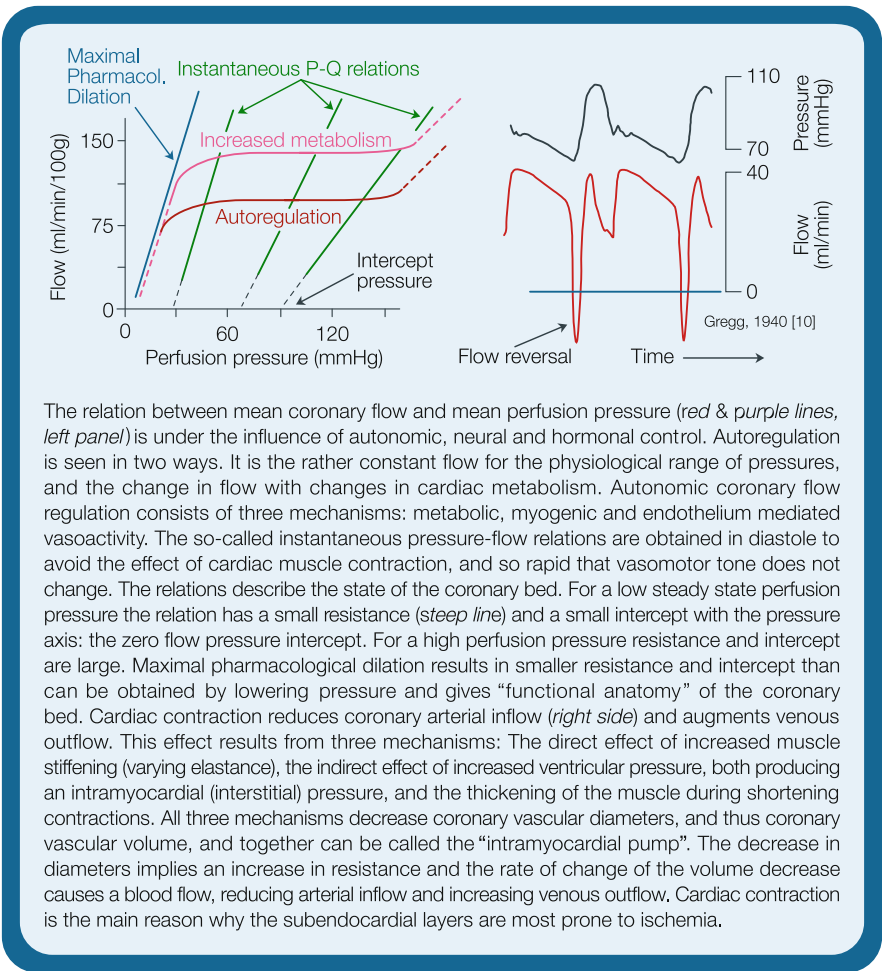
The relation between mean coronary flow and mean perfusion pressure (*red* & *purple lines, left panel*) is under the influence of autonomic, neural and hormonal control. Autoregulation is seen in two ways. It is the rather constant flow for the physiological range of pressures, and the change in flow with changes in cardiac metabolism. Autonomic coronary flow regulation consists of three mechanisms: metabolic, myogenic and endothelium mediated vasoactivity. The so-called instantaneous pressure-flow relations are obtained in diastole to avoid the effect of cardiac muscle contraction, and so rapid that vasomotor tone does not change. The relations describe the state of the coronary bed. For a low steady state perfusion pressure the relation has a small resistance (*steep line*) and a small intercept with the pressure axis: the zero flow pressure intercept. For a high perfusion pressure resistance and intercept are large. Maximal pharmacological dilation results in smaller resistance and intercept than can be obtained by lowering pressure and gives "functional anatomy" of the coronary bed. Cardiac contraction reduces coronary arterial inflow (*right side*) and augments venous outflow. This effect results from three mechanisms: The direct effect of increased muscle stiffening (varying elastance), the indirect effect of increased ventricular pressure, both producing an intramyocardial (interstitial) pressure, and the thickening of the muscle during shortening contractions. All three mechanisms decrease coronary vascular diameters, and thus coronary vascular volume, and together can be called the "intramyocardial pump". The decrease in diameters implies an increase in resistance and the rate of change of the volume decrease causes a blood flow, reducing arterial inflow and increasing venous outflow. Cardiac contraction is the main reason why the subendocardial layers are most prone to ischemia.

Description

The relations between arterial pressure and flow in the coronary bed are under the influence of the humoral-nervous systems, and under local control, i.e., autoregulation. There is also the mechanical effect of the contracting cardiac muscle on coronary flow. Several other mutual interactions of smaller magnitude between the coronary vasculature and the cardiac muscle exist, which will be discussed below. The quantitative contribution of humoral and nervous control will not be discussed here. For a comprehensive description of coronary hemodynamics see refs. [1–3].

Autoregulation of Coronary Flow

In the beating heart and in the physiological pressure range (40–140 mmHg) the relation between mean coronary flow and mean perfusion pressure shows a rather constant mean coronary flow (left part of Figure in the box). With increased and decreased cardiac metabolism the plateau of the curve increases and decreases, respectively. The fact that the plateau of the autoregulation curve depends on cardiac metabolism suggests that metabolic autoregulation is a primary effect that mainly plays a role in the smallest arterioles, which are in close contact with the cardiac muscle. A single mediator, originally thought to be adenosine, is too simple a theory for metabolic autoregulation. There is a fundamental difference in the equations required to express the effects of metabolic products such as adenosine, carbon dioxide, and pH, and ions, all of which cause vasodilatation, and the equations for oxygen which causes vasoconstriction. It is low oxygen content with increased usage that is postulated to cause metabolic vasodilatation. Mathematical modeling [4] and the proven relation between coronary vascular resistance and tissue and venous oxygen tension [5] suggest an important role of oxygen, and provide a statistically better fit to observed data than models based on vasodilating metabolic products.

Whereas metabolic autoregulation provides flow adaptation to tissue energy requirements, myogenic autoregulation provides adaptation to changes in transmural pressure. Myogenic autoregulation results from an intrinsic property of (smooth) muscle, that tries to maintain muscle tension constant (Fig. 18.1). An increase in pressure initially increases the vessel diameter and the wall stress. The subsequent vasoconstriction decreases vessel radius and increases wall thickness thereby reducing the wall stress (See Chap. 9). The myogenic response appears the strongest in the medium sized arterioles, and is a mechanism to minimize capillary pressure variations. The response time of metabolic and myogenic regulation is in the order of seconds. It is of interest to remark that almost the same relationship was found between coronary conductance and coronary venous PO_2 (reflecting tissue PO_2), for perfusion pressure changes and for pacing-induced
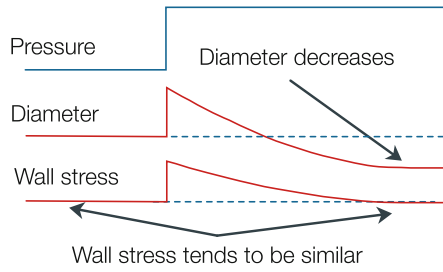
Fig. 18.1 The myogenic response. An increase in pressure increases vessel diameter and wall tension. Subsequent smooth muscle contraction reduces the diameter, to smaller than initial values, and restores wall stress
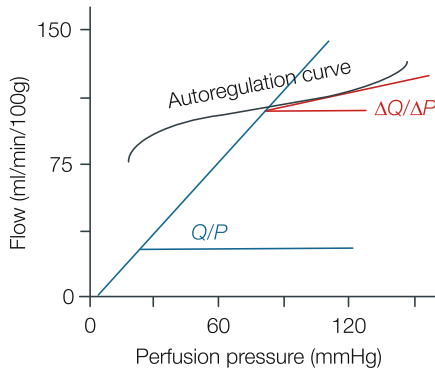
Fig. 18.2 Autoregulation gain, G, is defined as one minus the ratio of the local slope ($\Delta Q/\Delta P$) and the slope of the line through the origin (Q/P, i.e., 1/Resistance): $G = 1 - (\Delta Q/\Delta P)/(Q/P)$. In perfect autoregulation $G = 1$. Gain depends on perfusion pressure

changes in MVO_2 [6]. This suggests that tissue PO_2 may also play a part in pressure adaptation, in this case increases of pressure causing increasing PO_2 which causes vasoconstriction.

Endothelium mediated vasoactivity results from the fact that perfusion flow determines shear stress on the endothelial cells, which liberate vasodilators such as NO and prostaglandins. The main effect is in the larger, vessels, rather than in the resistance vessels [7]. Especially during strong vasodilation and thus large flow, increased diameters keep the pressure drop over the conduit system minimal.

When perfusion pressure changes the myogenic response and endothelium mediated regulation will be activated first, and metabolic regulation may follow. For a change in cardiac metabolism, the metabolic regulation will be initiated first and the other two will follow.

Autoregulation Gain

Autoregulation gain (Fig. 18.2), G, is a measure of the strength of autoregulation, and can be calculated as:

$$G = 1 - (\Delta Q / \Delta P) / (Q / P)$$
$$= 1 - (\Delta Q / Q) / (\Delta P / P)$$

with $\Delta Q/\Delta P$ the slope of the mean pressure – mean flow relation and Q/P the slope of the line through the point of determination, the working point, and the origin of the graph, the inverse of resistance. It can be seen that for perfect autoregulation the gain equals 1 and for no autoregulation, assuming the pressure-flow relation would go through the origin, the gain equals zero. Since the pressure-flow relation does, in general, not go through the origin, it has been suggested to use the slope of the instantaneous pressure-flow relation instead of Q/P. Autoregulation gain can be plotted as a function of pressure to obtain the range of regulation.

Reactive Hyperemia and Maximal Vasodilation

When cardiac oxygen demand increases, as in exercise, coronary flow will increase and the increase is called exercise hyperemia. During a (short) coronary occlusion the coronary vessels dilate and after the release of the occlusion flow is temporarily enhanced, a phenomenon called reactive hyperemia. In the normal coronary bed the maximal increase in flow is about fourfold.

Even during maximal exercise a brief coronary occlusion still results in reactive hyperemia [8]. It is possible to increase coronary flow pharmacologically (e.g., adenosine) and maximal pharmacologic vasodilation can lead to a smaller resistance than physiologic dilation (see left part of Figure in the box). When a coronary stenosis is present the magnitude of the reactive hyperemia is reduced. Quantification is then usually presented as Flow Reserve or Fractional Flow Reserve (see Chap. 5).

Instantaneous Pressure-Flow Relations

The coronary pressure-flow relations are under the influence of the vasomotor tone of the smooth muscle and the effect of the cardiac contraction on the vasculature. To get insight into the vasculature alone, the effect of cardiac contraction is to be minimized. This means that pressure-flow relations should be obtained in diastole.

Bellamy [9] studied pressure-flow relations in long diastoles obtained by vagal stimulation (Fig. 18.3). Since the smooth muscle is of the slow contracting fiber type, it is assumed that over a single long diastole, of about 1–2 s, vascular tone

Fig. 18.3 The instantaneous pressure-flow relation can be determined from a long diastole. It gives the 'state' of the bed, without the mechanical effect of cardiac muscle contraction, and during constant vasomotor tone. Adapted from ref. [9], used by permission
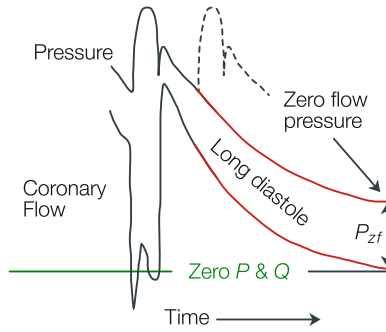
does not change. Thus the instantaneous pressure-flow relation describes the coronary vascular tree independently of the cardiac muscle contraction and for a constant vasomotor tone.

The instantaneous pressure-flow relations (see Figure in the box) show an intercept, P_{zf}, with the pressure axis, the so-called zero-flow pressure. The zero-flow pressure and the inverse slope (i.e., resistance) increase with vasomotor tone. Several explanations have been given for the intercept pressure, but none of them is generally accepted. Since the intercept pressure also is present with crystalloid perfusion, it is not the effect of plugging by blood cells [10]. Surface tension [11] has been proposed as a mechanism as well, but the changes in intercept with tone are hard to explain with this theory.

The most likely explanation is that the intercept pressure results from microvascular compliance which increases with the lowering of pressure [12, 13]. The zero-flow pressure thus may be an apparent intercept, which is related to the plateau of the pressure-volume relation of the arterioles [12]. Increased vasomotor tone increases the level of the plateau of the pressure-volume relation and this could explain the increase in the, apparent, intercept.

Cardiac Contraction and Coronary Flow

Coronary arterial inflow is impeded and venous outflow is augmented during cardiac contraction. When the coronary bed is vasodilated and cardiac muscle contractility is high, arterial flow may even reverse in early systole (see right part of the Figure in the box [14]).

The contracting cardiac muscle exerts its effect on the vasculature in three ways [3]. The increasing stiffness of the muscle in systole (see $E(t)$, Chap. 13) has a similar effect on the interstitial volume and the blood vessels as it has on the lumen of the ventricle (Fig. 18.4). This pumping action causes the vascular diameters and
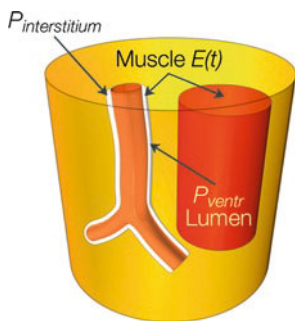
Fig. 18.4 Cardiac contraction implies increased stiffness of the muscle. For ventricular lumen and interstitium this increase in elastance results in a 'pumping' action. Ventricular pressure is also transmitted to interstitium, giving an intramyocardial pressure. Muscle thickening during shortening also affects the vessels. The result of these three mechanisms is decreased vascular volume and increased resistance
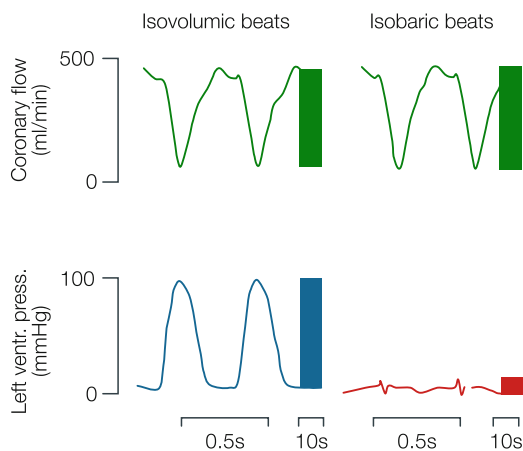
Fig. 18.5 Coronary flow during isovolumic beats (*left*), and isobaric contractions (*right*), of the isolated blood perfused cat heart. From ref. [15], used by permission

thus vascular volume to decrease in systole. Support for this mechanism is shown in the Fig. 18.5. This direct effect of the varying elastance, $E(t)$, is similar for isovolumic and isobaric contractions, i.e., contractions without pressure generation in the ventricular lumen. The ventricular load affects ventricular pressure and ventricular outflow, but when the aortic and coronary sinus pressure are unaffected, a similar pumping effect on coronary flow during both isovolumic and isobaric contractions is found [15].

The other effect is that of the pressure in the left ventricle, which, incidentally, also arises from the varying elastic properties of the cardiac muscle (Chap. 13). Ventricular pressure generates a so-called intramyocardial or interstitial pressure, which acts on the outer surface of the blood vessels. This partial explanation is called
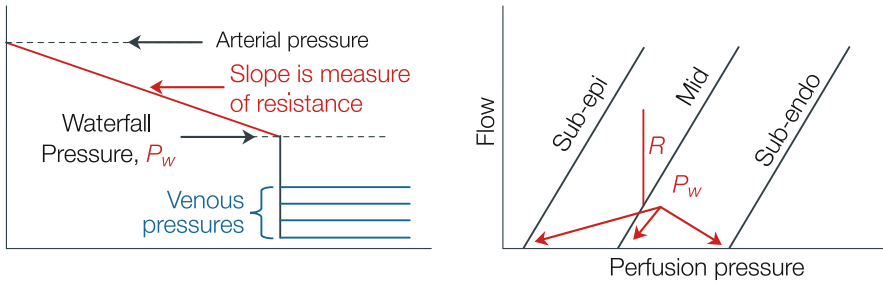
Fig. 18.6 The waterfall model is used to explain the effect of cardiac contraction on coronary arterial inflow. The waterfall pressure, P_w, is assumed to be proportional to left ventricular pressure with $P_w = P_{lv}$ sub-endocardially, and negligible sub-epicardially. Resistance $= (P_{arterial} - P_{waterfall})/$flow
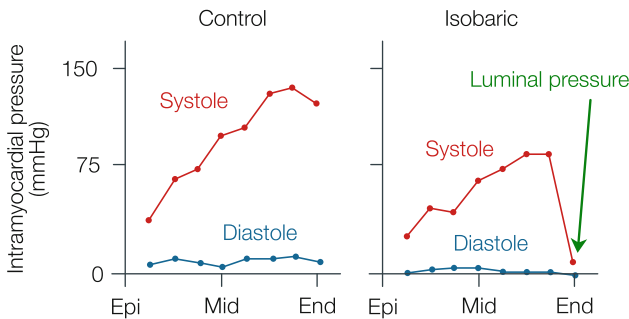
Fig. 18.7 Intramyocardial pressures measured in the beating heart using the servo-null technique. The intramyocardial pressure is high in isobaric beats where ventricular luminal pressure is negligible. Adapted from ref. [21], used by permission

the vascular waterfall (Fig. 18.6). The intramyocardial pressure is assumed to be equal to ventricular pressure at the subendocardium and negligible at the subepicardium [16]. However, there is some doubt regarding this assumption, since intramyocardial pressure is still considerable even when ventricular luminal pressure is negligible as in isobaric beats (Fig. 18.7). Also the waterfall model does not explain the increase in venous outflow during cardiac contraction [17]. Intramyocardial pressure decreases transmural pressure of the vessels and thus vascular diameters and vascular volume. Finally muscle shortening affects the vasculature since by shortening the muscles increase in diameter. The increase in muscle diameter takes place at the expense of the vessels, thereby decreasing their diameters [18]. These two effects, muscle elastance changes and muscle thickening, play complementary roles, since for isovolumic beats left ventricular pressure is high and so is intramyocardial pressure but muscle thickening is small because the muscles shorten little. For isobaric beats muscles shorten and thus thicken and this effect is larger than the pressure related effect. These two mechanisms also explain why cardiac contraction affects the subendocardial layers most and suggests the reason why the subendocardial

layers are more prone to ischemia than subepicardial layers. All these effects act directly on the vessels and are not coupled via vascular compliance as has been suggested earlier. This implies that not only during rhythmic contractions, but also in the steady state of contraction, i.e., systolic arrest, diameters are decreased and resistance is increased. Mean flow is indeed decreased in systolic arrest [19].

Since normal contraction is dynamic, the rate of change of vascular volume results in a blood flow. The vascular blood is therefore 'pumped', in a similar way as the ventricular pump, but since valves are absent, the blood is pumped to the arterial and to the venous side, with the amount depending on aortic and venous pressures. The inflow of blood, at the arterial side, is thus decreased and the outflow, at the venous side, is increased.

Detailed calculations have shown that the varying stiffness of the cardiac muscle, the thickening of the shortening muscle, and the increased intramyocardial pressure resulting from left ventricular pressure during contraction all contribute to decreased vessel size and therefore the increased resistance and intramyocardial pumping. The contribution of these effects depends on the layer, mode of contraction and the contractility [20].

The summary of the effects of cardiac contraction on the coronary vessels is given in Fig. 18.8. The pressure-flow relations show an intercept that depends on the layer, on contractility, left ventricular pressure, and muscle shortening [3, 20].

When it is assumed that coronary perfusion only takes place in diastole we can approximate the coronary fractional perfusion time, i.e., the perfusion time relative to the heart period T, as $T_d/T = 1 - T_s/T$, with T_d and T_s the duration of diastole and systole, respectively. Thus with a Heart Rate of 60 bpm, and the duration of systole being 0.35 s, the coronary fractional perfusion time is $1 - 0.35/1 = 0.65$ s/s. When Heart Rate is increased to 120 bpm, i.e., $T = 0.5$ s, as in exercise, and the ejection period decreases to 0.3 s the coronary fractional perfusion time is $1 - 0.3/0.5 = 0.4$ s/s, thereby decreasing coronary perfusion.
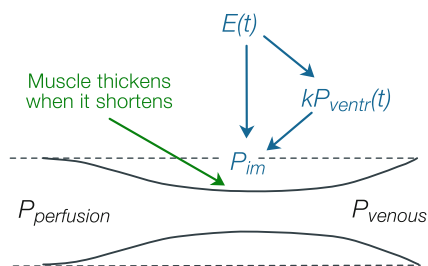
Fig. 18.8 Summary of the effects of cardiac contraction on coronary flow. Muscle contraction results in stiffer environment and in ventricular pressure, both leading to P_{im}. When the muscle shortens it thickens at the expense of the vasculature. These three mechanisms all play a role depending on the layer in the heart wall. The variations in vascular diameters result in 'pumping' of blood retrogradely to aorta and antegradely to the veins, the amounts depending on cardiac contraction, and aorta and venous pressures

Microvascular Aspects

Intramyocardial pressure has been measured for many years with different techniques [3, 21]. A recent method is the measurement with the servo-null technique, using micropipettes (diameter in the micron range) so as to cause minimal damage [21]. The results of these measurements are shown in Fig. 18.7. Thus intramyocardial pressure is not simply proportional to ventricular pressure. For the interstitial space the varying elastance hypothesis was applied to explain why intramyocardial pressure is present and similar in isobaric and isovolumic beats [22].

Both arteriolar and venular diameters decrease in systole. The decrease in arteriolar and venular diameters between diastole and systole in subendocardial layers are about 12 and 25%, respectively [23]. Thus venules are not being compressed completely as would be expected when intramyocardial pressure is close to ventricular pressure in subendocardial layers. A theoretical explanation has been given, and it is also shown that partial venous collapse protects arterioles from large changes in diameter [24].

Bridging. When an epicardial vessel, instead of running on the surface of the myocardium, is located in the heart wall, the vessel is greatly affected by cardiac contraction.

Perfusion pressure in layers. Microvascular perfusion pressure, expressed as arteriolar minus venular pressure (see Fig. 18.9) is considerably lower in subendocardial layers than in subepicardial layers [25]. This is caused by the pressure drop over the transmural arteries and transmural veins and may, in part, explain why the subendocardium is more vulnerable to ischemia than the subepicardial layers.

Coronary flow heterogeneity. Local flows are different between locations, and may vary from less than 50% to more than twice the mean overall perfusion flow. This variation is larger when the sample volume is smaller. Flow in small areas is
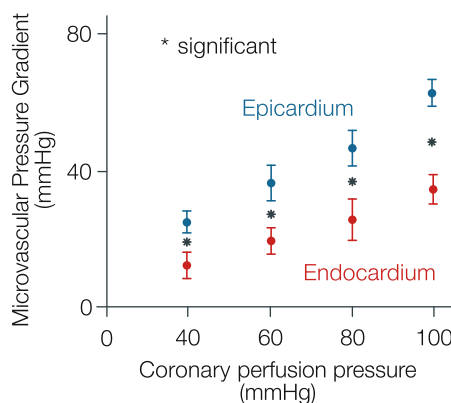
Fig. 18.9 The net perfusion pressure, expressed as microvascular pressure gradient, is significantly smaller in the sub-endocardium than in the sub-epicardium. Adapted from ref. [25], used by permission

not constant in time, but varies ('twinkling'). However, in areas where flow is large it remains large and where small it remains small. Large and small flows are not found at similar locations between animals. A partial explanation is based on the fractal rules of coronary geometry [26], but a complete explanation has not yet been given. Another explanation may be that cardiac myocytes are quite different in length and cross-section and larger cells require more oxygen.

The Gregg effect. Myocardial perfusion, in the absence of substrate and metabolite limitation, affects cardiac muscle contractility. It appears that increased perfusion opens Stretch Activated Channels, SAC's, thereby affecting both the Calcium handling and the contractile apparatus of the myocytes [27].

Vascular emptying in systole augments cardiac muscle contraction. During muscle shortening muscle diameter increases at the cost of the vascular volume. If the vascular volume cannot change, pressure is built up in the muscle cells and this intracellular pressure counteracts the force generated by the contractile apparatus so that the net force is smaller [18].

Both the endocardial and the vascular endothelium modulate cardiac muscle contraction. Removal or damaging of the endocardial endothelium results in a lower and shortened force generation [28]. NO may modulate cardiac performance such that it is matched to oxygen consumption and perfusion.

Coronary flow cools the heart. Cardiac efficiency is about 20–25% (Chap. 17), implying that about 75% of the oxygen consumed is converted into heat. This heat is transported by diffusion to mediastinum and ventricular lumen as well as by convection by the coronary flow (Chap. 17). At the normal level of coronary flow, i.e., ~90 ml/min/100 g, about 70% of the heat is carried away by the coronary flow. For lower flow the transport by diffusion increases and at a flow of 45 ml/min/100 g convection and diffusion contribute about equally to cardiac cooling [29].

Physiological and Clinical Relevance

Coronary Flow in Layers

Coronary heart disease is a major problem in the western world and understanding of the factors that determine the pathology of coronary function is therefore of utmost clinical importance.

The coronary flow has to be matched to cardiac metabolism and should thus vary with activity and exercise (Fig. 18.10). In the healthy organism coronary flow is matched to demand. Autoregulation assures that during variations in pressure coronary perfusion flow is maintained and that with increased metabolism flow is increased. When a stenosis is present (Chap. 5) the pressure distal to the stenosis may be too low for adequate perfusion and this is first experienced in exercise, when flow should increase. The explanation that cardiac ischemia is
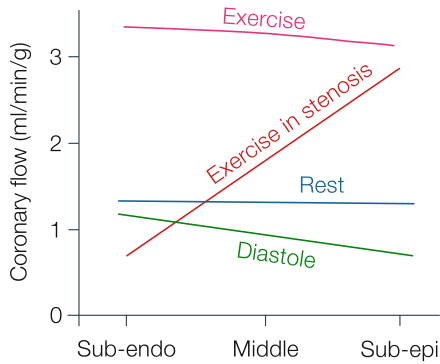
Fig. 18.10 Blood flow distribution in cardiac layers. In diastole mean flow is about 20% larger in sub-endocardial than in sub-epicardial layers (*green*). During rest mean flow is equally distributed over the different layers (*blue*). During exercise flow in the sub-epicardium tends to be smaller than in the sub-epicardium (*purple*). During exercise in the presence of a mild stenosis, coronary sub-endocardial flow will fall short (*red*)
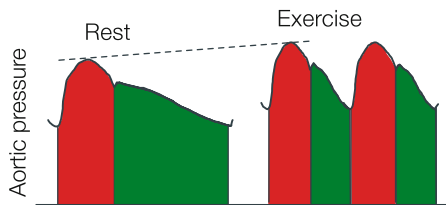
Fig. 18.11 The systolic (*red*) and diastolic (*green*) pressure-time areas. Their ratio is considered to be a measure of the myocardial, sub-endocardial, supply-demand ratio. During exercise the diastolic area decreases and the systolic area increases

earlier apparent in subendocardial layers than in subepicardial layers is partly due to cardiac contraction and partly the due to the pressure drop over the transmural vessels (Fig. 18.9).

Supply-Demand

Although the anatomy is such that coronary vascular resistance in diastole is the smallest in the subendocardial layers, contraction still reduces flow so much in this layer that perfusion only takes place during diastole. Thus the perfusion pressure and the duration of diastole are the main determinants of flow when the vasculature is dilated to its physiological maximum. This has led to the supply – demand ratio (see Chap. 16). The area under the systolic part of aortic or left

ventricular pressure curve is an index of oxygen consumption, see the Tension Time Index (Chap. 16). The area under the diastolic pressure curve is a measure of supply. The supply-demand ratio appears an acceptable indication of subendocardial ischemia [30]. In exercise the supply-demand ratio is strongly decreased (Fig. 18.11).

Coronary Stenosis

The effect of a coronary stenosis, in terms of perfusion, is quantified by coronary flow reserve, by fractional flow reserve and by fractional flow reserve. The hemodynamic effect of the stenosis is discussed Chap. 5.

References

1. Hoffman JIE, Spaan JAE. Pressure-flow relations in the coronary circulation. *Physiol Rev* 1990;70:331–390.
2. Spaan JA. *Coronary blood flow*. 1991, Dordrecht, Kluwer.
3. Westerhof N, Boer C, Lamberts RR, Sipkema P. Cross-talk between cardiac muscle and coronary vasculature. *Physiol Rev* 2006;86:1263–308.
4. Dankelman J, Spaan JAE, van der Ploeg CPB, Vergroesen I. Dynamic response of the coronary circulation to a rapid change in perfusion in the anaesthetised goat. *J Physiol (Lond)* 1989;419:703–715.
5. Vergroesen I, Noble MIM, Wieringa PA, Spaan JAE. Quantification of O_2 consumption and arterial pressure as independent determinants of coronary flow. *Am J Physiol* 1987;252:H545–H553.
6. Drake-Holland AJ, Laird JD, Noble MIM, Spaan JAE, Vergroesen I. Oxygen and coronary vascular resistance during autoregulation and metabolic vasodilation in the dog. *J Physiol* 1984;348:285–300.
7. Kuo L, Davis MJ, Chilian WM. Longitudinal gradients for endothelium-dependent and -independent vascular responses in the coronary microcirculation. *Circulation* 1995;92:518–525.
8. Duncker DJ, Bache RJ. Regulation of coronary blood flow during exercise. *Physiol Rev* 2008;88:1009–1086.
9. Bellamy RF. Diastolic coronary artery pressure-flow relations in the dog. *Circ Res* 1978;43:92–101.
10. Van Dijk LC, Krams R, Sipkema P, Westerhof N. Changes in coronary pressure-flow relation after transition from blood to Tyrode. *Am J Physiol* 1988;255:H476–H482.
11. Sherman IA. Interfacial tension effects in the microvasculature. *Microvasc Res* 1981;22:296–307.
12. Sipkema P, Westerhof N. Mechanics of a thin walled collapsible microtube. *Ann Biomed Eng* 1989;17(3):203–217.
13. Spaan JA. Coronary diastolic pressure-flow relation and zero flow pressure explained on the basis of intramyocardial compliance. *Circ Res* 1985;56:293–309.
14. Gregg DE, Green HD. Registration and interpretation of normal phasic inflow into the left coronary artery by an improved differential manometric method. *Am J Physiol* 1940;130:114–125.

15. Krams R, van Haelst, ACTA, Sipkema P, Westerhof N. Can coronary systolic-diastolic flow differences be predicted by left ventricular pressure of by time-varying intramyocardial elastance? *Basic Res Cardiol* 1989;84:149–159.
16. Downey JM, Kirk ES. Inhibition of coronary blood flow by a vascular waterfall mechanism. *Circ Res* 1975;36:753–760.
17. Spaan JA, Breuls NPW, Laird JD. Diastolic-systolic coronary flow differences are caused by intramyocardial pump action in the anesthetized dog. *Circ Res* 1981;49:584–593.
18. Willemsen MJ, Duncker DJ, Krams R, Dijkman M, Lamberts RR, Sipkema P, Westerhof N. Decrease in coronary vascular volume in systole augments cardiac contraction. *Am J Physiol* 2001;281:H731–H737.
19. Sipkema P, Takkenberg JJM, Zeeuwe PEM, Westerhof N. Left coronary pressure-flow relations of the beating and arrested rabbit heart at different ventricular volumes. *Cardiovasc Res* 1998;40:88–95.
20. Vis MA, Bovendeerd PH, Sipkema P, Westerhof N. Effect of ventricular contraction, pressure, and wall stretch on vessels at different locations in the wall. *Am J Physiol* 1997;272:H2963–H2975.
21. Mihailescu LS, Abel FL. Intramyocardial pressure gradients in working and nonworking isolated cat hearts. *Am J Physiol* 1994;266:H1233–H1241.
22. Westerhof N. Physiological Hypothesis. Intramyocardial pressure. *Basic Res Cardiol* 1990;85:105–119.
23. Yada T, Hiramatsu O, Kimura A, Goto M, Ogasawara Y, Tsujioka K, Yamamori S, Ohno K, Hosaka H, Kajiya F. In vivo observation of subendocardial microvessels in the beating porcine heart using a needle-probe videomicroscope with a CCD camera. *Circ Res* 1993;72:939–946.
24. Vis MA, Sipkema P, Westerhof N. Compression of intramyocardial arterioles during cardiac contraction is attenuated by accompanying venules. *Am J Physiol* 1997;273:H1002–H1011.
25. Chilian WM. Microvascular pressures and resistances in the left ventricular subendocardium and subepicardium. *Circ Res* 1991;69:561–570.
26. Bassingthwaighte JB, King RB, Roger SA. Fractal nature of regional myocardial blood flow heterogeneity. *Circ Res* 1989;65:578–590.
27. Lamberts RR, van Rijen MH, Sipkema P, Fransen P, Sys SU, Westerhof N. Increased coronary perfusion augments cardiac contractility in the rat through stretch-activated ion channels. *Am J Physiol* 2002;282:H1334–H1340.
28. Brutsaert DL. Cardiac endothelial-myocardial signaling: Its role in cardiac growth, contractile performance, and rhythmicity. *Physiol Rev* 2003;83:59–115.
29. Ten Velden GHM, Westerhof N, Elzinga G. Left ventricular energetics: heat loss and temperature distribution in the canine myocardium. *Circ Res* 1982;50:63–73.
30. Hoffman JIE, Buckberg JD. Myocardial supply:demand ratio – a critical review. *Am J Cardiol* 1978;41:327–332.

Chapter 19
Assessing Ventricular Function
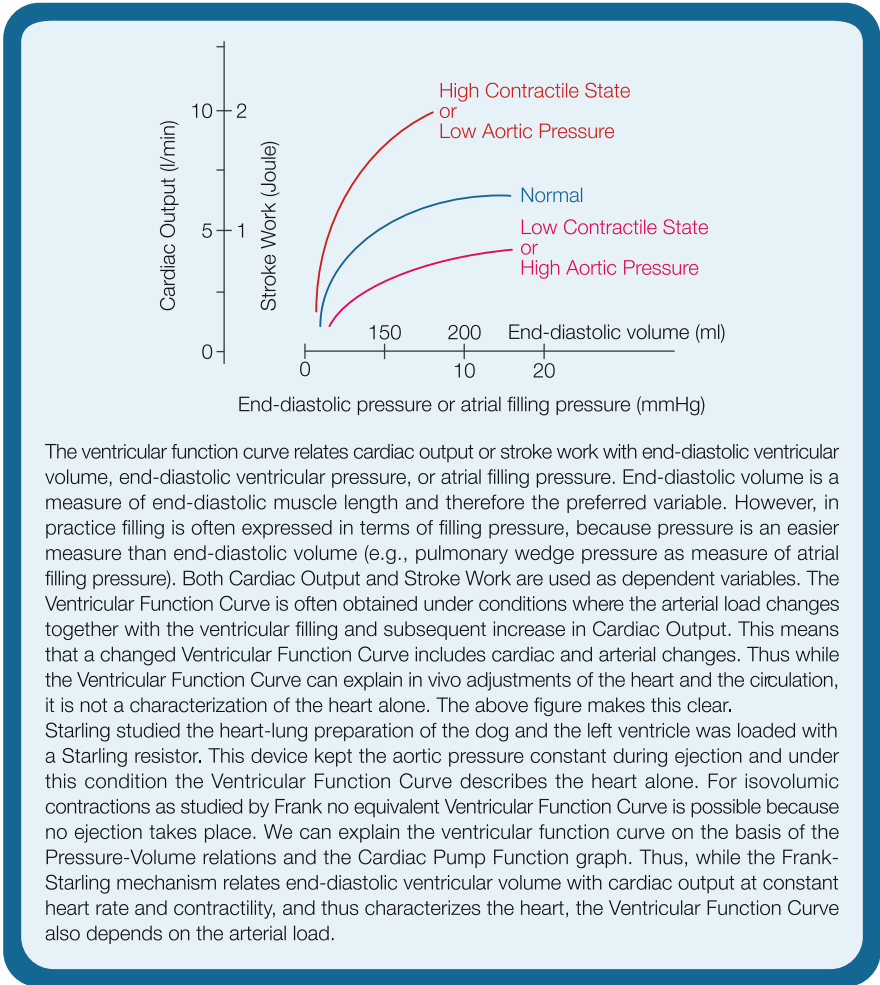
The ventricular function curve relates cardiac output or stroke work with end-diastolic ventricular volume, end-diastolic ventricular pressure, or atrial filling pressure. End-diastolic volume is a measure of end-diastolic muscle length and therefore the preferred variable. However, in practice filling is often expressed in terms of filling pressure, because pressure is an easier measure than end-diastolic volume (e.g., pulmonary wedge pressure as measure of atrial filling pressure). Both Cardiac Output and Stroke Work are used as dependent variables. The Ventricular Function Curve is often obtained under conditions where the arterial load changes together with the ventricular filling and subsequent increase in Cardiac Output. This means that a changed Ventricular Function Curve includes cardiac and arterial changes. Thus while the Ventricular Function Curve can explain in vivo adjustments of the heart and the circulation, it is not a characterization of the heart alone. The above figure makes this clear.

Starling studied the heart-lung preparation of the dog and the left ventricle was loaded with a Starling resistor. This device kept the aortic pressure constant during ejection and under this condition the Ventricular Function Curve describes the heart alone. For isovolumic contractions as studied by Frank no equivalent Ventricular Function Curve is possible because no ejection takes place. We can explain the ventricular function curve on the basis of the Pressure-Volume relations and the Cardiac Pump Function graph. Thus, while the Frank-Starling mechanism relates end-diastolic ventricular volume with cardiac output at constant heart rate and contractility, and thus characterizes the heart, the Ventricular Function Curve also depends on the arterial load.

Description

In the intact organism the Ventricular Function Curve is usually presented as the relation between Stroke Volume (or Cardiac Output or stroke work)) and ventricular filling. If we make a graph between filling volume and Cardiac Output, we can derive the Ventricular Function Curve from the pressure-volume relation as follows. If the aortic pressure and thus ventricular pressure in systole is kept constant (Starling experiment), Cardiac Output is proportional to end-diastolic volume (Chap. 13). In the intact organism, however, the pressure increases with increasing Cardiac Output, and this increase in pressure depends on the neural and humoral regulatory mechanisms. If changes are performed so rapidly that regulation cannot set in, we follow a family of curves: for larger filling Cardiac Output increases but the higher pressure counteracts this increase in part (see Fig. 19.1). Thus an increase in filling volume results in a smaller increase in Cardiac Output than under the assumption of a constant arterial pressure, as in Starlings' experiment. We thus see that the Ventricular Function Curve depends on the heart in combination with the arterial load, and therefore characterizes ventriculo-arterial coupling and not the heart alone. The relation between diastolic filling and Cardiac Output is therefore more difficult to interpret than the original experiments by Frank and Starling.

Before the cardiac Echo technique became available, ventricular filling pressure or diastolic ventricular pressure was easier to determine than end-diastolic volume and the Ventricular Function Graph was therefore often presented in the form of filling pressure and Cardiac Output. The graph is, in general, more linear when volume is used as independent variable than when filling pressure is used, because
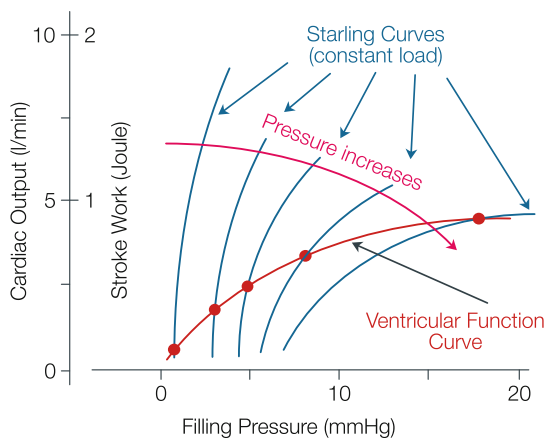
Fig. 19.1 The ventricular function curve is the relation between left ventricular filling pressure and cardiac output. The function curve depends on the pressure in systole, or simpler, aortic pressure, and is therefore load dependent. The family of *curves*, *blue lines*, can be derived from Starling's experiments each at constant aortic pressure. When the actual arterial load is present, increased filling results in increased output and increased pressure, i.e., a lower Starling curve

of the nonlinear diastolic pressure-volume relation. When circumferential strain is determined together with myocardial stroke work (Chap. 14), the so-called Preload Recruitable Stroke Work can be calculated and plotted as a function of end-diastolic strain and an almost perfectly linear relationship is found [1].

Global Left Ventricular Contractile Function Compared Between Patients

Indices of contractile function or contractility are dominated by the contribution of left ventricular (LV) cavity volume because arterial pressures are usually similar between patients. When end-systolic volume (ESV) and end-diastolic volume (EDV) are increased, while Stroke Volume, SV, is not changed, Ejection Fraction (EF) is decreased because EF$=SV$/EDV. MUGA, Multiple Gated Acquisitions, is the best method of assessment, at least in theory, because the radioactive counts from the LV cavity, when the blood is labeled, are proportional to volume. Other methods such as echocardiography (Echo) and Magnetic Resonance Imaging (MRI) depend on assumptions about geometry. There is nothing to be gained in this assessment from invasive measurements.

Invasive Assessment of Global Ventricular Function in the Patient

The maximum rate of rise of left ventricular pressure, dP_{LV}/dt_{max}, can be determined by measuring left ventricular pressure (LVP) with a catheter-tip manometer and passing the signal through an electronic differentiator. The signal has a prominent positive maximum, an index of global LV contractile function and contractility. There is also a prominent negative maximum, dP_{LV}/dt_{min}, which is a load dependent variable, and cannot be used as a measure of ventricular relaxation.

To be a measure of muscle function dP_{LV}/dt should be related to wall stress σ. This can be done using Laplace's law (Chap. 9).

$$\sigma = P_{LV} \cdot g_f$$

with g_f a geometry factor accounting for the (local) radius of curvature and myocardial wall thickness. By the chain rule, differentiating with respect to time, we obtain:

$$d\sigma/dt = g_f \cdot dP_{LV}/dt + P_{LV} \cdot dg_f/dt$$

This shows that it is important to determine dP_{LV}/dt_{max} during isovolumic conditions so that g_f may be assumed constant, i.e., $dg_f/dt = 0$, and

$$dP_{LV}/dt = (1/g_f) \cdot d\sigma/dt$$
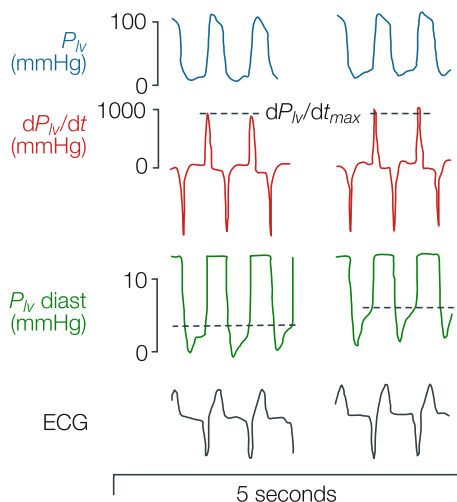
Fig. 19.2 Time derivative of left ventricular pressure, dP_{lv}/dt_{max}, as a measure of contractility. Increased filling, resulting in an increase in end-diastolic pressure (*stippled lines*) does not affect dP_{lv}/dt_{max} since this index is sensitive to inotropic interventions and not, in this range, to volume changes. Adapted from [2], used by permission

With changes in filling the geometric factor g_f will change limiting its use as contractility index. At low volumes, such as during cardiac surgery with open chest, a change in dP_{LV}/dt_{max}, may result both from changes in muscle function and filling. In the closed chest, and in the catheter laboratory the geometric factor does, in general, not change so that dP_{LV}/dt_{max} gives useful information on averaged global muscle function. At very large ventricular volumes an increase in the factor g_f may even result in a decrease in dP_{LV}/dt_{max}. Thus dP_{LV}/dt_{max} can be used only as a convenient volume independent index for changes in cardiac contractility in the catheter laboratory. In Fig. 19.2 the record on the left was obtained with the patient in head-up tilt and the record on the right with the patient in head-down tilt. It can be seen that the left ventricular end-diastolic pressure is higher in the right hand record due to the increase in ventricular volume, but dP_{LV}/dt_{max} is unchanged [2].

Merits and Drawbacks of dP_{LV}/dt_{max}, ESPVR and E_{max} as Assessments of Global Contractility

The theoretical gold standard for assessment of cardiac contractility is the slope of the End-Systolic Pressure-Volume Relation (ESPVR, Fig. 19.3), but in practice this ESPVR is usually only obtainable invasively, as during cardiac surgery. Volume changes are required and they can be obtained by, partial, occlusion and release of the vena cavae. An increase in contractility corresponds to a 'rotation' around V_d of
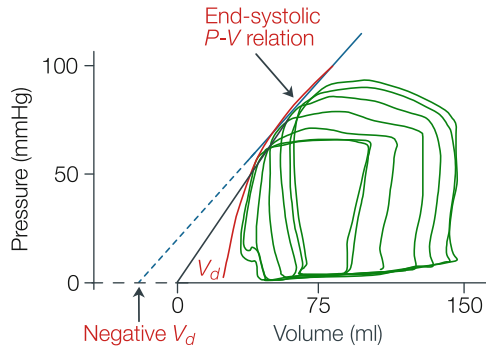
Fig. 19.3 End-systolic pressure-volume relation as a measure of global ventricular function. Several pressure-volume loops, preferably obtained with changes in cardiac filling, are required to determine this relation (*red line*). Approximations by assuming a straight relation (*blue line*, with negative intercept), or using a single loop and assuming linearity and zero intercept volume (*black line*) may lead to unacceptable errors
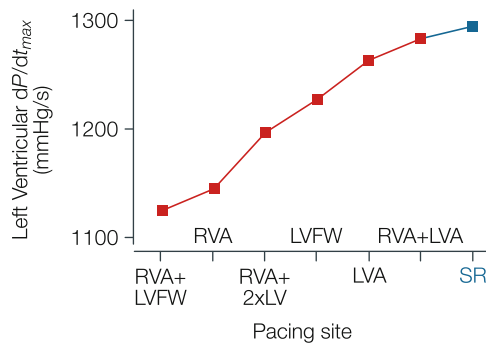
Fig. 19.4 dP_{lv}/dt_{max} depends on pacing site. During ventricular pacing from various sites $LVdP/dt$ max is compared with its value during sinus rhythm (SR). RVA = right ventricular apex; $LVFW$ = left ventricular free wall; LVA = left ventricular apex; $2xLV$ = LV free wall and apex. Redrawn from ref. [3], used by permission

the ESPVR (Chap. 13). The slope of the relation, E_{max}, is only an acceptable index of contractility if the relation is straight. For a curved relation the slope depends on the chosen pressure. The straight-line extrapolation often suggests a negative, physically impossible, and thus virtual, intercept with the volume axis. Thus in open thorax experiments, where volume and pressure can be measured, the ESPVR should be reported because it gives much more accurate information than the E_{max}.

The dP_{LV}/dt_{max} is unsuitable for comparing contractility of patients [4] because it is also an index of the synchronicity of contraction. Figure 19.4 shows that during a conduction defect, e.g., bundle branch block or inappropriate pacing sites, dP_{LV}/dt_{max} is different. In general, the dP_{LV}/dt_{max} is highest during sinus rhythm

(extreme right hand point in Fig. 19.4). The End-Systolic Pressure-Volume Relation, ESPVR, has the same shortcoming. In other words, the two quantities do not quantify muscle contractility but overall pump function.

Noninvasive Assessment of Global Ventricular Function in the Patient

By definition, noninvasive assessment rules out methods such as catheter-tip manometry and conductance catheter volume measurement. One approach that gained some popularity is calculating E_{max} by dividing peak aortic pressure, as an index of end-systolic left ventricular pressure, by end-systolic volume, obtained by Echo or MRI. In addition to the assumption of linearity of the ESPVR, the intercept volume is assumed to be negligible. These noninvasive approaches are subject to errors (Chap. 17).

The assessment of contractility is complicated by the nonlinearity of the ESPVR. Of course, if during an intervention mean arterial pressure does not change (pressure clamped by the baroreflex, [5]), the nonlinearity of the ESPVR does not play a role and the end-systolic pressure is moved to smaller volumes with increased contractility. If arterial pressure changes it is recommended that the changes in mean arterial pressure are accounted for. A control run should be compared in which the mean arterial pressure changes are reproduced with a pure vasoconstrictor or a pure vasodilator.

Assessment of Change in Regional Left Ventricular Function

Contractile function variables can be affected both by changes in global contractility and by regional dysfunction, e.g. myocardial infarction. In the latter case, regional contractile function is of clinical importance, but cannot be studied in absolute terms as is the case with global function indices such as the ESPVR and dP_{LV}/dt_{max}. The pragmatic approach therefore is to study local wall movement to see whether it is impaired or, in some cases such as hypertrophic cardiomyopathy, enhanced. Dysfunctional myocardium may respond to a positive inotropic intervention, e.g. post-extra-systolic potentiation or dobutamine infusion. This indicates if the tissue is viable and may improve with reperfusion. This approach is followed in Stress-Echo and Stress-MRI investigations.

Physiological and Clinical Relevance

The Ventricular Function Curve is very regularly used to demonstrate the effects of therapy on Cardiac Output.
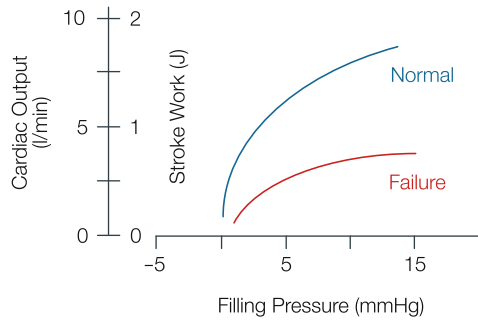
Fig. 19.5 Ventricular function curves under normal conditions, and in heart failure. The characterization pertains to ventriculo-arterial interaction and not to the heart alone

An example is given in Fig. 19.5, where the Ventricular Function Curve is shown in control and heart failure. Again, one should be aware of the fact that the graphs do not reflect the differences in the heart alone but also contain what is changed in the arterial load.

References

1. Glower DD, Spratt JA, Snow ND, Kabas JS, Davis JW, Olson CO, Tyson GS, Sabiston DC Jr, Rankin JS. Linearity of the Frank-Starling relationship in the intact heart: the concept of preload recruitable stroke work. *Circulation* 1984;71:994–1009.
2. Drake-Holland AJ, Mills CJ, Noble MIM, Pugh S. The response to changes in filling and contractility of various indices of human left ventricular mechanical performance. *J Physiol (Lond)* 1990;422:29–39.
3. Prinzen, FW, Peschar M. Relation between the pacing induced sequence of activation and left ventricular pump function in animals. *J Pacing Clin Electrophysiol* 2002;25:484–498.
4. Van den Bos GC, Elzinga G, Westerhof N, Noble MIM. Problems in the use of indices of myocardial contractility. *Cardiovasc Res* 1973;7:834–848.
5. Brooks CIO, White PA, Staples M, Oldershaw PJ, Redington AN, Collins PD, Noble MIM. Myocardial contractility is not constant during spontaneous atrial fibrillation in patients. *Circulation* 1998;98:1762–1768.

Part C
Arterial Hemodynamics

Chapter 20
Wave Travel and Velocity

Heart

Pressure

Wave speed, c, is

$c = \Delta x / \Delta t$

Distance

Δx

AORTA

Wave speed as a function of area compliance, $C_A = \Delta A / \Delta P$, wall elastic modulus, E_{inc}, wall thickness, h, and blood density is:

$c = \sqrt{A / \rho\, C_A}$
(Newton-Young, or Frank, or Bramwell-Hill equation)

$c = \sqrt{E_{inc}h / \rho D}$

Δt

Periphery

Time

(Moens-Korteweg equation)

Waves generated by the heart travel down the aorta and major conduit arteries. These waves may be pressure waves, flow or velocity waves or even diameter waves. The same wave speed applies to all waves. The ratio of the distance Δx, and the time it takes for the wave to travel over this distance, Δt, $\Delta x / \Delta t$, gives the wave speed or pulse wave velocity, c. The wave speed depends on vessel size and the elastic properties of the arterial wall. In the aorta of a healthy subject the wave speed is typically 4−5 m/s. In stiff aortas, having a low compliance (C_A) and a high wall elastic modulus (E_{inc}) the wave speed is higher. When compliance decreases by a factor of two, wave speed only increases by about 40%. The wave speed in peripheral arteries is higher than in central arteries since the elastic modulus is higher and diameter is smaller.

Description

The heart generates pressure and flow waves. Because of the elasticity of the aorta and the major conduit arteries, the pressure and flow waves are not transmitted instantaneously to the periphery, but they propagate through the arterial tree with a certain speed, which we call wave speed or pulse wave velocity (c). In analogy to waves created by stone dropped in a lake, the waves seen on the surface travel with a speed that is measured by the time it takes for the disturbance (wave) to cover a certain distance. The distance traveled by the wave over the time delay gives the wave speed, as schematically shown in the Figure in the box. Also, in analogy with the stone dropped in the lake, the wave transmission takes place even in the absence of blood flow and is not related to the velocity of the blood. When a stone is dropped in a river, the waves superimpose on the water flow, and the wave fronts traveling downstream go faster than the wave fronts that move upstream. In other words, the velocity of the blood adds to the wave speed. However, since blood flow velocity is much smaller (cm/s) than wave velocity (m/s) this effect is usually neglected.

Wave Speed Depends on Vessel Compliance

The wave speed can be related to the elastic modulus of the wall material via the Moens-Korteweg equation:

$$c = \sqrt{\frac{h \cdot E_{inc}}{2 \cdot r_i \cdot \rho}} = \sqrt{\frac{h \cdot E_{inc}}{D \cdot \rho}}$$

where E_{inc} is the incremental elastic modulus, ρ the blood density, h the wall thickness and r_i, and D the lumen radius and diameter. This equation is derived for non-viscous fluid but it is a good approximation for conduit arteries filled with blood. It is the so-called phase velocity i.e., the wave speed in a tube without reflections. From the Moens-Korteweg equation, Frank [1] and Bramwell and Hill [2] derived another expression relating wave speed to compliance:

$$c = \sqrt{A / \rho C_A} = \sqrt{V \Delta P / \Delta V \cdot \rho} = \sqrt{BM / \rho} = \sqrt{1 / \rho \cdot K}$$

with A the lumen area, $C_A = \Delta A / \Delta P$ the area compliance, ρ is blood density, and BM and K are Bulk Modulus and distensibility. Newton and Young derived this equation first, and Frank introduced it in hemodynamics and Bramwell and Hill introduced it in the Anglo-Saxon literature. It is therefore named Newton-Young, Frank, or Bramwell-Hill equation.

Phase Velocity and Apparent Phase Velocity

The phase velocity is the wave speed determined by the properties of the vessel wall and blood density alone as presented above, i.e., the effects of reflections (Chap. 21) are not included. When two arterial pressures are measured these waves include the effect of reflections and with reflections present the formulas become more complex and the wave speed derived is called the apparent wave velocity or apparent phase velocity. When Fourier analysis is performed (Appendix 1) on two waves measured a distance Δx apart, the wave speed for each harmonic can be obtained by using the time difference, called phase lag for sine waves, $\Delta\varphi$, between the two harmonics. The phase lag is $\Delta\varphi = 2\pi \Delta t/T = 2\pi f \Delta t$, with T the duration of one period, the inverse of the frequency, f, of the sine wave. The apparent wave velocity, c_{app}, is then calculated for each harmonic as

$$c_{app,n} = \frac{2\pi \cdot \Delta x}{T_n \cdot \Delta\varphi_n} = \frac{2\pi \cdot f_n \cdot \Delta x}{\Delta\varphi_n}$$

with n signifying the *nth* harmonic. If the frequency is given in Hz, Δx in cm, and $\Delta\varphi$ in radians, c_{app} will be in cm/s. The apparent wave velocity includes the effect of reflections and is therefore not a good measure of vessel compliance. Figure 20.1 shows the apparent wave velocity as a function of frequency. For high frequencies the apparent wave velocity approaches the true phase velocity because for high frequencies reflections become negligible (Chap. 23).
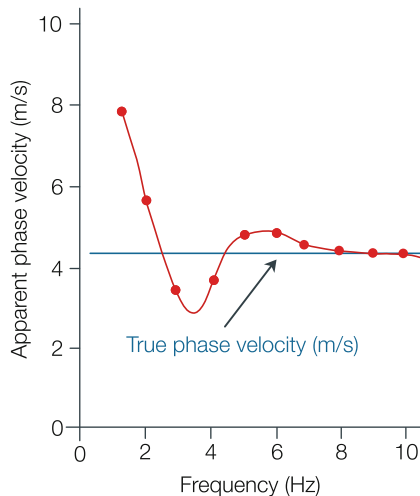
Fig. 20.1 The apparent wave velocity is close to the phase velocity for high frequencies
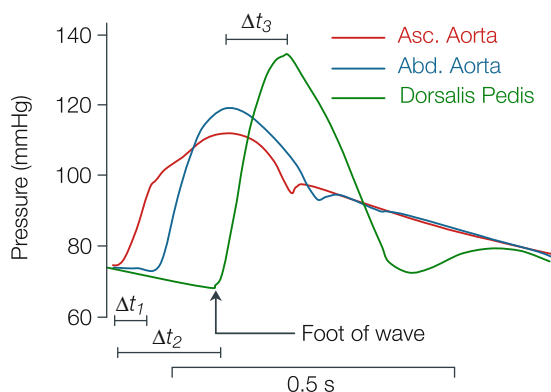
Fig. 20.2 Pressure waves at different locations of the human arterial tree. The time delay *t* of the foot of the waves divided by distance gives the pulse wave velocity (foot-foot pulse wave velocity). Adapted from ref. [3], used by permission

When the wave speed is determined from the foot of the wave (Fig. 20.2) the value is close to the apparent wave velocity at high frequencies, and thus close to the phase velocity. Therefore, the equations in the box may be applied to calculate area compliance or incremental modulus of the wall material. The 'top' of the wave (systolic pressure) cannot be used to estimate wave speed.

Methods to Obtain Wave Speed

- *Time delay or foot-to-foot method*. This is the most direct method. Wave speed is estimated from the time it takes for the foot of the pressure, diameter, or blood velocity wave, to travel between two sites a known distance apart. The so calculated foot-to-foot wave velocity is close to the phase velocity and can be used to derive vessel compliance. Figure 20.2 shows realistic time delays for pressure waves recorded in the human aorta and the lower limbs [3]. For instance, the delay of the foot of the wave between ascending and thoracic aorta is $\Delta t_1 = 0.056$ s, and the distance is $\Delta x_1 = 0.25$ m. Thus, the proximal aortic wave speed, equals 0.25/0.056 m/s and $c = 4.5$ m/s. The average wave speed from the aorta to the lower limb is $\Delta x_2/\Delta t_2 = 1.25$m/0.175 s or $c = 7.1$ m/s. Peripheral arteries are smaller, have relatively larger wall thickness, and are stiffer (higher E_{inc}). Therefore, by virtue of the Moens-Korteweg equation, they have a higher wave speed. Note that the estimated aorta-to-dorsalis pedis wave speed is an average wave speed for the entire arterial pathway traveled by the wave (aorta, iliac, femoral, and popliteal). The foot-to-foot method has been used in the above example to obtain the average wave speed between the ascending aorta and dorsalis pedis, with the foot-to-foot

time delay being estimated as $\Delta t_2 = 0.175$ s. If one had used the time delay based on peak systolic pressure ($\Delta t_3 = 0.102$ s, in Fig. 20.2), the estimated wave speed would have been $c = 1.25\text{m}/0.102\text{s} = 12.3$ m/s. This speed is much higher than the foot-to-foot estimate of $c = 7.1$ m/s. The overestimation is attributed partly to the fact that the artery is stiffer at higher distending pressures but is also partly attributed to wave reflections that contribute to peak systole. It is therefore generally accepted that the time delay should be calculated from the foot or the early up-slope of the wave rather than the systolic part.

- *Three-pressure method.* By measurement of three pressures some centimeters apart, reflections can be accounted for and the phase velocity can be derived [4]. However, the three pressures differ, in general, very little and errors are considerable.
- *Temporal and spatial derivative method.* For an artery without reflections wave speed can be calculated using the time derivative and spatial derivative of pressure [5]: $c = (dP/dt)/(dP/dx)$.
- *Wave speed derived from pressure and diameter measurements.* The Newton-Young equation permits the direct calculation of wave speed based on lumen cross-sectional area ($A = \pi D^2/4$) and area compliance C_A. Simultaneous measurements of lumen diameter and pressure can be obtained using ultrasound and photoplethysmography or tonometry, respectively. Calculation of area gives the cross-sectional area-pressure relation. Based on compliance and area and using Newton-Young equation, wave speed can be derived as a function of pressure.
- *Wave speed derived from flow and area measurements.* This method [6], see Fig. 20.3, is not often used, mainly because noninvasive flow and area measurements were not available in the past. MRI and ultrasonic technologies now make it possible to perform these noninvasive measurements. Imagine that the heart ejects into the aorta a certain volume ΔV over a period Δt. The ejected volume will be 'accommodated' in the aorta by means of an increase in the aortic cross-sectional area ΔA over a certain length Δx. The wave speed is the speed with
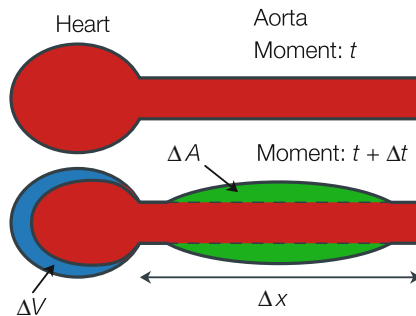
Fig. 20.3 Aortic area and flow changes can be used to derive wave speed

which the perturbation in area, ΔA, has traveled in the aorta, which is $\Delta x/\Delta t$. The volume ejected in the aorta is $\Delta V = \Delta A \, \Delta x$ or $\Delta x = \Delta V/\Delta A$. Dividing by Δt, we obtain:

$$c = \frac{\Delta x}{\Delta t} = \frac{\Delta V}{\Delta t \cdot \Delta A}$$

or since $\Delta V/\Delta t$ is equal to the volume flow ΔQ

$$c = \frac{\Delta Q}{\Delta A}$$

From this relation we see that when ejection takes place in a stiff artery where the change in area, ΔA, will be small, the wave speed will be high.

Physiological and Clinical Relevance

The above equations show that from wave speed wall elasticity (E_{inc}) and area compliance C_A can be derived if the artery's geometry (diameter and wall thickness) is known, thus, giving a good estimation of large vessel elasticity.

Time Delay or Foot-to-Foot Method

The wave speed between carotid artery and iliac or femoral artery can be measured noninvasively and is accepted as representative for aortic wave velocity, allowing for estimation of aortic elasticity. This noninvasive method is often used in hypertension research. Some limitations are: The estimation of length should account for the distance between the arch and the location of measurement in the carotid artery where the signal is measured. The ascending aorta is not included while changes in elasticity may be considerable just there. With aging the aorta becomes tortuous resulting in an underestimation of length and thus an underestimation in wave speed.

Wave Speed Depends on Pressure

Based on compliance and area and using Newton-Young equation, wave speed can be derived as a function of pressure as shown in Fig. 20.4. Clearly wave speed is a strong function of pressure, due to the nonlinear elastic properties of the arterial wall.
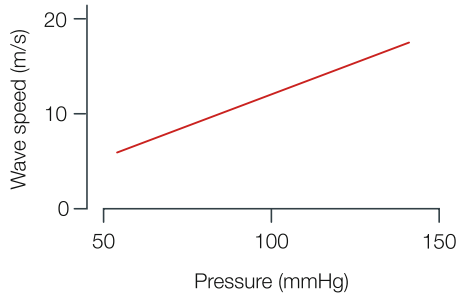
Fig. 20.4 Wave speed as a function of pressure derived from diameter (or pressure) measured non-invasively in the human brachial artery
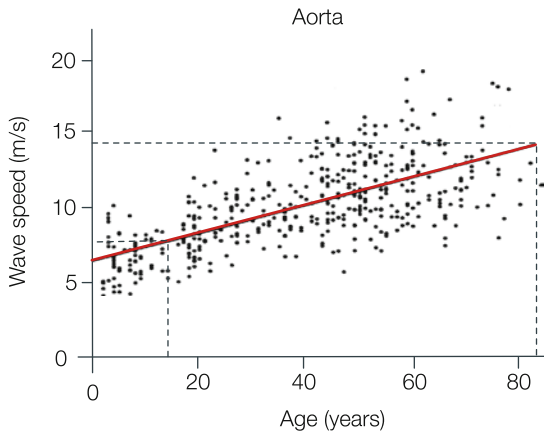
Fig. 20.5 Aortic pulse wave velocity as a function of age in individuals with low prevalence of atherosclerosis in Beijing. Note the increase by almost a factor of 2 corresponding with a fourfold decrease in compliance. From ref. [7], used by permission

Wave Speed Depends on Age

With age, wave speed increases as shown in Fig. 20.5 where data were measured in normal human subjects, in the absence of atherosclerosis. The increase in wave speed by about a factor two between the ages 15 and 80 years implies a decrease in compliance by a factor four. The increase in aortic stiffness with age is primarily attributed to a progressive thinning, fraying and fracture of elastic laminae, likely due to repetitive cyclic stress of the pulsing pressure.

Although all wall constituents are subjected to the same Pulse Pressure and thus to the same cyclic stretch, it is mainly the elastin that cannot be re-synthesized sufficiently rapidly [8]. The net result is gradual replacement of elastin with collagen.

The stiffer aorta implies reduced Windkessel function and higher Pulse Pressure (Chap. 24). The higher Pulse Pressure, in turn, may cause extra wear of the vessel wall resulting in more breakdown of elastin. It has been shown that Pulse Pressure is a better indicator of cardiovascular mortality and morbidity than systolic blood pressure [8].

References

1. Frank O. Die Elastizität der Blutgefässe. *Z Biol* 1920;71:255–272.
2. Bramwell JC, Hill AV. The velocity of the pulse wave in man. *Proc R Soc Lond [Biol]* 1922;93:298–306.
3. Remington JW, Wood EH. Formation of peripheral pulse contour in man. *J Appl Physiol* 1956;9:433–442.
4. Taylor MG. An experimental determination of the propagation of fluid oscillations in a tube with a visco-elastic wall; together with an analysis of the characteristics required in an electrical analogue. *Phys Med Biol* 1959;4:63–82.
5. Fry DL, Casper AG, Mallos AJ. A catheter tip method for measurement of the instantaneous aortic blood velocity. *Circ Res* 1956;4:627–632.
6. Vulliemoz S, Stergiopulos N, Meuli R. Estimation of local aortic elastic properties with MRI. *Magn Reson Med* 2002;47:649–654.
7. Avolio AP, Chen S-G, Wang R-P, Zhang C-L, Li M-F, O'Rourke MF. Effects of aging on changing arterial compliance and left ventricular load in a in a northern Chinese urban community. *Circulation* 1983;68:50–58.
8. Martyn CN, Greenwald SE. Impaired synthesis of elastin in walls of aorta and large conduit arteries during early development as an initiating event in pathogenesis of systemic hypertension. *Lancet* 1997;3502:953–955.
9. Mitchell GF, Moye LA, Braunwald E, Rouleau JL, Bernstein V, Geltman EM, Flaker GC, Pfeffer MA. Sphygmomanometrically determined pulse pressure is a powerful independent predictor of recurrent events after myocardial infarction in patients with impaired left ventricular function. *Circulation* 1997;96:4254–4260.

Chapter 21
Wave Travel and Reflection

The principle of wave travel and reflection of pressure and flow waves along the aorta and large arteries. Pulses, as models of the pressure and flow waves, are depicted as they travel along the aorta and after they are reflected at the end of this hypothetical vessel that is closed at the end. The main principle is that the forward pressure and flow wave are related through the characteristic impedance of the aorta (see Appendix 4). The characteristic impedance of large vessels is constant and frequency independent which implies that the forward waves of pressure and flow have the same shape. At the reflection site both pressure and flow are reflected and the magnitude of the reflection is the same for both. However, in this example of a closed end, the pressure wave is reflected "upright" while the flow wave is reflected "up side down", i.e., inversely with respect to pressure. For a tube without a closed end both pressure and flow are partially reflected, but flow is always "inverted" with respect to pressure. This basic principle pertains to all reflections, also for the reflections that take place at the heart. The backward waves return towards the heart with the same wave speed as the forward waves. The addition of forward and backward waves produces the measured wave. If no reflections exist the measured pressure and flow waves have the same wave shape. Thus reflections are the reason why pressure and flow differ in shape.

Description

Wave reflection takes place at all bifurcations and discontinuities of the vasculature. However, it turns out that the major part of the reflections occur at the arterioles, i.e., in the periphery where many bifurcations are present over short distances. This leads to *diffuse* reflection because waves are returning from many sites at different distances away and arriving in the proximal aorta at random moments in time. In addition, especially in the human, there appears to be a *distinct* reflection site in the distal abdominal aorta. An example of the distinct reflection is shown in Fig. 21.1. The moment the reflected wave returns at the heart depends on the distance of the reflection site, the wave speed, and how the wave is reflected (thus the phase of reflection coefficient). Since with age the wave speed increases, it has been suggested that reflected waves may return earlier in older subjects.

The amount of reflection is given by the reflection coefficient, which is defined for sinusoidal waves, as the ratio of the backward and forward waves and consists of a modulus or magnitude, and phase angle. Calculation of the reflection coefficient requires Fourier analysis (Appendix 1) because the coefficient is different for
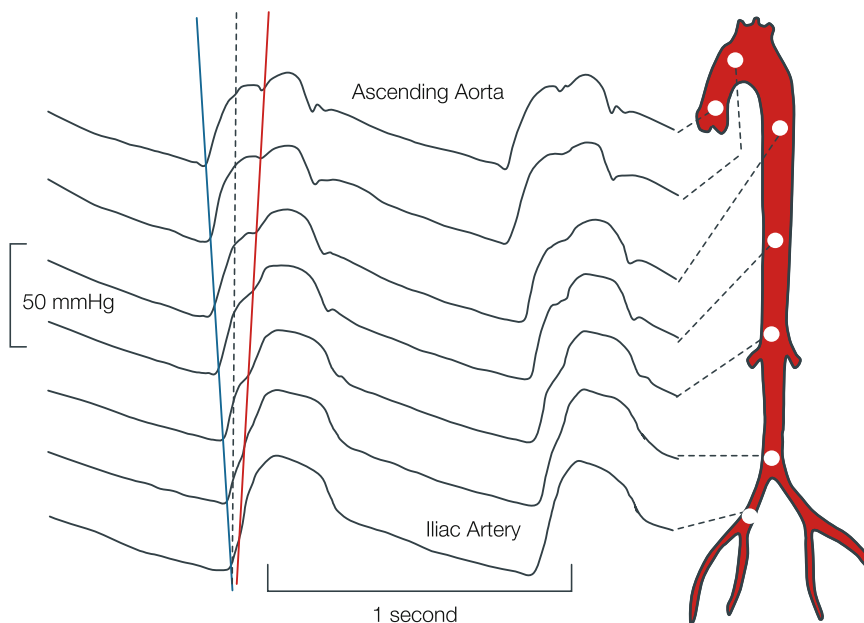
Fig. 21.1 Simultaneously measured pressures in the human aorta. The foot of the wave arrives later in the periphery and the reflected wave (inclination point) returns to the heart. The points are connected to show the later arrival of the reflected wave at the heart compared to the distal aorta. Adapted from ref. [1], used by permission

Fig. 21.2 The augmentation index (AI) is the augmented pressure (AP) divided by pulse pressure (PP). Calibration of blood pressure is not required
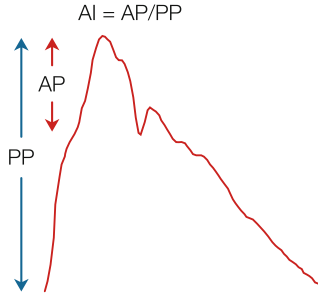
each harmonic. The modulus of the reflection coefficient is the same for pressure and flow but the phase angle of pressure and flow differ by 180° ('upside down', see Figure in the box). In approximation, the ratio of the amplitudes of full backward and forward waves can be used as a measure of the magnitude of reflection, usually in the form of the Reflection Index (see Chap. 22). The magnitude of the reflected wave with respect to the forward wave is related to the magnitude of the oscillation of the modulus of the input impedance (see Chap. 23).

The amount of reflection has also been related to the Augmentation Index, AI (Fig. 21.2). The Augmentation Index became very popular, in part because it can be determined noninvasively and calibration of the signal is not required so that, for instance, applanation tonometry can be used. However, the Augmentation Index depends not only on the magnitude of the reflected wave but also on its time of return. Recently is has been shown that by assuming a triangular wave shape for aortic flow and measured pressure the reflection magnitude can be calculated without the necessity to calibrate pressure and flow [2].

The arrival time of the reflected wave at the heart not only depends on the wave speed and the distance of the reflection site but also on how the waves are affected at the reflection site [3, 4]. For instance, when, at the reflection site, the waves are reflected 'out of phase' an apparent distance is introduced. This change in phase depends on the vascular properties such as characteristic impedance and the input impedance of the distal, 'loading' arterial bed. This phase change may therefore depend on age and vasoactive state. Thus, we cannot assume that the time the reflected wave arrives at the heart equals twice the distance to the reflection site divided by wave speed. Also if phases are changing with age the increased wave speed may be counteracted by changing phase angle of the reflection coefficient and arrival time may not be shortened [5, 6]. Pythoud et al. have suggested a possible solution [7].

Physiological and Clinical Relevance

The amount of diffuse reflection depends on the vasoactive state of the peripheral vascular bed. With increased vasoconstriction the so-called diffuse reflections increase and pressure and flow become less alike in shape. For examples see below,
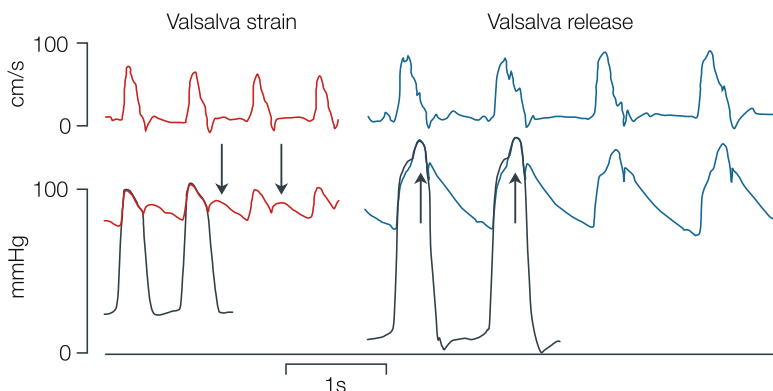
Fig. 21.3 During the Valsalva strain aortic pressure and flow in systole become alike because diffuse reflections decrease in amplitude and wave speed decreases so that the local reflection returns in diastole. After the release reflections return in systole and pressure and flow waves are different in shape. Adapted from ref. [8], used by permission
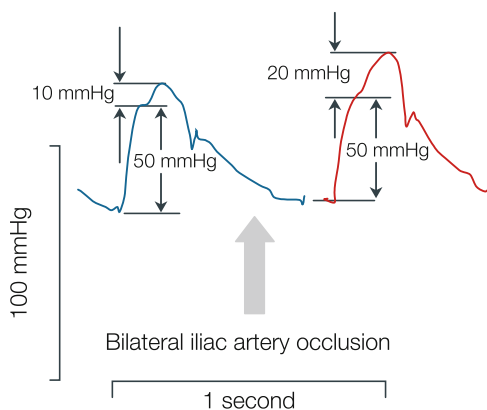
Fig. 21.4 Distinct reflection in the ascending aortic pressure is increased by mechanical compression of both iliac arteries. Adapted from ref. [1], used by permission

and also Chap. 22. Inversely, during vasodilation pressure and flow in the aorta become more alike: a pressure wave with an early peak, akin to the flow wave shape, is found in patients with a severely dilated state. With the Valsalva maneuver the transmural pressure in thoracic and abdominal aorta decreases [8]. This results in a more compliant aorta and a lower wave speed. The reflected waves arrive in diastole. The overall result is that reflections that return in systole are negligible leading to a similar shape of aortic pressure and flow in systole (Fig. 21.3).

An experiment where the distinct reflection is increased is shown in the Fig. 21.4. When both iliac arteries are manually occluded, the distinct reflection coefficient increases in magnitude and therefore the backward wave is increased resulting in a large Augmentation Index [1].
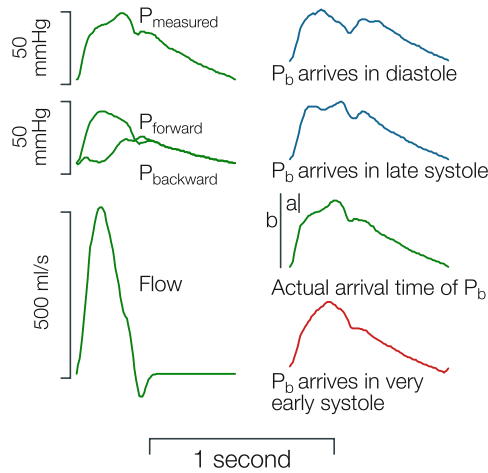
Fig. 21.5 The augmentation index, *a/b*, depends on the magnitude of reflection and time of return of the reflections. The pressure wave is separated into its forward and backward components (*left*). The backward wave is then shifted in time and the summated wave is calculated. It may be seen that the augmentation index strongly depends on the time of return of the reflected wave (*right*). Therefore the augmentation index cannot be used to quantify the magnitude of the reflection. Modified from ref. [2]

In hypertension, wave speed is increased. Resistance and thus diffuse reflections are also increased. This results in a large reflected pressure wave arriving at the heart in systole, and adding to the forward wave, resulting in a large Augmentation Index, and also in a higher Pulse Pressure and systolic pressure. The reflected flow wave is also large but subtracts from the forward flow wave resulting in a smaller net flow.

With increased reflection arriving in systole, the so-called supply-demand ratio of the cardiac muscle is negatively affected (see Chap. 16).

Not only is the magnitude of the reflected wave, but also its time of return is of importance. Thus the Augmentation Index does not only depend on the magnitude of reflection but it is affected by the moment the reflected waves return (see Fig. 21.5). Figure 21.6 shows the augmentation may be negative and positive depending on the moment the reflected wave arrives and on its magnitude. Thus a negative Augmentation Index does not imply negative reflection. Therefore estimation of the magnitude of the reflections cannot be carried out solely based on the Augmentation Index. Waveform analysis and the calculation of forward and backward waves allows for better estimation of reflection magnitude and time of return.

Reflection in the periphery causes a backward flow wave that may be seen as a reversal of the measured flow wave, Fig. 21.7. This negative part of the flow wave is greatly reduced in vasodilation, when the reflection and thus the backward flow wave is smaller. Also, mean flow is larger, and the measured flow wave does not exhibit a reversal.
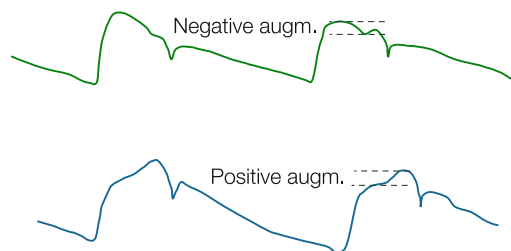
Fig. 21.6 With a small and late backward wave the augmentation may be negative (*top*, C beat). However, reflection is not negative. Early and large backward wave results in positive augmentation (*bottom*, type-A beat)
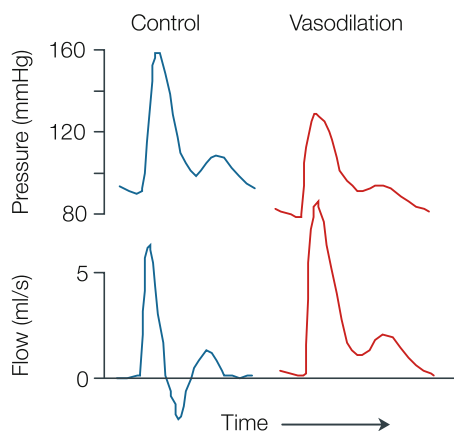
Fig. 21.7 Negative blood flow in part of the cardiac cycle results from inertia and reflections. With vasodilation the reflections decrease and flow reversal disappears (femoral artery). Adapted from ref. [9], used by permission

References

1. Murgo JP, Westerhof N, Giolma JP, Altobelli SA. Aortic input impedance in normal man: relationship to pressure wave forms. *Circulation* 1980;62:101–116.
2. Westerhof BE, Guelen I, Westerhof N, Karemaker JM, Avolio A. Quantification of wave reflection in the human aorta from pressure alone: a proof of principle. *Hypertension* 2006;48:595–601.
3. Sipkema P, Westerhof N. Effective length of the arterial system. *Ann Biomed Eng* 1975;3:296–307.
4. Westerhof BE, van den Wijngaard JP, Murgo JP, Westerhof N. Location of a reflection site is elusive: consequences for the calculation of aortic pulse wave velocity. *Hypertension* 2008;52:478–483.

5. Baksi AJ, Treibel TA, Davies JE, Hadjiloizou N, Foale RA, Parker KH, Francis DP, Mayet J, Hughes AD. A meta-analysis of the mechanism of blood pressure change with aging. *J Am Coll Cardiol* 2009;54:2087–2092.
6. Mitchell GF, Parise H, Benjamin EJ, Larson MG, Keyes MJ, Vita JA, Vasan RS, Levy D. Changes in arterial stiffness and wave reflection with advancing age in healthy men and women: the Framingham Heart Study. *Hypertension* 2004;43:1239–1245.
7. Pythoud F, Stergiopulos N, Westerhof N, Meister J-J. Method for determining distribution of reflection sites in the arterial system. *Am J Physiol* 1996;271:H1807–H1813.
8. Murgo JP, Westerhof N, Giolma JP, Altobelli SA. Manipulation of ascending aortic pressure and flow wave reflections with the Valsalva maneuver: relationship to input impedance. *Circulation* 1981;63:122–132.
9. O'Rourke MF, Taylor MG. Vascular impedance of the femoral bed. *Circ Res* 1966;18:126–139.

Chapter 22
Waveform Analysis

$$P_m = P_f + P_b \qquad Q_m = Q_f + Q_b$$
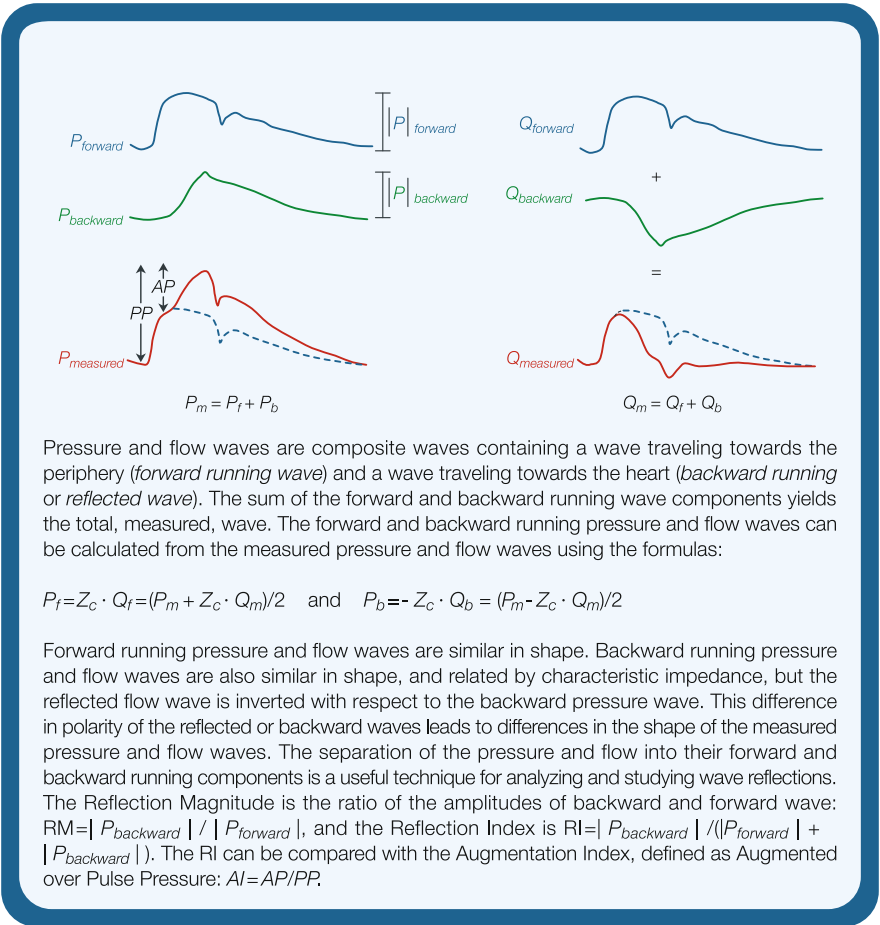
Pressure and flow waves are composite waves containing a wave traveling towards the periphery (*forward running wave*) and a wave traveling towards the heart (*backward running* or *reflected wave*). The sum of the forward and backward running wave components yields the total, measured, wave. The forward and backward running pressure and flow waves can be calculated from the measured pressure and flow waves using the formulas:

$$P_f = Z_c \cdot Q_f = (P_m + Z_c \cdot Q_m)/2 \quad \text{and} \quad P_b = - Z_c \cdot Q_b = (P_m - Z_c \cdot Q_m)/2$$

Forward running pressure and flow waves are similar in shape. Backward running pressure and flow waves are also similar in shape, and related by characteristic impedance, but the reflected flow wave is inverted with respect to the backward pressure wave. This difference in polarity of the reflected or backward waves leads to differences in the shape of the measured pressure and flow waves. The separation of the pressure and flow into their forward and backward running components is a useful technique for analyzing and studying wave reflections. The Reflection Magnitude is the ratio of the amplitudes of backward and forward wave: RM=| $P_{backward}$ | / | $P_{forward}$ |, and the Reflection Index is RI=| $P_{backward}$ | /(|$P_{forward}$ | + | $P_{backward}$ |). The RI can be compared with the Augmentation Index, defined as Augmented over Pulse Pressure: AI=AP/PP.

Description

At any location in the arterial tree, the measured pressure and flow waves are the sum of waves traveling from the heart towards the periphery (forward running waves) and waves traveling from peripheral arteries towards the heart (backward running waves). The backward running waves are often called reflected waves, simply because they arise from reflections of the forward running waves at arterial reflection sites.

Wave Separation Analysis: Forward and Backward Running Components

Consider the schematic diagram given in Fig. 22.1. As mentioned above, at any arterial location the measured pressure and flow waves (shown on the left) are the sum of their forward and backward running components [1, 2]. So, we may write

$$P_m = P_f + P_b$$

and

$$Q_m = Q_f + Q_b$$

The forward running flow wave and the forward running pressure wave, are related through the local characteristic impedance of the vessel (for the determination of Z_c
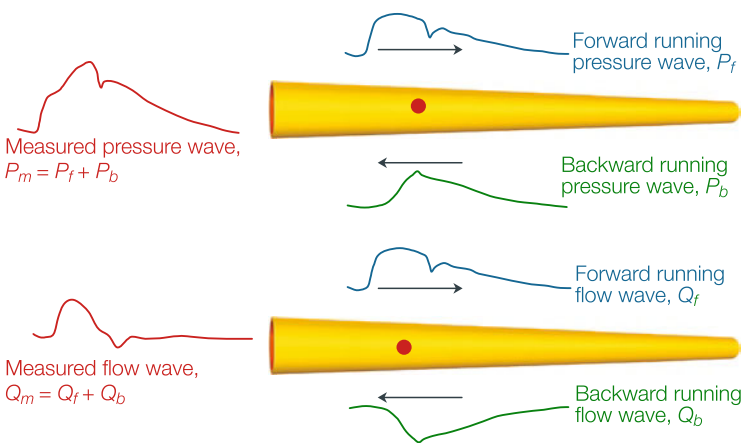
Fig. 22.1 Principle of the separation of pressure and flow waves into their forward and backward running components

see Appendix 4 and [1–3]) $P_f = Z_c \cdot Q_f$. The reflected flow and the reflected pressure wave are also related by the characteristic impedance, $P_b = -Z_c \cdot Q_b$. The minus sign results from the fact that flow is reflected 'upside down' in comparison with pressure (Chap. 21). Substituting Q_f and Q_b into the above equations we obtain:

$$P_f = Z_c \cdot Q_f = (P_m + Z_c \cdot Q_m) / 2$$

and

$$P_b = -Z_c \cdot Q_b = (P_m - Z_c \cdot Q_m) / 2$$

The above formulas are simple to use when the characteristic impedance, Z_c, is a real number, which means that we neglect the blood viscosity and the viscoelasticity of the wall. This is often a good approximation, especially when referring to conduit arteries, in which case we may calculate Z_c as:

$$Z_c = \rho \cdot c / A$$

with ρ blood density, c the local pulse wave velocity and A the luminal cross-sectional area. If, however, wall friction and viscoelasticity cannot be neglected, as in smaller vessels, then the same analysis holds and same equations apply, with the exception that the characteristic impedance Z_c is a complex number. In this case the analysis should be done in the frequency domain. This implies Fourier analysis (Appendix 1) of the measured pressure and flow waves, application of the above relations for each harmonic and inverse Fourier to reconstruct the time functions of the waves.

After the derivation of P_f and P_b the magnitude of reflection and the arrival time of the reflected wave can be calculated. The magnitude of reflection can be expressed by the Reflection Magnitude, which is the ratio of the amplitudes of backward and forward waves: $RM = P_b / P_f$. The Reflection Index, RI, is the ratio of the amplitudes of the backward wave and the sum of the forward and backward waves: $RI = P_b / (P_f + P_b)$. The RI can be qualitatively compared with the Augmentation Index (see Figure in the Box and Fig. 22.2). Waveform analysis requires measurement of pressure and flow to calculate P_f and P_b. The arrival time of the reflected wave can be determined from the foot of the wave (see Fig. 22.2). In the calculation of RM and RI calibration of pressure and flow are not required since they are ratios [4]. It was also suggested that pressure alone may suffice if (aortic) flow is assumed to be triangular in wave shape ('triangulation method') [4, 5].

The Augmentation Index, AI, is derived from the measured pressure wave without the need for application of wave separation. However, while the Reflection Index gives a good measure of the magnitude of (total) reflection, the Augmentation Index depends on the delay, magnitude and the shape of the reflected wave and the shape of the forward wave, and therefore cannot give a quantitative description of reflection magnitude. In Chap. 21 it was shown that for the same magnitude and wave shape of the backward and forward waves the delay between them strongly determines the Augmentation Index.

Another approach to the analysis of pressure and flow in a given arterial location is to look at very small portions of the traveling wave (dP or dQ). This is called
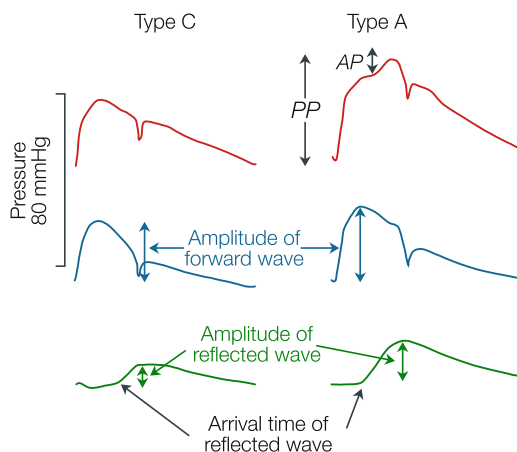
Fig. 22.2 Analysis of aortic pressure waves (*red*) into their forward (*blue*) and reflected, or backward, waves (*green*). The Type C beat pertains to a young adult and the Type A beat to an old subject. Augmented pressure over pulse pressure is the augmentation index, AI = AP/PP

wave intensity analysis [6]. The application of 'wavelets' to separate the pressure and flows into their forward and backward running components leads to identical results on reflections when compared to the method expressed by the equations given above [7].

Physiological and Clinical Relevance

The analysis of arterial pressure and flow waves into their forward and backward running components can be used to quantify the role of wave reflections in certain physiological and pathological situations. Figure 22.2 shows the aortic pressure waves measured in young healthy adult, type C beat, and an older subject, type A beat [1]. Figure 22.2 also shows the forward and backward running pressure components. For the type C beat we observe that the amplitude of the reflected wave is rather small and in the order of 12 mmHg. Further, the rise in the reflected wave arrives relatively late in systole. The net effect is that the addition of the reflected wave onto the forward wave does not lead to a significant increase in late systolic pressure. In contrast, in the old subject (Fig. 22.2, right), we observe a considerably larger amplitude of the reflected wave, which also arrives early in systole. Here the addition of the reflected wave to the forward wave leads to a very pronounced late systolic peak, resulting in a considerable increase in systolic pressure. The late systolic peak in the Type A beat results from wave reflection (Chap. 21) and has been related to the Augmentation Index, AI, defined as the ratio *AP/PP*. The limitation of the AI has been discussed in Chap. 21. The RI and RM, mentioned above appear to give better quantification of reflection in magnitude and timing.

Practical Determination of Characteristic Impedance

In practice, the characteristic impedance of large vessels can be determined in two ways. The first is by averaging of the modulus of the input impedance between the fourth and tenth harmonic (Chap. 23). The second method is by taking the slopes of the aortic pressure and flow waves during the early part of the ejection period, ΔP and ΔQ, and calculating their ratio: $Z_c = (\Delta P/\Delta t)/(\Delta Q/\Delta t)$ [3]. Both methods (see also Appendix 4) rely on the fact that characteristic impedance is a pressure-flow relation in the absence of reflections. Reflections are small in early systole and at high frequencies (see Chap. 23).

Reflections Depend on the Vascular Bed and on Its Vasoactive State

Wave reflections in the pulmonary circulation are less significant than in the systemic arterial tree [8]. Aortic pressure and flow and common pulmonary artery pressure and flow, are broken down in their forward and backward components (Fig. 22.3). When the systemic bed is dilated, with nitroprusside, reflections
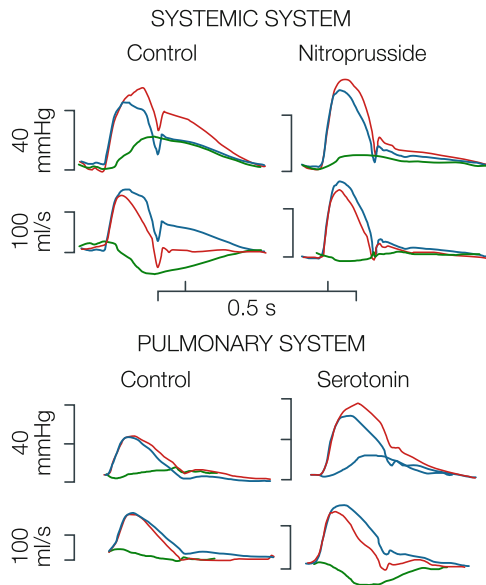
Fig. 22.3 Pressure and flow in aorta and common pulmonary artery are broken down in their forward and backward components. *Red lines*, *blue lines*, and *green lines* give measured waves, forward waves, and backward waves, respectively. With vasodilation and vasoconstriction backward waves are reduced and increased, respectively. Adapted from ref. [8], used by permission

decrease, and when the pulmonary arterial system is constricted, with serotonin, reflections increase. It should be noticed that when reflections decrease in magnitude, the pressure and flow waves become similar in shape, while the inverse happens with increased reflections.

References

1. Murgo JP, Westerhof N, Giolma JP, Altobelli SA. Aortic input impedance in normal man: relationship to pressure wave forms. *Circulation* 1980;62:105–116.
2. Westerhof N, Sipkema P, van den Bos GC, Elzinga G. Forward and backward waves in the arterial system. *Cardiovasc Res* 1972;6:648–656.
3. Li JK. Time domain resolution of forward and reflected waves in the aorta. *IEEE Trans Biomed Eng* 1986;33:783–785.
4. Westerhof BE, Guelen I, Westerhof N, Karemaker JM, Avolio A. Quantification of wave reflection in the human aorta from pressure alone: a proof of principle. *Hypertension* 2006;48:595–601.
5. Mitchell GF. Triangulating the peaks of arterial pressure. *Hypertension* 2006;48:543–545.
6. Hughes AD, Parker KH. Forward and backward waves in the arterial system: impedance or wave intensity analysis? *Med Biol Eng Comput* 2009;47:207–210.
7. Parker KH. An introduction to wave intensity analysis. *Med Biol Eng Comput* 2009;47:175–188. Review.
8. Van den Bos GC, Westerhof N, Randall OS. Pulse-wave reflection: can it explain the differences between systemic and pulmonary pressure and flow waves? *Circ Res* 1982;51:479–485.

Chapter 23
Arterial Input Impedance
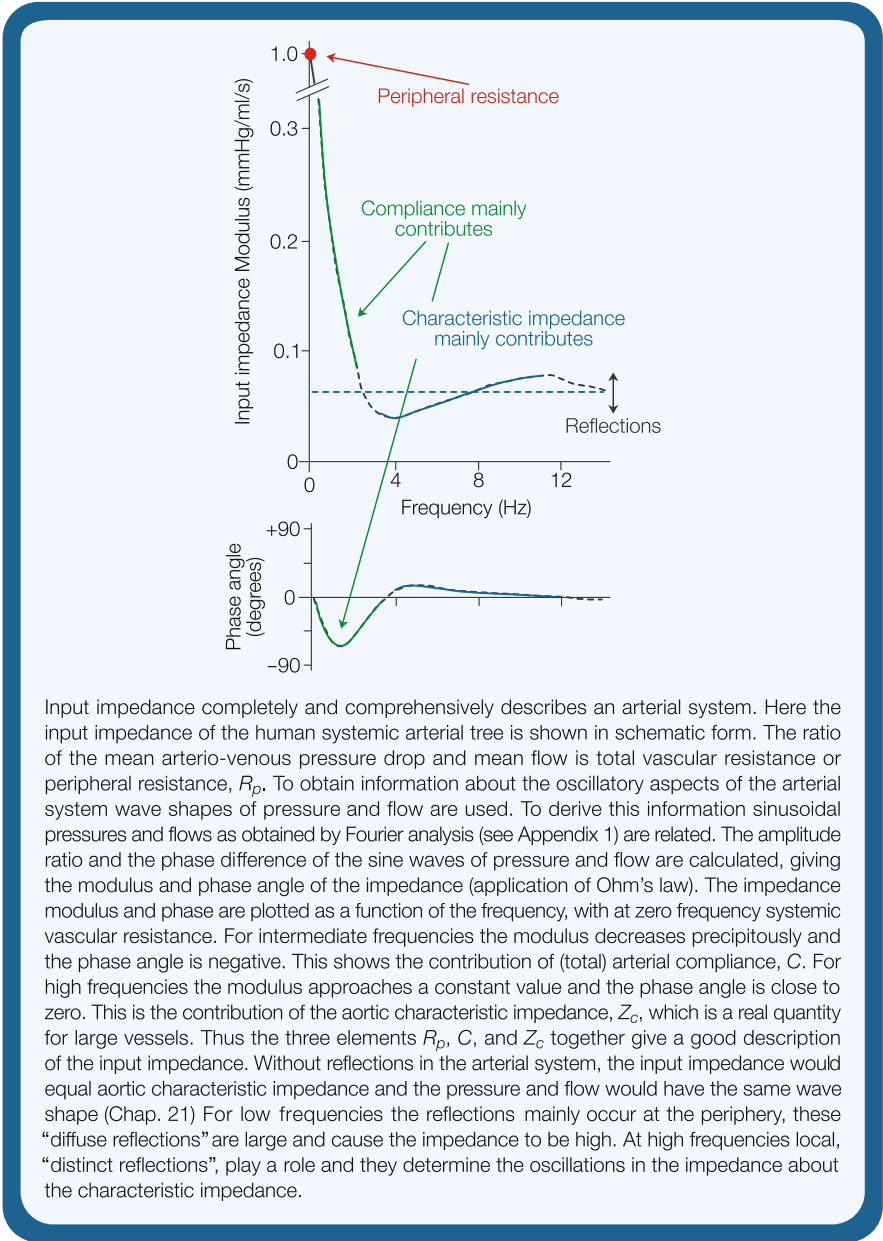
Input impedance completely and comprehensively describes an arterial system. Here the input impedance of the human systemic arterial tree is shown in schematic form. The ratio of the mean arterio-venous pressure drop and mean flow is total vascular resistance or peripheral resistance, R_p. To obtain information about the oscillatory aspects of the arterial system wave shapes of pressure and flow are used. To derive this information sinusoidal pressures and flows as obtained by Fourier analysis (see Appendix 1) are related. The amplitude ratio and the phase difference of the sine waves of pressure and flow are calculated, giving the modulus and phase angle of the impedance (application of Ohm's law). The impedance modulus and phase are plotted as a function of the frequency, with at zero frequency systemic vascular resistance. For intermediate frequencies the modulus decreases precipitously and the phase angle is negative. This shows the contribution of (total) arterial compliance, C. For high frequencies the modulus approaches a constant value and the phase angle is close to zero. This is the contribution of the aortic characteristic impedance, Z_c, which is a real quantity for large vessels. Thus the three elements R_p, C, and Z_c together give a good description of the input impedance. Without reflections in the arterial system, the input impedance would equal aortic characteristic impedance and the pressure and flow would have the same wave shape (Chap. 21) For low frequencies the reflections mainly occur at the periphery, these "diffuse reflections" are large and cause the impedance to be high. At high frequencies local, "distinct reflections", play a role and they determine the oscillations in the impedance about the characteristic impedance.

Description

Definition of Impedance

Impedance is the relation between the pressure difference and flow of a linear system, for sinusoidal or oscillatory signals. Impedance completely describes the system and it can be derived from pulsatile pressure difference and pulsatile flow and the application of Fourier analysis. Inversely, when the impedance is known, a given flow allows for the calculation of pressure and vice versa. Systemic arterial and pulmonary arterial input impedance are a comprehensive description of the systemic and pulmonary arterial tree. Input impedances of organ systems may be derived as well. The longitudinal, transverse and characteristic impedance are discussed in Appendix 3.

Derivation of Input Impedance

In the calculations of input impedance, Z_{in}, we use both the mean values and the pulsatile part of the pressure and flow. We apply Fourier analysis of the aortic pressure and flow because the calculations can only be performed for sinusoidal signals. The details and limitations of Fourier analysis are discussed in Appendix 1. To derive impedance Ohm's law is applied. For each pair of sine waves of pressure and flow (i.e., harmonics) we calculate the ratio of the amplitudes and the phase angle difference between them. To apply Ohm's law, i.e., to calculate impedance and peripheral resistance, the system must be in the steady state, time-invariant, and linear. This means that the arterial system may not vary in time, e.g., vasomotor tone should be constant, and that the relation between pressure and flow is linear, e.g., if a sine wave of pressure is applied a sine wave of flow should result. For a time-varying system the calculation of impedance does not lead to interpretable results. The coronary circulation, where resistance and arterial compliance vary over the heartbeat, the calculation of impedance from pressure and flow using Fourier analysis does not lead to reasonable results. For a nonlinear system the calculation of impedance also does not lead to interpretable results. An example is the calculation of 'impedance' from ventricular pressure and aortic flow, where the aortic valves make the system nonlinear, and where the results are not useful. The arterial system is not perfectly linear but the variations of pressure and flow over the heartbeat are sufficiently small so that linearity is approximated and the derived impedance is a meaningful description. It has been shown that some of the scatter of the input impedance data (Fig. 23.1) results from nonlinearity [2].
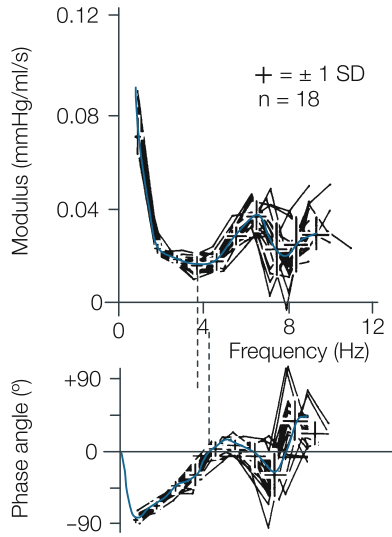
Fig. 23.1 Scatter in the input impedance (type A beat) is caused, in part, by noise on the pressure and flow signals especially affecting the small amplitudes of high harmonics. Non-linearity of the arterial system also contributes to the scatter. The *blue line* is drawn through the averaged values. The *vertical dashed lines* indicate that the modulus minimum and phase zero crossing are not at the same frequency, implying that a single tube with real, 'in phase' reflection is not a good model of the entire arterial tree. From ref. [1], by permission

Limitations

The limitations of linearity and time-invariance also hold for the calculation of peripheral resistance. Mean aortic pressure divided by mean aortic flow only gives information on peripheral resistance if, over the period of determination, peripheral resistance does not vary. Also, mean left ventricular pressure over mean aortic flow does not lead to a sensible result because the system includes the valves and is not linear.

Fourier analysis and subsequent calculation of the input impedance only gives information at frequencies that are multiples of the Heart Rate, i.e., harmonics (Appendix 1). By pacing the heart at different rates, the frequency resolution can be increased.

Because the information contained in the signals for high frequencies is small, the higher harmonics (Appendix 1) are subject to noise, so that the impedance at high frequencies often scatters considerably. This limitation can be partly circumvented by analyzing more than one heartbeat and averaging the results. This can be done by using, for instance, an entire respiratory cycle (steady state of oscillation) or by analyzing a series of beats individually (Fig. 23.1) followed by averaging of the impedances [1].

In the systemic circulation venous pressure may be neglected (Chap. 6), so that the use and Fourier analysis of aortic pressure and flow gives a sufficiently accurate approximation of the input impedance. However, in the analysis of the pulmonary circulation venous pressure cannot be neglected.

Hemodynamic Elements

In Appendix 2 the basic hemodynamic elements are discussed. For a resistor it holds that the sine waves of pressure and flow are in phase, i.e., the phase angle is zero. For compliance the flow is advanced with respect to pressure. This is seen as $-90°$ in the impedance phase angle. For inertance flow is delayed, and shows as $+90°$ for the impedance phase. The modulus of the impedance decreases with frequency, $1/\omega C$ for compliance, and increases with frequency, ωL, for the inertance, respectively. In Appendix 4 characteristic impedance is discussed. It is shown that the characteristic impedance of a large artery, like the aorta, the mass effects and compliance effects interact in such a way that sinusoidal pressure and flow waves are in phase, and their ratio is constant. Thus the phase angle of the characteristic impedance is then zero and its modulus is constant and independent of frequency, i.e., $Z_c = \sqrt{Z_l'}\ Z_t' = \sqrt{L'/C_A} = \sqrt{\rho\Delta P/\Delta A \cdot A}$. This means that the amplitude ratio of pressure and flow is the same for all frequencies and the phase angle is zero. Thus for large vessels the characteristic impedance is similar to a resistance and is often called characteristic resistance, and modeled as a resistor. However, characteristic impedance is non-existent at zero Herz and no energy is lost in it. Thus when modeling characteristic impedance with a resistor these limitations must be kept in mind.

Explanation of Input Impedance

Although the input impedance gives a comprehensive description of the arterial system its practical use is limited.

The Windkessel. However, the description of the impedance given in the box suggests three important parameters describing input impedance. These three parameters form the basis of the Windkessel models Chap. 24). The original two-element Windkessel, proposed by Frank, consists of peripheral resistance, R_p, and total arterial compliance, C. From the information on input impedance, which became available in the 1960s, the idea of aortic characteristic impedance, Z_c, as third Windkessel element appeared [3]. However, we should keep in mind that when the characteristic impedance is modeled with a resistor the mean pressure over mean flow will be $R_p + R_c$, while it should be R_p only. Although this error is not large for the systemic circulation where R_c is about 7% of R_p, it leads to errors when, for instance the three-element Windkessel is used to estimate total arterial compliance. To correct for these shortcomings, a fourth element, the total arterial inertance (see Chap. 24) was introduced [4].

Wave transmission. From wave transmission we can explain the impedance as follows. For a reflectionless system the input impedance equals aortic characteristic impedance and, inversely, the difference between input impedance and characteristic impedance results from reflections. For low frequencies the reflections from bifurcating arteries and other discontinuities mainly in the periphery, where bifurcations occur over short distances, return to the proximal aorta. The effect of the diffuse reflected waves is that impedance strongly differs from aortic characteristic impedance. For high frequencies, where wavelengths are less than the length of the arterial system, the waves return out of phase, and cancel each other out so that the arterial system appears reflectionless. Also damping which is stronger for the high frequencies causes less reflections to return. For high frequencies input impedance is, therefore, close to the characteristic impedance, i.e., constant modulus and phase angle close to zero. The oscillations of the impedance modulus around the characteristic impedance, and the oscillations in phase angle, result from distinct reflections. It has been suggested that in the human these reflections may occur at the aortic bifurcation or at the level of the renal arteries. This is considered a distinct reflection site and the reflections lead to the inclination point in systolic pressure and the pressure augmentation (type A beat, Chap. 22). The ratio of backward and forward running wave amplitudes is related to the magnitude of the oscillations in the impedance modulus [1].

Effective Length of the Arterial System

The frequencies where the minimum in the input impedance modulus and the zero crossing of the phase angle occur have been used to estimate the 'effective length' of the arterial system. The effective length of the arterial system is used as a conceptual description to determine at what distance from the ascending aorta the major reflections arise. In this concept it is assumed that the arterial system behaves like a single tube, the aorta, with a single resistance, the peripheral resistance at its distal end. To derive the effective length is then simple. Since the aortic characteristic impedance is a real number (no phase angle), the reflection coefficient is real as well. Let us consider a sinusoidal pressure and flow, with a wavelength four times the length of the aorta. When the forward pressure wave travels a quarter wave length to reach the end of the tube, and again one quarter wave length to return at the heart, the forward and reflected waves of pressure are 180° out of phase and thus cancel, and the measured pressure wave has negligible amplitude. For the flow waves the same holds, but the flow waves are reflected 180° out of phase (Chap. 21). Thus the forward and reflected flow waves are 360° out of phase: 180° results from the reflection and the other 180° results from traveling half a wavelength. This means that forward and backward flow waves are in phase and the measured flow about twice the forward or backward wave. Thus for a frequency where this model system is a quarter of a wavelength long, pressure is negligible,

and flow is large, and the modulus of the input impedance is small and the phase angle is zero. This is called the quarter wavelength principle.

Quantitatively we describe this phenomenon as follows. The wave speed, c, equals wavelength, λ, times frequency, f, thus, $c = \lambda \cdot f$. When the length of the tube is a quarter wave length, $l = \lambda/4$, and the minimum of the impedance is found at frequency $f = c/\lambda$, $= c/4 \cdot l$ or $l = c/4 \cdot f$. With a wave speed in the aorta of 6 m/s and the frequency of the minimum in the impedance modulus or zero crossing of the phase at 4 Hz, the effective length equals $600/4\cdot4 \sim 38$ cm. However, the assumption of a single tube, loaded with the peripheral resistance as model of the systemic arterial tree, is too simple and often unrealistic. When the reflection coefficient is not real, i.e., when the phase of the pressure and flow waves are changed at the reflection site, the calculation may even lead to an effective length longer than the arterial system [5]. When the impedance modulus minimum and zero crossing of the phase angle are not found at the same frequency, the assumption that the arterial system can be modeled with a single tube and a peripheral resistance is violated. Since the distinct reflection coefficient is not a real quantity in the mathematical sense, the arrival time of the reflected wave at the heart not only depends on wave speed and distance to the distinct reflection site, but also depends on the phase angle of the reflection coefficient [6].

External Power

The power produced by the heart equals (I/T). $\int P(t) \cdot d(t)$, with integration over the heart period T (in practice the ejection period since otherwise flow is negligible), and is called total external power. When mean aortic pressure and Cardiac Output are multiplied the mean power is obtained (see Chap. 15). The difference is called oscillatory or pulsatile power, which is about 15% of total power. We can also calculate power by means of the input impedance. Using Ohm's law, mean power is then $CO^2 \cdot R_p$. Oscillatory power must calculated for each harmonic (n), separately from flow Q_n and $Z_{in,n}$, and then added as: $\Sigma Q_n^2 \cdot |Z_{in,n}| \cos \phi_n$, with $|Z_{in,n}|$ the impedance modulus and ϕ_n the impedance phase angle. The sum of mean power and oscillatory power equals total power. It has been suggested that the minimum of the modulus of the input impedance should relate to Heart Rate since power was then thought to be minimal. However, we see that not the modulus alone but the real part of the input impedance (modulus times cosine of the phase angle) determines power and the real part has often no clear minimum.

Impulse Response

Conceptually, it is rather awkward that while pressure and flow are functions of time, the input impedance is expressed as a function of frequency. There exists a characterization of the arterial system in the time domain. This characterization is

the so-called impulse response function, which is the pressure that results from an impulse of flow, i.e., a short lasting flow, short with respect to all travel and characteristic times of the arterial system, typically about 1–5 ms in duration. Because the impulse has a height with dimension ml/s and the duration is in seconds, the area under the impulse is ml. The pressure response resulting from this impulse is normalized with respect to the volume of the impulse and the units of the impulse response are therefore mmHg/ml. The calculation of the impulse response function from measured pressure and flow is complicated but straightforward [7]. When the measured flow is broken up in a number of short impulses, the proper addition of the impulse responses leads to the pressure as a function of time.

The input impedance and impulse response function form a 'Fourier pair'. Fourier analysis of the impulse response function leads to the input impedance and inverse transformation of input impedance leads to the impulse response function [7].

If the impulse response is short in duration with respect to the time constant of variation of the time varying system, it may be used to obtain a characterization of that system as a function of time. For example, if the duration of the impulse response is less than 100 ms, and the system under study varies with a typical time of a few hundred milliseconds, the system can be characterized by the impulse response. In this way input impedance of the coronary arterial system was derived in systole and diastole [8].

Physiological and Clinical Relevance

As discussed above, derivation of input impedance requires sophisticated analysis of pressure and flow waves, the data show scatter (Fig. 23.1), and interpretation requires models. Thus, routine clinical applications are seldom carried out. However, impedances calculated in the human and mammals have led to a much better understanding of arterial function. For instance, the input impedance of the arterial system, when normalized to peripheral resistance, is similar in mammals [9]. This explains, in part, why aortic pressures and flows are so similar in shape in mammals (Chap. 30).

The arterial system can be described in terms of Windkessel models and distributed models. The main arterial parameters describing input impedance are peripheral resistance, total arterial compliance and aortic characteristic impedance (Box Figure). Arterial function is often easier to understand when the three Windkessel parameters given as description of the arterial system. With the modern computing techniques the calculation of the parameters of the Windkessel model can be performed rapidly and gives directly interpretable results. For instance, a change in total arterial compliance, which is often not obvious from the impedance plot, can be obtained directly, while the impedance calculations can be avoided.

In terms of wave transmission the pressure and flow waves can be better analyzed in terms of forward and backward running waves than in terms of impedance

(Chap. 22). The amplitude ratio of the backward and forward waves appears to relate with the oscillations of the modulus of the impedance around the characteristic impedance.

The Characteristic Pressure Wave Shapes in Old and Young Subjects

The examples shown in Figs. 23.2 and 23.3 make clear that, although the pressure and flow waves result from the interaction of the heart and arterial load, major features of the pressure wave shape arise from the arterial system and can therefore be related to aspects of the input impedance.

   Greater reflections result in greater differences in the wave shapes of pressure and flow and in more deviation of the input impedance from the aortic characteristic impedance (Type A beat).
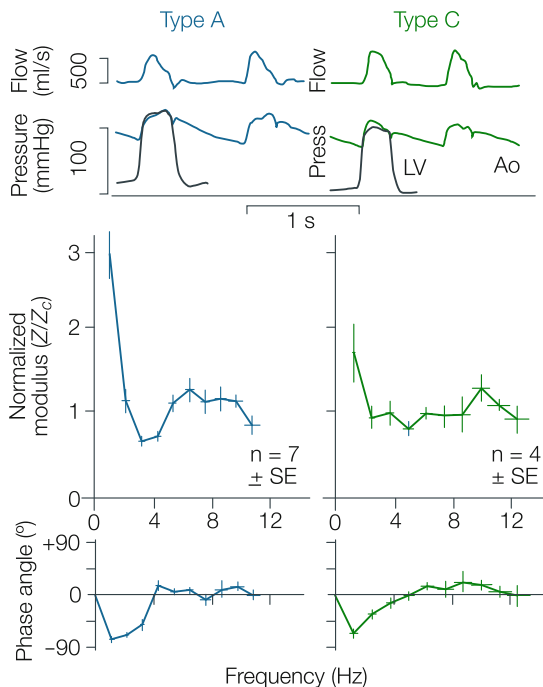
Fig. 23.2 Types of beats relate to input impedance. In older subjects, Type A, with high pulse wave velocity, the distinct reflection returns in systole and augments the pressure wave. The impedance oscillates about the characteristic impedance. In young subjects, Type C, reflections are smaller and return in diastole. The impedance oscillates less. Adapted from ref. [1], used by permission
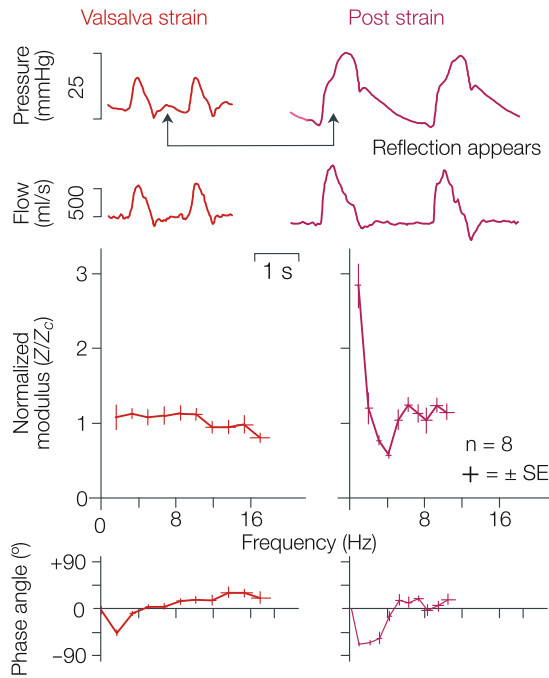
Fig. 23.3 The Valsalva strain maneuver increases intra-thoracic and intra-abdominal pressures. The thus lower transmural pressure increases arterial compliance and lowers pulse wave velocity. Reflections diminish and return later, in diastole. An almost reflectionless situation appears where pressure and flow resemble each other (*top*) and input impedance is close to aortic characteristic impedance. In the release phase the reverse is true, reflections return in systole and are large. Adapted from ref. [10], used by permission

Changes in Reflection

In the Fig. 23.3 (left side) we see that during the Valsalva maneuver aortic pressure resembles aortic flow in wave shape [10]. During the Valsalva maneuver intra-thoracic and intra-abdominal pressures increase. The transmural pressure of the aorta decreases and the compliance increases leading to a decreased pulse wave velocity. As a result reflections return slower and arrive late in the cardiac cycle, in diastole. Reflections are probably also decreased in magnitude. The result is an almost reflectionless arterial system. Pressure and flow become similar in shape and the input impedance is close to the characteristic impedance of the aorta. After the release of the Valsalva maneuver, cardiac filling and transmural pressure are increased, Cardiac Output and pulse wave velocity are increased as well and reflections return in systole, and a large augmentation in the pressure is seen (Fig. 23.3 right side).

Hypertension

In Fig. 23.4 we see the relation between systolic hypertension and the changes in the arterial system represented as input impedance. With increasing age systolic pressure increases and diastolic pressure even decreases somewhat. The main age-related change in the arterial system is decrease of arterial compliance. The decrease in compliance can be seen in the impedance graph: the modulus decreases less rapidly with increasing frequency (1) and the characteristic impedance is increased (2). The pulse wave velocity is also increased and therefore the waves reflected at the level of the lower abdominal aorta return earlier at the heart and augment the pressure wave in the ascending aorta. The result is larger oscillations of the impedance around the characteristic impedance and a larger Pulse Pressure (3). Peripheral resistance also increases somewhat and the result is a small increase in mean pressure (4).
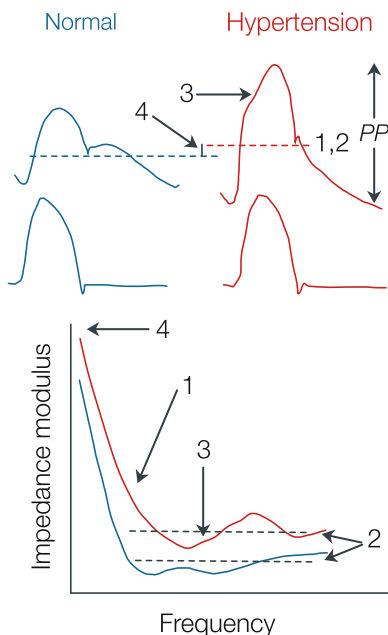
Fig. 23.4 In hypertension peripheral resistance and thus mean pressure is increased (4). Compliance is decreased resulting in a larger pulse pressure, PP, a less rapid decrease in imped-ance modulus with frequency (1), and larger characteristic impedance (2). Reflections are increased, the impedance oscillates more about the characteristic impedance (3), and the wave is augmented (3). Adapted from ref. [11], used by permission

References

1. Murgo JP, Westerhof N, Giolma JP, Altobelli SA. Aortic input impedance in normal man: relationship to pressure wave forms. *Circulation* 1980;62:105–1116.
2. Stergiopulos N, Meister J-J, Westerhof N. Scatter in the input impedance spectrum may result from the elastic nonlinearity of the arterial wall. *Am J Physiol* 1995;269:H1490–H1495.
3. Westerhof N, Elzinga G, Sipkema P. An artificial system for pumping hearts. *J Appl Physiol* 1971;31:776–781.
4. Stergiopulos N, Westerhof BE, Westerhof N. Total arterial inertance as the fourth element of the windkessel model. *Am J Physiol* 1999;276:H81–H88.
5. Sipkema P, Westerhof N. Effective length of the arterial system. *Ann Biomed Eng* 1975;3:296–307.
6. Westerhof BE, van den Wijngaard JP, Murgo JP, Westerhof N. Location of a reflection site is elusive: consequences for the calculation of aortic pulse wave velocity. *Hypertension* 2008; 52:478–483.
7. Sipkema P, Westerhof N, Randall OS. The arterial system characterized in the time domain. *Cardiovasc Res* 1980;14:270–279.
8. Van Huis GA, Sipkema P, Westerhof N. Coronary input impedance during the cardiac cycle as obtained by impulse response method. *Am J Physiol* 1987;253:H317–H324.
9. Westerhof N, Elzinga G. Normalized input impedance and arterial decay time over heart period are independent of animal size. *Am J Physiol* 1991;261:R126–R133.
10. Murgo JP, Westerhof N, Giolma JP, Altobelli SA. Manipulation of ascending aortic pressure and flow reflections with the Valsalva maneuver: relationship to input impedance. *Circulation* 1981;63:122–132.
11. O'Rourke MF. Pulsatile arterial haemodynamics in hypertension. Aust N Z J Med 1976;6(suppl 2):40–48.

Chapter 24
The Arterial Windkessel

The analogy between the fire engine with the Windkessel and the arterial system. The peripheral resistance is the summed resistance of all small arteries, arterioles and capillaries. Total arterial compliance is the sum of the compliances of all arteries, mainly the conduit arteries. The Windkessel model can help us to understand how the arterial system functions, can be used as a realistic load in isolated heart studies, can be used in modeling, and can form the basis for estimating arterial system parameters. Adapted from [1], used by permission.

Description

Figure 24.1 shows the three-element Windkessel as model for the load on the heart. This (hydraulic) model) as load of the real heart results in ventricular and aortic pressure and aortic flow that are similar to those measured *in vivo* Three Windkessel models are given in Fig. 24.2. Otto Frank, 1899, popularized the original two-element Windkessel. He reasoned that the decay of diastolic pressure in the ascending aorta,
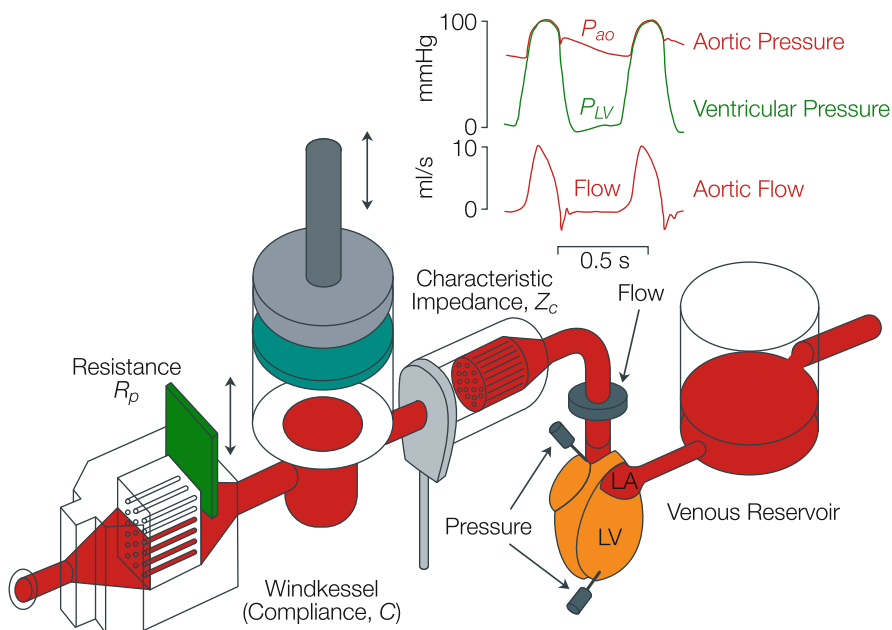
Fig. 24.1 The three-element Windkessel is a lumped model of the entire systemic arterial tree and mimics the load on the heart. Its three parameters have a physiologic meaning (see Chap. 23). The peripheral resistance equals the resistance of all small arteries, arterioles and capillaries. The total arterial compliance equals the sum of the compliances of all arteries, it is mainly located in the conduit arteries, with the greater part in the (proximal) aorta. The characteristic impedance of the proximal aorta, Z_c, related with Pulse Wave Velocity, c, through aortic cross-sectional artery, A, by $Z_c = \rho \cdot c \cdot A$, and forms the link of the Windkessel with transmission line models. When this model is used to load an isolated heart, the pressures and flow generated by this heart in combination with the artificial arterial tree are as in the intact animal (*inset at top*).

when flow is zero, can be described by an exponential curve. The time constant, τ, i.e., the time for pressure to decrease to 37% of the starting pressure, is given by the product of peripheral resistance, R_p, and the total arterial compliance, C, $\tau = R_p C$. The larger the resistance the slower the blood, stored in the compliant conduit vessels, leaves the system and the longer the time constant will be. Also, the larger the compliance the more blood is stored, and the longer the time constant will be. Frank's objective was to derive Cardiac Output from aortic pressure. By measuring the pulse wave velocity over the aorta (carotid to femoral) together with, averaged, cross-sectional area, and using the Newton-Young equation (Chap. 20) area compliance, C_A, can de estimated. When aortic length is also known volume compliance, C, is derived. Using τ and C, the peripheral resistance can be calculated from $R_p = \tau/C$. From mean pressure and resistance, using Ohm's law, mean flow is then found. The assumption that all compliance is located in the aorta, thus neglecting the compliance of the smaller conduit vessels, introduces a small error. After pulsatile flows could be measured, and arterial input impedance could be determined (Chap. 23), the shortcomings of the two-element Windkessel became clear.
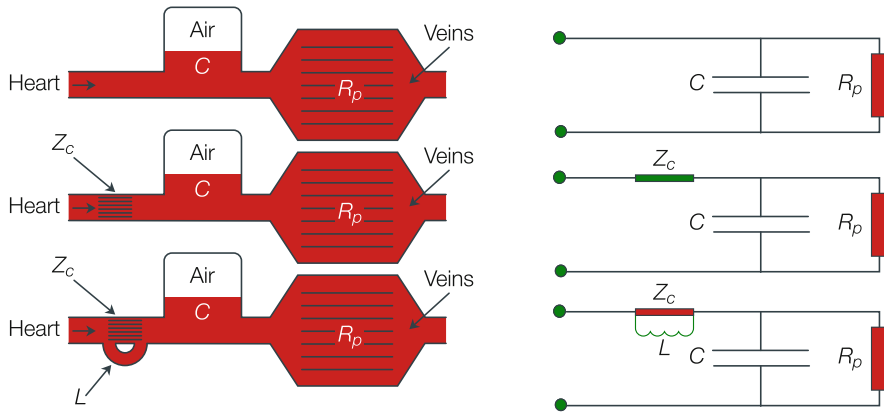
Fig. 24.2 The three Windkessels: The hydraulic version (*left*) and electrical version (*right*). The two-element Windkessel (Frank) contains total peripheral resistance (R), and total arterial compliance (C). The three-element Windkessel contains the aortic characteristic impedance, (Z_c). The four-element Windkessel contains total arterial inertance, playing a role at the very low frequencies. This fourth element also solves the problem that characteristic impedance, although having the dimension resistance, is not a real resistor and therefore, in the three-element Windkessel model mean pressure over mean flow equals $Z_c + R$ instead of R. Adapted from ref. [1], used by permission

The three-element Windkessel is based on Frank's two-element Windkessel with the addition of the characteristic impedance [2]. Input impedance shows, at high frequencies, a constant impedance modulus and a phase angle of about zero degrees (Chap. 23). This is not in line with the impedance of the two-element Windkessel that exhibits a continuously decreasing modulus and a phase angle that approaches $-90°$ for high frequencies (Fig. 24.3). From a wave transmission and reflection standpoint, it can be reasoned that for high frequencies reflections in the proximal aorta cancel out and for a reflectionless aorta the input impedance equals its characteristic impedance (Chap. 22). Or, in other words, for high frequencies the input impedance equals the characteristic impedance of the proximal aorta. Aortic characteristic impedance is a real number, i.e., its modulus is constant with a value $Z_c = \sqrt{\rho} \, \Delta P/(\Delta A \cdot A)$ and its phase angle is zero (Appendix 4). This behavior is also characteristic of a resistance. Therefore, a resistor has often been used to mimic the characteristic impedance of the proximal aorta. The introduction of the characteristic impedance or characteristic resistance as the third element of the Windkessel can be seen as bridging the lumped models and the transmission line models. However, the characteristic impedance is only present for oscillatory pressure and flow and does not dissipate energy while a resistor does (Chap. 23).

The approximation of characteristic impedance by a resistor leads to errors in the low frequency range. When, for instance, total arterial compliance is determined from aortic pressure and flow by parameter estimation of the three elements of the Windkessel, the compliance is consistently overestimated.

The fourth element of the Windkessel was introduced to circumvent the inconsistency resulting from modeling the characteristic impedance by a resistance [3].
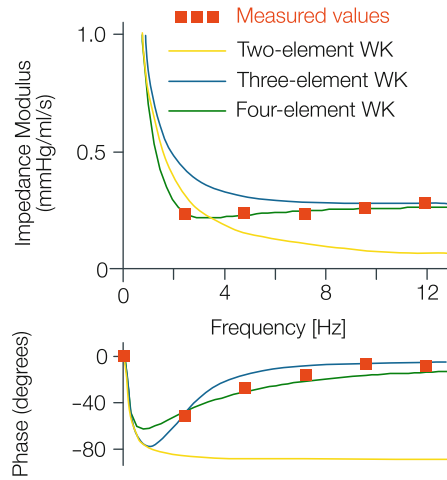
Fig. 24.3 The input impedances of the two-element, three-element and four-element Windkessel models, compared with the measured input impedance. The two-element Windkessel clearly falls short, especially in the high frequency range. The three-element Windkessel is less accurate at very low frequencies, as a result of the representation of the characteristic impedance by a resistance.

The four-element Windkessel is also shown Fig. 24.2 and its input impedance in Fig. 24.3. It has been established that the inertance term equals total inertance of the arterial system. Using this four-element Windkessel model, total arterial compliance is estimated accurately from pressure and flow.

In summary, the characteristic impedance introduces transmission concepts into the Windkessel model and provides for a correct behavior of the model at high frequencies. The total arterial inertance improves the very low frequency behavior of the Windkessel [2, 3].

When flow is zero, as in diastole, the decrease of aortic pressure, is characterized by the decay time (Fig. 24.4), which equals R_pC for all three Windkessel models, if we start with some delay after valve closure (about 10% of the heart period). The Windkessel models only mimic the behavior of the entire arterial system, or sub-systems, at their entrance. This lumped description of the entire arterial system means that pressures within these models have little meaning. The measurement of pressure distal of the characteristic impedance, for instance, does not represent the pressure in the more distal arterial system.

How the Arterial Tree Reduces to a Windkessel

For very low frequencies the wavelengths are very long, longer than the arterial system. This implies that all pressure variations occur simultaneously, and the system reduces to a (two-element) Windkessel. For very high frequencies the wavelengths are short and the reflections returning from the many reflection
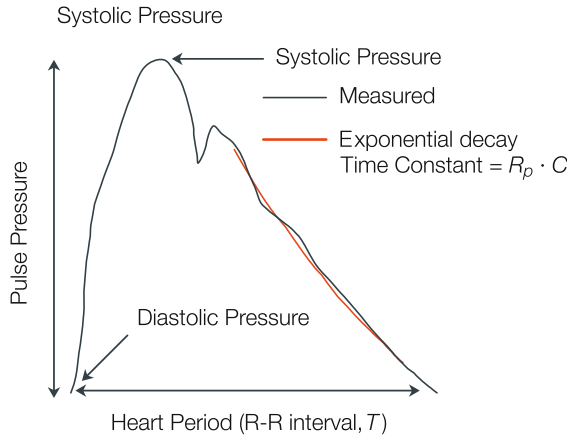
Fig. 24.4 The Windkessel models predict an exponential decay of aortic pressure when flow is zero, i.e., in diastole. This decay is characterized by the decay time that equals $R_p \cdot C$, with R_p peripheral resistance and C total arterial compliance. The decay is described by $P(t) = P_0 \cdot e^{-t/R_pC}$

sites, arrive at random times and cancel. Then the input impedance approaches the characteristic impedance of the aorta. In terms of reflections the Windkessel takes into account the diffuse reflections but not the distinct reflections (see Chap. 21).

Other Lumped Models

Other lumped models are partly Windkessel models with more elements and partly tube models. More elements in the Windkessel may evolve to transmission line models, but often the parameters lose their physiologic meaning. Tube models consist of single tubes, loaded with a resistor or with a Windkessel model. Two tube models may consist of two tubes in parallel or in series (Chap. 25). Wave transmission, not existing in the Windkessel models, is present in the tube models, which gives them certain advantages.

Physiological and Clinical Relevance

Windkessel models, especially the three-element Windkessel, can explain the behavior of the input impedance and gives a meaning to the three main parameters that describe the arterial system (Chap. 23). Windkessel models also find their use as load for the isolated ejecting hearts (Fig. 24.1). The Windkessel parameters may be changed and cardiac pump function studied [4]. Figure 24.5 shows an example of changes in peripheral resistance and total arterial compliance while cardiac contractility, Heart Rate and cardiac filling are maintained constant. In such a study we can compare changes in resistance and compliance on pressure and flow.
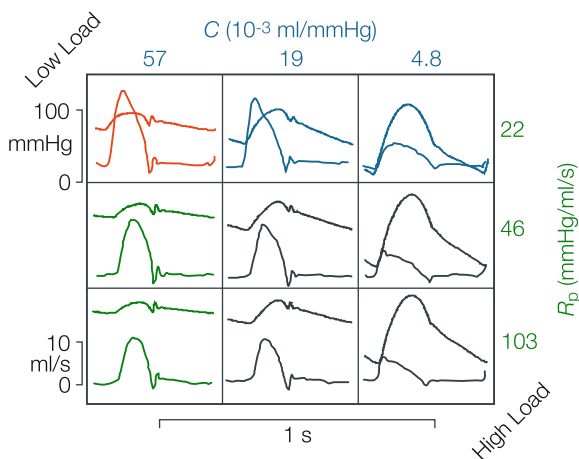
Fig. 24.5 Aortic pressure and flow resulting from an isolated cat heart pumping into a three-element Windkessel. The effect of changes in peripheral resistance (increasing downwards, *green*) and arterial compliance (decreasing to the right, *blue*) are shown. The control condition is the *left top panel*, *red*. The advantage of the use of such a model is that all venous and cardiac parameters can be kept constant while a single parameter of the load; here resistance or compliance can be varied. Adapted from ref. [4] used by permission

The three-element Windkessel model can, at least qualitatively, explain the changes in systolic and diastolic blood pressure with age. With aging peripheral resistance increases somewhat more than Cardiac Output decreases, resulting in a (small) increase in mean pressure. Total arterial compliance, mostly aortic compliance, decreases considerably (factor ~3; see Chap. 20) and therefore Pulse Pressure increases as well. The result is a strong increase in systolic pressure and a decrease in diastolic pressure (Fig. 24.6).

Another use of the Windkessel models is the estimation of arterial parameters. Several methods have been proposed to derive total arterial compliance [5]. These methods are (see Fig. 24.7):

- *The Stroke Volume over Pulse Pressure method*. This method is rather old [6] but has been reintroduced recently [7]. The method assumes that Stroke Volume is ejected in the conduit vessels (aorta) and that there is no run-off through the periphery. Therefore this ratio overestimates compliance [8] and should be used in comparisons only.
- *The decay time method described above*.
- *The area method*, where the area under the diastolic aortic pressure divided by the pressure difference between start and endpoint is set equal to decay time.

$$RC = \int_{t_1}^{t_2} \frac{P}{P_1 - P_2} dt$$

Knowing the R_pC time and calculating R_p, i.e., the ratio of mean pressure and mean flow, the compliance can be derived [9, 10].
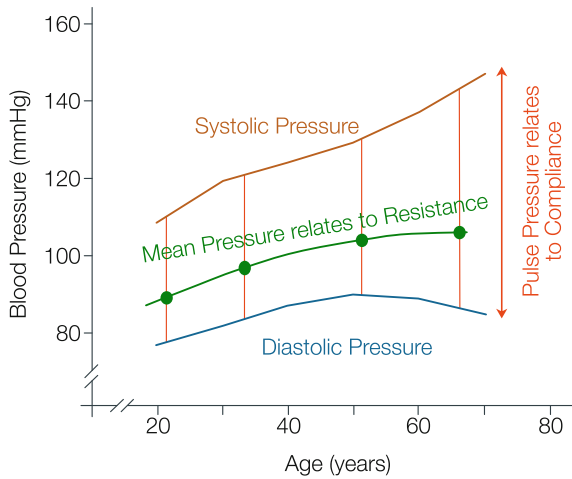
Fig. 24.6 Pressure as a function of age. While systolic pressure continuously increases with age (*brown*), diastolic pressure even decreases for higher ages (*blue*). Mean pressure (*green*) increases initially but hardly changes at higher ages. The increase in mean pressure mainly relates to an increase in peripheral resistance, while the increase in pulse pressure (*vertical red lines*) mainly results from the decrease in total arterial compliance
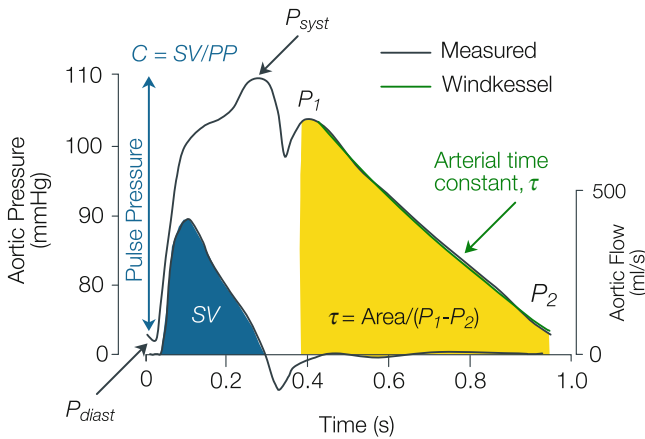
Fig. 24.7 Determination of total arterial compliance: (1) Stroke volume divided by Pulse Pressure (*blue*). (2) The decay time, τ, of diastolic aortic pressure, $\tau=R_pC$ (*green*). (3) Area method: The area under the diastolic aortic pressure divided by the pressure difference in diastole (P_1-P_2) is used as a measure of the decay time (*yellow*). Methods 2 and 3 use $R_p=P_{mean}/Q_{mean}$, and then calculate $C=R_pC/R_p$

The two-area method is based on the following equation:

$$\int_{t_1}^{t_2} Qdt = C \cdot (P_2 - P_1) + \frac{1}{R_p} \int_{t_1}^{t_2} Pdt$$

The equation is applied to two periods of the cardiac cycle; the period of onset of systole to peak systole and the period from peak systole to the end of diastole. Thus two equations with two unknowns, R_p and C, are obtained [11].

- *The Pulse Pressure method* is based on fitting the systolic and diastolic pressures predicted by the two-element Windkessel with measured aortic flow as input, to the measured values of systolic and diastolic pressure. Although the two-element Windkessel does not produce correct wave shapes, the low frequency impedance is very close to the actual impedance and systolic and diastolic pressure are mainly determined by low frequencies [12]. The method is practical when flow can be measured noninvasively (e.g., MRI, US) and aortic systolic and diastolic pressures can be derived from noninvasive pressures (via Brachial of Carotid artery.
- *The parameter estimation method* fits the three-element or four-element Windkessel using pressure and flow as a function of time. When aortic flow is fed into the Windkessel the pressure is predicted. This pressure can be compared to the measured pressure. By minimization of the Root Mean Square Errors, RMSE, of the difference between measured and predicted pressures the best Windkessel parameters are obtained. In this way all the Windkessel parameters can be derived including a good estimate of characteristic impedance. Using the three-element Windkessel compliance is overestimated [8], but this is not the case using the four-element Windkessel [3]. Also, inversely, pressure may be used as input and minimization of flow errors is then performed [5].
- *The transient method* can be applied when pressure and flow are not in the steady state. Peripheral resistance can then not be calculated from mean pressure and mean flow, because aortic flow is not equal to peripheral flow. Using the three-element Windkessel with flow as input, pressure may be calculated while storage of blood in the large conduit arteries is accounted for. By curve fitting of the Windkessel parameters to obtain minimal difference between measured and predicted pressure the Windkessel parameters can be estimated accurately [13].
- *The input impedance method* fits the input impedance of the three-element or four-element Windkessel model to the measured input impedance, by minimization of the RMSE, in a way similar to method mentioned above.
- *The wave velocity method*. A method, not based on the Windkessel but on transmission of waves is mentioned here too. Using the Moens-Korteweg equation wave speed (in practice the foot-to-foot wave velocity, $c_{f\text{-}f}$) can be related to compliance as $c_{f\text{-}f} = \sqrt{V \Delta P / \Delta V \rho}$ (see Chap. 20). When the wave speed between carotid and iliac arteries is measured, length l, and average cross-sectional area of the aorta is also determined, volume V can be calculated and total aortic compliance, $\Delta V / \Delta P$, is obtained. Since the ascending aorta and other arteries are not included, total aortic compliance is lower than total arterial compliance.

It should be emphasized that all Windkessel-based methods imply accurate pressure measurement in the proximal aorta. The first three methods require measurement of Cardiac Output only, while the next five methods require ascending aortic flow wave shape. The wave velocity method requires two accurate measurements of pressure, flow or diameter, in terms of time.

Finally the three- or four-element Windkessel models can be used in lumped models of the whole cardiovascular system in combination with lumped cardiac models (see ref. [14] as an example).

References

1. Westerhof N, Lankhaar JW, Westerhof BE. The arterial Windkessel. *Med Biol Eng Comput* 2009;47:131–141.
2. Westerhof N, Elzinga G, Sipkema P. An artificial system for pumping hearts. *J Appl Physiol* 1971;31:776–781.
3. Stergiopulos N, Westerhof BE, Westerhof N. Total arterial inertance as the fourth element of the windkessel model. *Am J Physiol* 1999;276:H81–H88.
4. Elzinga G, Westerhof N. Pressure and flow generated by the left ventricle against different impedances. *Circ Res* 1973;32:178–186.
5. Stergiopulos N, Meister J-J, Westerhof N. Evaluation of methods for estimating total arterial compliance. *Am J Physiol* 1995;268:H1540–H1548.
6. Hamilton WF, Remington JW. The measurement of the stroke volume from the pressure pulse. *Am J Physiol* 1947;148:14–24.
7. Chemla D, Hébert JL, Coirault C, Zamani K, Suard I, Colin P, Lecarpentier Y. Total arterial compliance estimated by stroke volume-to-aortic pulse pressure ratio in humans. *Am J Physiol* 1998;274:H500–H505.
8. Segers P, Brimioulle S, Stergiopulos N, Westerhof N, Naeije R, Maggiorini M, Verdonck P. Pulmonary arterial compliance in dogs and pigs: the three-element windkessel model revisited. *Am J Physiol* 1999;277:H725–H731.
9. Liu Z, Brin KP, Yin FCP. Estimation of total arterial compliance: and improved method and evaluation of current methods. *Am J Physiol* 1986;251:H588–H600.
10. Randall OS, Esler MD, Calfee RV, Bulloch GF, Maisel AS, Culp B. Arterial compliance in hypertension. *Aust N Z J Med* 1976;6:49–59.
11. Self DA, Ewert RD, Swope RP, Latham RD. Beat-to-beat estimation of peripheral resistance and arterial compliance during +Gz centrifugation. *Aviat Space Environ Med* 1994;65:396–403.
12. Stergiopulos N, Meister J-J, Westerhof N. Simple and accurate way for estimating total and segmental arterial compliance: the pulse pressure method. *Ann Biomed Eng* 1994;22:392–397.
13. Toorop GP, Westerhof N, Elzinga G. Beat-to beat estimation of peripheral resistance and arterial compliance during pressure transients. *Am J Physiol* 1987;252:H1275–H1283.
14. Segers P, Stergiopulos N, Westerhof N. Quantification of the contribution of cardiac and arterial remodeling in hypertension. *Hypertension* 2000;36:760–765.

Chapter 25
Distributed Models and Tube Models
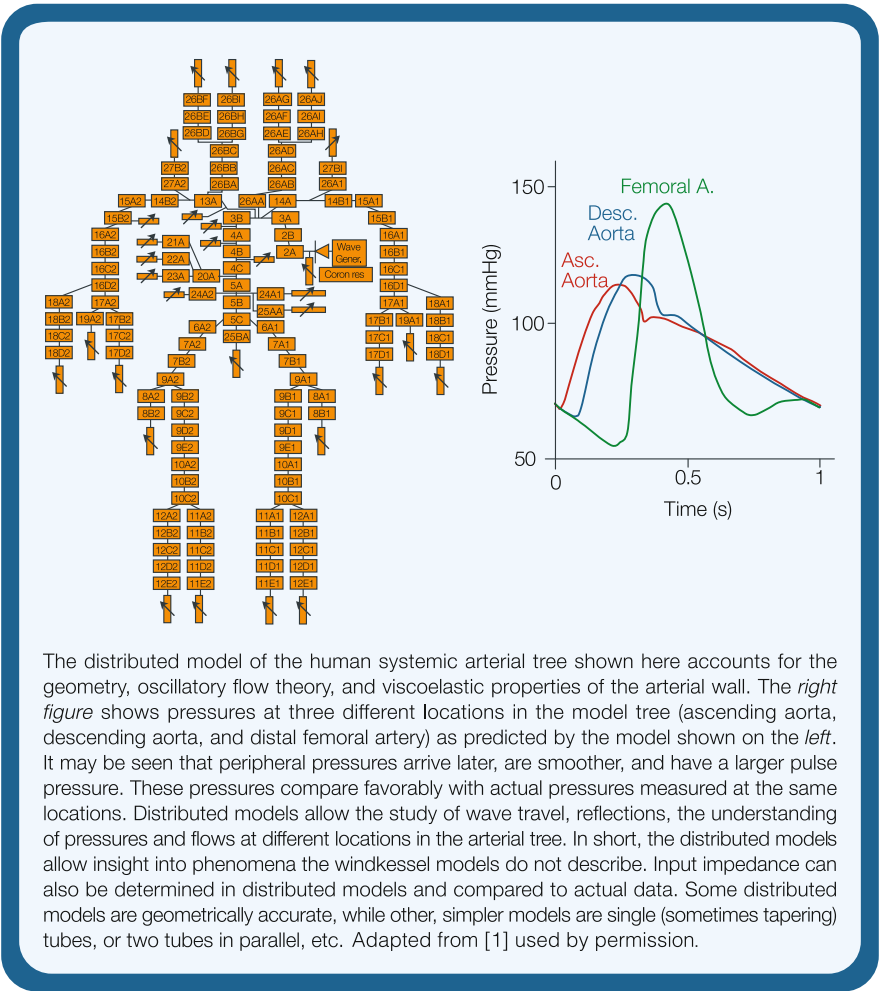
The distributed model of the human systemic arterial tree shown here accounts for the geometry, oscillatory flow theory, and viscoelastic properties of the arterial wall. The *right figure* shows pressures at three different locations in the model tree (ascending aorta, descending aorta, and distal femoral artery) as predicted by the model shown on the *left*. It may be seen that peripheral pressures arrive later, are smoother, and have a larger pulse pressure. These pressures compare favorably with actual pressures measured at the same locations. Distributed models allow the study of wave travel, reflections, the understanding of pressures and flows at different locations in the arterial tree. In short, the distributed models allow insight into phenomena the windkessel models do not describe. Input impedance can also be determined in distributed models and compared to actual data. Some distributed models are geometrically accurate, while other, simpler models are single (sometimes tapering) tubes, or two tubes in parallel, etc. Adapted from [1] used by permission.

Description

The Windkessel models give an overall, lumped description of the arterial tree, but do not permit studies on pressure and flow wave propagation in the arterial tree. Modeling wave propagation requires the use of tube models or distributed models that account for arterial geometry, such as the one shown in the Figure in the box. The basic idea of distributed models is to break up the arterial tree into small segments, whose geometry and mechanical properties are known. The wave transmission characteristics of each arterial segment can be described using Womersley's oscillatory flow theory (Chap. 8) or electrical transmission line theory (Appendix 3).

Distributed models of the arterial tree can also be constructed based on the one-dimensional (simplified) form of the blood flow equations describing the conservation of mass and momentum:

$$\partial Q / \partial x + \partial A / \partial t = 0$$

$$\partial Q / \partial t + \partial (Q^2 / A) / \partial x = -(1 / \rho) \cdot A \cdot \partial P / \partial x - 2\pi r_i \cdot \tau / \rho$$

where A is the vessel cross-sectional area and τ is wall shear stress, usually estimated using Poiseuille's law. The two equations above have three variables: pressure P, flow Q, and area A. Therefore a constitutive law relating cross-sectional area, A, to pressure, P, is needed to form a system of three equations with three unknowns, which can be easily solved using different numerical techniques (i.e., finite differences, or method of characteristics).

Distributed models have been extensively used to study different aspects of pressure and flow propagation, such as the effects of viscoelasticity, the effects of different forms of arterial disease on pressure and flow waves, wave reflections, the relation of peripheral to central pressure waves, etc. [1–3]. Distributed models predict pressure and flow waves that are fairly accurate and compare well to actual waves measured in the human. This can be seen in Fig. 25.1, where measured arterial pressure waves in the human are compared to predicted pressure waves of a standard distributed model. Beyond an apparently good qualitative agreement, well known aspects of pressure wave propagation in arteries, such as the systolic pressure amplification, the smoothing of the pulse and the appearance of a secondary reflection in the diastolic part of a pressure wave in a peripheral artery are well predicted.

Global aspects of the distributed models, such as the aortic impedance (Fig. 25.2), also compare favorably to reality. Figure 25.2 shows the modulus and phase of the input impedance derived from a distributed human systemic arterial model as well as the input impedance measured in a young healthy adult. Figure 25.2 also shows that the distributed model predicts all the typical features of the arterial input impedance. The rapid drop in modulus for the first few harmonics, the relatively flat modulus in the medium and high frequency range correspond with experimental data. The phase reaches negative values for low frequencies and
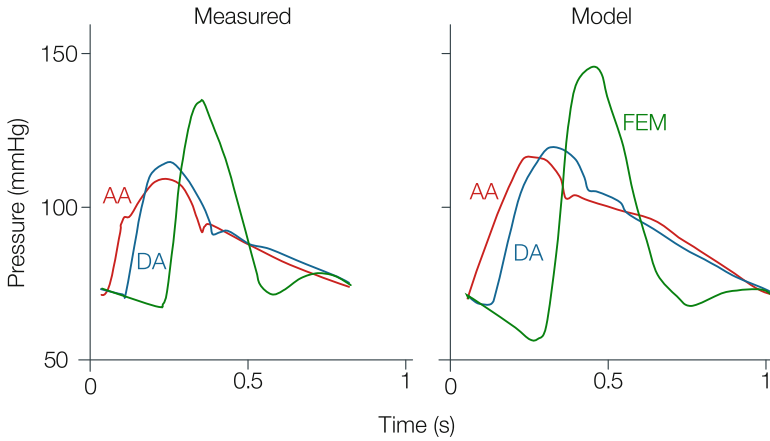
Fig. 25.1 Central and peripheral pressure waves of a distributed model, compared with actual pressure waves measured in similar locations in the human. *AA* ascending aorta, *DA* descending aorta, and *FEM* femoral artery
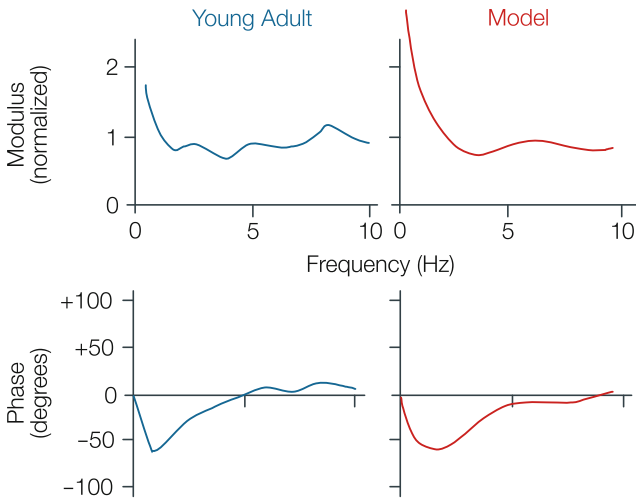
Fig. 25.2 Input impedance measured in a young healthy adult (*left*), compared with the input impedance of a distributed model (*right*). The impedance modulus is normalized to aortic characteristic impedance to facilitate comparison

then returns small values as the measured data. Detailed information on arterial geometry seems not of great importance since Taylor has shown that a randomly distributed model (in terms of vessel lengths) resembles arterial input impedance and wave travel [4, 5].

Single Tube and Two-Tube Models

Windkessel models and distributed models of the arterial tree represent the two extremes of available models of the arterial tree: the former are simple, contain three to five global parameters and therefore are easy to use but lack all aspects of wave travel. The distributed models offer a fairly complete representation of the arterial tree in terms of hemodynamics but require a large number of parameters namely geometry and elasticity of all arterial segments, and therefore are rather cumbersome in their use. Given the above limitations, several researchers have proposed models that are relatively simple but allow for the phenomena of wave travel and reflections. The simplest are the single tube and the asymmetric T-tube models. The single tube models are, as the name suggests, the combination of a tube representing mainly the aorta connected to a peripheral resistor or Windkessel as a model of the peripheral beds. The simplicity of the model is also its main handicap in the sense that all distal reflections come from a single point. A slightly more realistic model is a single tube with geometric tapering as model of the aorta. Asymmetric T-tube models, on the other hand, appear to yield a better description of the arterial tree in terms of input impedance and wave reflections. The asymmetric T-tube model consists of two parallel tubes, a short and long one representing the arterial tree of the upper extremities (head and arms) and a larger size tube accounting the thoracic and abdominal aorta and their branches including the legs [6, 7]. The two tubes terminate either with a resistance or a Windkessel as model of the corresponding terminal bed [2, 6, 7].

Physiological and Clinical Relevance

Distributed models have been used mostly for research as analytical tools because they are realistic for simulating a variety of physiological and pathological situations. Although, in principle, distributed models can be used to derive useful parameters of the arterial tree based on *in vivo* measurements, clinical use is difficult because of the large number of parameters required to construct a 'per patient' model.

In arterial modeling research the choice of model should depend on the degree of detail required and the focus desired. To understand the effect of total arterial compliance on integrated quantities such as aortic pressure and Cardiac Output, the Windkessel models suffice. To model detailed effects, such a local flows and pressures and their transmission, one needs to use distributed models.

References

1. Westerhof N, Bosman F, De Vries CJ, Noordergraaf A. Analog studies of the human systemic arterial tree. *J Biomech* 1969;2:121–143.
2. Stergiopulos N, Young DF, Rogge TR. Computer simulation of arterial flow with applications to arterial and aortic stenosis. *J Biomech* 1992;25:1477–1488.

3. O'Rourke HF, Avolio AP. Pulsatile flow and pressure in human systemic arteries: studies in man and in a multi-branched model of the human systemic arterial tree. *Circ Res* 1980;46: 363–372.
4. Taylor MG. The input impedance of an assembly of randomly branching elastic tubes. *Biophys J* 1966;6:29–51.
5. Taylor MG. Wave transmission through an assembly of randomly branching elastic tubes. *Biophys J* 1966;6:697–716.
6. Campbell KB, Burattini R, Bell DL, Kirkpatrick RD, Knowlen GG. Time-domain formulation of asymmetric T-tube model of the arterial system. *Am J Physiol* 1990;258:H1761–H1774.
7. O'Rourke MF. Pressure and flow waves in systemic arteries and the anatomical design of the arterial system. *J Appl Physiol* 1967;23:139–149.

Chapter 26
Transfer of Pressure

Aortic pressure

Transfer function:
$T(\omega) = P_p(\omega)/P_{ao}(\omega)$

Amplitude ratio

Inverse Fourier Analysis

Frequency (Hz)

Phase difference (Radians)

Radial pressure

Fourier Analysis
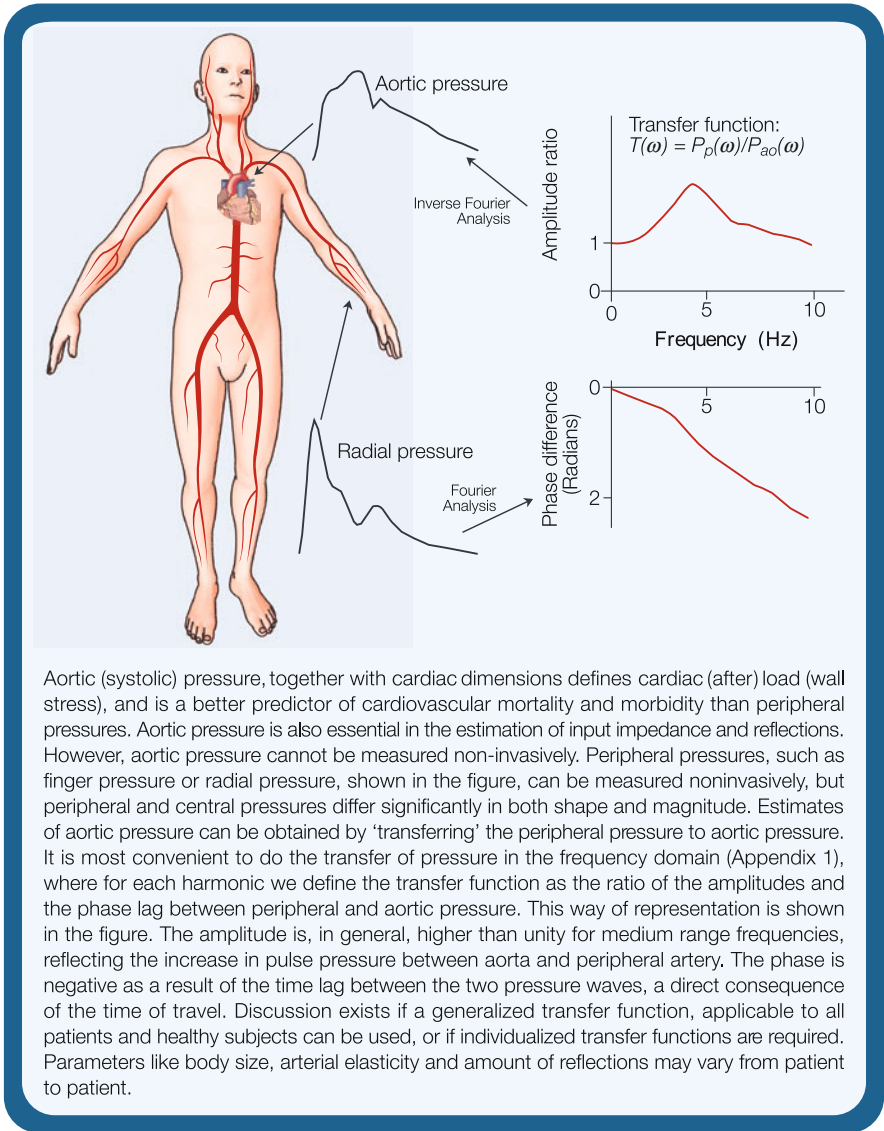
Aortic (systolic) pressure, together with cardiac dimensions defines cardiac (after) load (wall stress), and is a better predictor of cardiovascular mortality and morbidity than peripheral pressures. Aortic pressure is also essential in the estimation of input impedance and reflections. However, aortic pressure cannot be measured non-invasively. Peripheral pressures, such as finger pressure or radial pressure, shown in the figure, can be measured noninvasively, but peripheral and central pressures differ significantly in both shape and magnitude. Estimates of aortic pressure can be obtained by 'transferring' the peripheral pressure to aortic pressure. It is most convenient to do the transfer of pressure in the frequency domain (Appendix 1), where for each harmonic we define the transfer function as the ratio of the amplitudes and the phase lag between peripheral and aortic pressure. This way of representation is shown in the figure. The amplitude is, in general, higher than unity for medium range frequencies, reflecting the increase in pulse pressure between aorta and peripheral artery. The phase is negative as a result of the time lag between the two pressure waves, a direct consequence of the time of travel. Discussion exists if a generalized transfer function, applicable to all patients and healthy subjects can be used, or if individualized transfer functions are required. Parameters like body size, arterial elasticity and amount of reflections may vary from patient to patient.

Description

Peripheral pressures can be measured noninvasively by different techniques. For example, (calibrated) finger pressure can be reliably measured by photoplethysmography [1], and (un-calibrated) radial artery [2] and carotid artery pressure waveforms can be obtained with applanation tonometry [3]. Both techniques are commercially available. However, most clinicians and family physicians use peripheral pressures and typically brachial pressure obtained with the classical sphygmomanometer. Brachial pressure, systolic and diastolic values only, is then used as a substitute for aortic pressure, or, even more so, as a global arterial pressure indicator. However, peripheral and central aortic pressures are not the same. The pressure waveform and the systolic and diastolic pressures can be substantially different between locations (see Figure in the box). In general, systolic pressure increases as we move from central to peripheral sites, a phenomenon called 'systolic peaking', which is attributed to wave reflections in the peripheral vascular beds. Diastolic pressure tends to be slightly lower in peripheral vessels than in central arteries. Recently is has been made clear that not only peripheral and aortic pressures differ in magnitude and wave shape, but that aortic pressure is a better indicator of cardiac morbidity and mortality than peripheral pressure [4]. Also the effect of blood pressure lowering appears to have different effects on aorta and peripheral pressures [4, 5].

Definition of Transfer function

One way to obtain aortic pressure from a noninvasively measured peripheral pressure wave is to apply a so-called pressure transfer function. In essence, we define a transfer function, T, which is the ratio of the peripheral pressure wave, P_p, to the aortic pressure wave, P_{ao}. The two pressures can only be related to each other in the frequency domain. Therefore we have to apply Fourier analysis (see Appendix 1) and for every harmonic, we define the amplitude of the transfer function as the ratio of amplitudes of the peripheral and aortic pressure wave and the phase of the transfer function as the difference in the phase between the peripheral and aortic pressure. The approach is similar to the derivation of input impedance (Chap. 23), where pressure and flow are related. This is mathematically expressed as [6–8]:

$$T(\omega) = P_p(\omega) / P_{ao}(\omega)$$

The amplitude and the phase of the transfer function between the radial artery and the aorta is shown schematically in the Figure in the box. The zero-frequency value of the transfer function is the ratio of mean peripheral arterial pressure to mean aortic pressure. Because of the small drop in mean pressure between the aorta and the peripheral artery, this ratio is only slightly lower than 1. The amplitude of the

transfer function is, in general, higher than unity for medium range frequencies, reflecting the increase in Pulse Pressure at the peripheral site. For high frequencies the transfer function is difficult to obtain accurately because the amplitudes of the harmonics are small. The amplitude of the transfer function decreases for high frequencies to negligible values because high frequencies are little reflected and damped while traveling. The phase is negative, as a result of the phase lag between the two waves, a direct consequence of the time it takes for the aortic wave to travel towards the periphery. The mean slope of the phase is determined by wave speed.

Several techniques are commercially available to obtain central from peripheral pressures, see [2, 6]. These methods use a 'generalized transfer function', which is the average of a (large) number of transfer functions measured in a group of human subjects.

Calibration of Noninvasively Determined Pressure Wave Shapes

Applanation tonometry [2], and echo tracking of wall motion [9] are ways to obtain peripheral pressure wave shapes noninvasively, but calibration is not available. Sphygmomanometrically obtained, and thus quantitative values of systolic, $P_{syst,br}$ and diastolic, $P_{diast,br}$ pressure, in the brachial artery, can help in the calibration of noninvasively obtained carotid artery pressure [3], a surrogate of aortic pressure. It is assumed that mean pressure and diastolic pressure are not different between brachial to carotid artery: $P_{diast,br} = P_{diast,car}$, and $P_{mean,br} = P_{mean,car}$.

By assuming that mean pressure in the carotid artery, $P_{mean,car}$, equals $P_{mean,car} = (P_{syst,car} + P_{diast,car})/2$ and in the brachial artery $P_{mean,br} = (P_{syst,br} + 2P_{diast,br})/3$. Rearrangement leads to:

$$P_{syst,car} \approx 2/3\, P_{syst,br} + 1/3\, P_{diast,br} \approx 0.67\, P_{syst,br} + 0.33\, P_{diast,b}$$

If instead it is assumed that $P_{mean,car} \approx 0.4\, P_{syst,car} + 0.6\, P_{diast,car}$, we find:

$$P_{syst,car} \approx 0.83\, P_{syst,br} + 0.15\, P_{diast,br}$$

Physical Basis and Simple Mathematical Model for Transfer Function

A simple approach, which helps to understand the physical basis of the transfer function, is to consider the entire arterial pathway from the aorta to the peripheral site as a single tube. The aortic pressure wave, P_{ao}, consists of its forward running component, $P_{f,ao}$, and its backward running component or reflected wave, $P_{b,ao}$. At the peripheral site the forward and backward running wave components are $P_{f,p}$ and, $P_{b,p}$, respectively (see Fig. 26.1).
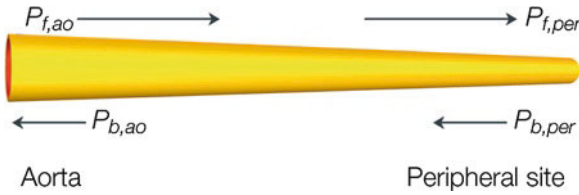
Fig. 26.1 The forward and backward waves, P_f and P_b, travel from aorta, to periphery, and back

As a first approximation, we may assume that the forward wave at the peripheral site is identical to the forward wave at the aorta with the exception of a time delay between the two waves. This time delay is equal to the time it takes for the forward wave to travel from the aorta to the peripheral site, i.e., $\Delta t = l/c$, l being the distance and c the wave speed. In the frequency domain the time delay is expressed as a phase lag, which is equal to $\omega \Delta t$, and we may write

$$P_{f,p} = P_{f,ao} \cdot e^{i\omega\Delta t}$$

Following a similar reasoning, the reflected wave at the peripheral site is equal to the reflected wave in the aorta. However, because the reflected wave travels in the opposite direction, the aortic wave now lags the peripheral wave by the same time delay Δt. The transfer function, T, can thus be written as:

$$T(\omega) = P_p(\omega)/P_{ao}(\omega) = [P_{f,p}(\omega) + P_{b,p}(\omega)]/[P_{f,ao}(\omega) + P_{b,ao}(\omega)]$$

and thus:

$$T(\omega) = [P_{f,ao}(\omega)\cdot e^{i\omega\Delta t} + P_{b,ao}(\omega)\cdot e^{-i\omega\Delta t}]/[P_{f,ao}(\omega) + P_{b,ao}(\omega)]$$

Dividing by $P_{f,ao}$ and taking into account that $P_{b,aow}/P_{f,ao}$ is equal to the reflection coefficient, Γ, we obtain the following final expression for the transfer function T:

$$T(\omega) = \left[e^{i\omega\Delta t} + \Gamma(\omega)e^{-i\omega\Delta t}\right]/\left[1 + \Gamma(\omega)\right]$$

This single tube model suggests that the transfer function depends primarily on the reflection coefficient at the distal site, $\Gamma(\omega)$, and on the time of travel, Δt, of the waves between the two sites [10]. The model, of course, is an oversimplification of reality, because it does not take into account the effects of wave damping, and non-linear elasticity. The model applies to a single uniform vessel and thus cannot be applied when several significant reflection sites exist between the aorta and the peripheral site, e.g., major bifurcations. The model gives, however, reasonable predictions of the transfer function between the aorta and the brachial artery, as shown Fig. 26.2 [10].
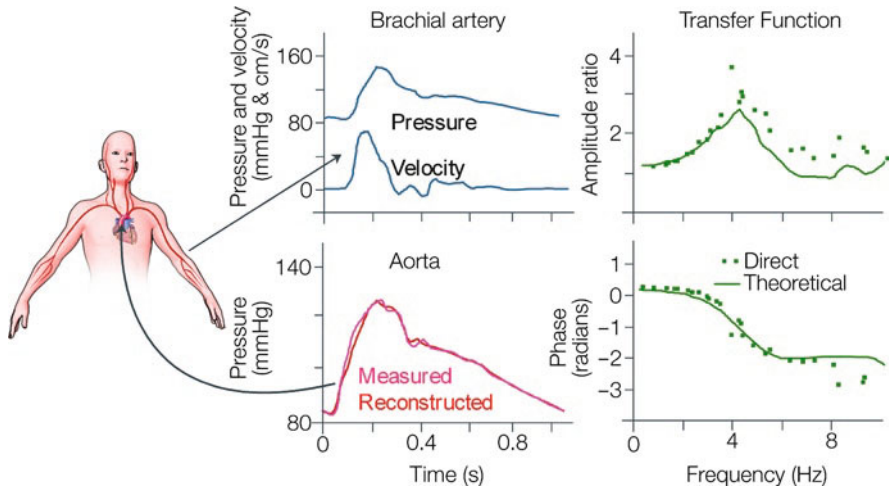
Fig. 26.2 Aorta pressure can be derived from pressure and velocity or flow waves in the brachial artery, together with the travel time of the waves between these two sites. The brachial pressure and flow (or velocity) can be used to calculate forward and reflected pressures. When the backward pressure wave is advanced and the forward pressure wave is delayed in time, subsequent addition results in aortic pressure. The theoretical transfer function (green) is close to the measured data. Adapted from ref. [10], used by permission

Physiological and Clinical Relevance

Figure 26.3 shows aortic pressure and brachial pressure measured in an individual under control conditions as well as after administration of nitroglycerin [5]. Figure 26.3 also shows that the transfer of pressure depends on the state of the vascular tree. Under control conditions, systolic brachial pressure is approximately 150 mmHg, overestimating aortic pressure by 10 mmHg. Under nitroglycerin, systolic pressure in aorta drops significantly. Notice the disappearance of the late systolic reflected wave (decreased augmentation), apparently due to reduced reflections resulting from vasodilatory effects of nitroglycerin. Brachial systolic pressure, however, remains practically unchanged, now overestimating aortic pressure by more than 30 mmHg. This example demonstrates that peripheral pressure waves are not a reliable substitute for aortic pressure and their relation may vary depending on different physiological parameters, such as arterial vasomotor tone. Therefore, peripheral waves cannot give an accurate estimation of the load on the heart. The recent epidemiological study by Williams et al. [4] shows these differences as well and discusses its implications: in treatment and prediction on the basis of aortic pressure is preferred.

From a clinical standpoint it is thus aortic pressure and not peripheral pressure that is of primary importance in a number of aspects. Aortic systolic pressure is the main determinant of cardiac (after) load, and aortic diastolic drives coronary perfusion.
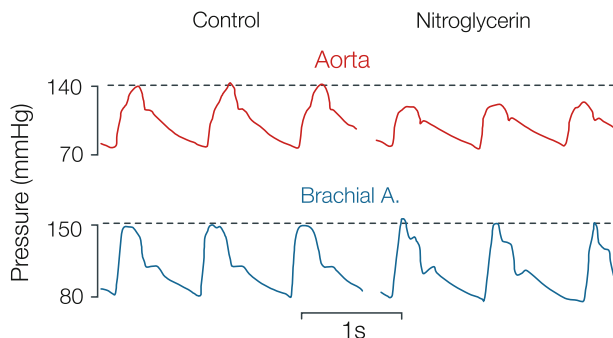
Fig. 26.3 Simultaneous recordings of aortic and brachial pressure waves under control conditions, and after administration of nitroglycerin. During vasodilation systolic blood pressure in the brachial artery is not affected while systolic aortic pressure is lowered. Adapted from ref. [4], used by permission

The aortic pressure waveform can be used to derive reliably arterial compliance based on a variety of methods (Chap. 24). During ejection, aortic pressure can be taken as a surrogate of left ventricular pressure and, together with noninvasive measurements of left ventricular volume, can be used to estimate cardiac parameters such as End-Systolic elastance (Chaps. 13 and 18).

A major drawback of the transfer function technique is that a generalized function does not exist. Parameters like body size, arterial elasticity and peripheral resistance, which vary from patient to patient, are important determinants of pressure transfer. Thus on the one hand the generalized transfer function may not be precise but is easily applicable [7], but on the other hand the individually derived transfer function improves the results little [11].

References

1. Eeftinck Schattenkerk DW, van Lieshout JJ, van den Meiracker AH, Wesseling KR, Blanc S, Wieling W, van Montfrans GA, Settels JJ, Wesseling KH, Westerhof BE. Nexfin noninvasive continuous blood pressure validated against Riva-Rocci/Korotkoff. *Am J Hypertens* 2009;22:378–383.
2. Adji A, O'Rourke MF. Determination of central aortic systolic and pulse pressure from the radial artery pressure waveform. *Blood Press Monit* 2004;9:115–121.
3. Van Bortel LM, Balkestein EJ, van der Heijden-Spek JJ, Vanmolkot FH, Staessen JA, Kragten JA, Vredeveld JW, Safar ME, Struijker Boudier HA, Hoeks AP. Non-invasive assessment of local arterial pulse pressure: comparison of applanation tonometry and echo-tracking. *J Hypertens* 2001;19:1037–1044.
4. Williams B, Lacy PS, Thom SM, Cruickshank K, Stanton A, Collier D, Hughes AD, Thurston H, O'Rourke M; CAFE Investigators; Anglo-Scandinavian Cardiac Outcomes Trial Investigators; CAFE Steering Committee and Writing Committee. Differential impact of blood pressure-lowering drugs on central aortic pressure and clinical outcomes: principal results of the Conduit Artery Function Evaluation (CAFE) study. *Circulation* 2006;113:1213–1225.

5. Kelly RP, Gibbs HH, O'Rourke MF, Daley JE, Mang K, Morgan JJ, Avolio AP. Nitroglycerin has more favourable effects on left ventricular afterload than apparent from measurement of pressure in a peripheral artery. *Eur Heart J* 1990;11:138–144.

6. Chen CH, Nevo E, Fetics B, Pak PH, Yin FCP, Maughan WL, Kass DA. Estimation of central aortic pressure waveform by mathematical transformation of radial tonometry pressure. Validation of a generalized transfer function. *Circulation* 1997;95:1827–1836.

7. Hope SA, Tay DB, Meredith IT, Cameron JD. Comparison of generalized and gender-specific transfer functions for the derivation of aortic waveforms. *Am J Physiol* 2002;283:H1150–H1156.

8. Karamanoglu M, O'Rourke MF, Avolio AP, Kelly RP. An analysis of the relationship between central aortic and peripheral upper limb pressure waves in man. *Eur Heart J* 1993;14:160–167.

9. Hoeks APG, Brands PJ, Smeets FA, Reneman RS. Assessment of distensibility of superficial arteries. *Ultrasound Med Biol* 1990;16:121–128.

10. Stergiopulos N, Westerhof BE, Westerhof N. Physical basis of pressure transfer from periphery to aorta: a model based study. *Am J Physiol* 1998;274:H1386–H1392.

11. Westerhof BE, Guelen I, Stok WJ, Lasance HA, Ascoop CA, Wesseling KH, Westerhof N, Bos WJ, Stergiopulos N, Spaan JA. Individualization of transfer function in estimation of central aortic pressure from the peripheral pulse is not required in patients at rest. *J Appl Physiol* 2008;105:1858–1863.

Chapter 27
Mechanotransduction and Vascular Remodeling

Blood vessels respond to pressure and flow, more exactly to hoop stress and wall shear. Short term. A pressure increase results in a smooth muscle contraction and thus in a diameter decrease, so that hoop stress normalizes (myogenic response, see Chapter 18). A flow increase implies an increase in wall shear stress, which is sensed by the endothelium (glycocalix). The endothelium liberates NO which is a smooth muscle dilator. The increase in diameter reduces the wall shear stress. This is called Flow Mediated Dilation (left panel). Long term. Sustained high blood pressure implies a high wall hoop stress that leads to wall thickening (hypertrophy), and normalization of hoop stress. Increased flow gives increased wall shear stress and leads to increase in vessel diameter. In general, vascular remodeling leads to a restoration to control levels of hoop stress and wall shear stress (right panel). From [1], used by permission.

Description

One of the fundamental characteristics of living tissues is their ability to respond to changes in their mechanical environment.

Although often referred to the macroscopic quantities of pressure and flow, vascular responses are better associated with wall hoop stress and wall shear stress. We recall that wall hoop stress (σ) is related to transmural pressure through the law of Laplace, $\sigma = P \cdot r_i / h$ (see Chap. 9), and that wall shear stress (τ) is related to flow, or axial pressure drop, $\Delta P/l$, through the law of Poiseuille, $\tau = 4\eta \cdot Q/\pi \, r_i^3 = (\Delta P/l)/(r_i/2)$ (Chap. 2).

Short Term Arterial Adaptation

Pressure effects. In the short term, under physiologic conditions, an increase in transmural pressure increases hoop stress, and, via the myogenic response (Chap. 18) of the smooth muscle, vessel diameter decreases and hoop stress is normalized (See Laplace's Law, Chap. 9). Thus the increase in vascular tone counterbalances the increased pressure.

Flow effects. Acute changes in blood flow lead to adjustments in vessel caliber, via endothelium-dependent vasodilation or vasoconstriction. A flow increase, leads to an increase in shear stress, which is sensed by the endothelium, and followed by vasodilation. Vasodilators, e.g., NO, are released and the smooth muscle relaxes. Muscle relaxation results in vasodilation and increase in vessel diameter, thereby normalizing the shear stress. In Chap. 2 we mentioned that wall shear stress is neither the same in similar vessels in different mammals, nor the same in different vessels in a single animal. Yet it appears that local endothelial cells have a desired set-point of shear stress.

Mechanotransduction

Mechanotransduction refers to the many mechanisms by which cells convert mechanical stimuli into chemical activity. One such mechanism is flow-induced vasorelaxation, whereby increased wall shear stress causes smooth muscle relaxation (Figure in the box, at left).

This aspect of mechanotransduction only takes place when the endothelium is intact. The search for the mechanism was based on the finding by Furchgott that Acetylcholine, ACh, only relaxes the smooth muscle if the vascular endothelium is intact [2]. The factor liberated by the endothelium was named Endothelium Derived Relaxing Factor, EDRF [2]. Palmer et al. showed that EDRF is Nitric Oxide NO, a small molecule that also plays a role in synaptic transmission [3]. Thus in shear rate dependent dilation NO plays a major role as the dilating factor. The shear stress needs to be higher than a certain threshold value before diameter changes occur (Fig. 27.1, left). The level of the stress, and its duration, need to be of sufficient magnitude to elicit a response (Fig. 27.1, right). This is a relation akin to the strength-duration curve defining the response of nerve tissue. Also it has been shown that it is mainly the mean shear stress that causes vasodilation and not the magnitude of oscillations about the mean stress (Fig. 27.2). Shear stress dependent
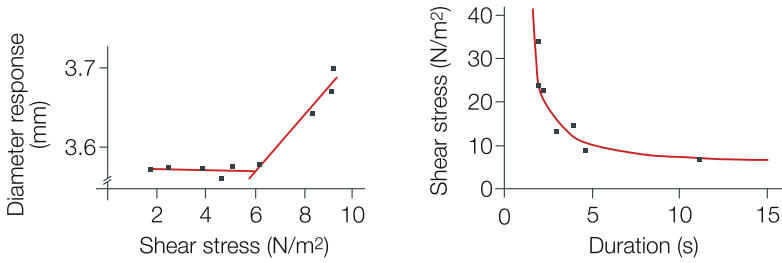
Fig. 27.1 The diameter response relates linearly with shear stress, above a threshold value (*left panel*). Strength (stress magnitude) and duration of the stress determine the response to shear stress. They relate inversely, like a strength-duration curve (*right panel*). Adapted from ref. [4], used by permission
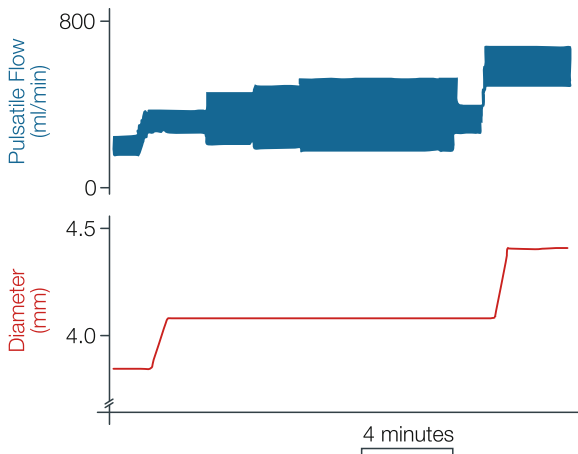
Fig. 27.2 An increase mean flow (*top trace*) induces an increase in diameter (*bottom trace*), as shown in the early part of the tracings. The subsequent increase in the pulsatility of flow, at the same mean flow, has no detectable effect on diameter. A further increase in mean flow induces the final increase in the diameter (last part of the tracings). Adapted from ref. [4], used by permission

arterial dilatation is abolished by the NO synthesis inhibitor L-NAME, by hyaluronidase, and by intraluminal hyperglycemia.

At present it is accepted knowledge that the glycocalyx (a gel layer 0.5 μm thick between the endothelium and the blood in the lumen) is the sensor of changes in shear stress, although some researchers maintain that the sensor is the endothelial cell membrane and/or its cytoskeleton. The suggestion that signaling arises from the periphery, and is transmitted "upstream", is unlikely [5].

Long Term Vascular Adaptation

Growth and remodeling are processes that allow the living tissue to maintain an optimal environment under physiological development (Chap. 2) as well as under

various pathologic conditions. The arterial wall responds to prolonged changes in transmural pressure or flow by means of geometrical adaptation (e.g., hypertrophy), structural adaptation (e.g., change in scleroprotein content, stiffening) and functional adaptation (e.g., changes in endothelial function or vascular smooth muscle tone).

Pressure effects. In the long term an increase in pressure leads to a thickening of the arterial wall (hypertrophy). Wall thickening lowers wall hoop stress down to control (normotensive) levels, thus counterbalancing the increase in pressure. An example of such adaptation is shown in Fig. 27.3.

Flow effects. Chronic changes in flow lead to remodeling. Long-term, flow-induced remodeling implies reorganization of cellular and extracellular wall components. The adaptive response to changes in blood flow has been studied in various animals and it was found that the vessel inner diameter adapts to preserve the level of wall shear at the intimal surface. Kamiya and Togawa [6] first demonstrated that the adaptive response to an increase in flow leads to normalization in wall shear stress. They constructed an arterio-venous shunt between the carotid artery and jugular vein of a dog, which led to a significant increase in blood flow in the ipsilateral carotid and a decrease in blood flow in the contralateral one. Six to 8 months after the operation, carotid diameter was increased in the segment with high flow and decreased in the segment with low flow. The diameter change preserved wall shear stress within 15% of the pre-operation levels, despite the severe increase or decrease in flow.

Similar findings were reported by Langille [1, 7] on the rabbit carotid artery, where a reduction in flow led to a reduction in internal diameter and restoration of wall shear stress (see Fig. 27.4). Remodeling in response to increased flow appears to be associated with cell hyperplasia, structural changes in internal elastic lamina and adventitia as well as with the contractile properties of the artery. The endothelium and nitric oxide synthesis are the main mediators in the vessel adaptation to flow. For example, inhibition of nitric oxide synthesis totally abolishes the capacity of the pig carotid artery to remodel and maintain control levels of wall shear in the presence of an arterio-venous shunt [8].

| Control | Hypertensive | Severely hypertensive |
| P_{SYS} = 140 mm Hg | P_{SYS} = 200 mm Hg | P_{SYS} = 240 mm Hg |

━ 50 μm
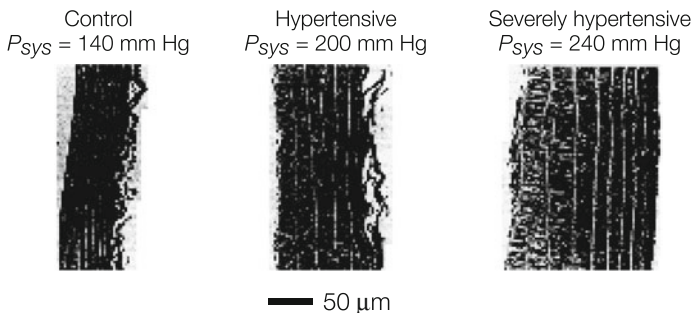
Fig. 27.3 Thoracic aortic walls of rats fixed under their *in vivo* pressure and stained with Azan. Sections are parallel to the longitudinal axis of the vessel with the intimal surface facing leftward. Adapted from ref. [9], used by permission
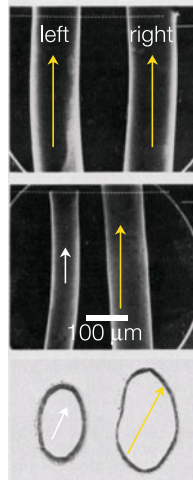
Fig. 27.4 Scanning electron micrographs of methacrylate casts of left and right common carotid arteries of a normal rabbit (*top*) and 2 weeks after left carotid flow was reduced (*middle*), as indicated by *white arrow*. Cross-sections after 2 weeks of left common carotid flow reduction are given in the *bottom panel*. Adapted from ref. [7], used by permission

Residual Stress in Relation to Growth and Remodeling

In Chap. 10 it was mentioned that both cardiac tissue and vascular tissue are not at a zero stress state when all loads are removed [10]. It was also postulated that residual stresses help maintain a uniform stress distribution across the wall (Chap. 10). When, for different physiological or pathological reasons, the biomechanical environment to which the wall is subjected is changed, mechanical stresses within the arterial wall will also be altered and their distribution will not be uniform. A remodeling process will likely take place in order to restore stresses and strain to control levels.

Remodeling leads to changes in geometry and structure, with addition or resorption of mass. Consequently, the zero stress state will change. Changes in the zero stress state, or changes in the opening angle allow for the monitoring of arterial wall remodeling. Figure 27.5 shows changes in wall thickness and opening angle in various positions along the aorta of rats, which received a very tight banding of the thoracic aorta just below the diaphragm. For the aorta above the banding site, which was exposed to higher pressure, we observe a progressive thickening of the aortic wall during the entire post-surgery period (normalization of hoop stress). The opening angle, however, shows a non-monotonic evolution. Initially, the opening angle increases, indicative of higher growth in the internal wall layers. Later, as the wall thickens and stress levels are restored, the opening angle returns to control levels as well. This demonstrates that remodeling is dependent on the local stress distribution and also that wall remodeling affects the residual stress distribution within the arterial wall.
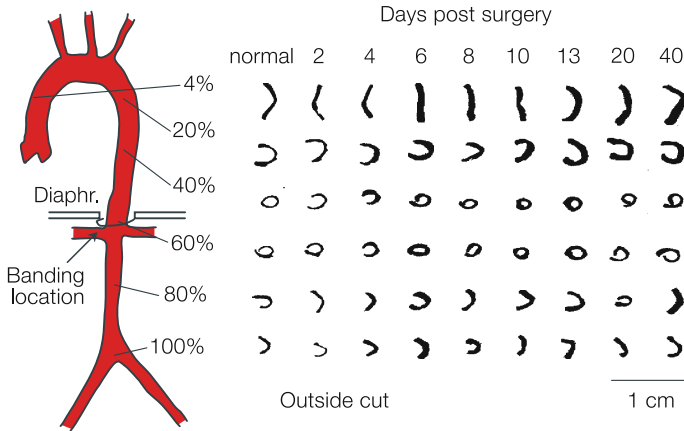
Fig. 27.5 Photographs of aortic rings cut open radially to reveal their Zero Stress State (ZSS). The first column shows the ZSS in normal rats. The other columns show the change in ZSS after hypertension was induced by banding of the aorta above the celiac trunk. Adapted from ref. [10], used by permission

Physiological and Clinical Relevance

Arterial Remodeling in Hypertension

In presence of essential hypertension, vascular resistance increases due to alterations in resistance vessel architecture, decrease in lumen diameter and increase in media thickness/lumen diameter ratio. This corresponds to an inward eutrophic remodeling, as schematically shown in Fig. 27.6. The type of remodeling in resistance vessels depends on the type of hypertension and treatment. Human renal hypertension leads to inward hypertrophic remodeling. During anti-hypertensive treatment the situation is often reversed and outward eutrophic remodeling and hypertrophic remodeling is observed. Figure 27.6 shows the different types of remodeling that can be distinguished, as suggested by Mulvany [11].

Arterial Remodeling in Hypertension: Large Arteries

Remodeling due to hypertension is known to increase wall thickness and restore wall hoop stress. In terms of compliance and elastic properties, arterial remodeling tends to be vessel specific. Aortic and carotid artery compliances are reduced in hypertension. Radial artery compliance and incremental elastic modulus (Fig. 27.7), however, seem to be preserved in hypertensive patients [12]. It is important here to acknowledge the nonlinear nature of the compliance and elastic modulus curves. Compliance is expressed as a function of pressure (structural property) and elastic
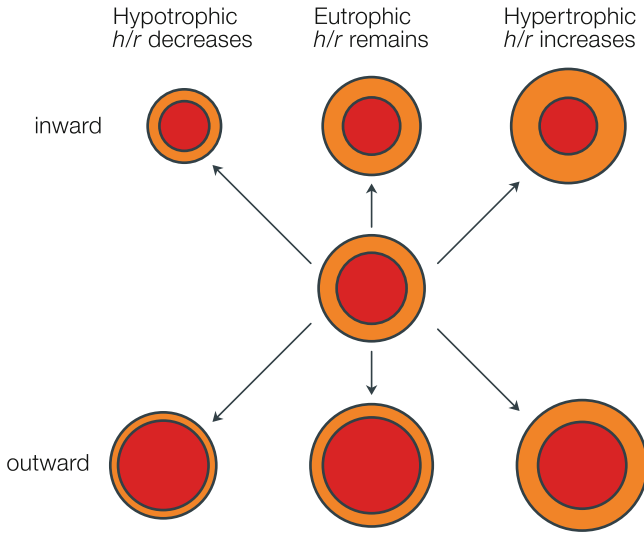
Fig. 27.6 Classification of different types of arterial remodeling, i.e. a structurally determined change. Adapted from ref. [11], used by permission

modulus as a function of stress or strain (material property). We observe that at their corresponding operating pressure, normotensive and hypertensive radial arteries exhibit the same compliance, which is indicative of some kind of structural remodeling aiming to maintain normotensive compliance levels. Further, the incremental modulus-stress curve is identical in normotensive and hypertensive patients, which means that the intrinsic elastic properties of the wall material remained the same. This example demonstrates nicely the capacity of the radial artery to remodel in hypertension in a manner that normalizes wall stress by thickening, maintains control compliance levels despite exposure to higher pressure and preserves the intrinsic elastic properties of the arterial tissue.

Flow Mediated Dilatation, as a Means to Evaluate Endothelial Function

Metabolic vasodilatation within an organ causes a fall in peripheral resistance so that blood flow in the artery supplying the organ increases (Figure in the box, top trace). The increased flow causes an increase in wall shear stress (middle trace). The mechano-sensor within the arterial wall, the endothelium, detects the wall shear and produces arterial dilatation, so that the increased flow required downstream is accommodated and wall shear stress normalized. The vasodilation is mediated by the endothelium-dependent relaxing factor (EDRF), now known to be nitric oxide (NO). The response is abolished if the animal is pretreated with a NO synthase
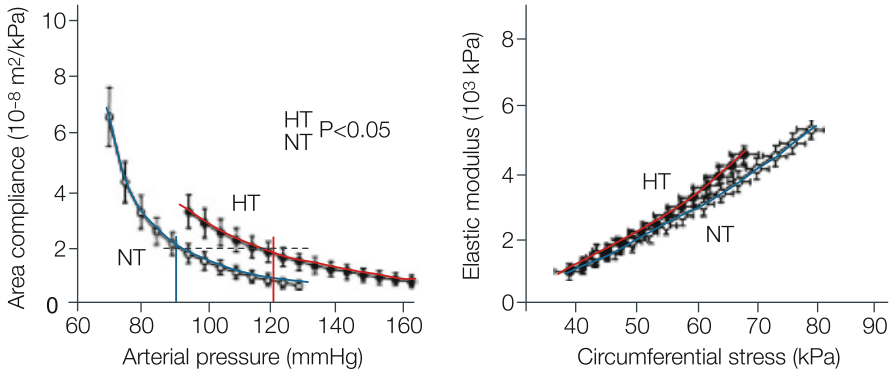
Fig. 27.7 Radial artery area compliance (*left*) and elastic modulus (*right*) measured *in vivo* in a group of normotensive (NT, $n=22$) and hypertensive subjects (HT, $n=25$). When compared at their corresponding mean operating pressures (NT: 90 mmHg; HT: 121 mmHg) area compliance was similar despite significant concentric hypertrophy (*left panel*). In normotensive subjects wall thickness is 0.28 mm compared to 0.40 mm in hypertensive patients. Internal diameter is the same and equal to 2.50 mm in both groups. The incremental elastic modulus-stress curve (*right panel*) was essentially the same in normotensives and hypertensives, suggesting similar tissue material properties in the two groups. Adapted from ref. [12], used by permission

inhibitor or when the endothelium is removed or made nonfunctional. The increase in diameter in the supply artery is called Flow Mediated Dilatation (FMD).

Flow Mediated Dilation can be studied noninvasively in arteries. For instance, brachial artery diameter can be measured during control and during post-occlusion reactive hyperemia where flow is increased. The increased wall shear stress causes endothelium dependent dilation which can be measured noninvasively (Ultrasound, Wall tracking). An endothelium independent vasodilator, (e.g., sublingual glyceryl trinitrate, GTN), is used to test muscle relaxation of the artery without involvement of the endothelium [13, 14].

Low Shear and Atheroma

According to Caro [15], and substantial subsequent literature, atheromatous plaques develop preferentially at sites with low shear. In the light of the recent knowledge, we can postulate with some confidence that this is because less NO production is taking place in the sites of low shear, and NO being an anti-atheromatous factor.

It can also be appreciated why diabetic patients and people with glucose intolerance have accelerated athero-thrombotic disease, as the hyperglycemia inhibits the production of NO in response to shear stress [16]. Hyperinsulinaemia occurs in patients pre-disposed to type-2 diabetes (metabolic syndrome or insulin resistance) and may occur with excess insulin administration in type 1 diabetes. The hyperinsulinaemia results in more dilated arteries than normal, and therefore shear stress is

lower than normal (shear stress is inversely related to the radius to the third power, see Chap. 2); compensation for this is the insulin-induced increase in basal NO production. Thus diabetic hyperinsulinaemia creates an arterial tree with overall low shear stresses, predisposing to atheroma, and the accompanying diabetic hyperglycemia also inhibits the response to increased shear as generated by exercise, further predisposing the patient to arterial lesions.

References

1. Langille LB. Blood flow-induced remodeling of the artery wall. In: *Flow-dependent regulation of vascular function*. 1995, edited by Bevan JA, Kaley G and Rubanyi GM. New York, Oxford University Press, 1995.
2. Furchgott RF, Zawadzki JV. The obligatory role of endothelial cells in the relaxation of arterial smooth muscle by acetylcholine. *Nature* 1980;288(5789):373–376.
3. Palmer RMJ, Ferrige AG, Moncada S. Nitric oxide release accounts for the biological activity of endothelium-derived relaxing factor. *Nature* 1987;27:524–526.
4. Kelly R, Snow HM. Characteristics of the response of the iliac artery to wall shear stress in the anaesthetised pig. *J Physiol* 2007;582:731–743.
5. Markos F, Ruane-O'Hora T, Snow HM, Kelly R, Wainwright C, Skene K, Drake-Holland AJ, Noble MI. Dilatation in the femoral vascular bed does not cause retrograde relaxation of the iliac artery in the anaesthetized pig. *Acta Physiol* 2008;194(3):207–213.
6. Kamiya A, Togawa T. Adaptive regulation of wall shear stress to flow change in canine carotid artery. *Am J Physiol* 1980;239:14–29.
7. Langille BL, O'Donnell F. Reductions in arterial diameter produced by chronic decreases in blood flow are endothelium-dependent. *Science* 1986;231:405–407.
8. Tronc F, Wassef M, Esposito B, Henrion D, Glagov S, Tedgui A. Role of NO in flow-induced remodeling of the rabbit common carotid artery. *Arterioscler Thromb Vasc Biol* 1996;16:1256–1262.
9. Matsumoto T, Hayashi K. Stress and strain in hypertensive and normotensive rat aorta considering residual strain. *J Biomech Eng* 1996;118:62–73.
10. Fung YC, Liu SQ. Change of residual strains in arteries due to hypertrophy caused by aortic constriction. *Circ Res* 1989;65:1340–1349.
11. Mulvany MJ. Vascular remodelling of resistance vessels: can we define this? *Cardiovasc Res* 1999;41:9–13.
12. Laurent S, Girerd X, Mourad J-J, Lacolley P, Beck L, Boutouyrie P, Mignot J-P, Safar M. Elastic modulus of the radial artery wall material is not increased in patients with essential hypertension. *Arterioscler Thromb* 1994;14:1223–1231.
13. Lambert J, Aarsen M, Donker AJM, Stehouwer CDA. Endothelium-dependent and -independent vasodilation of large arteries in normoalbuminuric insulin-dependent diabetes mellitus. *Arterioscler Thromb Vasc Biol* 1996;16:705–711.
14. Lavi T, Karasik A, Koren-Morag N, Kanety H, Feinberg MS, Shechter M. The acute effect of various glycemic index dietary carbohydrates on endothelial function in nondiabetic overweight and obese subjects. *J Am Coll Cardiol* 2009;53:2283–2287.
15. Caro C, Fitzgerald J, Schroeter R. Arterial wall shear and distribution of early atheroma in man. *Nature* 1969;223:1159–1160.
16. Kelly R, Ruane-O'Hara T, Noble MIM, Drake-Holland AJ, Snow HM. Effect of hyperglycaemia on endothelial dependent dilatation in the iliac artery of the anaesthetized pig. *J Physiol* 2006;573:133–145.

Chapter 28
Blood Flow and Arterial Disease
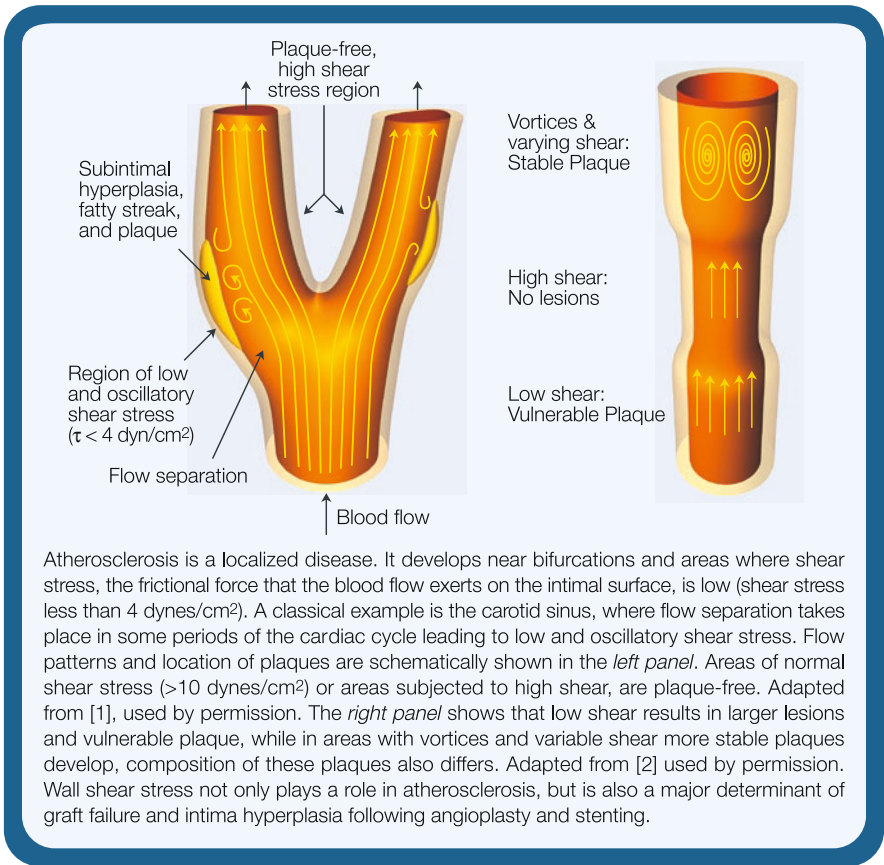
Atherosclerosis is a localized disease. It develops near bifurcations and areas where shear stress, the frictional force that the blood flow exerts on the intimal surface, is low (shear stress less than 4 dynes/cm2). A classical example is the carotid sinus, where flow separation takes place in some periods of the cardiac cycle leading to low and oscillatory shear stress. Flow patterns and location of plaques are schematically shown in the *left panel*. Areas of normal shear stress (>10 dynes/cm2) or areas subjected to high shear, are plaque-free. Adapted from [1], used by permission. The *right panel* shows that low shear results in larger lesions and vulnerable plaque, while in areas with vortices and variable shear more stable plaques develop, composition of these plaques also differs. Adapted from [2] used by permission. Wall shear stress not only plays a role in atherosclerosis, but is also a major determinant of graft failure and intima hyperplasia following angioplasty and stenting.

Description

Hemodynamic forces not only regulate blood vessel geometry and structure, i.e., remodeling, but they can be considered also as main factors influencing the development of different forms of vascular disease, such as atherosclerosis, and aneurysms. Of particular importance is the role of shear stress, the minute force resulting from the friction that the flowing blood exerts on the luminal surface, on the localization and development of atherosclerosis.

Atherosclerosis is associated with genetic predisposition and systemic factors such as hypertension, hyperlipidemia, smoking, etc. However, the localized nature of the disease, which occurs principally in areas of disturbed flow such as near bifurcations and curvatures, cannot be explained by systemic factors that apply equally throughout the vasculature. It is recognized today that atherosclerosis develops in areas where shear stress is low, typically less than 4 dyn/cm^2, or 0.4 Pa, and changes direction during the cardiac cycle. An example is the wall of the carotid sinus, where local shear is low and flow separates during the decelerating phase of the heart cycle, leading to flow separation and thus flow reversal and change in shear stress direction (left panel of Figure in the box). Other areas where low shear stress co-localizes with atherosclerosis are the coronaries, the infrarenal aorta and the femoral artery.

Shear Stress and Endothelial Function

Apart from its non-thrombogenic protective role, the endothelial layer constitutes the mechano-sensing element, which senses the local flow conditions and produces autocrine and paracrine factors for the functional regulation of the arterial wall. Studies of endothelial cells *in vitro* and *in vivo* have revealed the deleterious effect of low and oscillatory, vortex-related, shear stress on endothelial function. Under physiological shear ($\sigma > 10$ dyn/cm^2) endothelial cells align in the direction of flow whereas they do not when exposed to low shear ($\sigma < 4$ dyn/cm^2). Low and oscillatory shear stress lead to inhibition of NO-synthase, greater endothelial cell cycling and increase in apoptosis. Low and oscillatory shear also contribute to local endothelial dysfunction, which may lead to enhanced monocyte adhesion, increased platelet activation, increased vasoconstriction, increased smooth muscle cell proliferation, and increased oxidant activity, thus constituting a likely model for atherogenesis. Recently, it has been shown that low shear stress in combination with flow patterns like vortices determine the type of plaque, both in composition and vulnerability (right panel of Figure in the box). Low shear results in vulnerable plaque while vortex-based shear results in more stable plaque [2]. High shear stress induces an atheroprotective endothelial phenotype, increases NO production, and decreases the expression of vasoconstrictors, inflammatory response mediators, adhesion molecules and oxidants.

Detailed discussion on the relation between shear stress and endothelial function can be found in the review articles by Davies et al. [3] and Malek et al. [1].

Physiological and Clinical Relevance

Assessing Risk for Atherosclerosis

Ultrasound measurements in the carotid artery of healthy young adults aged 28–38 years revealed a significant inverse relation between the measured intima-media thickness and local shear stress. This suggests that there is a prognostic value in the assessment of local wall shear levels using noninvasive techniques, such as ultrasound Doppler or MRI.

Since the velocity profile near a bifurcation depends strongly on the geometry, it has been suggested that there exist 'geometrical risk' factors for atherosclerosis. Certain branching geometries, i.e., high curvatures and large angles, would predispose to atherosclerosis because they would lead more easily to flow separation and low shear stress regions.

Shear Stress and Intima Hyperplasia in Vein Grafts

Intima hyperplasia in vein grafts is also sensitive to wall shear. Dobrin et al. [4] examined the effect of all mechanical factors (pressure, extension, and shear stress) on intima hyperplasia and medial thickening in autogenous vein grafts in dogs. Autologous vein grafts were used to bypass a segment of the femoral artery. The femoral artery on one side was ligated, so that all femoral blood flow passed through the graft. The femoral artery at the opposite side was left patent, which permitted only part of the flow to pass through the vein graft. A stiff cuff was placed over the middle section of the vein grafts impeding radial expansion. Cross-sectional areas are given in Fig. 28.1. The results show that intima hyperplasia is greater on both sides, in the distended, low shear, regions, than in the regions constrained by the cuffs, thus at high shear. Furthermore, intima hyperplasia was globally lower on the side with high flow, obtained by femoral artery ligation, as compared to the side were femoral artery was left patent, i.e., low flow.

Shear Stress and Intima Hyperplasia in Bypass Grafts

High shear stress inhibits neointima formation in artificial ePTFE grafts. Animal experiments have shown that exposure of implanted grafts to higher shear, by means of distal arterio-venous fistulas, leads to a decrease in the thickness of the already existing neointima hyperplasia.
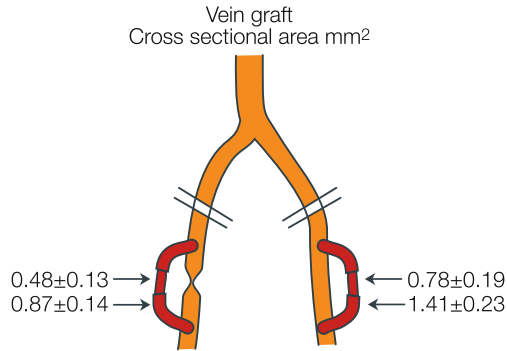
Fig. 28.1 Intimal hyperplasia in vein grafts. Adapted from ref. [4], used by permission

Low and oscillatory wall shear stress patterns may also be responsible for the failure of bypass grafts. In the vicinity of an end-to-side anastomosis, blood flow is greatly disturbed. This is mainly due to the abrupt change in geometry. For vascular grafts, intima hyperplasia develops preferentially at the 'toe' and the 'heel' of the anastomosis. These are exactly the locations where flow separation, low wall shear stress and large gradients of wall shear stress take place.

Intima Hyperplasia Following Angioplasty and Stenting

Restenosis is an undesirable occlusive response to stent implantation after balloon angioplasty. In contrast to balloon angioplasty, where acute or sub acute recoil represents the major mechanism of restenosis, stent restenosis is exclusively attributed to neointima proliferation, a tissue reaction often termed intima hyperplasia (IH). Morphological studies have demonstrated that neointima is caused by early smooth muscle cell ingrowth, which is then gradually replaced by extracellular matrix.

There is a good deal of scientific evidence that intima hyperplasia is sensitive to flow. Kohler and Jawien [5] studied the effects of flow on intima hyperplasia after balloon injury of the rat common carotid. Flow was increased, by ~35%, by ligation of the opposite common carotid artery or decreased, also by ~35%, by ligation of the ipsilateral internal carotid. Two weeks after the intervention, intima thickness, indicated by the distance between the artery lumen and arrow, was significantly smaller in the high flow group (Fig. 28.2a) as compared with low-flow group (Fig. 28.2b).

There appears also to be strong clinical evidence for the relation between post interventional flow and patency of balloon angioplasty. If local flow, and thus wall shear stress, after balloon angioplasty is high, the artery is expected to remain patent. This observation, common to many physicians practicing balloon angioplasty,
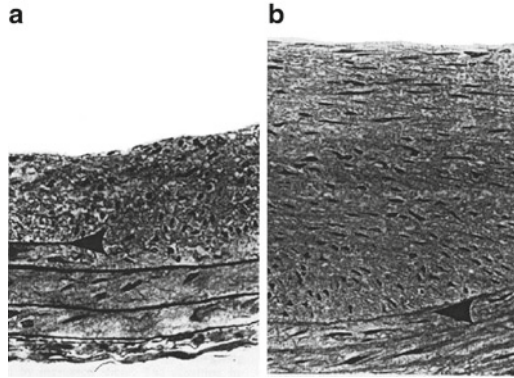
Fig. 28.2 Histological sections of the rat carotid artery subjected to high flow (**a**) and low flow (**b**) indicating the degree of intimal hyperplasia 2 weeks after balloon injury. Adapted from ref. [5], used by permission

is substantiated by recent studies reporting increased long-term patency after angioplasty in lower extremity arteries when flows are high. Direct clinical proof of the inverse relationship between wall shear stress and intima thickness was given by Wentzel et al. [6].

The restenosis problem following stent placement has been drastically reduced with the use of drug-eluting stents. Drug-eluting stents with the capability to deliver anti-inflammatory or anti-proliferative drugs directly to the adjacent arterial tissue, inhibit neointima hyperplasia and restenosis.

References

1. Malek AM, Alper SL, and Izumo S. Hemodynamic shear stress and its role in atherosclerosis. *JAMA* 1999;282:2035–2042.
2. Cheng C, Tempel D, van Haperen R, van der Baan A, Grosveld F, Daemen MJ, Krams R, and de Crom R. Atherosclerotic lesion size and vulnerability are determined by patterns of fluid shear stress. *Circulation* 2006;113:2744–2753.
3. Davies PF, Barbee KA, Lal R, Robotewskyj A, and Griem ML. Hemodynamics and atherogenesis. Endothelial surface dynamics in flow signal transduction. *Ann N Y Acad Sci* 1995;748: 86–102; discussion 102–103.
4. Dobrin PB, Littooy FN, and Endean ED. Mechanical factors predisposing to intimal hyperplasia and medial thickening in autogenous vein grafts. *Surgery* 1989;105:393–400.
5. Kohler T and Jawien A. Flow affects development of intimal hyperplasia after arterial injury in rats. *Arterioscler Thromb* 1992;12:963–971.
6. Wentzel JJ, Krams R, Schuurbiers JC, Oomen JA, Kloet J, Van der Giessen WJ, Serruys PW, and Slager CJ. Relationship between neointimal thickness and shear stress after Wallstent implantation in human coronary arteries. *Circulation* 2001;103:1740–1745.

Part D
Integration

Chapter 29
Determinants of Pressure and Flow
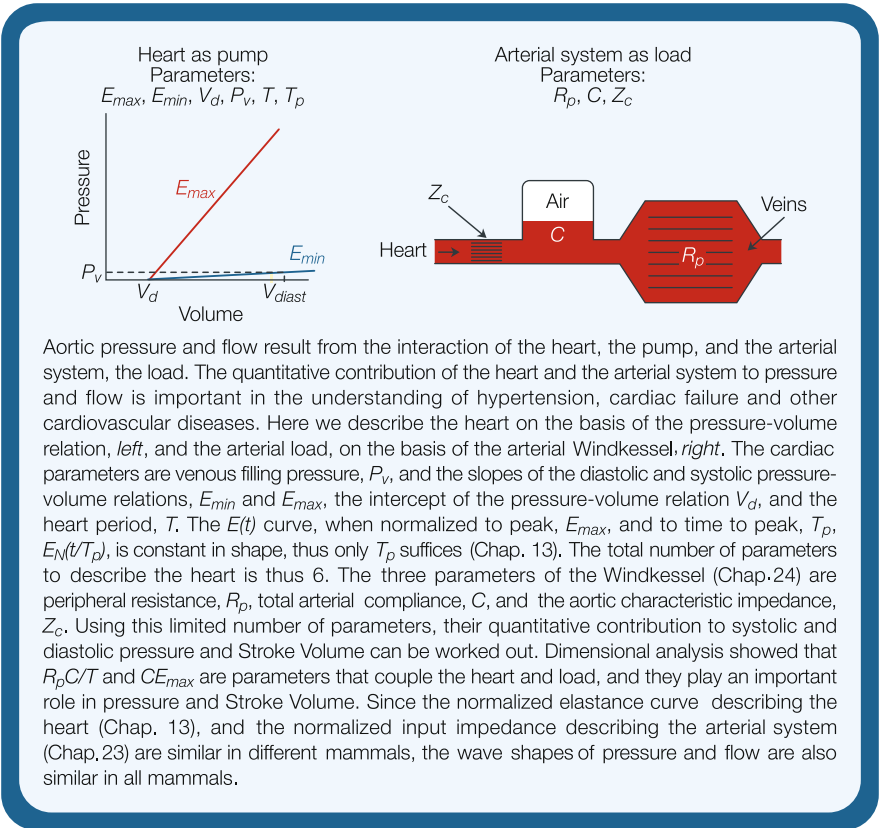
Aortic pressure and flow result from the interaction of the heart, the pump, and the arterial system, the load. The quantitative contribution of the heart and the arterial system to pressure and flow is important in the understanding of hypertension, cardiac failure and other cardiovascular diseases. Here we describe the heart on the basis of the pressure-volume relation, *left*, and the arterial load, on the basis of the arterial Windkessel, *right*. The cardiac parameters are venous filling pressure, P_v, and the slopes of the diastolic and systolic pressure-volume relations, E_{min} and E_{max}, the intercept of the pressure-volume relation V_d, and the heart period, T. The $E(t)$ curve, when normalized to peak, E_{max}, and to time to peak, T_p, $E_N(t/T_p)$, is constant in shape, thus only T_p suffices (Chap. 13). The total number of parameters to describe the heart is thus 6. The three parameters of the Windkessel (Chap. 24) are peripheral resistance, R_p, total arterial compliance, C, and the aortic characteristic impedance, Z_c. Using this limited number of parameters, their quantitative contribution to systolic and diastolic pressure and Stroke Volume can be worked out. Dimensional analysis showed that R_pC/T and CE_{max} are parameters that couple the heart and load, and they play an important role in pressure and Stroke Volume. Since the normalized elastance curve describing the heart (Chap. 13), and the normalized input impedance describing the arterial system (Chap. 23) are similar in different mammals, the wave shapes of pressure and flow are also similar in all mammals.

Description

Blood pressure and Cardiac Output result from the interaction of the heart and arterial load. However, quantitative information about the contribution of both the heart and arterial load to pressure and flow under different physiological conditions and during various diseased states is limited. To quantitatively analyze the cardiac and arterial contributions to systolic and diastolic pressure and Stroke Volume, we make use of the simplified descriptions of the cardiac pump and the arterial load. The heart is described by the varying elastance model (Chap. 13), and the arterial system is described by the three-element Windkessel model (Chap. 24). Using these models the contribution of each parameter to pressure and flow can be quantified.

Dimensional Analysis

Dimensional analysis, or the concept of similitude, is a powerful method to systematically derive relations of a system and offers two major advantages [1]. First, it reduces the number of variables, and second, it groups the cardiac and arterial parameters in dimensionless terms, which are automatically scaled to Heart Rate and body size. This will be a particularly important issue when we discuss comparative physiology (Chap. 30). The parameters that describe the heart as a pump, including venous filling pressure, and the arterial system as the load are given in the box. The total number of parameters is nine, namely six for the heart and three for the arterial system.

The dependent variables systolic and diastolic pressure (P_s and P_d) and Stroke Volume, SV, can be written as a function of these nine cardiac and arterial parameters. Dimensional analysis implies that when the variables and the parameters are non-dimensionalized, the number of non-dimensional parameters can be reduced by three. Three is the number of reference dimensions (time, force and length), describing the variables [1]. Thus six non-dimensional parameters remain. An intelligent choice is the following [2]:

$$P_s / P_v = \Phi_1(Z_c / R_p, R_p C / T, CE_{min}, E_{max} / E_{min}, E_{min} V_d / P_v, T_p / T)$$

$$P_d / P_v = \Phi_2(Z_c / R_p, R_p C / T, CE_{min}, E_{max} / E_{min}, E_{min} V_d / P_v, T_p / T)$$

$$SV \cdot E_{min} / P_v = \Phi_3(Z_c / R_p, R_p C / T, CE_{min}, E_{max} / E_{min}, E_{min} V_d / P_v, T_p / T)$$

The symbols are explained in the box. The next step is to find the dependence of the non-dimensional variables on the non-dimensional parameters. The dependence of $E(t)$ on time and its magnitude are similar when normalized (Fig. 29.1) and the contribution of T_p/T to P_s/P_v, P_d/P_v, and $SV \cdot E_{min}/P_v$ is small and is neglected. It turns out experimentally that the parameter $E_{min} \cdot V_d / P_v$ does not contribute to P_s/P_v and P_d/P_v; that Z_c / R_p does not determine P_d/P_v and SV/V_d; while E_{max} / E_{min} does not
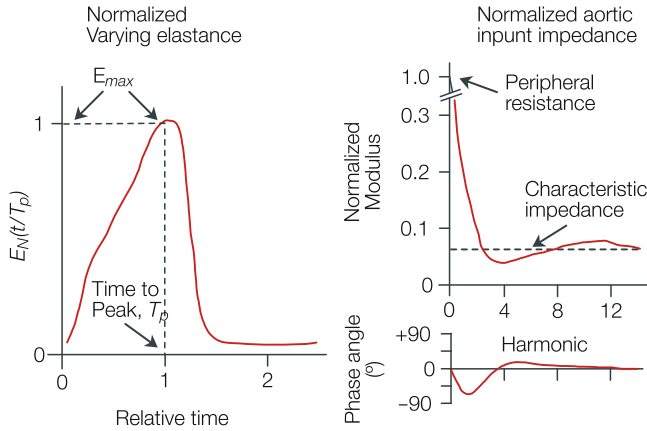
Fig. 29.1 The normalized elastance curve and the normalized input impedance, are independent of animal size, and the result is that wave shapes of aortic pressure and flow that look alike in mammals, with pressure even the same in magnitude

determine $SV \cdot E_{min}/P_v$. The contribution of Z_c/R_p to P_s/P_v turns out to be small [2] and is neglected. The relations then can be simplified to:

$$P_s / P_v \approx \Phi_1 (R_p C / T, CE_{min}, E_{max} / E_{min})$$

$$P_d / P_v \approx \Phi_2 (R_p C / T, CE_{min}, E_{max} / E_{min})$$

$$SV \cdot E_{min} / P_v \approx \Phi_3 (R_p C / T, CE_{min}, E_{min} \cdot V_d / P_v)$$

In all non-dimensional variables we see that the parameters $R_p C/T$, and $C \cdot E_{min}$ appear. We call them ventriculo-arterial coupling parameters. This emphasizes the fact that the interaction of pump and load determines pressure and flow.

The Frank-Starling mechanism also emerges clearly from the above equations. Leaving all parameters the same, the pressures are simply proportional to venous pressure, P_v, the SV is also related to filling pressure, but in a more complex way. In reality the diastolic Pressure-Volume relation is not straight and therefore the effect of filling is more complex than shown here.

The pressures also are dependent on E_{max}/E_{min} a measure of contractility of the heart. The Stroke Volume is also described by the rather complex term $E_{min} \cdot V_d / P_v$, which is related to diastolic ventricular filling and can be written as $V_d / (V_{diast} - V_d)$, with V_{diast} end-diastolic ventricular volume.

On the basis of the results obtained with the dimensional analysis we can perform a sensitivity analysis of pressure and Stroke Volume to individual parameters. The results are given in the Table 29.1.

We note that the normalized parameters $R_p C/T$, CE_{min}, E_{max}/E_{min} do not depend on body size, so that for similar venous pressures, aortic systolic and diastolic

Table 29.1 The quantitative contribution of heart and arterial system parameters to pressure and Stroke Volume

	P_{sys}	P_{dias}	SV
Z_c	+9	0	0
R_p	+41	+90	−28
C	−10	+22	+5
T	−50	−90	+28
E_{max}	+40	+32	+33
E_{min}	−100	−100	−100
P_v	+100	+100	+100

Percent changes in pressure and Stroke Volume, SV, resulting from an increase in a single cardiac or arterial parameter. Thus a 20% change in heart period (T) results in a 10% change in systolic pressure and an 18% in diastolic pressure. The *minus sign* indicates a decrease with an increase in a parameter. For identification of parameters see the box

pressures will be similar in all mammals (see Chap. 30). Stroke Volume does depend on body size. The wave shapes of aortic pressure and flow result from the shape of the $E(t)$ curve, describing the pump, and the input impedance, describing the arterial load. Both, when normalized, are body size independent [3, 4], explaining why aortic pressure and flow look alike in all mammals (Chap. 30).

Physiological and Clinical Relevance

The analysis shows in quantitative terms the contribution of cardiac and arterial parameters to blood pressure and Stroke Volume. It may be seen from Table 29.1 that resistance has a much stronger effect on systolic blood pressure than compliance has. However, changes in compliance are often considerably larger than resistance changes. For instance, between the ages of 20 and 70 years compliance may decrease by a factor of 3 (Chap. 20), thus increasing systolic blood pressure by 15%, while the age related resistance increase is about 10% resulting in a systolic pressure increase of slightly over 4%.

On the basis of the dimensionless parameters shown above it may be suggested to use E_{max}/E_{min} as a measure of contractility instead of E_{max} alone, because this ratio is size independent, while the E_{max} alone is, of course, depending on the ventricular volume.

The theoretical results can be compared with biological data. Experimental data [5] obtained from the isolated heart loaded with a Windkessel model (Chap. 24) indeed show that compliance changes alone have a small effect on systolic blood pressure and a larger effect on diastolic blood pressure (Fig. 29.2). When compliance is decreased *in vivo* (Chap. 11) other parameters also change and systolic
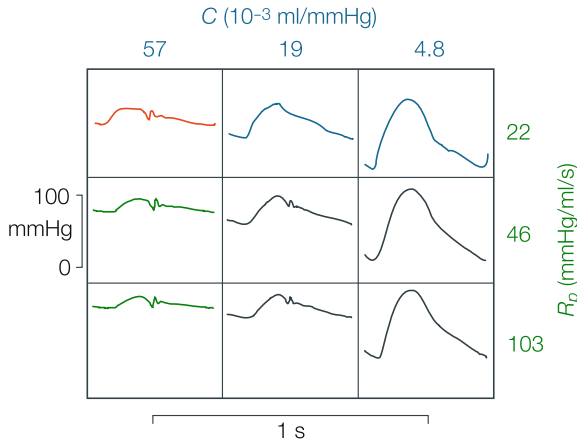
Fig. 29.2 Aortic pressure resulting from an isolated cat heart pumping into a three-element Windkessel. The effect of changes in peripheral resistance and total arterial compliance are shown. All cardiac parameters and Z_c are kept constant. Note that mean pressure depends on resistance, and pulse pressure is strongly affected by compliance. Adapted from ref. [5], used by permission

pressure increases and diastolic pressure decreases [6]. The main difference between the *ex vivo* and *in vivo* results is the adaptation of the heart during the decrease in compliance. The heart, was unchanged including diastolic filling Fig. 29.2, while *in vivo* the heart adapts and Cardiac Output diminishes less than in the *ex vivo* situation (see Fig. 11.6, Chap. 11). Thus, the changed cardiac function *in vivo* has an effect on blood pressure.

Contribution of Arterial System and Heart in Systolic Hypertension

The increase in aortic pressure with age is shown in Fig. 29.3. In the literature it is well established that hypertension results in ventricular hypertrophy and therefore a higher E_{max}. However, it is often not realized that hypertrophy causes changes in the properties of the cardiac pump such as increased wall thickness (i.e. increased E_{min} and E_{max}) and that these changes may, in turn, contribute to a further increase in blood pressure. Since Cardiac Output decreases little with age, the increase in mean pressure results mainly from the increase in peripheral resistance. Similarly the increase in Pulse Pressure with maintained Stroke Volume mainly results from the decrease in total arterial compliance.

Using the models, as given in the box, the contributions of the heart and arterial system to systolic aortic pressure in four groups of hypertensive patients were calculated and the results are shown in Fig. 29.4 [7]. It may be seen that in concentric remodeling the increase in systolic blood pressure is mainly the result of the
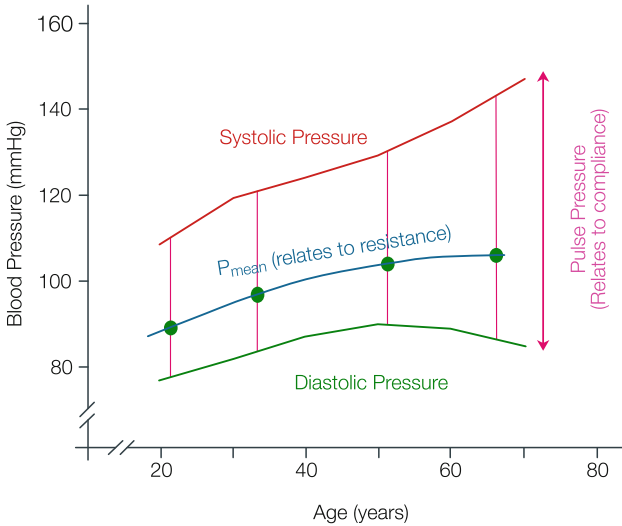
Fig. 29.3 Aortic pressure as a function of age. The increase in mean pressure relates mainly to peripheral resistance. The increase in pulse pressure results mainly from decreased total arterial compliance
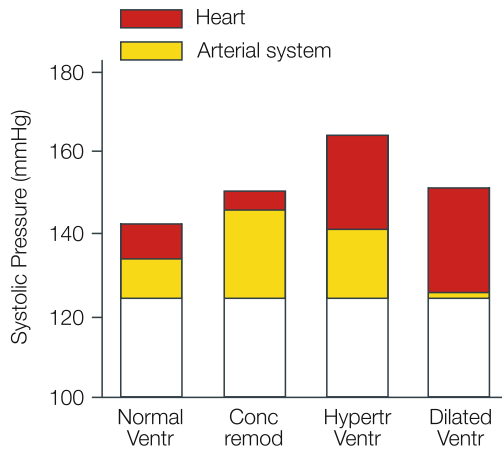
Fig. 29.4 Cardiac and arterial contributions to systolic pressure increase in four groups of hypertensive patients. Several stages in cardiac changes are depicted, (1) normal ventricle; (2) concentric remodeling; (3) hypertrophied ventricle; and (4) dilated left ventricle. Cardiac and arterial parameters derived from ref. [3]. The *white bar* gives the systolic pressure of the normal cardiovascular system. In concentric remodeling most of the pressure increase results from the change in the arterial system. When the ventricle is dilated in hypertension most of the pressure increase is caused by the heart. Adapted from ref. [7], used by permission

altered arterial system, while in eccentric hypertrophy the contribution to the increased systolic pressure is mainly the result of changed cardiac properties. This example therefore shows that both heart and arterial system need to be considered in hypertension research.

References

1. Munson BR, Young DF, Okiishi TH. *Fundamentals of fluid mechanics.* 1994, New York, Wiley.
2. Stergiopulos N, Meister J-J, Westerhof N. Determinants of Stroke Volume and systolic and diastolic aortic pressure. *Am J Physiol* 1996;270:H2050–H2059.
3. Senzaki H, Chen C-H, Kass DA. Single-beat estimation of end-systolic pressure-volume relation in humans: a new method with the potential for noninvasive application. *Circulation* 1996;94:2497–2506.
4. Westerhof N, Elzinga G. Normalized input impedance and arterial decay time over heart period are independent of animal size. *Am J Physiol* 1991;261:R126–R133.
5. Elzinga G, Westerhof N. Pressure and flow generated by the left ventricle against different impedances. *Circ Res* 1973;32:178–186.
6. Randall OS, van den Bos GC, Westerhof N. Systemic compliance: does it play a role in the genesis of essential hypertension? *Cardiovasc Res* 1984;18:455–462.
7. Segers P, Stergiopulos N, Westerhof N. Quantification of the contribution of cardiac and arterial remodeling to hypertension. *Hypertension* 2000;36:760–765.

Chapter 30
Comparative Physiology

Aortic and ventricular pressure are similar in shape and magnitude in mammals. The only difference is the Heart Rate (HR, $1/T_{period}$). The aortic flow wave shape is similar as well but its magnitude depends on body size. This strong similarity results from the relations between the basic parameters describing the cardiovascular system. To compare parameters we make use of the so-called allometric equation: $PA = PA_0\, M^e$, with PA the parameter of interest, PA_0 a reference value, M body mass, and e the exponent. Double logarithmic plots give linear relations with slope e, similar values of the exponent means that the ratio of the parameters is independent of animal size. The R_pC-time of aortic pressure decay in diastole, with R_p peripheral resistance and C total arterial compliance, and the heart period, T_{period}, both scale as $M^{1/4}$. The ventriculo-arterial coupling parameter R_pC/T_{period} is independent of body mass and thus the same in mammals. Volume parameters such a heart size and Stroke Volume, SV, are proportional to body mass. Heart Rate scales as $M^{-1/4}$. Since CO equals HR times SV, it is proportional to $M^{3/4}$. Basal metabolism is proportional to CO, and thus also proportional to $M^{3/4}$. The coupling parameter CE_{min}, and the ratio's E_{max}/E_{min} and $T_{diastole}/T_{period}$, are independent of body mass. The limited data available on the $E(t)$ curve, when scaled to its maximum and time of peak suggest similarity as well. The ratio of peripheral resistance and aortic characteristic impedance is independent of animal size, implying that normalized aortic input impedance is identical in mammals. Since all parameters prescribing aortic pressure and flow wave shapes are independent of animal size, the pressure and flow waves are similar in mammals. Pressures even have the same magnitude, while Cardiac Output scales to $M^{3/4}$. Similar mean pressure (at brain level) is probably a necessary condition for brain perfusion, while the similar diastolic pressure and constant fraction of diastole, $T_{diastole}/T_{period}$, are conditions to provide sufficient subendocardial coronary perfusion. The similar pressures in mammals imply stringent conditions on pressure and suggest that even borderline hypertension is abnormal. Since Stroke Volume is proportional to body mass CO and basal metabolism scale to $M^{3/4}$ rather than to body mass, thereby limiting cardiac metabolic reserve in small mammals.

Description

Comparative physiology is based on the allometric equation [1]:

$$PA = PA_0 \cdot M^e$$

with *PA* the parameter of interest, PA_0 a reference value, *M* body mass, and *e* the exponent. When the logarithm of both sides is taken the equation can be rewritten as:

$$\log PA = \log PA_0 + e \log M$$

This equation states that, when a parameter *PA* is plotted against body mass *M*, in a double logarithmic plot, a straight line with slope *e* is obtained, If two parameters have the same slope (same *e*), the ratio of the parameters does not depend on body mass, i.e., the ratio is independent of the size (mass) of the animal.

The coupling parameter R_pC/T (see Chap. 29) is an example of the study of comparative physiology, where it is shown that the characteristic time of the arterial system, R_pC-time, and the characteristic time of the heart, the heart period, *T*, have the same exponent (Fig. 30.1) implying that their ratio is independent of body mass [2]. The similar Pulse Pressure found in mammals can be understood on the basis of this mass-independence as follows. Total arterial compliance, *C*, is proportional to Stroke Volume divided by Pulse Pressure, *PP* so that $C \propto SV/PP$. Mean pressure is equal to Peripheral Resistance, R_p, times Cardiac Output: $P_{mean} = R_p \cdot CO$. The Cardiac Output equals Heart Rate times Stroke Volume, and Heart Rate $= 1/T$. Therefore, $P_{mean}/PP \propto R_pC$-time/T. This implies that, with similar mean pressure, the Pulse Pressure, and therefore also the systolic and the diastolic pressures are the same in mammals. The ratio of Pulse Pressure and mean pressure, PP/P_{mean}, is called the fractional Pulse Pressure.
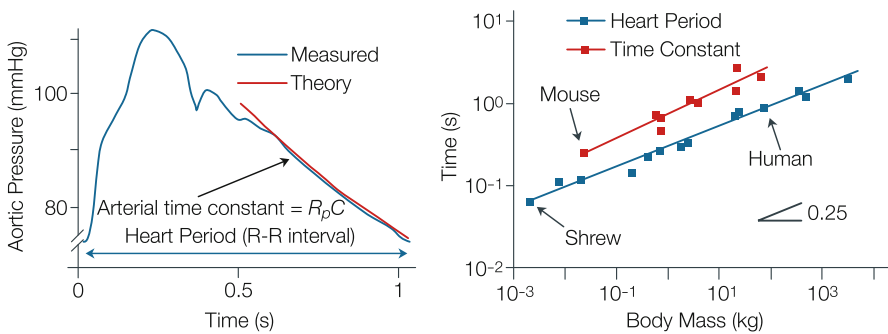
Fig. 30.1 Aortic pressure (*left*) and a log-log plot of heart period, $T_{period} =$ R-R interval, and R_pC-time (*right*). The aortic pressure shows an exponential decay in diastole, characterized by the arterial parameter R_pC-time, i.e., peripheral resistance, R_p, times total arterial compliance, *C*. The heart period, T_{period}, is a cardiac parameter. Both times show an increase with body mass with an exponent of 1/4. This implies that the ratio of the two, the ventriculo-arterial coupling parameter R_pC/T_{period} is the same in mammals. Adapted from ref. [2], used by permission
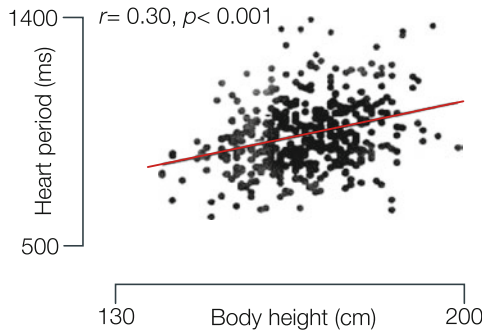
Fig. 30.2 Heart period relates to body height in humans. Slope is (length)$^{0.9}$ or mass$^{0.27}$, which is close to 1/4 as found between mammals. Adapted from ref. [3], used by permission

The finding that the heart period increases with body mass, predicts, even in a single species, that heart period increases also with body length. This was indeed shown to be the case in the human (Fig. 30.2).

In general, volumes are proportional to body mass, i.e., M^{+1} and so are cardiac volume and Stroke Volume [4]. With $CO = HR \cdot SV$, it follows that CO is proportional to $M^{3/4}$. This is indeed what is found and is shown Fig. 30.3.

Other comparative data are scarce but if we assume similar material properties, and with volumes proportional to body mass [4, 5], it follows that the slope of the diastolic and systolic pressure-volume relations, are proportional to M^{-1}, and also that total arterial compliance, C, is proportional to body mass. Thus, the coupling parameters CE_{min} and CE_{max} (see Chap. 29), are independent of body mass. The ratio of E_{max} and E_{min} equals systolic over diastolic pressure for isovolumic beats and this ratio is similar in mammals, thus E_{max}/E_{min} is size independent. In the data published on the $E(t)$ curve, those of man and dog are not dissimilar in shape, when normalized with respect to time of peak and peak value [6]. Quantitative data on a whole range of mammals is not available yet.

When we plot the characteristic impedance and peripheral resistance as a function of body mass we find parallel lines again (Fig. 30.4). This implies that this ratio is similar in mammals. Therefore the aortic input impedance (Fig. 30.5) when scaled with respect to the characteristic impedance or peripheral resistance and plotted as a function of harmonic, i.e., as multiples of the Heart Rate (Appendix 1) is similar [2].

When a three-element Windkessel is assumed as acceptable model of the systemic arterial tree (Chap. 24), the input impedance can be written as:

$$Z_{in}/Z_c = \frac{1 + R_p/Z_c + 2\pi \cdot nR_pC/T}{1 + 2i\pi \cdot nR_pC/T}$$

where n is the harmonic number and $1/T$ is Heart Rate. With R_pC/T and R/Z_c independent of animal size, the normalized arterial input impedance is basically similar for all mammals (Fig. 30.5, blue line). Thus, the aortic pressure and flow wave
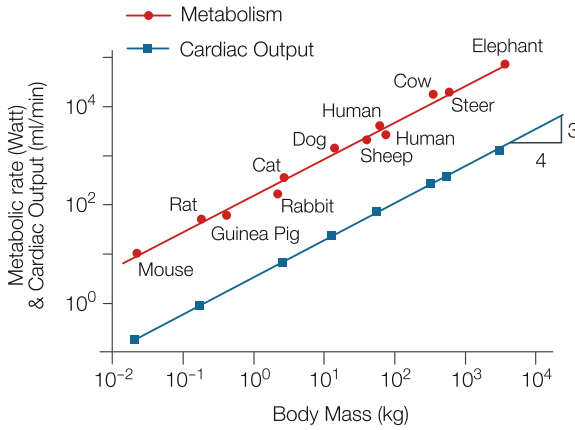
Fig. 30.3 Cardiac output and basal metabolism are proportional and increase with body mass to the power 3/4. Data on metabolic rate from ref. [1] and data on CO from ref. [5], used by permission
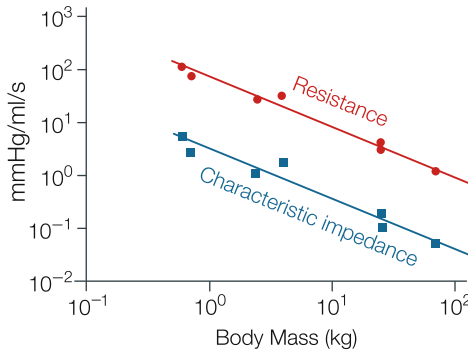
Fig. 30.4 Peripheral resistance and aortic characteristic impedance scale similarly with body mass. Therefore their ratio is independent of animal size. Adapted from ref. [2], used by permission

shapes are related in a similar way in all mammals. This in turn implies that with similar pressure wave shapes, the flow waves are similar too.

The non-dimensional ventriculo-arterial coupling parameters, CE_{max} and R_pC/T (decay time of diastolic aortic pressure over heart period, Chap. 29) are independent of animal size. Together with the above the final result is that in all mammals pressure waves are similar in shape and magnitude and flow waves are also similar in shape, but the magnitude relates to body mass to the power 3/4. It was also shown (Chap. 17) that the size of the heart results in optimal external power production [7].

It has also been suggested that shear stress would be similar in mammals too (Chaps. 27 and 28). Shear stress is proportional to Q/r^3, and since CO scales to $M^{3/4}$, and r to $M^{1/3}$, shear stress scales to $M^{3/4}/M = M^{-1/4}$. Shear stress is probably not very tightly controlled (Chaps. 27 and 28) and certainly is not the same in different vessels and different in similar arteries between animals (Chap. 2).
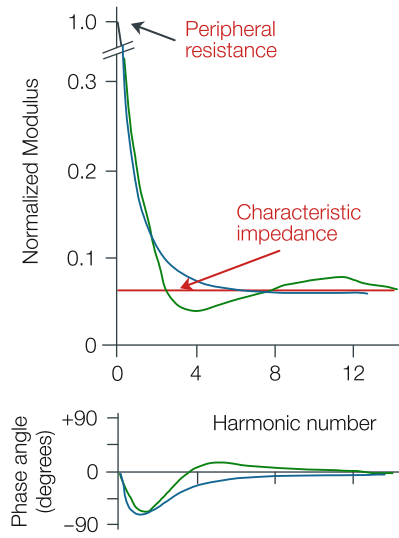
Fig. 30.5 Normalized input impedance is similar in mammals (*green*). This implies that the ratios of the harmonics of pressure and flow are similar and thus their wave shapes are the same. The normalized three-element Windkessel is shown in *blue*
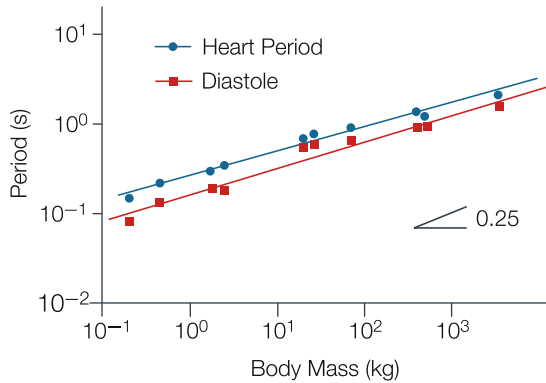
Fig. 30.6 Heart period and duration of diastole are plotted as a function of body mass. The *parallel lines* imply that diastole is a fixed fraction of the heart period. Adapted from ref. [2], used by permission

The allometric relations of heart period and duration of diastole are given in Fig. 30.6. The slopes of the relations are not different, which means that diastole is a constant fraction of the heart period. Subendocardial perfusion mainly takes place in diastole, and thus depends on diastolic pressure and the duration of diastole. With similar diastolic pressures and similar coronary fractional perfusion time (Chap. 18) perfusion conditions are also similar in mammals [2].

Basal Whole Body and Cardiac Metabolism

Basal whole body metabolism and Cardiac Output are both proportional to body mass as $M^{3/4}$ (Fig. 30.3). Why CO is proportional to $M^{3/4}$ was explained above. Apparently metabolism is related to CO, but other suggestions have been given [8]. Basal metabolism and CO may be closely related because oxygen carrying capacity of the blood is similar in mammals.

Cardiac Metabolism

Experimental data show that Cardiac metabolism increases with body mass to the power 3/4. Oxygen consumption is proportional to the Pressure Volume Area, PVA, times Heart Rate, HR. Therefore it holds approximately: $VO_2 \propto [P_{systolic} \, SV + \frac{1}{2} P_{systolic} \cdot (V_{end\text{-}systolic} - V_d)] \cdot HR$ (see Chap. 16). Since volumes are proportional to body mass (scale to M^1), pressure is size independent, and HR scales as $M^{-1/4}$, VO_2 relates to body mass to the power 3/4 as well.

Thus since cardiac metabolism increases with body mass to the power 3/4 and cardiac mass is proportional to body mass, cardiac metabolism per gram heart tissue increases with body mass to the power $-1/4$. This means that cardiac metabolism per gram is higher in small than in large animals.

Mitochondrial relative volume, as a measure of maximal energy expenditure per unit mass, decreases with body mass as $M^{-0.05}$ [9]. In other words, the difference between maximal metabolism and resting metabolism, i.e. the metabolic reserve, decreases in smaller mammals.

Pulse Wave Velocity and Reflections

Experimental data suggest that pulse wave velocity is independent of animal size. This can be seen from basic vascular data where the Young modulus of elasticity, E, and wall thickness over radius, h/r_i, are species independent and, as a consequence wave speed (Moens-Korteweg equation),

$$c = \sqrt{\frac{h \cdot E}{2 \cdot r_i \cdot \rho}}$$

is independent of body size as well.

The return of the reflected waves at the heart equals traveled length over wave speed and phase of the reflection coefficient. Length of the arteries is proportional to $M^{1/3}$, so that the return time of reflections is also proportional to $M^{1/3}$. The heart period is proportional to $M^{1/4}$. This small difference in power, and the possible difference in reflection phase angle, makes reflections that return from the periphery arrive in the about the same part of the cardiac cycle in most mammals.

In summary, the rigorous control of blood pressure appears to demand that Heart Rate is coupled to the R_pC-time of the arterial system. This, in combination with a *SV* that is proportional to body mass, results in the 3/4 power law of *CO* and whole body metabolism.

Physiological and Clinical Relevance

Comparative physiology of the cardiovascular system shows that the heart and arterial system act to produce similar magnitude and wave shape of pressures and similar wave shapes of flow in mammals. This strongly suggests that pressure magnitude and wave shape are important. It has indeed been shown that high pressure, e.g., hypertension, is a strong indicator of cardiovascular pathology. Recent epidemiological data point to the strong relation between Pulse Pressure and cardiovascular morbidity and mortality [10, 11]. The magnitude of Pulse Pressure, together with the about $2.5 \cdot 10^9$ pulsations in a human lifetime, may play a role in fatigue and fracture of the arterial wall. Martyn and Greenwald [12] argue that the synthesis of elastin is slow and that damage, resulting from pulsations, takes years to repair. The decrease in elastin may be the reason that with age aortic diameter increases and the wall becomes stiffer, because vessel elasticity becomes gradually more determined by the collagen, which gradually replaces elastin.

It has been suggested that all mammals have the same number of heartbeats over their life span (about $1.4 \cdot 10^9$ beats). Thus small animals with high Heart Rates live shorter than large animals with low Heart Rates. Vascular damage has been proposed as possible explanation [12]. Another explanation for the longer life span of large mammals is that metabolism per gram decreases with increasing body mass. The lower metabolic rate per cell may imply a lower production of oxygen radicals and less cellular damage. However, animals in zoological gardens and humans in western society live much longer than predicted on the basis of the number of their heart beats.

References

1. Schmidt-Nielsen K. *Scaling. Why is animal size so important?* 1984, London & New York, Cambridge University Press, pp 57.
2. Westerhof N, Elzinga G. Normalized input impedance and arterial decay time over heart period are independent of animal size. *Am J Physiol* 1991;261:R126–R133.
3. Smulyan H, Marchais SJ, Pannier B, Guerin AP, Safar ME, London GM. Influence of body height on pulsatile hemodynamic data. *J Am Coll Cardiol* 1998;31:1103–1109.
4. Holt JP, Rhode EA, Kines H. Ventricular volumes and body weight in mammals. *Am J Physiol* 1968;215:704–714
5. Altman PL, Dittmer DE (eds). *Biological handbook.* 1971, Bethesda, Federation of American Societies of Experimental Biology, pp 278, 320, 336–341.
6. Senzaki H, Chen C-H, Kass DA. Single beat estimation of end-systolic pressure-volume relation in humans: a new method with the potential for noninvasive application. *Circulation* 1996;94:2497–2506.

7. Elzinga G, Westerhof N. Matching between ventricle and arterial load. *Circ Res* 1991;68:1495–1500.

8. West GB, Woodruff WH, Brown JH. Allometric scaling of metabolic rate from molecules and mitochondria to cells and mammals. *Proc Natl Acad Sci USA* 2002;99:2473–2478.

9. Barth E, Stämler G, Speiser B, Schaper J. Ultrastructural quantification of mitochondria and myofilaments in cardiac muscle from 10 different animal species including man. *J Mol Cell Cardiol* 1992;24:669–681.

10. Benetos A, Safar M, Rudnichi A, Smulyan H, Richard JL, Ducimetieere P, Guize L. Pulse pressure: a predictor of long-term cardiovascular mortality in a French male population. *Hypertension* 1997;30:1410–1415.

11. Mitchell GF, Moye LA, Braunwald E, Rouleau JL, Bernstein V, Geltman EM, Flaker GC, Pfeffer MA. Sphygmomanometrically determined pulse pressure is a powerful independent predictor of recurrent events after myocardial infarction in patients with impaired left ventricular function. *Circulation* 1997;96:4254–4260.

12. Martyn CN, Greenwald SE. Impaired synthesis of elastin in walls of aorta and large conduit arteries during early development as an initiating event in pathogenesis of systemic hypertension. *Lancet* 1997;3502:953–955.

Part E
Appendices

Appendix 1
Times and Sines: Fourier Analysis
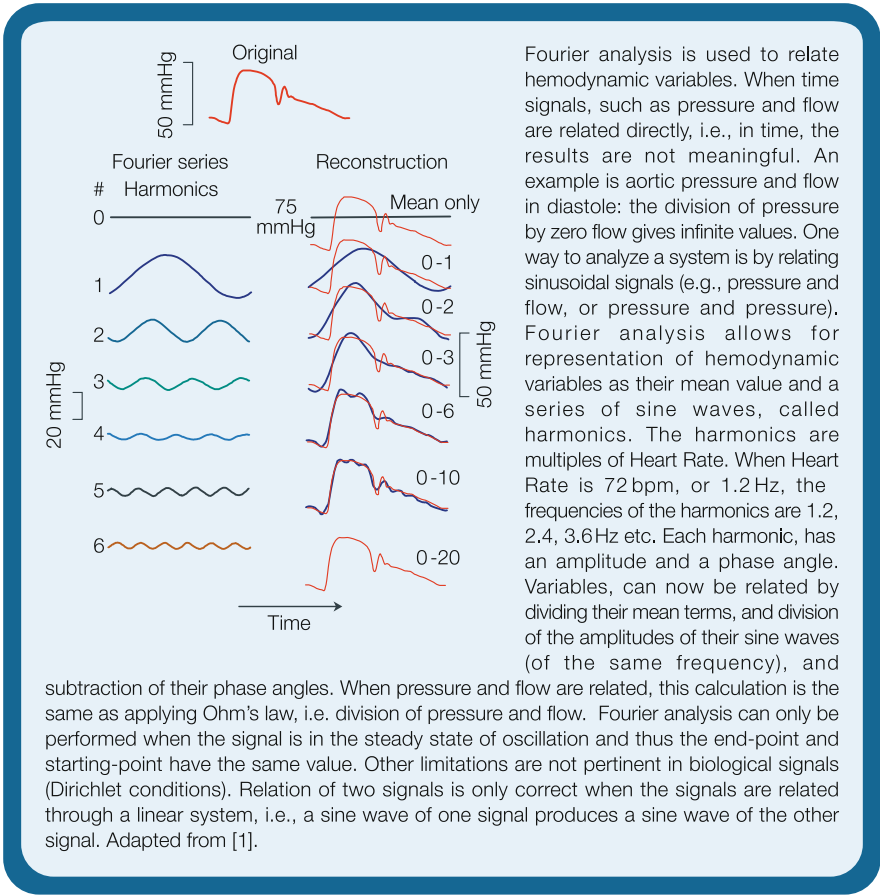
Fourier analysis is used to relate hemodynamic variables. When time signals, such as pressure and flow are related directly, i.e., in time, the results are not meaningful. An example is aortic pressure and flow in diastole: the division of pressure by zero flow gives infinite values. One way to analyze a system is by relating sinusoidal signals (e.g., pressure and flow, or pressure and pressure). Fourier analysis allows for representation of hemodynamic variables as their mean value and a series of sine waves, called harmonics. The harmonics are multiples of Heart Rate. When Heart Rate is 72 bpm, or 1.2 Hz, the frequencies of the harmonics are 1.2, 2.4, 3.6 Hz etc. Each harmonic, has an amplitude and a phase angle. Variables, can now be related by dividing their mean terms, and division of the amplitudes of their sine waves (of the same frequency), and subtraction of their phase angles. When pressure and flow are related, this calculation is the same as applying Ohm's law, i.e. division of pressure and flow. Fourier analysis can only be performed when the signal is in the steady state of oscillation and thus the end-point and starting-point have the same value. Other limitations are not pertinent in biological signals (Dirichlet conditions). Relation of two signals is only correct when the signals are related through a linear system, i.e., a sine wave of one signal produces a sine wave of the other signal. Adapted from [1].

Description

Fourier analysis breaks a periodic signal up in a series of sine waves, called harmonics. Any repetitive physiological signal, such as pressure or flow in the steady state can be written as a Fourier series:

$$f(t) = \frac{a_0}{2} + \sum_{n=1}^{N} [a_n \cos\frac{2\pi t}{T} + b_n \sin\frac{2\pi}{T}t], \text{n harmonic number, and N} \geq 0$$

The T is period of the signal, with 1/T the frequency; thus here Heart Rate. The Fourier coefficients a_n and b_n, can be straightforwardly calculated and are not obtained by curve fitting:

$$a_n = \frac{1}{T}\int_0^T f(t)\cos(n\frac{2\pi t}{T})dt, \text{with n} \geq 0$$

$$b_n = \frac{1}{T}\int_0^T f(t)\sin(n\frac{2\pi t}{T})dt, \text{with n} > 1$$

A practical way to write the Fourier series is in terms of modulus, M, and phase, φ

$$M_n^2 = a_n^2 + b_n^2, \text{and tan } \varphi_n = b_n / a_n.$$

Thus if, for example, the Fourier series of pressure and flow are expressed this way, the impedance modulus (Chap. 23) is obtained by division of the modulus of pressure and flow (with the same n), and the impedance phase angle is obtained by subtraction of the phase angles of pressure and flow. Similarly the transfer function can be obtained from two pressure signals (Chap. 26).

The technique to perform Fourier analysis is now readily available and therefore easy to perform.

In the left part of the Figure in the box the individual harmonics are given each having an amplitude and phase angle. The phase angle is best seen from the starting point of the sine wave. We see that the amplitudes of the harmonics are decreasing in amplitude. On the right hand side of the Figure in the box, the reconstruction is presented, which is simply the addition of the sine waves at the same moments in time. Using ten harmonics the signal is almost completely reconstructed, and with 20 harmonics the signal is completely reconstructed. This means that aortic pressure is described by approximately 15 harmonics. It turns out that the smoother the signal the fewer harmonics are required to describe it. Ventricular pressure can be described by about ten harmonics. Thus, in general, the information in hemodynamic signals such as pressure, flow and diameter contains information up to 15 harmonics, i.e., 15 times the Heart Rate.

This knowledge is important with respect to measurement techniques. To describe a sine wave at least two points are required (the Nyquist criterion [2]). Thus sampling should be done with at least twice the highest frequency, i.e. the highest

harmonic, in the signal. In hemodynamics this means that the sampling rate should be at least twice as high as the frequency of the highest harmonic, thus 30 times the Heart Rate. If dealing with human hemodynamics, with a Heart Rate of 60 bpm, the frequency is 1 cycle per second 1 (1 Hz) and sampling should be done with a rate higher than 30 samples per second. If we measure in the rat with a rate of 420 bpm, or 7 Hz, sampling rate should be at least 210 samples per second.

Along the same lines one can reason that equipment used in hemodynamics should be sufficiently fast so that 15 times the Heart Rate can be accurately measured. For instance, in human use a pressure-manometer system should at least be accurate up to about 15 Hz, and when used during exercise with a Heart Rate of 180 bpm (3 Hz) at least up to 45 Hz.

In practice we use a large safety factor of about 3 or 4, and therefore a sampling rate of 100 Hz is certainly sufficient for the human at rest. In exercise the sampling rate should be increased by the same factor as the increase in Heart Rate.

Limitations

The following limitations apply to the use of Fourier analysis [1].

1. Fourier analysis may only be performed on periodic signals. In practice this means that the signal value at the start and end of the period to be analyzed should be the same. In other words only single heart beats or multiples of full beats, e.g., a respiratory cycle, where start values and end values of the signals are equal may be analyzed.
2. Fourier analysis can always be performed on signals in the steady state of oscillation. However, the calculation of the relation between two signals only leads to useful results when the system is linear, which means that sine wave input leads to sine wave output. The system should also be time invariant. The calculation of impedance or transfer function is then performed along the lines given in Fig. A1.1. The modulus ratio and the phase difference of the same harmonic number are calculated. Despite the nonlinear relations between pressure and diameter and pressure and flow etc., in many situations nonlinearity is not so strong that large errors result. However, the scatter in modulus and phase of the input impedance (Chap. 23) has been suggested to result from nonlinearity of the arterial system [3].
3. The amplitudes of the higher harmonics decrease in amplitude and are therefore more subject to noise than the lower harmonics. Thus the high frequency information should be considered with care.
4. Fourier analysis gives data at multiples of the Heart Rate only. Thus the frequency resolution is limited. Pacing of the heart at different rates, including high Heart Rates, improves the frequency resolution and also high frequency information.

It is also advisable to analyze a number of beats (~10) in the steady state to reduce noise [4]. This can be done by analysis per beat, and averaging the derived harmonics
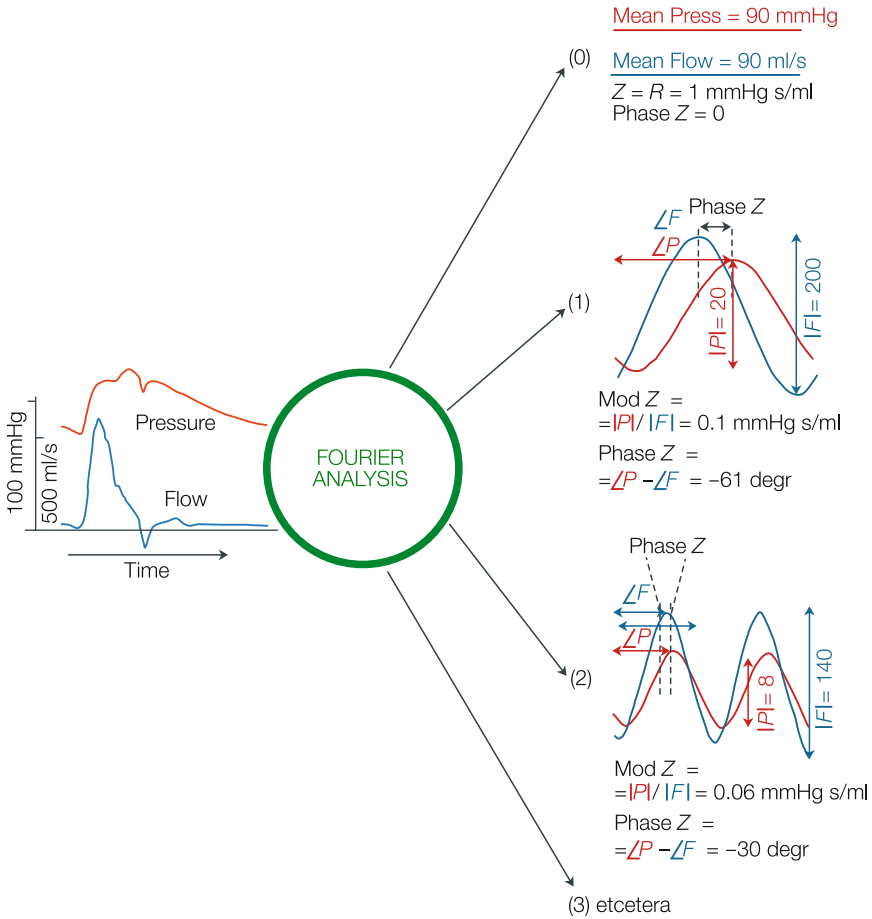
Fig. A1.1 Use of Fourier analysis in relating two time signals, here pressure and flow. For each harmonic the ratio of the moduli (amplitudes) and their phase difference, describes the relation, here impedance. In pressure transfer two pressures are analyzed

of these beats. It is, in principle, equally accurate to analyze a series of beats. When the Heart Rate is 75 bpm, i.e., 1.25 Hz, and a series of ten beats is analyzed, harmonics are obtained at multiples of 0.125 Hz. However, only the 10th, 20th, 30th, etc. harmonics, thus 1.25 Hz, 2.50 Hz, etc., contain accurate information.

Physiological and Clinical Relevance

Fourier analysis teaches us that hemodynamic signals contain at most ~15 harmonics. Higher harmonics disappear in the noise. Thus equipment should be able to measure >15 times the Heart Rate accurately. In the Pressure and flow measure-

ment techniques to be used in the human (Heart Rate 60 bpm) should thus have a flat frequency response up to >15 Hz. In the mouse, with a Heart Rate of 600 bpm the frequency response should be accurate up to >150 Hz.

Fourier analysis and the subsequent calculation of the amplitude ratio and phase angle difference per harmonic of two hemodynamic signals give information about a linear and time invariant system. An example is input impedance (Chap. 23). An important other example is the calculation of the pressure transfer function (Chap. 26). When radial and aortic pressure are measured, the Fourier analysis of these two signals and subsequent calculation of their amplitude and phase relation leads to the transfer function, which describes the arterial system in between these two sites. Once the transfer function is known, radial pressure can be used to derive aortic pressure as long as the arterial system does not change.

Nonlinearity of the system e.g., cardiac valves, the pressure-flow relation over a stenosis etc., does not allow calculations based on this linear approach. For instance, systemic vascular resistance and impedance can be calculated from aortic pressure minus venous pressure and aortic flow but not from ventricular pressure and flow.

The oscillatory flow theory is also based on sinusoidal relations between pressure drop over and flow through a segment of artery (Chap. 8).

References

1. Westerhof N, Sipkema P, Elzinga G, Murgo JP, Giolma JP. Arterial impedance. *In*: Hwang NHC, Gross DR, Patel DJ. *Quantitative cardiovascular studies*. 1979, Baltimore, MD; University Park Press.
2. Hamming RW. *Digital filters*. 1977, Englewood Cliffs, NJ, Prentice Hall.
3. Stergiopulos N, Meister J-J, Westerhof N. Scatter in the input impedance spectrum may result from the elastic nonlinearity of the arterial wall. *Am J Physiol* 1995;269:H1490–H1495.
4. Murgo JP, Westerhof N, Giolma JP, Altobelli SA. Aortic input impedance in normal man: relationship to pressure wave forms. *Circulation* 1980;62:105–116.

Appendix 2
Basic Hemodynamic Elements
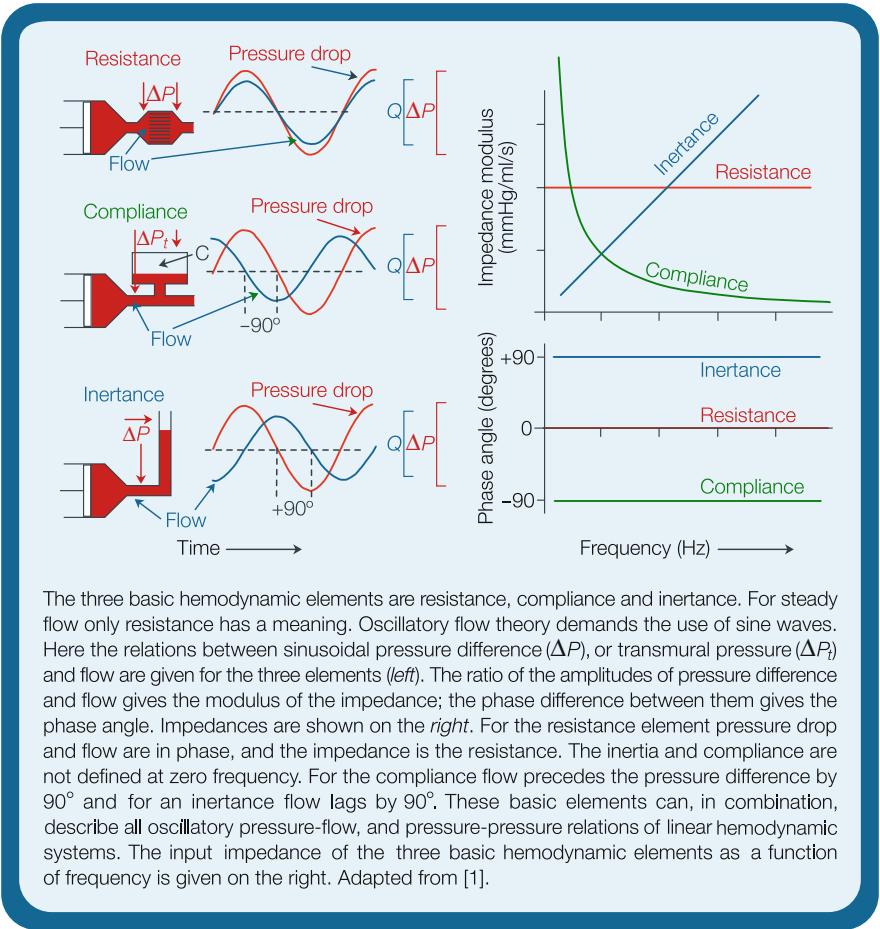
The three basic hemodynamic elements are resistance, compliance and inertance. For steady flow only resistance has a meaning. Oscillatory flow theory demands the use of sine waves. Here the relations between sinusoidal pressure difference (ΔP), or transmural pressure (ΔP_t) and flow are given for the three elements (*left*). The ratio of the amplitudes of pressure difference and flow gives the modulus of the impedance; the phase difference between them gives the phase angle. Impedances are shown on the *right*. For the resistance element pressure drop and flow are in phase, and the impedance is the resistance. The inertia and compliance are not defined at zero frequency. For the compliance flow precedes the pressure difference by 90° and for an inertance flow lags by 90°. These basic elements can, in combination, describe all oscillatory pressure-flow, and pressure-pressure relations of linear hemodynamic systems. The input impedance of the three basic hemodynamic elements as a function of frequency is given on the right. Adapted from [1].

Description

The impedance of the three basic hemodynamic elements [1] is shown in the right hand side of the Figure in the box. For the resistance, the pressure drop and flow are in phase and their amplitude ratio gives the value of the resistance. For the compliance, the sine wave of flow precedes the pressure drop, and they are −90° out of phase, i.e., a quarter of the whole sine wave for all frequencies. The modulus of the impedance, $|Z(\omega)|$ equals $1/\omega \cdot C$, with C compliance and ω the circular frequency, $\omega = 2\pi \cdot f$, f being the frequency in Hz (cycles per second). Increasing frequency implies decreasing impedance modulus. For the inertance the impedance modulus equals $|Z(\omega)| = \omega \cdot L = 2\pi \cdot f \cdot L$, the impedance increases with frequency, and the phase angle is +90° for all frequencies.

Physiological and Clinical Relevance

All linear and time invariant hemodynamic systems, for instance the entire systemic arterial tree, the pulmonary vascular system, or a pressure transfer function can be quantitatively described by a combination of these three basic elements. Linear means that when the input (e.g., pressure) is a sine wave, the output (e.g., flow) should also be a sine wave.

Limitations

The arterial system is not linear. For instance, the pressure-volume relation of the arteries is not straight. Other aspects such as inlet length, curvature of vessels, etc., result in nonlinear behavior. Nevertheless, in most practical aspects this nonlinearity does not affect the results obtained by linear analyses much. Often "piece-wise" linearity is sufficient: for a pressure of 120/80, Pulse Pressure is relatively small and over this range of 40 mmHg the system can be considered linear. Over the range 160/120 again linearity holds, but over the range 160/80 this may not be the case anymore. Thus, systemic vascular resistance and aortic input impedance can be calculated and this information is meaningful. However, the relation between mean and oscillatory ventricular pressure and aortic flow does not contain useful information because of the strong nonlinearity of the aortic valves.

Reference

1. Westerhof N, Sipkema P, Elzinga G, Murgo JP, Giolma JP. Arterial impedance. *In*: Hwang NHC, Gross DR, Patel DJ. *Quantitative cardiovascular studies.* 1979, Baltimore, MD; University Park Press.

Appendix 3
Vessel Segment

A segment of blood vessel is an important building block of arterial models. In principle, distributed models, single or two-tube models, and lumped models are based on these building blocks. The basic elements constituting the building block are inertance, $L = \rho l/\pi\, r_i^2$, resistance, $R = 8\eta l/\pi\, r_i^4$, and compliance, $C \approx 3\,\pi\, r_i^3 l/2Eh$. When we give these parameters per unit length a prime is added, L', R', and $C' = C_A$, and C_A is area compliance. The inertance and resistance describe the relation between pressure drop (ΔP) and flow (Q), and in combination are called the longitudinal impedance, $Z_l = i\omega L + R$. Accounting for oscillatory flow theory a combination of resistances and inertances are used. For large arteries resistance may be omitted, for very small arteries and arterioles only resistance remains. The compliance accounts for the change in diameter with transmural pressure (P_t). The diameter change implies storage of blood and relates to the difference of flows into and out of the segment. The relation between the flow difference and transmural pressure is called transverse impedance, $Z_t = 1/i\omega C$. When accounting for viscoelastic wall properties a combination of resistances and compliances is required.

Description

The relation between the pressure drop and flow of a uniform segment of blood vessel is shown in the Figure in the box. The relation consists of a longitudinal impedance, which is described by Womersley's oscillatory flow theory [1, 2], and a transverse impedance [3], describing the pressure-area (or volume) relation of the segment. The combination of longitudinal and transverse impedances gives characteristic impedance and wave propagation (Appendix 4).

The Longitudinal Impedance

The longitudinal impedance Z_l, is given in Fig. A3.1 and is described by Womersley's oscillatory flow theory [1]. For small arteries, i.e., for small values of Womersley's α, the longitudinal impedance per length is described by Poiseuille's equation and $Z_l' = R' = 8\eta/\pi r_i^4$. For large values of α, i.e. large arteries, longitudinal impedance per unit length reduces to an inertance only and equals $Z_l' = i\,\omega\,L' = i\omega\,4\rho/3\pi \cdot r_i^2$.

The Transverse Impedance

The transmural pressure difference, i.e., the oscillatory pressure between lumen and external environment, is related to volume changes (see Chap. 11). Volume changes can be related to flow, and therefore we can use the term transverse impedance. The transverse impedance for a viscoelastic wall material is shown in Fig. A3.2 [3].
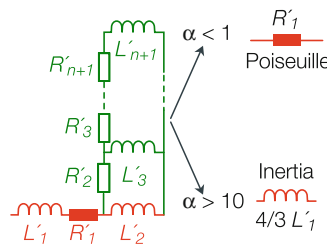
Fig. A3.1 The longitudinal impedance of a segment of artery of unit length, in electrical terms. The ladder network results from oscillatory flow theory. For small arteries or low frequencies, i.e., low α, as in the periphery, only resistance contributes. For large arteries or high frequencies, i.e., large α, the inertia is only of importance. $R'_n = 8\eta n/\pi r_i^4$, and $L'_n = \rho/(2n-1)\pi r_i^2$. Adapted from ref. [1], used by permission
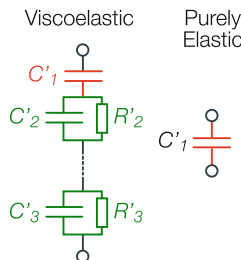
Fig. A3.2 The transverse impedance of a segment of artery of unit length, in electrical form. The dashpot-spring representation is shown in Chap. 10. The ladder network (*green*) results from viscoelasticity. For a purely elastic wall only compliance C_l' remains. Adapted from ref. [3], used by permission

For large conduit arteries, where the wall is almost purely elastic, this can be simplified to a single compliance, C and compliance per unit length is $C' = C_A = \Delta A/\Delta P$, with C_A area compliance (Chap. 11). The expression for compliance is:

$$C / l = C_A = 3\pi \cdot r_i^2 \cdot (r_i + h)^2 / E \cdot h \cdot (2r_i + h), \quad \text{or when } h \ll r_i, C \approx 3\pi \cdot r_i^3 \cdot l / 2E \cdot h.$$

The transverse impedance per length is $Z_t' = 1/i\ \omega \cdot C_A$.

Large and Small Arteries

From the above formulas we see that inertance is proportional to r_i^{-2}, and resistance to r_i^{-4}. This implies that resistance increases most strongly towards the periphery and this is why it is the overriding element there. The transverse impedance is proportional to r_i^{-3}, and increases towards the periphery, meaning that peripheral vessels contribute little to overall compliance. In other words compliance is mainly located in the conduit arteries. We should remember that all three basic elements are determined not only by the material properties but also by the geometry.

Physiological and Clinical Relevance

From the above we see that with smaller radius, as found towards the periphery, the importance of resistance becomes greater than inertance and compliance and in the very small arterioles only the resistance remains, 'Resistance Vessels'. In large conduit blood vessels, as the human aorta, the resistance term becomes negligible and inertance and compliance accurately describe the segment.

All models based on tubes. i.e., single tube, two-tube and distributed models, use the vessel segment as building block, and these building blocks are based on the description of longitudinal and transverse impedance.

References

1. Jager GN, Westerhof N, Noordergraaf A. Oscillatory flow impedance in electrical analog of arterial system. *Circ Res* 1965;16:121–133.
2. Womersley JR. *The mathematical analysis of the arterial circulation in a state of oscillatory motion.* 1957, Wright Air Dev. Center, Tech Report WADC-TR-56-614.
3. Westerhof N, Noordergraaf A. Arterial viscoelasticity. A generalized model. *J Biomech* 1970;3:357–379.

Appendix 4
Wave Speed and Characteristic Impedance
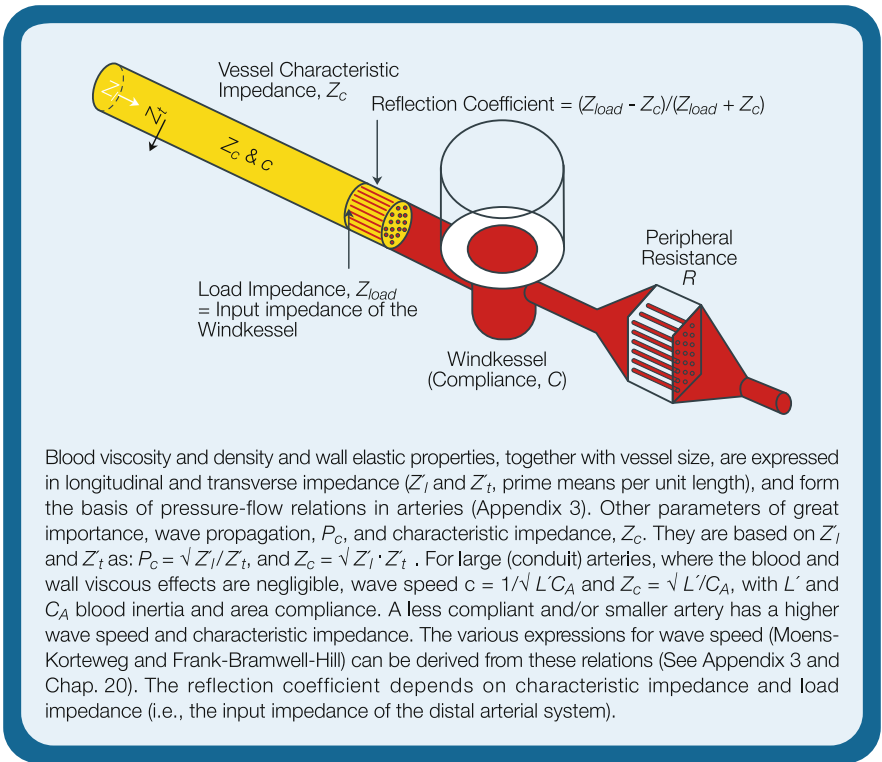
Blood viscosity and density and wall elastic properties, together with vessel size, are expressed in longitudinal and transverse impedance (Z'_l and Z'_t, prime means per unit length), and form the basis of pressure-flow relations in arteries (Appendix 3). Other parameters of great importance, wave propagation, P_c, and characteristic impedance, Z_c. They are based on Z'_l and Z'_t as: $P_c = \sqrt{Z'_l/Z'_t}$, and $Z_c = \sqrt{Z'_l \cdot Z'_t}$. For large (conduit) arteries, where the blood and wall viscous effects are negligible, wave speed $c = 1/\sqrt{L'C_A}$ and $Z_c = \sqrt{L'/C_A}$, with L' and C_A blood inertia and area compliance. A less compliant and/or smaller artery has a higher wave speed and characteristic impedance. The various expressions for wave speed (Moens-Korteweg and Frank-Bramwell-Hill) can be derived from these relations (See Appendix 3 and Chap. 20). The reflection coefficient depends on characteristic impedance and load impedance (i.e., the input impedance of the distal arterial system).

Description

Wave speed, c, and characteristic impedance, Z_c, are two important vessel parameters determining its wave transmission and reflection properties. These two quantities can be derived from so-called wave transmission theory, in analogy to what happens in telegraph lines, or antenna cables, for the transmission of electromagnetic waves. The characteristic impedance $Z_c = \sqrt{Z_l'\ Z_t'}$, with Z_l' and Z_t' the longitudinal and transverse impedance per length as given in Appendix 3. For large vessels like the aorta (large Womersley's α) is $Z_c = \sqrt{Z_l'\ Z_t'} = \sqrt{L'/C_A} = \sqrt{\rho \Delta P/\Delta A \cdot A}$,

The propagation constant, P_c, gives transmission properties: wave speed and the damping constant and is $P_c = \sqrt{Z_l'/Z_t'}$. The P_c consists of a real (giving damping) and imaginary part, $\mathrm{im}[P_c]$, giving wave speed, $c = \mathrm{i}\,\omega\,/\mathrm{im}[P_c]$. Since propagation is virtually always determined in large vessels (large α) we can write $P_c = \sqrt{Z_l'/Z_t'} = \mathrm{i}\,\omega \cdot \sqrt{L'C_A}$ and wave speed $c = \mathrm{i}\,\omega/\mathrm{im}[P_c] = 1/\sqrt{L'C_A}$. This is the so-called phase velocity.

Inserting the relations given in Appendix 3 for large vessels gives $c = \sqrt{A/\rho C_A} = \sqrt{A \cdot \Delta P/\Delta A \cdot \rho} = \sqrt{V \Delta P/\Delta V \cdot \rho} = \sqrt{1/\rho K}$ with $K =$ distensibility (Chap. 11 and 20; Frank or Bramwell-Hill equation for wave speed).

Using $A = \pi r_i^2$ and thus $\Delta A = 2\pi r_i \cdot \Delta r_i$, we arrive at $c = \sqrt{r_i \cdot \Delta P/2\Delta r_i \cdot \rho}$. This form is useful in the estimation of wave speed from changes in radius and pressure. Using $C_A \approx 3\pi \cdot r_i^3/2E_{inc} \cdot h$ and from Womersley's theory $L' = 4\rho/3\pi \cdot r_i^2$ (Appendix 3), gives $c = \sqrt{C_A L'} = \sqrt{E \cdot h/2r_i \cdot \rho}$, and using $\Delta P/\Delta r_i = h/r_i \cdot (\Delta \sigma/\Delta r_i)$ also gives $c = \sqrt{E_{inc}\,h/2r_i \cdot \rho}$ (Chap. 20, Moens-Korteweg). Sometimes $L' = \rho/\pi \cdot r_i^2$ is used, which leads to $c = \sqrt{2E_{inc}\,h/3r_i \cdot \rho}$. The difference in the square root of 2/3 and 1/2 is about 15%. When reflections are present the apparent wave velocity is measured, which deviates from the phase velocity (Chap. 20). However, by using sharp corners in the waveform, i.e., high frequencies in the signal, reflections may be assumed negligible (see section "Calculation of Characteristic Impedance") and the phase velocity is approached.

The choice of formula depends on the information desired. If local compliance is to be derived, the Frank or Bramwell-Hill equation is preferred. If the material constant, E_{inc}, is to be obtained the Moens-Korteweg equation is to be used.

When the heart ejects it has to accelerate the blood into a compliant aorta. Thus what the heart encounters first during ejection is the combination of the effects of compliance and inertance. Inertance increases the load but compliance makes it easier to eject. The combined effect is given by the characteristic impedance $Z_c = \sqrt{L'/C_A}$, and Z_c is called characteristic impedance because it is characteristic for the vessel and it impedes the flow. Since $Z_c = \sqrt{L'/C_A}$ it implies that the characteristic impedance of the aorta is a real number and frequency independent. If we take the proximal aorta as an example, the ventricle encounters, during the initial part of ejection, an impedance to flow that is the characteristic impedance of the proximal aorta. If the heart were loaded with the peripheral resistance directly the initial load would be much higher, because systemic peripheral resistance is about 15 times larger than the characteristic impedance of the aorta. If the aorta were infinitely long or if no reflections would return to the heart (Chap. 21), the characteristic impedance would be the load on the heart and the pressure and flow waves would have the same shape.
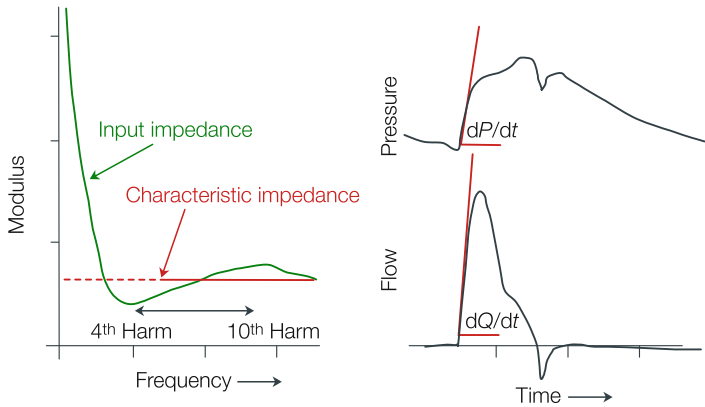
Fig. A4.1 The characteristic impedance can be estimated from the input impedance modulus at high frequencies: Z_c=averaged |Zin| for harmonics 4–10. Characteristic impedance also can be estimated from the slope of the initial phase of aortic pressure and aortic flow, where reflections are assumed minimal: $Z_c = dP/dt/dQ/dt = dP/dQ$

Calculation of Characteristic Impedance

Since, for high frequencies, corresponding to short time scales, the arterial tree approaches a reflectionless system, the input impedance at high frequencies is close to the characteristic impedance of the vessel where the impedance is determined (Chap. 23). This allows for an estimation of characteristic impedance from the modulus of the input impedance at high frequencies (Fig. A4.1, left). In practice the averaged impedance modulus between the fourth to tenth harmonic is used [1].

It is also assumed that early in ejection when no reflections are returning yet from the periphery, the pressure and flow are related through the characteristic impedance [2]. This allows calculation of characteristic impedance from the ratio of the slopes of (aortic) pressure and flow (Fig. A4.1, right).

Calculation of Reflection Coefficient

The reflection coefficient is defined as (see Figure in box):

$$\Gamma = \left(Z_{load} - Z_c\right)/\left(Z_{load} + Z_c\right)$$

With Z_{load} the impedance of the load of the artery and Z_c its characteristic impedance. For an artery loaded with a resistor R the reflection coefficient equals: $\Gamma = (R - Z_c)/(R + Z_c)$. For details see [1, 3].

The reflection coefficient is between 0 and 1, when zero, no reflection takes place and when 1 full reflection occurs. The reflection coefficient is complex in the mathematical

sense and a function of frequency, which implies that waves may be reflected out of phase. Thus the reflected sine wave is, in general, not only smaller than the forward wave, but also out of phase with it. Since a phase shift relates to a time shift, the reflected wave may appear to reflect from greater of shorter distance [4]. Only when the tube has a large diameter, and Z_c is real, and the load is also real, thus a resistor, the reflection coefficient is real and the pressure wave is reflected in-phase.

Physiological and Clinical Relevance

Wave transmission is easily studied noninvasively and can give information about vessel compliance without the need of invasive measurements (Chap. 20). A decrease in aortic compliance with age by a factor of 3 increases the pulse wave velocity by about 70% ($\sqrt{3}$), assuming constant radius. Decreased compliance also results in increased characteristic impedance, which affects reflection. Both the decrease in compliance and the increase in characteristic impedance lead to a higher Pulse Pressure if ejection flow is unaltered.

For large vessels where the wave speed is usually studied (aorta, carotid artery, and large leg and arm arteries) the viscous properties of blood and the viscosity of the wall are negligible so that damping of the waves does not play a role. In these arteries the compliance and inertance together determine wave speed and characteristic impedance (Appendix 4 and Chap. 20). When smaller vessels are studied the situation gets much more complex, the wave is not only transmitted but also damped.

Reflection occurs at every bifurcation and discontinuity, thus at all locations where characteristic impedances are different. Reflection can cause an apparent time delay suggesting that the reflected wave has traveled longer than the distance to the reflection site suggests. In aging the reflected wave will return earlier to the heart as a result of the increased wave speed, but this effect is counteracted by an altered phase shift [1].

It can be seen that $c/Z_c = A/\rho$, and with $\rho \sim 1$ in the cgs system, it holds that $c/Z_c = A$. Thus, if the input impedance is determined from velocity instead of volume flow, and pressure, characteristic impedance equals wave speed.

References

1. Nichols WW, O'Rourke MF. *McDonald's blood flow in arteries.* 2005, New York, NY: Oxford University Press, 5th edn.
2. Li JK-J. Time domain resolution of forward and reflected waves in the aorta. *IEEE Trans Biomed Eng* 1986;BME-33:783–785.
3. Milnor WR. *Hemodynamics.* 1989, Baltimore & London; Williams & Wilkins, 2nd edn.
4. Westerhof BE, Guelen I, Westerhof N, Karemaker JM, Avolio A. Quantification of wave reflection in the human aorta from pressure alone: a proof of principle. *Hypertension* 2006;48:595–601.

Appendix 5
Basic Aspects

$\Delta P_{axial} = P_1 - P_2$
$\Delta P = R \times \text{Flow}$

$\Delta P_{transmural} = P_{in} - P_{out}$

P_1

P_2

$A = \pi r_i^2$

Radius r_i

$P_{in} \approx (P_1 + P_2)/2$

Flow direction

Surface or Lateral Area $= 2\pi r_i l$

Length l

P_{out}

The pressure difference, P_1-P_1, in the direction of the axis, inside the blood vessel, causes the flow. The pressure inside, which is about $P_{in} = (P_1 + P_2)/2$ minus the pressure outside, P_{out} is the transmural pressure. Changes in transmural pressure cause changes in diameter. The axial pressure drop in large arteries is small. Two areas are of importance: The cross-sectional area, $A = \pi r_i^2$, where pressure acts to push blood forward (*red*), and the lateral area, which equals $A = 2\pi r_i l$, which is used in exchange with the environment (*ochre*).

Description

Pressure and Flow

Pressure is the force applied per unit area. In hemodynamics we always think of pressure in terms of a pressure difference. The pressure difference along the axis, or pressure gradient, is the pressure that causes the flow of blood. The pressure difference between

the inside and outside of a vessel or the heart, which is often called transmural pressure, causes the wall distension.

Flow (Q) is given in ml/s or in liters/minute (Cardiac Output), and variably called *flow*, *volume flow* or *flow rate*. The *velocity*, or *flow-velocity* of blood, v, is given in cm/s. The volume flow, and the flow velocity averaged over the cross-sectional area of a vessel are related through the cross-sectional area, A, $v{\cdot}A = Q$.

Pressure and flow result from the properties of the heart as a pump and the characteristics of the arterial system. However, the so generated pressure and flow, can be used to obtain the properties of the arterial system and the heart. For instance, aortic minus venous pressure divided by aortic flow gives total peripheral resistance. For other applications see Chaps. 14 and 23.

Pulsatile and Oscillatory Pressure and Flow

Pressure and flow vary during the cardiac cycle and are therefore called pulsatile pressure and flow. When pressure and flow are subjected to Fourier analysis and written as a series of sine waves (Appendix 1) we call them oscillatory pressure and flow. The zero term equals the mean value and the harmonics are the oscillatory terms. Womersley's oscillatory flow theory pertains to sinusoidal pressure-flow relations.

Area

In the Figure in the box the two areas of a blood vessel are shown. The area $A = \pi r_i^2$, the so-called cross-sectional area, is the area where the pressure acts to cause flow. The law of Poiseuille connects the pressure gradient to flow via this area to the second power, namely to r_i^4. The cross-sectional area of the human aorta is about 6 cm^2 and of an arteriole it is about 30 μm^2. The total cross-sectional area of all capillaries together is about 5,000 cm^2 or 0.5 m^2.

The lateral area or exchange area is the area involved in the exchange of oxygen, substrates and metabolites between tissue and blood. This area is calculated as: $2\pi r{\cdot}l$, with l length. The total exchange area of all capillaries together is about 6,000 m^2.

Wave Speed Differs from Flow Velocity

Blood flow velocity is the speed with which the molecules and cells in the blood move from heart to periphery on the arterial side and back ('venous return') on the venous side. The, mean, velocity of blood in the aorta is about 15 cm/s, maximum velocity of blood in systole in the aorta is about 100 cm/s, and in the capillaries the average velocity is about 0.5 mm/s.

Wave speed or wave velocity is the velocity with which the pressure wave, the diameter variation and the flow wave travel. The wave speed pertains to pulsatile phenomena, and depends on vessel size and vessel elasticity (Chap. 20). The values of wave speed are between 4 and 10 m/s, thus much higher than the blood flow velocity.

Wave speed and flow velocity are, in the context of this book, not related. Even without net blood flow-velocity, waves may be present.

The phase velocity (Moens-Korteweg; Frank; Newton-Young) is the wave speed in a reflectionless artery. When reflections are present the wave speed is called apparent phase velocity. The relation can be seen in Fig. 20.1.

Volume, Flow, and Circulation Time

Volume of a compartment, flow to a vascular bed (or whole system), and circulation time can be determined using an identifiable, nontoxic indicator that does not leave the compartment under study. Examples of indicators are dyes, radioactive tracers, or cold saline (thermodilution technique). For the last indicator a correction for disappearance from the circulation is made.

Blood volume can be determined by an intravenous injection of an amount, m_d, of a dye. The measurement of the concentration of the marker, $[C]$, in a blood sample, after complete mixing, allows for the calculation of the blood volume, V. The measured concentration in the blood is $[C]$ and this equals m_d/V, thus it follows that $V = m_d/[C]$. The injection may be performed in any blood vessel and the sample may be taken from any vessel as well.

Blood flow can be determined from a rapid injection of an indicator, amount m_d, and measurement of the concentration-time curve of the indicator in the blood. This is called the indicator dilution technique to determine mean flow. The flow is calculated as m_d/area under the time-concentration curve. In the indicator dilution technique, flow is determined at the location of injection, while the location of detection of the concentration-time curve is free. For instance, injection of a dye in the left atrium, guarantees good mixing, and allows for the estimation of Cardiac Output. The measurement of the concentration-time curve may take place in any artery and is thus rather free to choose.

In the indicator dilution technique cold saline is often used, and the method is then called the thermodilution technique. The most frequently used method is by flow guided catheter, injection of cold saline in the right atrium or right ventricle and measurement of the temperature in the pulmonary artery. The commercially available apparatuses correct for heat loss.

Circulation time is obtained by rapidly injecting an indicator at one location, x_1, and measurement of the arrival time at another location, x_2. Circulation time alone is of limited use but in combination with flow it allows estimation of the vascular volume between the two points. The volume of vascular bed between x_1 and x_2 equals the circulation time between x_1 and x_2 times volume flow. The circulation time of the entire circulation is about 1 min.

The Navier-Stokes Equations

The Navier-Stokes [1] equations form the basis of all fluid dynamics, including hemodynamics, and can be found in textbooks on fluid mechanics (Appendix 6). They are the equations of motion of the fluid due to the forces acting on it such as pressure and gravity, and the equations include the effect of fluid density and viscosity. It is a group of three sub-equations, each for one of the three spatial dimensions.

An exact mathematical solution of these general equations is not possible because of their nonlinear character, so that large computers are required to solve them for each situation. The software to solve the equations is available. One of the terms representing this method is Computational Flow Dynamics.

Under simplifying assumptions the Navier-Stokes equations can be solved. Poiseuille's law, Oscillatory Flow Theory and Bernoulli's equation, etc., are examples of simplified forms of the Navier-Stokes equations.

Reference

1. Munson BR, Young DF, Okiishi TH. *Fundamentals of fluid mechanics*. 1994, New York, Wiley.

Appendix 6
Books for Reference

Bevan JA, Kaley G, Rubanyi GM. *Flow-dependent regulation of vascular function.* 1995, New York, Oxford University Press.

Braunwald E (Ed). *Heart disease*, 2001, Philadelphia & Sydney, WB Saunders, 6th edn.

Burton AC. *Physiology and biophysics of the circulation.* 1972, Chicago, Year Book Medical Publishers, 2nd edn.

Caro CG, Pedley TJ, Schroter RC, Seed WA. *The mechanics of the circulation.* 1978, Oxford & New York, Oxford University Press.

Chien KR (Ed). *Molecular basis of cardiovascular disease.* Philadelphia & London, Saunders, 1999.

Cowen SC, Humphrey JD. *Cardiovascular soft tissue mechanics.* 2002, Dordrecht & Boston, Kluwer Acad. Publishers.

Crawford MH, DiMarco JP, Paulus WJ. *Cardiology.* 2004, Edinburgh & London, Mosby.

Drzewiecki GM, Li JK-J. *Analysis and assessment of cardiovascular function.* 1999, New York & Heidelberg, Springer-Verlag.

Fozzard HA, Haber E, Jennings RB, Katz AM, Morgan HE. *The heart and cardiovascular system: scientific foundations.* 1991, New York; Raven Press, 2nd edn.

Fung YC. *Biomechanics. Mechanical properties of living tissues.* 1981, New York & Heidelberg, Springer-Verlag.

Fung YC. Biodynamics. *Circulation.* 1984, New York & Heidelberg, Springer-Verlag.

Fung YC. *Biomechanics.* 1990, New York & Heidelberg, Springer-Verlag.

Fung YC, Perrone N, Anliker M. *Biomechanics.* 1972, Englewood Cliffs, Prentice-Hall.

Glantz SA. *Mathematics for biomedical applications.* 1979, Berkeley, University California Press.

Guyton AC, Hall JE. *Textbook of medical physiology*, 2000, Philadelphia & Sydney, WB Saunders, 10th edn.

Hwang NHC, Gross DR, Patel DJ. *Quantitative cardiovascular studies.* 1979, Baltimore, MD, University Park Press.

Hwang NHC, Normann NA. *Cardiovascular flow dynamics and measurements*. 1977, Baltimore, MD, University Park Press.

Jaffrin MY, Caro CG. *Biological flows*. 1995, New York, Plenum Press.

Milnor WR. *Hemodynamics.* 1989, Baltimore & London, Williams & Wilkins, 2nd edn.

Munson BR, Young DF, Okiishi TH. *Fundamentals of fluid mechanics.* 1994, New York, John Wiley & Sons, 2nd edn.

Nichols WW, O'Rourke MF. *McDonald's blood flow in arteries.* 2005, New York, NY, Oxford University Press, 5th edn.

Noble MIM. *The cardiac cycle.* 1979, Oxford & London, Blackwell Scientific Publications.

Noordergraaf A. *Hemodynamics.* 1969, In Bio-engineering, H.P. Schwan Ed. New York, McGraw-Hill.

O'Rourke MF. *Arterial function in health and disease.* 1982, Edinburgh & London, Churchill Livingstone.

O'Rourke MF, Kelly RP, Avolio AP. *The arterial pulse.* 1992, Philadelphia PA, Lea & Febiger.

Ottesen JT, Olufsen MS, Larsen JK. *Applied mathematical models in human physiology.* 2004, Philadelphia PA, Society Industrial and Applied Mathematics (SIAM).

Sagawa K, Maughan L, Suga H, Sunagawa K. *Cardiac contraction and the pressure-volume relationship.* 1988, New York & Oxford, Oxford University press.

Schmidt-Nielsen L. *Scaling.* 1984, New York, Cambridge University Press.

Spaan JAE. *Coronary blood flow.* 1991, Dordrecht & Boston. Kluwer Academic Publishers.

Strackee J, Westerhof N. *The physics of heart and circulation.* 1992, Bristol & Philadelphia, Institute of Physics Publishing.

Talbot SA, Gessner U. *Systems physiology.* 1973, New York & London, John Wiley & Sons.

Weibel ER. *Symmorphosis.* 2000, Cambridge, Harvard University Press.

Westerhof N, Gross DR. *Vascular dynamics.* 1989, New York & London, Plenum Press.

Yin FCP. *Ventricular/vascular coupling.* 1986, New York & Heidelberg, Springer-Verlag.

Appendix 7
Symbols

a	Acceleration (m/s^2)
A	Area (cm^2)
A^*	Amplitude
AI	Augmentation index (dimensionless)
b	Constant
bpm	Heart rate (beats per minute)
c	Pulse wave velocity or wave speed (m/s)
$c_{f\text{-}f}$	Foot-to-foot wave velocity (m/s)
c_{app}	Apparent wave velocity
C	Compliance $\Delta V/\Delta P$ (ml/mmHg)
C_A	Area compliance (cm^2/mmHg)
C_D	Diameter compliance (cm/mmHg)
CO	Cardiac output (l/min)
d	Derivative
∂	Partial derivative
d, D	Diameter (cm)
D	Distensibility ($\Delta V/V\Delta P$, 1/Bulk Modulus)
E	Elastance (mmHg/ml)
E_{es}	End-systolic elastance or maximal elastance (mmHg/ml)
E_{inc}	Incremental modulus of elasticity (mmHg/ml)
E_m	Murray energy term
E_{max}	Maximal or end-systolic elastance, slope of the ESPVR (mmHg/ml)
E_{min}	Diastolic elastance (mmHg/ml)
E_p	Peterson modulus ($r_0\Delta P/\Delta r_0$, mmHg)
EF	Ejection fraction (%)
ESPVR	End-systolic pressure-volume relation
$E(t)$	Time varying elastance
f	Frequency (Hz, 1/s)
F	Force (N)
FFR	Fractional flow reserve
FMD	Flow mediated dilation

g	Gravity (m/s^2)
g_f	Geometry factor
G	Gain (dimensionless)
G	Conductance (1/R, ml/mmHg s)
h	(Wall) thickness
HR	Heart rate (beats per minute, bpm)
Ht	Hematocrit
i	$\sqrt{-1}$
J_o, J_1	Bessel functions, order 0, 1
l	Length (cm)
L	Inertia (mmHg/ml/s^2)
l_{inlet}	Inlet length (cm)
m	Mass (kg)
m_d	Amount of substance, e.g., dye (g or M)
M	Body mass (kg)
P	Pressure (mmHg, kPa)
P_c	Propagation constant
P_{es}	End-systolic pressure (mmHg, kPa)
P_f	Forward or incident pressure wave
P_m	Measured pressure wave
P_b	Backward or reflected pressure wave (mmHg, kPa)
P_s, P_d	Systolic and diastolic blood pressure (mmHg, kPa)
P_v	Venous filling pressure (mmHg, kPa)
P_{mean}	Mean blood pressure (mmHg, kPa)
P_{O2}	Partial oxygen pressure (mmHg)
PP	Pulse pressure ($P_s - P_d$, mmHg, kPa)
PVA	Pressure volume area (mmHg ml)
Q	(Volume) flow ml/s or l/min
Q^f	Forward flow wave
Q^b	Backward flow wave
r	Radius
r_i, r_o	Internal and external radius
R	Resistance (mmHg/ml/s)
R_c	Characteristic resistance
R_p	Peripheral resistance
Re	Reynolds number ($2\rho \cdot v \cdot r/\eta$, dimensionless)
RPP	Rate pressure product (mmHg s)
SV	Stroke volume (ml)
St	Strouhal number ($2\omega \cdot r/v$)
t	Time (s)
T	Transfer function
T	Heart period (s), transfer function
TTI	Tension time index (mmHg s)
T_{su}	Surface tension (N/m)
v	Velocity (cm/s)

V	Volume (ml)
V_d	Intercept volume (ml)
V_{ed}	End-diastolic volume (ml)
V_{es}	End-systolic volume (ml)
V_{O2}	Oxygen consumption (per beat)
W	Work, energy (Joule)
WSS	Wall shear stress (kPa)
x	Location
z	Height difference
Z	(Input) impedance (modulus in mmHg/ml/s phase in degrees)
Z_c	Characteristic impedance (modulus in mmHg/ml/s phase in degrees)
ZSS	Zero stress state
α	Womersley's parameter ($\alpha^2 = r^2 \omega \rho / \eta$, dimensionless)
β	Stiffness parameter (β-stiffness)
ε	Strain $\Delta l/l$ (dimensionless)
ε_t	Transverse strain (dimensionless)
ϕ	Phase angle (degrees or radians π radians $= 180°$)
γ	Shear rate (1/s)
η	(Absolute or dynamic) viscosity (cP or Pa.s)
λ	Wave length (cm)
π	3.1415…
ρ	(Blood) density (g/cm^3)
σ	Stress and hoop stress (Pa $=$ N/m^2)
τ	Shear stress (Pa) and decay time (s)
ω	Circular frequency ($2\pi f$)
Δ	Difference, 'gradient'
Γ	Reflection coefficient (dimensionless)
K	Distensibility
θ	Angle (degrees)

Appendix 8
Units and Conversion Factors

	SI-system (kg m s)	cgs-system (g cm s)	Medical units
Area Compliance, C_A	1 m²/Pa = 1 m⁴/N	10⁴ cm⁴/dyn	1.33·10⁶ cm²/mmHg
Compliance, C	1 m³/Pa = 1 m⁵/N	10⁵ cm⁵/dyn	1.33·10⁸ ml/mmHg

Bulk Modulus	1 Pa = 1 N/m²	10 dyn/
		    cm² = 1.36gwt/
		    cm²
			7.5·10⁻³ mmHg

Diameter Compliance, C_D	1 m¹/Pa = 1 m³/N	10³ cm⁴/dyn	1.33·10⁴ cm/mmHg

Distensibility	1 Pa⁻¹ = 1 m²/N	0.1 cm²/
		    dyn = 0.75 cm²/
		    gwt
			133 mmHg⁻¹

Density, ρ	1 kg/m³	10⁻³ g/cm³	
Elastance, E	1 Pa/m³ = 1 N/m⁵	10⁻⁵ dyn/cm⁵	7.5·10⁻⁹ mmHg/ml
Energy – work, W	1 J = 1 N·m = Pa·m³	10⁷ erg (dyn·cm)	7.5·10³ mm Hg·ml = 0.24 Calᵃ
Flow, Q	1 m³/s	10⁶ cm³/s = 10⁶ ml/s	(1 l/min = 16.66 ml/s)
dQ/dt	1 m³/s²	10⁶ ml/s²	
Force, F	1 N = 1 kg·m/s²	10⁵ dyn = 1g·cm/s² ~10² g (wt)	
Frequency, f	Hz = s⁻¹	Hz = s⁻¹	min⁻¹ (60 bpm = 1 Hz)
Frequency circular, ω	2πf Hz		
Inertance, L	1 Pa·s²/m³ = N·s²/m⁵	10⁻⁵ dyn·s²/cm⁵	7.5·10⁻⁹ mmHg·s²/ml

(Incremental)
    Young Modulus
	1 Pa = 1 N/m²	10 dyn/
		    cm² = 1.36 gwt/
		    cm²
			7.5·10⁻³mmHg

Phase angle, degrees		With 360° = 2π radians	
Power, W	1 W = 1 J/s	10⁷ erg/s	7.5·10³ mmHg·ml/s

Pressure, P and
    stress, σ
	1 Pa = 1 N/m²	10 dyn/
		    cm² = 1.36 gwt/
		    cm²
			7.5·10⁻³ mmHg

dP/dt	1 Pa/s	10 dyn/cm²/s	7.5·10⁻³ mmHg/s
Resistance, R	1 Pa·s/m³ = N·s/m⁵	10⁻⁵ dyn·s/cm⁵	7.5·10⁻⁹ mmHg·s/ml

(continued)

(continued)

	SI-system (kg m s)	cgs-system (g cm s)	Medical units
Shear rate, γ	s^{-1}	s^{-1}	s^{-1}
Shear stress, τ	1 Pa = 1 N/m^2	10 dyn/cm^2 = 1.36 g/cm^2	$7.5 \cdot 10^{-3}$ mmHg
Velocity (wave)	m/s	m/s	m/s
Viscosity, η	1 Pa·s = 1 N·s/m^2	10 dyn·s/cm^2 = 10 Poise	
Decay time ($R \cdot C$)	s	s	s
$L \cdot C^{b}$	s^2	s^2	s^2
1 ml O$_2$^{c}	~20 J	$20 \cdot 10^7$ erg (dyn·cm)	150 mmHg·ml = 4.8 cal
1 ml O$_2$/min^{b}	~0.33 W	$0.33 \cdot 10^7$ erg/s	2.5 mmHg·ml/s

[a] 1 Cal = 10^3 cal

[b] When L and C are expressed per length: $1/\sqrt{L'C'}$ = m/s (velocity)

[c] For fatty acids and glucose metabolism; not for protein metabolism

1 kPa = 7.5 mmHg = 10 cm H$_2$O = mN/mm^2

Contractile efficiency is the inverse of the slope of the relation between Pressure Volume Area and oxygen consumption per beat

Economy of contraction is defined as oxygen consumption used for isovolumic contractions

Efficiency is the ratio of external, or produced mechanical power, and input power or oxygen consumption per time

Strain, Reynolds number, and Womersley's parameter, do not have a dimension, but one needs to work in a single system

Index